

Improving Transportation Infrastructure Resilience against Hurricanes, other Natural Disasters, and Weathering: Part I - Analysis of failure of transportation signs due to Hurricane Maria

Volume 1

FINAL REPORT
June 2022

Submitted by:

Gustavo Pacheco-Crosetti, PhD, PE
Professor

Héctor J. Cruzado, PhD, PE
Professor

Antonio J. Roig
Graduate Student

Transportation Infrastructure Research Center – TIRC
Polytechnic University of Puerto Rico
377 Ponce de Leon Ave, San Juan, PR 00918

External Project Manager:
Juan Carlos Rivera, Engineer
Puerto Rico Highway and Transportation Authority

In cooperation with

Rutgers, The State University of New Jersey
And
Puerto Rico
Department of Transportation and Public
Works And
U.S. Department of Transportation
Federal Highway Administration

Disclaimer Statement

The contents of this report reflect the views of the authors, who are responsible for the facts and the accuracy of the information presented herein. This document is disseminated under the sponsorship of the Department of Transportation, University Transportation Centers Program, in the interest of information exchange. The U.S. Government assumes no liability for the contents or use thereof.

The Center for Advanced Infrastructure and Transportation (CAIT) is a Regional UTC Consortium led by Rutgers, The State University. Members of the consortium are Atlantic Cape Community College, Columbia University, Cornell University, New Jersey Institute of Technology, Polytechnic University of Puerto Rico, Princeton University, Rowan University, SUNY - Farmingdale State College, and SUNY - University at Buffalo. The Center is funded by the U.S. Department of Transportation.

1. Report No. CAIT-UTC-REG17		2. Government Accession No.		3. Recipient's Catalog No.	
4. Title and Subtitle Improving Transportation Infrastructure Resilience against Hurricanes, other Natural Disasters, and Weathering: Part I - Analysis of failure of transportation signs due to Hurricane Maria				5. Report Date June 2022	
				6. Performing Organization Code CAIT/PUPR	
7. Author(s) Gustavo Pacheco-Crosetti (https://orcid.org/0000-0001-5346-6144) Héctor J. Cruzado (https://orcid.org/0000-0003-0268-5296)				8. Performing Organization Report No. CAIT-UTC-REG17	
9. Performing Organization Name and Address Transportation Infrastructure Research Center – TIRC Polytechnic University of Puerto Rico 377 Ponce de Leon Ave, San Juan, PR 00918				10. Work Unit No.	
				11. Contract or Grant No. 69A3551847102	
12. Sponsoring Agency Name and Address Center for Advanced Infrastructure and Transportation Rutgers, The State University of New Jersey 100 Brett Road Piscataway, NJ 08854				13. Type of Report and Period Covered Final Report 10/01/2018 - 5/29/2020	
				14. Sponsoring Agency Code	
15. Supplementary Notes U.S. Department of Transportation/OST-R 1200 New Jersey Avenue, SE Washington, DC 20590-0001					
16. Abstract On September 20, 2017, Hurricane Maria made landfall in Puerto Rico with maximum sustained winds of 155 mph. Other researchers have estimated that, while crossing the island, the hurricane produced 3-second gust wind speeds of up to 155 mph at 33 feet above ground for flat open terrain. Hurricane Maria caused significant damage to several and different types of structures throughout Puerto Rico, including guide traffic sign mounted on I-beams. The objectives of this research were to Volume 1) estimate the wind speeds that caused damages on guide traffic sign mounted on I-beams, and to suggest improvements to its design and construction to increase resiliency; Volume 2) identify the most common modes of failures experienced by small traffic signs during Hurricane Maria, estimate the gust wind speeds at which small traffic signs failed during Hurricane Maria, and suggest improvements to the design and construction of small traffic signs to increase their resiliency by reducing risk of failure in future extreme weather events; and Volume 3) perform a comprehensive field study to identify the cantilever-type traffic signs that experienced damages due to the wind loads. Some of the main highways of Puerto Rico were travelled to locate failed traffic signs, inspect them, estimate wind pressure, and determine the mode of failure. Based on study findings, a review of the design specifications and improvement on quality control during construction was recommended to guarantee a structure that is more resilient to future events.					
17. Key Words Hurricanes, wind damages, highway signs, transportation resilience			18. Distribution Statement		
19. Security Classification (of this report) Unclassified		20. Security Classification (of this page) Unclassified		21. No. of Pages 393	
				22. Price	

Acknowledgments

The authors would like to thank the Puerto Rico Highway and Transportation Authority (PRHTA) and the Puerto Rico Department of Transportation and Public Work (PRDOT) for all the information and collaboration they provided during the development of the project.

The authors also thank the Center for Advanced Infrastructure & Transportation (CAIT) at Rutgers University, and the Federal Highway Administration (FHWA), for their support in the development of the project.

Finally, thanks to Polytechnic University of Puerto Rico personnel and the students that participated in this project for their cooperation and assistance.

TABLE OF CONTENT

1	INTRODUCTION	1
2	LITERATURE REVIEW	7
2.1	HURRICANE MARIA	7
2.2	GROUND-MOUNTED BREAKAWAY SIGNS (GMBS).....	10
2.3	WIND LOADS ON SIGNS.....	19
3	RESEARCH PROGRAM	23
3.1	OBJECTIVES AND SCOPE.....	23
3.2	METHODOLOGY.....	23
4	FIELD INSPECTION.....	25
4.1	GEOLOCATION OF DOCUMENTED CASES	25
4.2	TRAFFIC SIGN FAILURES.....	27
4.2.1	<i>Foundation Failure</i>	27
4.2.2	<i>Slippage Failure</i>	28
4.2.3	<i>Fuse Plate Fracture</i>	31
4.2.4	<i>Undetermined Cases</i>	32
5	CASE STUDIES	35
5.1	FAILURE MODEL ANALYSIS.....	35
5.2	CASE 1.....	38
5.3	CASE 2.....	42
5.4	CASE 3.....	44
5.5	RESULTS	47
6	CONCLUSIONS AND RECOMMENDATIONS.....	48
	REFERENCES.....	52

List of Figures

Figure 1.1: Trajectories of tropical cyclones in the past century on the North Atlantic Ocean Basin (NOAA, n.d.)	1
Figure 1.2: Trajectories of tropical cyclones that have affected Puerto Rico in the past 150 years (NOAA, n.d.).....	2
Figure 1.3: Trajectory of Hurricane Maria through Puerto Rico (NOAA, n.d.).....	3
Figure 1.4: Gust speeds estimates for Hurricane Maria (FEMA, 2018)	4
Figure 1.5: Guide sign with breakaway I-beams	5
Figure 2.1: 2017 North Atlantic Hurricane Track Map (NOAA, 2017)	8
Figure 2.2: Satellite image of Hurricane Maria nearing peak intensity (Pasch, Penny, & Berg, 2019)	8
Figure 2.3: Hurricane Maria sustained and gust speed measurements (FEMA, 2018)	9
Figure 2.4: San Juan radar pre and post hurricane Maria (Climate.gov, 2018)	10
Figure 2.5: Puerto Rico road system (PRDOT, 2011).....	11
Figure 2.6: Dual post ground-mounted breakaway sign	12
Figure 2.7: Single post ground-mounted breakaway sign (Source: Google Maps)	12
Figure 2.8: Side view of the main components of a breakaway sign	13
Figure 2.9: Fuse plate.....	14
Figure 2.10: Hinge plate.....	14
Figure 2.11: Acting elements of a breakaway sign.....	15
Figure 2.12: Breakaway mechanism activated.....	15
Figure 2.13: Breakaway base for unidirectional impact.....	16
Figure 2.14: Sign to post connections using wind beams (PRDOT, 2000)	17
Figure 2.15: Fuse plate geometry (PRDOT, 2000).....	18
Figure 2.16: Hinge plate geometry (PRDOT, 2000)	18
Figure 2.17: Hinge joint detail for the ground mounted breakaway post (PRDOT, 2000)	19
Figure 2.18: Wind loads on sign cases required by ASCE 7 (ASCE, 2017).....	22
Figure 4.1: Location of documented cases (adapted from Google Earth Pro)	26
Figure 4.2: Foundation failure of Sign 6.....	27
Figure 4.3: Foundation failure of Sign 5	28
Figure 4.4: Slotted fuse plate slippage failure of Sign 9	29
Figure 4.5: Slotted fuse plate slippage failure of Sign 7	29
Figure 4.6: Sign 12 before (top left; Source: Google Earth Pro) and after failure	30
Figure 4.7: Slippage failure at the base of Sign 4	31
Figure 4.8: Fuse plate rupture of Case 2	32
Figure 4.9: Undetermined mode of failure of Sign 8.....	33
Figure 4.10: Undetermined mode of failure of Sign 10.....	33
Figure 4.11: Sign 11 before and after failure (Source: Google Maps)	34
Figure 5.1: Failure model for determination of wind speed	36
Figure 5.2: Case 1.....	38
Figure 5.3 Case 1 location (adapted from Google Earth).....	38
Figure 5.4: Case 1 dimensions.....	39
Figure 5.5 Fuse plate retrieved from Case 1	39
Figure 5.6: (a) Waterjet cutting machine, (b) specimens tension tested, and (c) rupture specimens. .	40
Figure 5.7 Case 1, Scenario A	41
Figure 5.8: Case 1, Scenario B	41
Figure 5.9: Case 2.....	42

Figure 5.10: Case 2 location (adapted from Google Earth)	42
Figure 5.11: Case 2 dimensions	43
Figure 5.12 Case 2, Scenario A.....	43
Figure 5.13: Case 2, Scenario B.....	44
Figure 5.14: Case 3.....	44
Figure 5.15: Case 3 location (adapted from Google Earth)	45
Figure 5.16: Case 3 dimensions	45
Figure 5.17: Assumed scenario for Case 3	46
Figure 6.1: Effect of raising the location of fuse plate of Case 1, Scenario B	50
Figure 6.2: Recommendation of inserting exit number into main sign.....	50
Figure 6.3: Rotating spring-loaded hinge.....	51

List of Tables

Table 1.1: Estimated damages due to major hurricanes in the past decades	2
Table 1.2: Approximate relationship between wind speeds in ASCE 7 and Saffir/Simpson Hurricane Scale (ASCE, 2017)	5
Table 2.1: Number and size of breakaway posts and wind beams (PRDOT, 2000)	17
Table 2.2: Fuse and hinge plates data (PRDOT, 2000)	18
Table 4.1: Signs geolocated and documented	26
Table 5.1: Case 1 fuse plate tensile test results	40
Table 5.2: Case 3 fuse plate tensile test results	46
Table 5.3: Data and results from the three cases	47

1 Introduction

Due to its location in the Caribbean Sea, the archipelago of Puerto Rico is constantly at risk of being impacted by tropical storms and hurricanes. Most of these tropical cyclones are formed in the Atlantic Ocean, near the west of Africa, moving from East to West, and then to the North, impacting the islands on the Caribbean Sea and parts of Central America and North America, as it can be appreciated in Figure 1.1. That trajectories of some of the tropical cyclones that have affected Puerto Rico are shown in Figure 1.2, with the color of the trajectory indicating the category of the event. Tropical storms and hurricanes have caused loss of lives and substantial damages in Puerto Rico. As a sample of this, Table 1.1 presents the damages (not adjusted to inflation) of the major hurricanes that have made landfall in Puerto Rico in the past several years. Several other tropical storms and non-major hurricanes have also made landfall in Puerto Rico during the same period, also causing substantial damages.

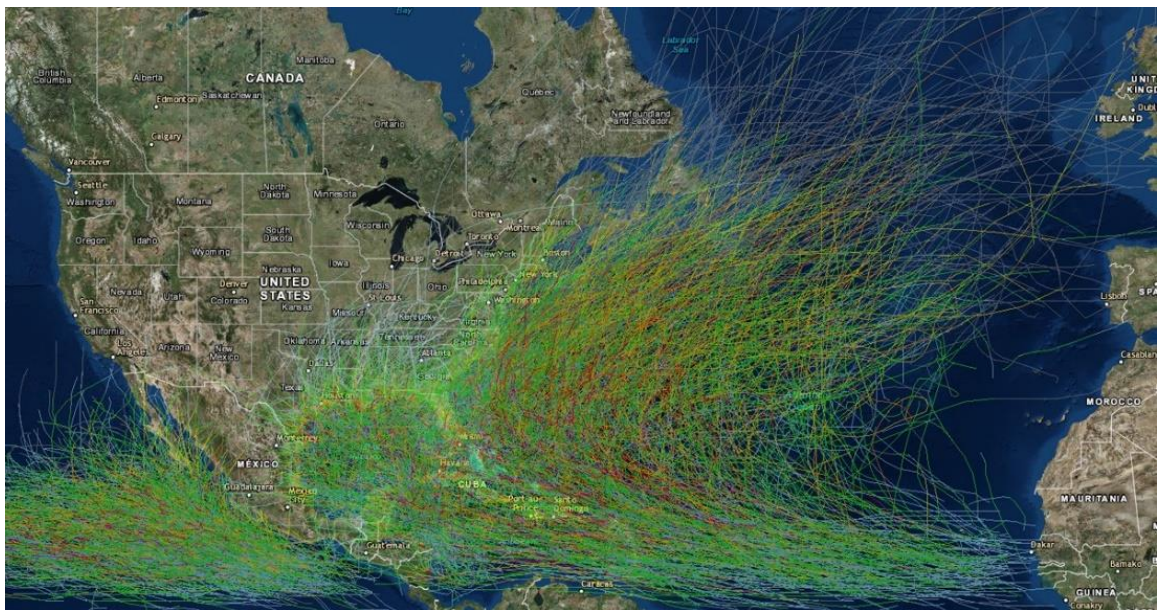


Figure 1.1: Trajectories of tropical cyclones in the past century on the North Atlantic Ocean Basin (NOAA, n.d.)

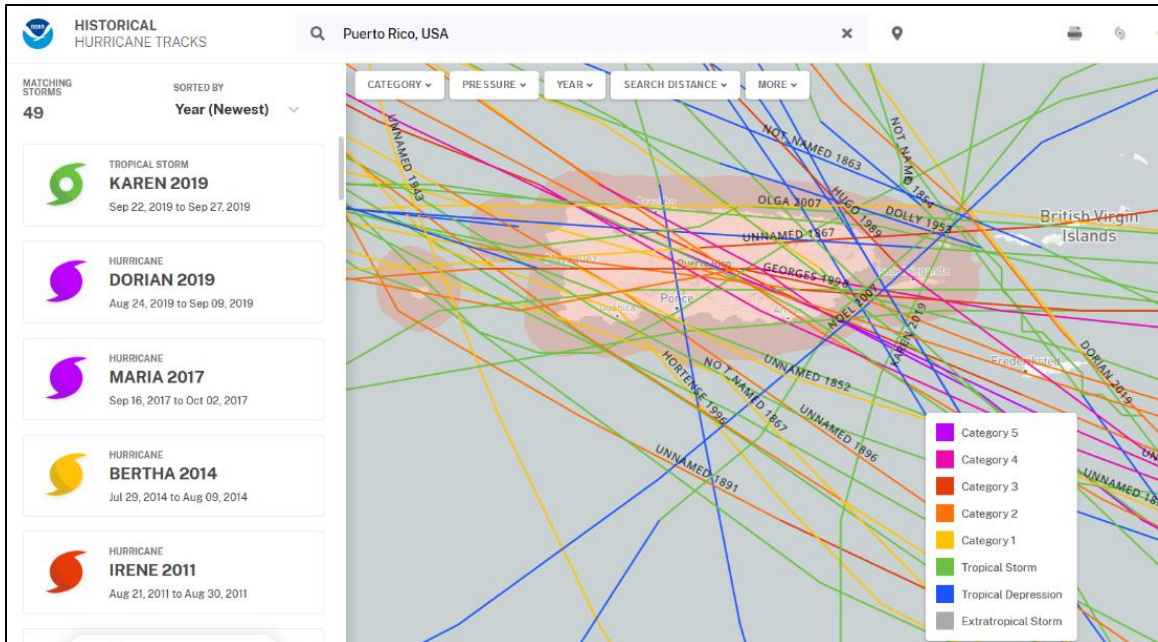


Figure 1.2: Trajectories of tropical cyclones that have affected Puerto Rico in the past 150 years (NOAA, n.d.)

Table 1.1: Estimated damages due to major hurricanes in the past decades

Hurricane	Year	Damages in US billions of dollars (unadjusted to inflation)
Hugo	1989	\$1.5
Georges	1998	\$2.0 - 8.0
Maria	2017	\$100

Hurricane Maria made landfall in Puerto Rico on September 20, 2017, as a strong category 4 hurricane with sustained winds of 155 mph. As shown in Figure 1.3, the hurricane crossed the main island of Puerto Rico from the southeast to the northwest, leaving as a category 3 hurricane with sustained winds of 110 mph. Besides the strong winds, the hurricane brought heavy rains, reaching 40 inches of rainfall in 48 hours (NWS, 2017). The rain caused severe flooding in several parts of the island that were furthered exacerbated in coastal regions due to the storm surge. The hurricane also caused a large quantity of landslides with a large concentration on the center of the island, where the topography presents higher elevations (NWS, 2017).

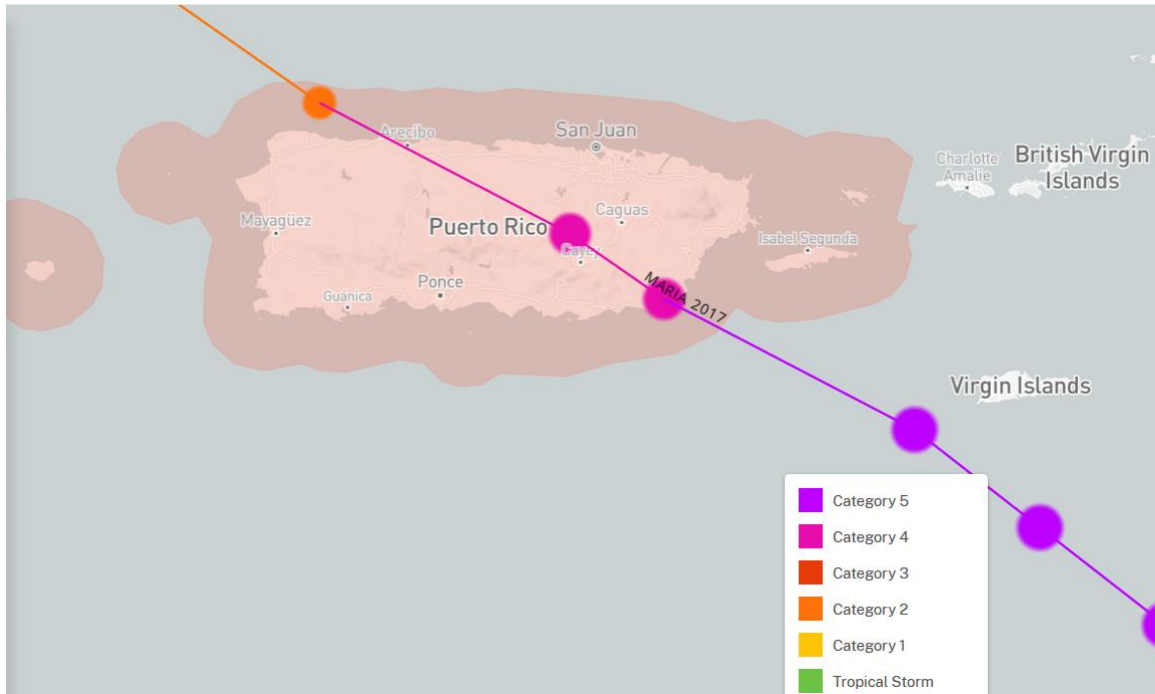


Figure 1.3: Trajectory of Hurricane Maria through Puerto Rico (NOAA, n.d.)

Hurricane Maria and its effects were extensively studied. Among the developed studies, researchers estimated the peak gust wind speeds that the hurricane produced. This type of research is extremely relevant, as they can be used to verify if the design wind speeds are adequate to lead to the construction of resilient structures against similar future weather event. Figure 1.4 presents one of these estimates; it should be considered that the estimates are for 3-second gusts 33 feet above ground for flat open terrain. In the figure, it can be seen that the maximum gust wind speed estimated was 140 mph. In other consulted studies, the maximum gust wind speed estimates range from 130 mph (Pacific Disaster Center, 2017) to 151 mph (Hubbard, 2018). No study estimating gust wind speeds higher than 155 mph, the sustained wind speed of Maria at the time of landfall, was found during the development of this study, and up to the end of year 2020. A recent report by the National Institute of Standards and Technology (2021) on Hurricane Maria included

topographic effects on their wind gust estimates, and presented in some spots speed higher than 155 mph.

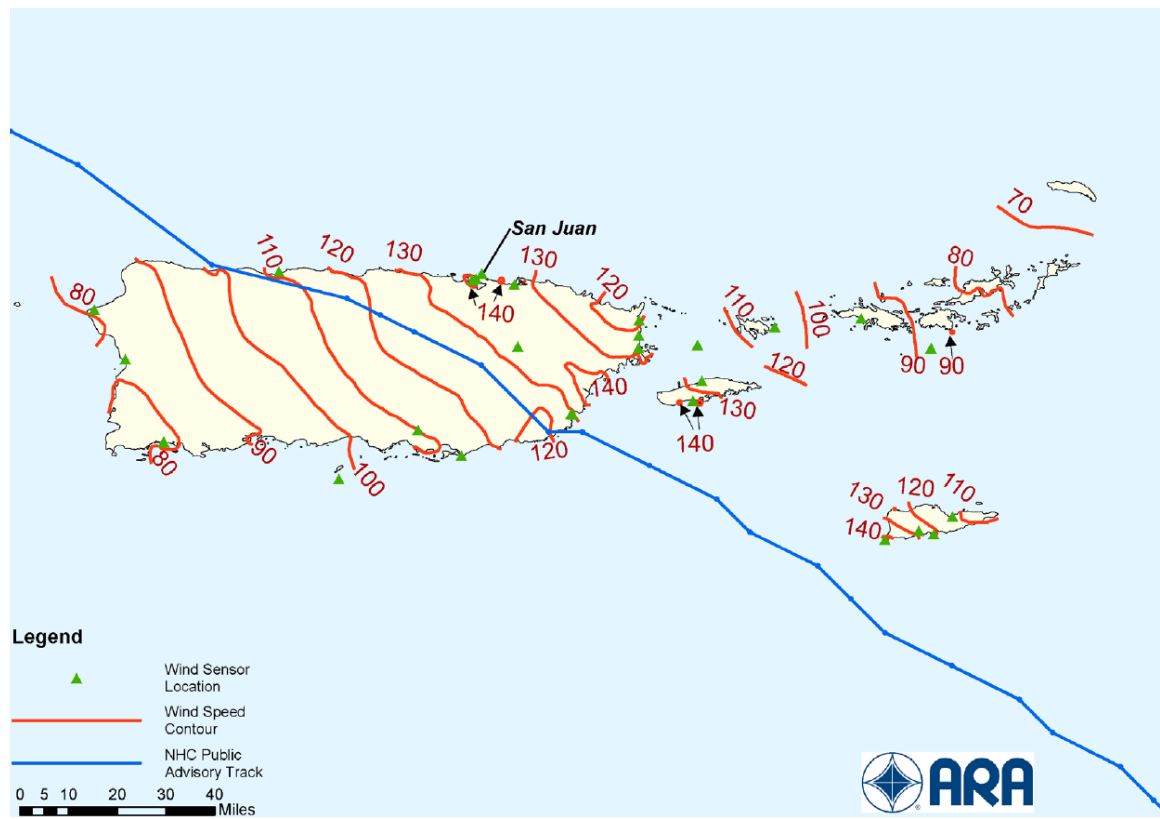


Figure 1.4: Gust speeds estimates for Hurricane Maria (FEMA, 2018)

The ASCE Standard ASCE/SEI 7-16 offers an approximate relationship between the sustained wind speed over water with gust wind speed over water and over land. This relationship is presented in Table 1.2. Performing a linear interpolation, it can be estimated that, for the sustained wind speed of 155 mph that Hurricane Maria had at the time of landfall, the expected gust wind speed over water and over land would be 189 mph and 171 mph, respectively. A point of interest is that the gust wind speed over land of 171 mph estimated using the table of the ASCE Standard is significantly higher than the gust wind speeds estimated by the different studies consulted for this research.

Table 1.2: Approximate relationship between wind speeds in ASCE 7 and Saffir/Simpson Hurricane Scale (ASCE, 2017)

Saffir-Simpson Hurricane Category	Sustained Wind Speed Over Water (mph)	Gust Wind Speed Over Water (mph)	Gust Wind Speed Over Land (mph)
1	74 – 95	90 – 116	81 – 105
2	96 – 110	117 – 134	106 – 121
3	111 – 129	135 – 157	122 – 142
4	130 – 156	158 – 190	143 – 172
5	> 157	> 191	> 173

Hurricane Maria caused significant damage to several and different types of structures throughout Puerto Rico, including, but not limited to guide traffic sign mounted on I-beams. Often, these signs have a smaller size sign attached on top indicating the exit number, like the one shown in Figure 1.5. This type of sign has breakaway posts designed to protect drivers and passengers in case a vehicle impacts the structure.



Figure 1.5: Guide sign with breakaway I-beams

The objectives of this research were to:

- Estimate the gust wind speeds that caused damages on guide traffic sign mounted on I-beams during Hurricane Maria.
- Suggest improvements to the design and construction of guide traffic sign mounted on I-beams to increase their resiliency by avoiding or reducing the risk of failure in future extreme weather events.

This report covers all the stages of this research project. Chapter 2 presents a literature review on three topics: (1) Hurricane Maria's general meteorological data, (2) breakaway traffic signs, and (3) calculation of wind loads on signs. In Chapter 3 the research program of this project is presented, including the objectives, scope, and methodology. Chapter 4 presents the field inspection information with the geolocation of the documented cases are presented. Also in Chapter 4, examples of the traffic sign failures are presented within each of the three categories of failure: foundation failure, slippage failure, and fuse plate fracture. Chapter 5 describes the three case studies selected in the failure category of fuse plate fracture with their respective location, geometric data, laboratory test result of the failed plate, and the wind speed estimated to have caused the failure. Finally, Chapter 6 presents the summary, conclusions, and recommendations, including suggestions on how to make the structures studied in this project more resilient.

2 Literature Review

This chapter first covers meteorological aspects of Hurricane Maria. Then, general aspects of the design and construction of ground-mounted breakaway signs are presented. Finally, a comparison is made between the calculation of wind loads on signs in the procedures of AASHTO and ASCE.

2.1 Hurricane Maria

The Caribbean basin experiences the hurricane season for six months out of the year, from June 1 to November 30. The month of September is when normally the highest number of storms develop. From August to October 2017, the Atlantic basin was subjected to 17 storms, with six of them becoming major hurricanes (category 3 or higher on the Saffir-Simpson scale), as shown in Figure 2.1. Three of the six major hurricanes (Harvey, Irma, and Maria) impacted the U.S. and its territories with an estimated \$265 billion in damages (FEMA, 2018). Out of this, \$90 billion were caused by Maria in Puerto Rico and the U.S. Virgin Islands (FEMA, 2018).

Hurricane Maria development started off the west coast of Africa as a tropical wave on September 12. It became a tropical depression and then a tropical storm, both on September 16. It turned into a hurricane on September 17 and a major hurricane on September 18 (Pasch, Penny, & Berg, 2019). Maria made landfall on the island of Dominica on September 19. Afterwards, it reached its maximum intensity of 172.6 mph with a minimum pressure of 908 mb (see Figure 2.2), but then went through an eyewall replacement that weakened it as it neared Puerto Rico. It made landfall in the southeast coast of Puerto Rico on September 20 at approximately 1015 UTC with an estimated

sustained wind speed of 155 mph (Pasch, Penny, & Berg, 2019), close to the lower limit of 157 mph for a category 5 hurricane.

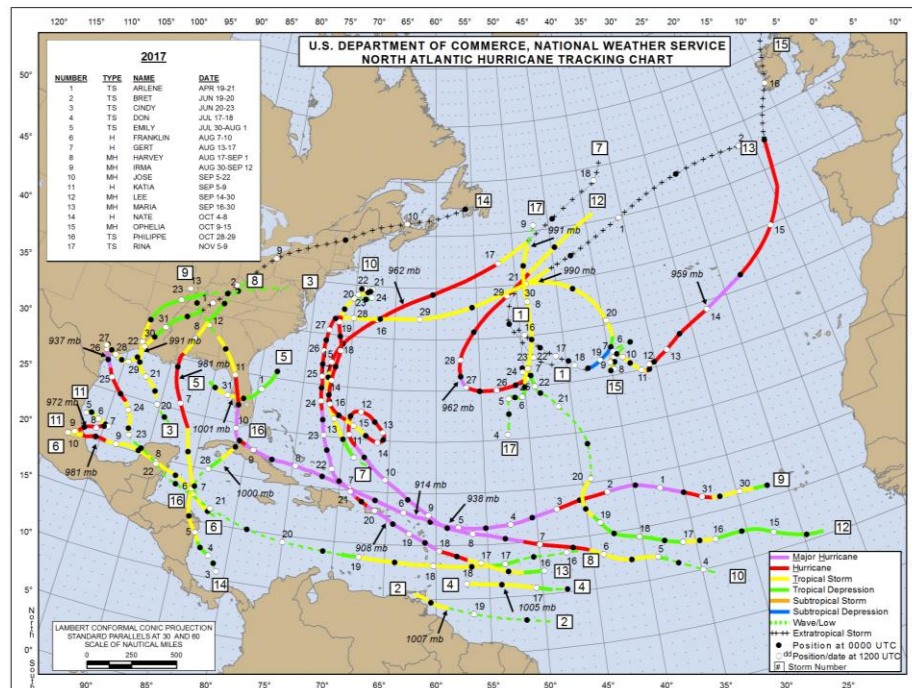


Figure 2.1: 2017 North Atlantic Hurricane Track Map (NOAA, 2017)

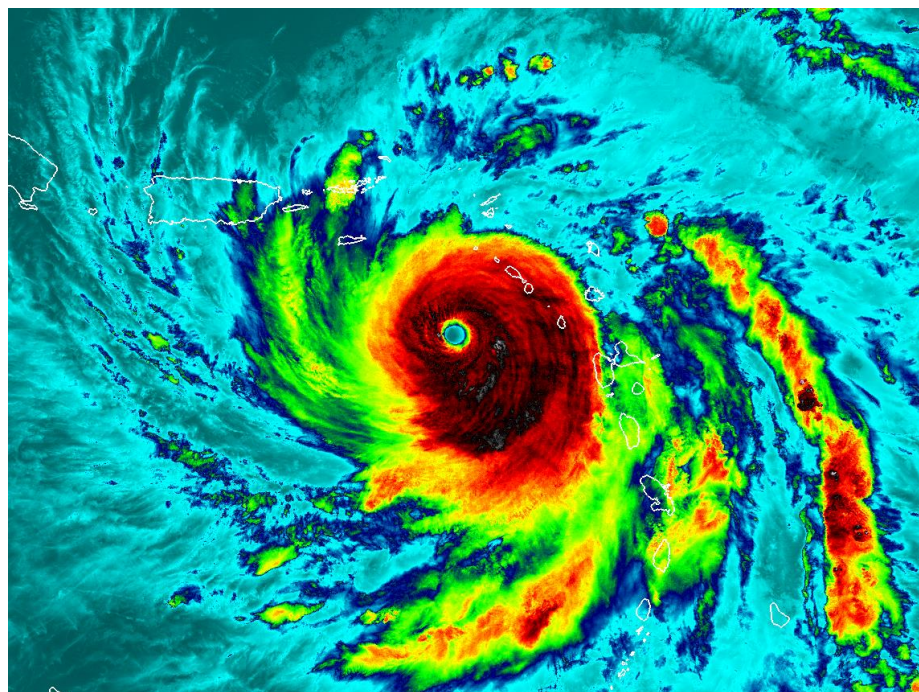


Figure 2.2: Satellite image of Hurricane Maria nearing peak intensity (Pasch, Penny, & Berg, 2019)

Maria's estimated landfall wind speed at Puerto Rico was an extrapolation of the weakening trend of Maria noted by an aircraft report after the eye replacement several hours earlier (Pasch, Penny, & Berg, 2019). Figure 2.3 shows the maximum sustained and gust wind speeds measured in Puerto Rico for hurricane Maria. Two important factors to consider are that (1) several instruments failed during the hurricane and (2) the measurements may have been made at terrains or heights that differ from the standards of 33-ft height and flat open terrain (FEMA, 2018).

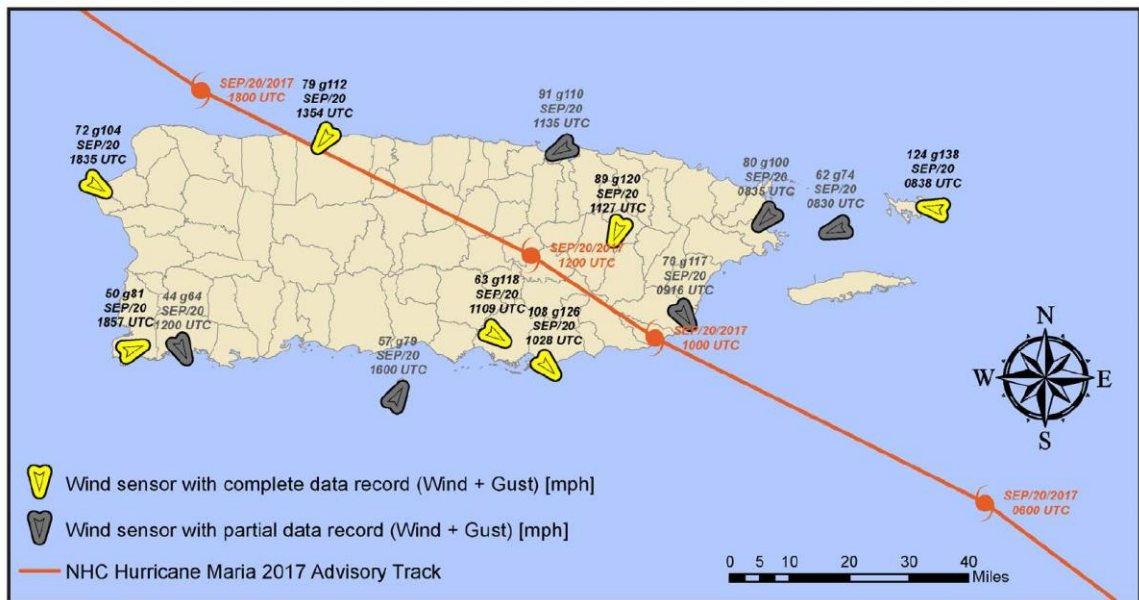


Figure 2.3: Hurricane Maria sustained and gust speed measurements (FEMA, 2018)

As the hurricane approached Puerto Rico, the main meteorological tool available to track and gather information was the San Juan WSR-88D doppler radar. The weather radar, operated by the Federal Aviation Administration and the National Weather Service, was designed for a 134 mph (60 m/s) wind speed (NEXRAD , 1996). The radar was functional until 0950 UTC on September 20, thereafter the radar was damaged and destroyed (see Figure 2.4) before Maria made landfall in Puerto Rico.



Figure 2.4: San Juan radar pre and post hurricane Maria (Climate.gov, 2018)

2.2 Ground-Mounted Breakaway Signs (GMBS)

The regulation, specifications and all the aspects of traffic signs in the United States are defined by the Federal Highway Administration (FHWA). The FHWA is a division of the United States Department of Transportation. The general document defining highway signs is the *Manual on Uniform Traffic Control Devices* (MUTCD) by the FHWA. The MUTCD contains general standards and guidelines on how traffic signs are designed, installed, and utilized. In the United States all traffic signs or traffic control devices must legally conform to these standards as defined in the MUTCD.

The origin of the breakaway signs required features has its roots in the *Report 350: Recommended Procedures for the Safety Performance Evaluation of Highway Features* by the National Cooperative Highway Research Program (NCHRP) published in 1989. Additionally, because of changes in transportation vehicles throughout the years, all devices that are to be placed on roadways must be tested according to the *Manual for Assessing Safety Hardware* (MASH) by the FHWA. The majority of the design standards

outlined in the MUTCD were developed by the American Association of State Highway and Transportation Officials (AASHTO).

The current standard by AASHTO that regulates breakaway signs is the *LRFD Specifications for Structural Supports for Highway Signs, Luminaires, and Traffic Signals*. As previously mentioned, the term breakaway refers to signs that are designed to yield when impacted by a vehicle. The method of yielding may be a fracture component, a plastic hinge, a slip plane, or a combination of these. The criteria used to determine if a yielding mechanism is considered a breakaway system is defined in the MASH.

The road system in Puerto Rico is composed of approximately 9,000 miles of paved roads, and it is divided into primary, primary urban, secondary, and tertiary roads, as shown in Figure 2.5. Throughout the road system in Puerto Rico, there are thousands of traffic signs of different geometries, colors, and sizes alongside roads and highways providing crucial information to the drivers. Of the many types of ground-mounted breakaway signs, the focus of this report is the double I-beam post as shown Figure 2.6, and the single I-beam post as shown in Figure 2.7.

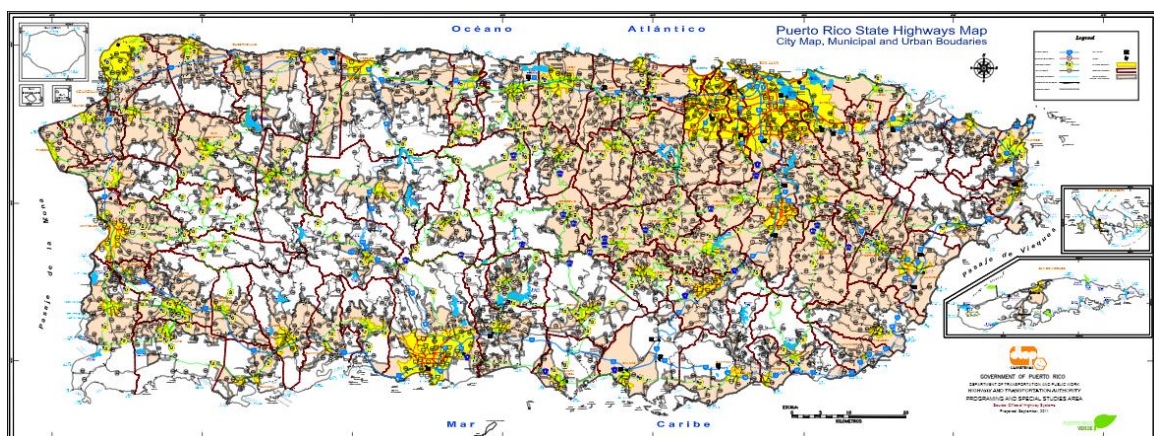


Figure 2.5: Puerto Rico road system (PRDOT, 2011)



Figure 2.6: Dual post ground-mounted breakaway sign



Figure 2.7: Single post ground-mounted breakaway sign (Source: Google Maps)

The objective of the breakaway design feature is to reduce the damage to the vehicle in the event it impacts a sign structure (AASHTO, 2011), therefore protecting the life of the passengers of the impacting vehicle. As seen in Figure 2.8, breakaway signs have three main components that are designed to minimize the resistance to impact: (1) the fuse and hinge plates, (2) the upper and lower beams forming the single post design, and (3) the breakaway base plate. The fuse plate (see example in Figure 2.9) and the hinge plate (see example in Figure 2.10) vary in geometry, depending on the size of the sign and the post utilized. As a vehicle impacts one of the signs posts, the perforated fuse plate yields and fractures, the breakaway base allows the post to slide backwards, and the hinge plate bends backwards allowing the post to rotate, as shown in Figure 2.11 and Figure 2.12.

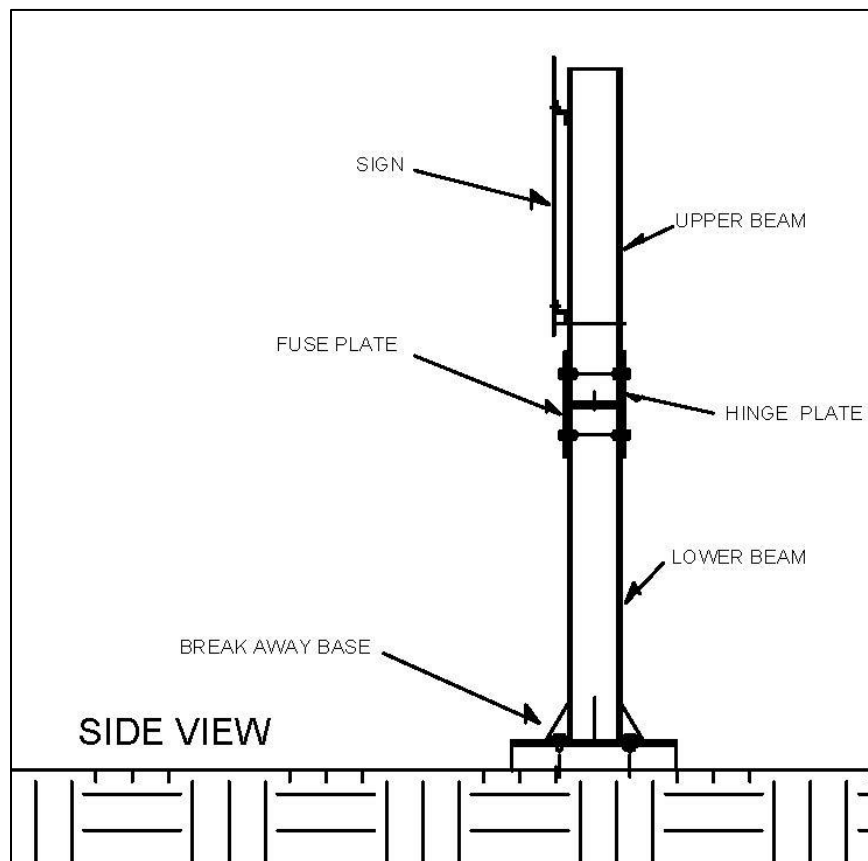


Figure 2.8: Side view of the main components of a breakaway sign



Figure 2.9: Fuse plate



Figure 2.10: Hinge plate

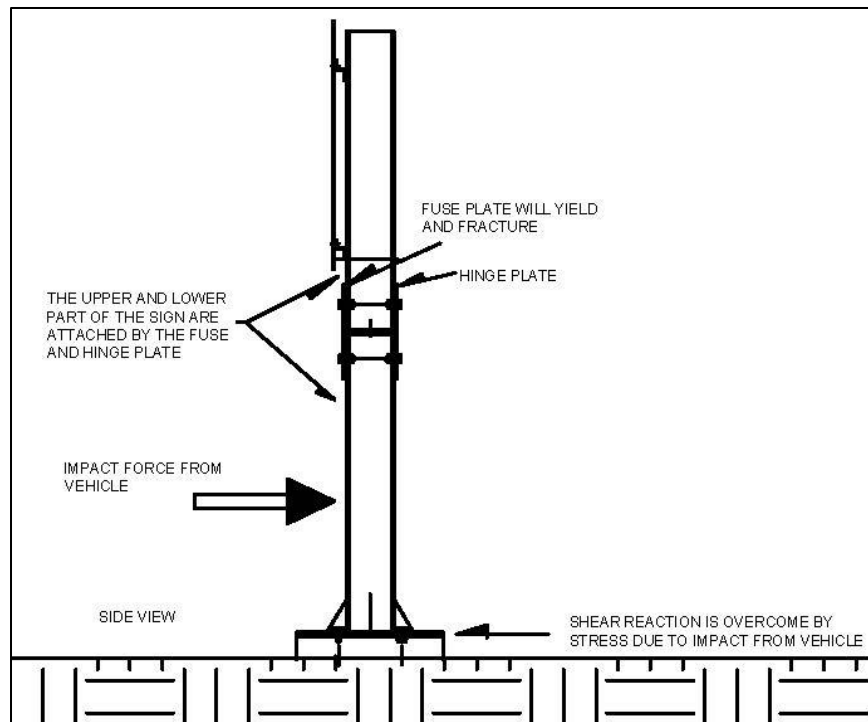


Figure 2.11: Acting elements of a breakaway sign

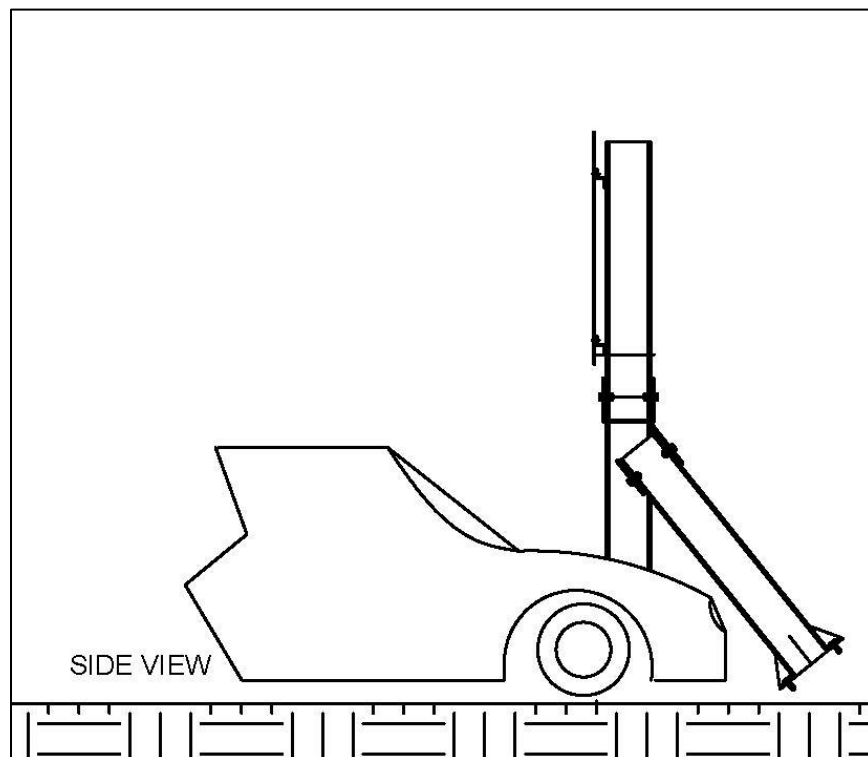


Figure 2.12: Breakaway mechanism activated

Figure 2.13 illustrates a unidirectional slip base, meaning the breakaway post is designed to be impacted in one general direction, or parallel to the direction of vehicular flow. There are other types of slip bases for the breakaway system. For example, the multidirectional slip base design, conceptually acts like the unidirectional slip base without regards to the direction of the impact (AASHTO, 2011).



Figure 2.13: Breakaway base for unidirectional impact

From 1999 to 2000, the Department of Transportation and Public Works of Puerto Rico (PRDOT) released standard drawings regarding the ground-mounted breakaway signs. Some sections of those drawings are reproduced here. Figure 2.14 shows Z-beams being denoted as “wind beams” to connect signs to posts. Table 2.1 is used to determine the required number and section of breakaway posts and wind beams. The geometry of the fuse and hinge plates are presented in Figure 2.15, Figure 2.16 and Table 2.2. The assembly of the fuse and hinge plates is presented in Figure 2.17.

It should be pointed out that breakaway systems are not always required. As an alternative, structural supports of signs may be protected with guardrails or other barriers (AASHTO, 2015).

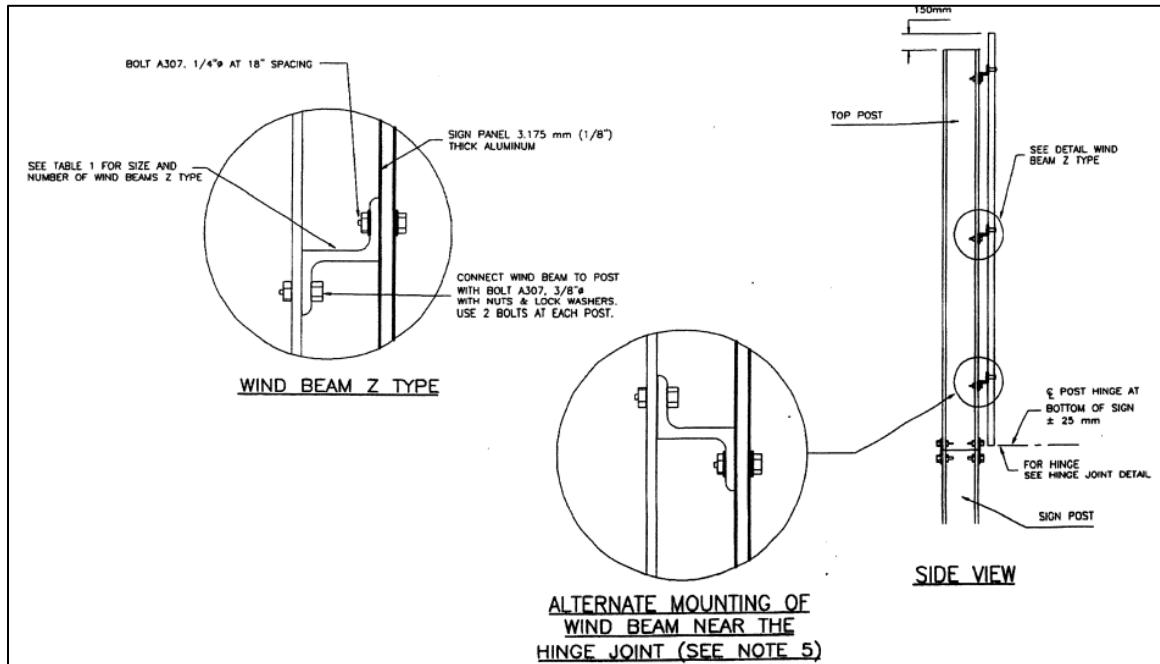


Figure 2.14: Sign to post connections using wind beams (PRDOT, 2000)

Table 2.1: Number and size of breakaway posts and wind beams (PRDOT, 2000)

HEIGHT OF SIGN FT (MTS) *	NUMBER OF WIND BEAMS	1 POST			2 POST		3 POST
		WIND BEAM Z 4 x 2.85			WIND BEAM Z 4 x 2.85		WIND BEAM Z 3 x 2.33
		SIGN LENGTH FT (MTS)*			SIGN LENGTH FT (MTS)*		SIGN LENGTH FT (MTS)*
4' (1.22)	2	4' (1.22)	8' (2.44)	13.8' (4.21)**	16' (4.86)	22.5' (4.86)	28' (8.54)
8' (2.44)	3	W 6 x 12	W 6 x 12	W 8 x 18	W 6 x 12	W 8 x 18	W 6 x 12
12' (3.66)	4	W 6 x 12	W 8 x 18	W 10 x 33	W 8 x 18	W 10 x 22	W 10 x 22
16' (4.88)	5	W 8 x 18	W 10 x 33	W 12 x 40	W 10 x 33	W 10 x 33	W 10 x 33
20' (6.10)	6	W 10 x 22	W 12 x 40	W 12 x 53	W 12 x 40	W 12 x 53	W 12 x 40
		W 10 x 33	W 12 x 53	W 12 x 53	W 12 x 53	W 12 x 53	W 12 x 53

* THE CONTRACTOR SHALL USE THE NUMBER OF POSTS AND POST SIZE TABULATED FOR A SIGN PANEL LENGTH (L) AND FOR A SIGN PANEL HEIGHT (H) EQUAL TO OR GREATER THAN THE ACTUAL SIGN PANEL LENGTH (L) AND SIGNPANEL HEIGHT

** MAXIMUM LENGTH FOR THE NUMBER OF POSTS SHOWN

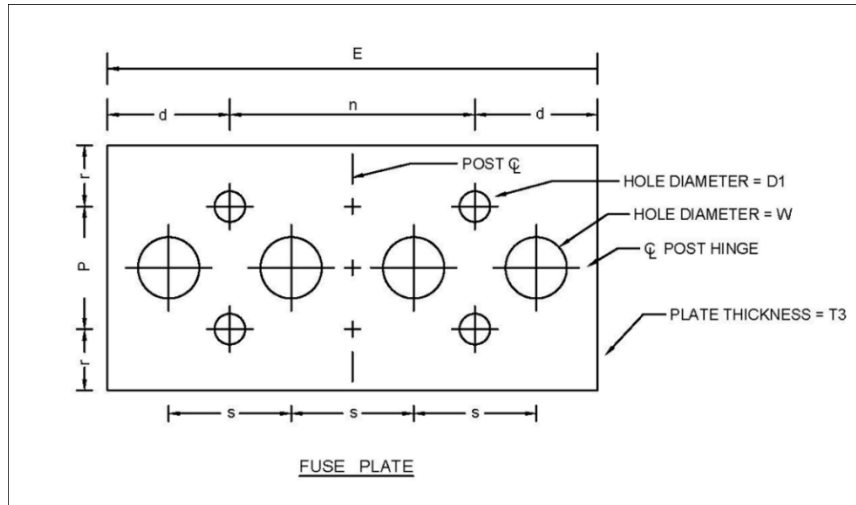


Figure 2.15: Fuse plate geometry (PRDOT, 2000)

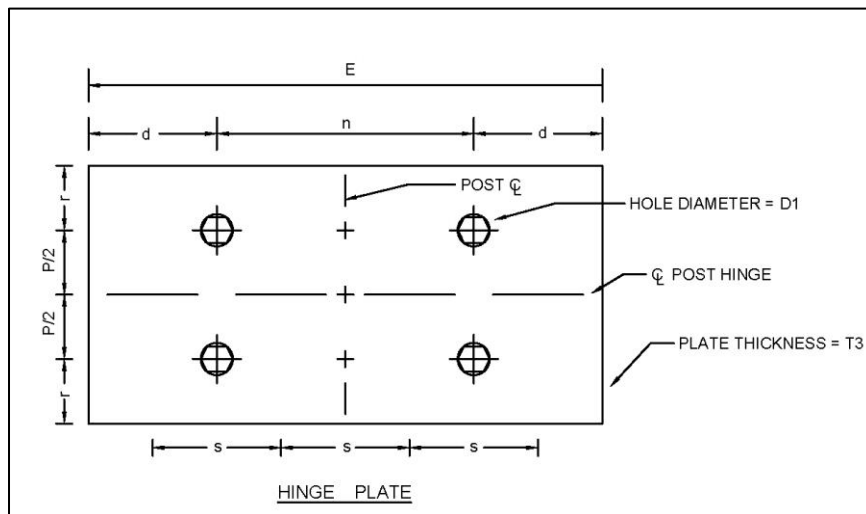


Figure 2.16: Hinge plate geometry (PRDOT, 2000)

Table 2.2: Fuse and hinge plates data (PRDOT, 2000)

POST SECTION	BOLT SIZE (IN.)	E (IN.)	P (IN.)	D1 (IN.)	d (IN.)	n (IN.)	r (IN.)	s (IN.)	T3 (IN.)	W (IN.)
W6 x 12 W8 x 15 W10 x 17	5/8 ϕ	4 5/16	2 15/16	11/16	1 1/8	2 1/16	1 1/16	1	1/4	13/16
W8 x 18 W10 x 22	3/4 ϕ	5 1/2	3 3/4	13/16	1 1/2	2 1/2	1 3/8	1 3/16	3/8	1 1/16
W10 x 33 W12 x 40	1 1/8 ϕ	8 1/4	5 11/16	1 3/16	2 3/16	3 7/8	2 3/16	1 15/16	1/2	1 11/16
W12 x 53	1 1/2 ϕ	10 3/4	7 1/3	1 9/16	2 13/16	5 1/8	2 5/8	2 1/2	1/2	2

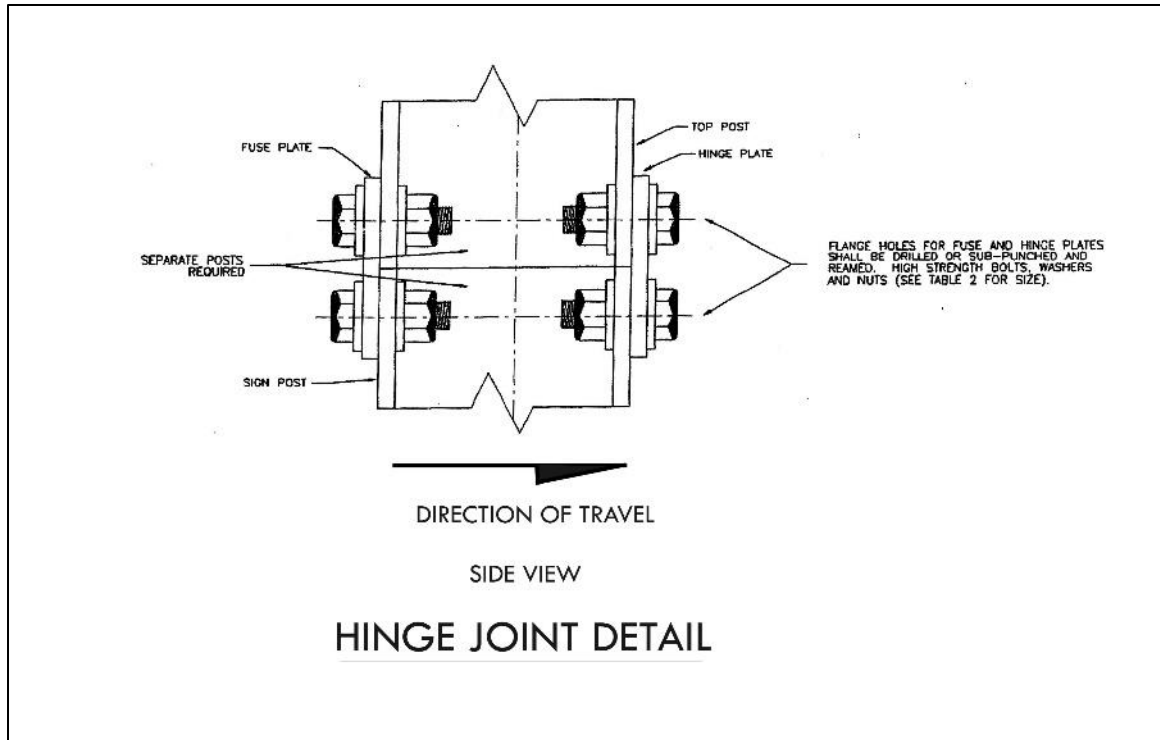


Figure 2.17: Hinge joint detail for the ground mounted breakaway post (PRDOT, 2000)

2.3 Wind Loads on Signs

In the U.S., there are two references that are the most widely used for the calculation of wind loads on signs and their supporting structures. These are:

- *LRFD Specifications for Structural Supports for Highway Signs, Luminaires, and Traffic Signals* by AASHTO, for which the first edition was published in 2015. This edition was based on previous editions that used the ASD methodology instead of the LRFD methodology.
- *Minimum design loads and associated criteria for buildings and other structures* (ASCE Standard ASCE/SEI 7-16) by ASCE.

The wind loads section of AASHTO Specifications is based on previous versions of the ASCE 7 Standard, so in fact both documents offer similar procedures for the calculation of wind loads on signs.

In the AASHTO Specifications, the design wind pressure in pounds per square foot (psf) is calculated as:

$$P_z = 0.00256K_zK_dGV^2C_d \quad (2-1)$$

where:

K_z = height and exposure factor

K_d = directionality factor

G = gust effect factor

V = basic wind speed in miles per hour

C_d = drag coefficient

Meanwhile, in the ASCE Standard, the design wind force in pounds (lb) is calculated as:

$$F = 0.00256K_zK_{zt}K_dK_eGV^2C_fA_s \quad (2-2)$$

where:

K_{zt} = topographic factor

K_e = ground elevation factor

C_f = net force coefficient

A_s = gross area of sign in ft²

The two main differences between the AASHTO and ASCE procedures that may lead to significant differences in the calculation of wind loads are:

- The Gust Effect Factor (G): The ASCE 7 Standard offers a procedure to calculate G in accordance with the fundamental frequency of the structure. Meanwhile, the AASHTO Specifications indicates that the ASCE 7 states that all structures with a fundamental frequency of 1 Hz or with a height to least

horizontal dimension ratio greater than 4 should be considered wind-sensitive, and since most of the structures covered by the specification meet the second criteria, the minimum value of G that may be used is 1.14.

- AASHTO's Drag Coefficient (C_d) vs ASCE's Force Coefficient (C_f): For rectangular signs, the determination of C_d is based only on the dimensions of the sign. Meanwhile, the determination of C_f requires the sign dimensions plus its elevation with respect to the ground.

Other differences are the inclusion of the topographic factor (K_{zt}) and the ground elevation factor (K_e) in the ASCE 7 Standard, but not on the AASHTO Specifications, which may also lead to significant differences for signs not located on flat terrain or for signs located at high elevations above sea level, respectively. Additionally, although the AASHTO Specification only considers a uniform pressure acting over the sign, the ASCE 7 Standard considers three different cases (as shown in Figure 2.18):

- Case A: Resultant force acting on the sign's geometric center.
- Case B: Resultant force acting at a distance e from the geometric center.
- Case C: The total area of the sign is divided into segments and a resultant force is calculated for each segment.

Summarizing, in terms of wind loads calculations, the ASCE Standard is not only the basis for the AASHTO Specifications, but it also considers more variables and is more detailed. Therefore, the ASCE approach is considered to be most advanced and comprehensive than the AASHTO method.

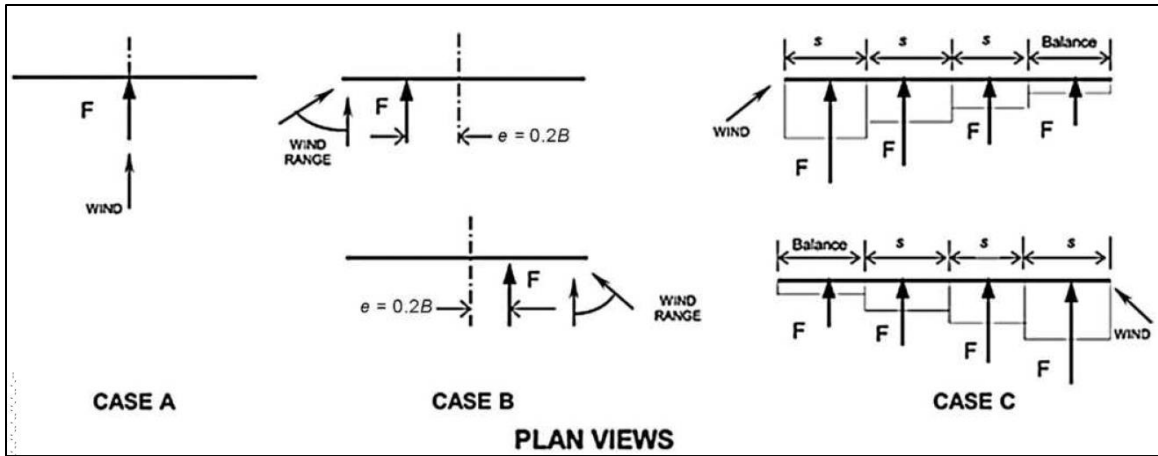


Figure 2.18: Wind loads on sign cases required by ASCE 7 (ASCE, 2017)

3 Research Program

In this chapter, the program for this research project is presented, including the objectives, scope, and methodology.

3.1 Objectives and Scope

The objectives of this research were to:

- Estimate the gust wind speeds that caused damages on guide traffic sign mounted on I-beams.
- Suggest improvements to the design and construction of guide traffic sign mounted on I-beams to increase their resiliency by avoiding or reducing the risk of failure in future extreme weather events.

In this study, only signs mounted on I-beams with breakaway systems that failed due to the winds of Hurricane Maria in Puerto Rico were considered.

3.2 Methodology

During the first stage of this research, some of the main highways of Puerto Rico were travelled to locate failed traffic signs, inspect them, and determine the mode of failure. Three modes were identified: foundation failure, slippage failure, and fuse plate fracture. Some cases presented a combination of these modes of failures.

For cases involving fuse plate rupture, the appropriate failure mechanism was identified and analyzed to estimate the wind speed that caused the damage. Three case studies of fuse plate failure were selected, for which field measurements were collected. For two of the cases, the ruptured fuse plates were acquired and used to obtain specimens that were tested in tension, determining the ultimate stress of the material.

Afterwards, the structures were analyzed to estimate the wind pressure that caused the failures on them. Then, these wind pressures were used to estimate the corresponding 3-second gust speed at 33 feet height for open terrain by applying the wind load provisions of ASCE/SEI 7-16. These estimates were then compared with estimates from other studies.

Finally, suggestions on how to improve the resiliency of these sign structures were developed.

4 Field Inspection

Puerto Rico's primary highways were traveled to locate signs mounted on I-beams with breakaway systems that failed during Hurricane Maria. This chapter presents the location of the failed sign structures, and the three modes of failure were identified.

4.1 Geolocation of Documented Cases

Twelve cases of failed signs mounted on I-beams with breakaway systems were geolocated and documented. Table 4.1 indicated the location of the twelve cases and their mode of failure. As it can be seen in the table, three modes were identified: foundation failure, slippage failure, and fuse plate fracture. Also, some signs were classified as having an undetermined failure mode, as they presented a combination of modes, negating the possibility of definitively determining which mode acted first. The failure modes are explained in the following section.

Also indicated in Table 4.1 is if each sign is protected by a guardrail. It can be seen in the table that, out of the twelve cases documented for this project, nine structures were protected by guardrails. Still, all twelve cases had breakaway systems. The reader should recall that breakaway systems are not required if the sign structure is protected by a guardrail or another type of barrier.

The location of twelve cases is presented in Figure 4.1. In the figure, the red line represents the path of Hurricane Maria, and the three red markers correspond to signs that were selected as case studies for their mode of failure, which was fuse plate fracture. The green markers correspond to cases that were not selected as case studies because they had other different modes of failures.

Table 4.1: Signs geolocated and documented

ID	Latitude	Longitude	Failure Mode	Protected by guardrail
Case 1	18° 8'10.53"N	65°49'40.19"W	Fuse plate fracture	No
Case 2	18°14'58.21"N	65°58'5.16"W	Fuse plate fracture	No
Case 3	18°15'56.68"N	66° 2'21.25"W	Fuse plate fracture	Yes
Sign 4	17°59'10.45"N	66°36'14.29"W	Slippage failure	Yes
Sign 5	17°59'8.99"N	66°36'0.12"W	Foundation failure	Yes
Sign 6	17°59'17.82"N	66°36'56.50"W	Foundation failure	Yes
Sign 7	18° 4'9.58"N	66°13'6.58"W	Slippage failure	Yes
Sign 8	17°59'30.31"N	66°18'3.13"W	Undetermined	Yes
Sign 9	18° 7'1.50"N	66° 8'6.19"W	Slippage failure	Yes
Sign 10	18° 7'16.54"N	65°49'13.93"W	Undetermined	Yes
Sign 11	18°21'55.76"N	66° 4'11.51"W	Undetermined	Yes
Sign 12	18° 8'42.84"N	66° 6'18.86"W	Undetermined	No

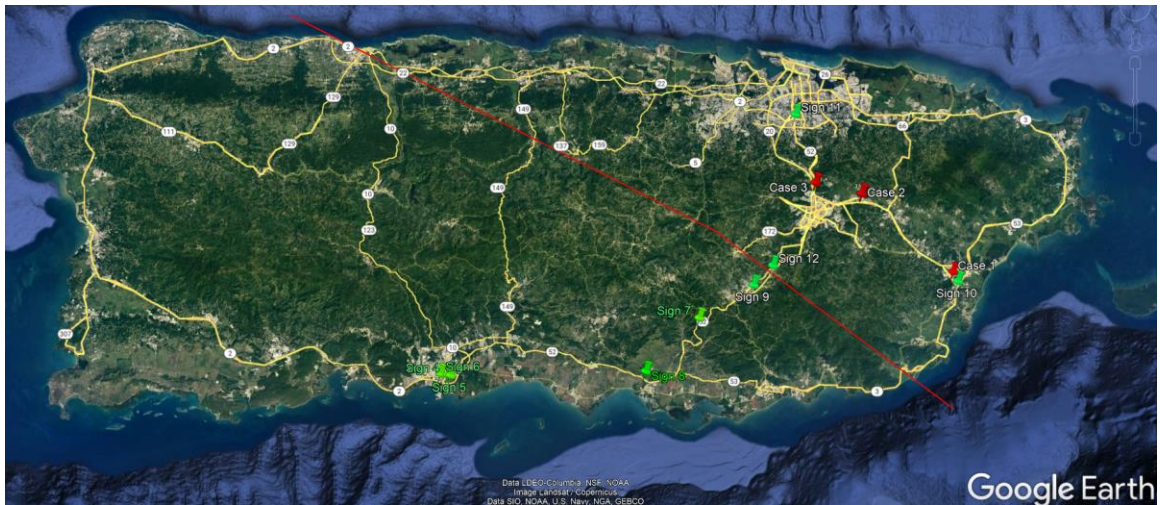


Figure 4.1: Location of documented cases (adapted from Google Earth Pro)

4.2 Traffic Sign Failures

Three modes of failures were identified: foundation failure, slippage failure, and fuse plate fracture. These modes of failure are covered in this section.

4.2.1 Foundation Failure

Foundation failure occurs when none of the structural members on top of the foundation initially failed under the wind loads, but one or more of the posts overturns. The overturn could be due to the foundation not being deep enough, to the foundations not being adequately constructed, to the soil being significantly weakened due to the heavy rainfall of a hurricane, or to a combination of these factors. Sign 6, presented in Figure 4.2, was a case of foundation failure in which one of the posts started to overturn. Meanwhile, Sign 5 was another case of foundation failure in which the structure collapse due to the overturning of both posts, as presented in Figure 4.3.



Figure 4.2: Foundation failure of Sign 6



Figure 4.3: Foundation failure of Sign 5

4.2.2 Slippage Failure

During this project it was found that, sometimes, a fuse plate different from the one shown in Figure 2.15 is used. Instead, a slotted fuse plate is employed. Plate slippage occurs when the bolts holding the slotted fuse plate together to the upper and lower part of the post are loosened, probably due to the effects of cyclic loading caused by the wind or the frictional resistance being exceeded. Once this slotted fuse plate is loosened, the upper post is only being supported by the hinge plate, which eventually causes the hinge plate to bend. This was the mode of failure of Sign 9, shown in Figure 4.4. Notice in this figure that the slotted fuse plate is undamaged, while the hinge plate is bend.

Similarly, Sign 7 was another case of slotted fuse plate slippage, as shown in Figure 4.5. This time, the hinge plate was ruptured, probably because the upper beams are shorter than the lower beams.

Slippage failure may also be caused by the cyclic wind loading causing the bolts connecting the post to the base to become loosened. This appears to have been the case of

Sign 12. As shown in Figure 4.6, this was a dual post for which the bolts at the base of one of the posts became loosened, causing this post to be blown off its base.

Another case of slippage failure at the base of the posts was Sign 4, as shown in Figure 4.7. It can be noticed in the figure that the breakaway base support is partially deformed.



Figure 4.4: Slotted fuse plate slippage failure of Sign 9



Figure 4.5: Slotted fuse plate slippage failure of Sign 7



Figure 4.6: Sign 12 before (top left; Source: Google Earth Pro) and after failure



Figure 4.7: Slippage failure at the base of Sign 4

4.2.3 Fuse Plate Fracture

Fuse plate fracture occurs when the wind loads on the sign cause the fuse plate to fail in tension, which eventually leads to the bending of the hinge plate, like the case shown in Figure 4.8. It was determined that this mode of failure has a mechanism that allows the estimation of wind speed. Therefore, they were selected as case studies. As previously mentioned, three cases of fuse plate fracture were documented as the three red markers depicted in Figure 4.1 and denoted as Cases 1, 2, and 3 in Table 4.1. It can be noted in Figure 4.1 that the three case studies were at some point located in the right front quadrant of the hurricane, which is the quadrant with the strongest winds. The three case studies are discussed in more detail in the following chapter.



Figure 4.8: Fuse plate rupture of Case 2

4.2.4 Undetermined Cases

Three of the twelve documented cases presented a combination of mode of failures. Most probably, one of the modes acted first, making that mode the main culprit of the failure. Still, because the failed structure showed a combination of modes, it cannot be conclusively determined which mode acted first.

Sign 8, demonstrated a combination foundation failure and fuse plate rupture, as shown in Figure 4.9. It is probable that one of the posts had a foundation failure that lead to the other post having fuse plate rupture.

Sign 10, shown in Figure 4.11, experienced a combination of slotted fuse plate slippage and foundation failure. This case did not have a hinge plate, nor were the posts cut into lower and upper beams. Instead, for each post, the web and one of the flanges of the wide-flange section were cut, with the uncut flange acting as the hinge plate.

Sign 11 was dual post sign for which only one post was left partially standing after the hurricane, as shown in Figure 4.11. The partially standing post experienced fuse plate rupture, while the fallen post experienced foundation failure or slippage failure.



Figure 4.9: Undetermined mode of failure of Sign 8



Figure 4.10: Undetermined mode of failure of Sign 10



Figure 4.11: Sign 11 before and after failure (Source: Google Maps)

5 Case Studies

Three identified signs that failed due to fuse plate rupture were selected as case studies to be analyzed for wind speed determination. This chapter presents first the analysis procedure followed to determine the wind speed at failure. Afterwards, each case study is presented, including the estimated wind speed at failure.

5.1 Failure Model Analysis

The model adopted for the failure mechanism consists in a static moment equilibrium about the hinge plate, between the wind pressure over the sign (which produces the overturning moment), and the tension stresses on the fuse plate (which produced the restoring moment). This model, presented in Figure 5.1, is consistent with the model of other authors (Pfeifer, 1993; Paulsen, Pfeifer, Holloway, & Reid, 1995). The nomenclature for this model is as follows:

S = sign height

B = sign width

$A_s = B S$ = area of the sign

h = height of top of sign above ground

d_t = moment arm of the tension force, from the edge of the I-beam to the center of the rupture fuse plate; equals the depth of the W-section (d) plus the half of the width of the fuse plate ($t/2$)

d_w = moment arm of the wind pressure, from the rupture plane to the center of the sign

A_t = total area in tension of the fuse plate in the rupture plane; equals the addition of the thickness of the fuse plate (t) times the net width of the fuse plate at the rupture plane (b_n)

P_w = wind pressure on the sign

F_w = total wind force on the sign; equivalent to F in Equation (2-2)

F_u = tensile ultimate strength of fuse plate steel

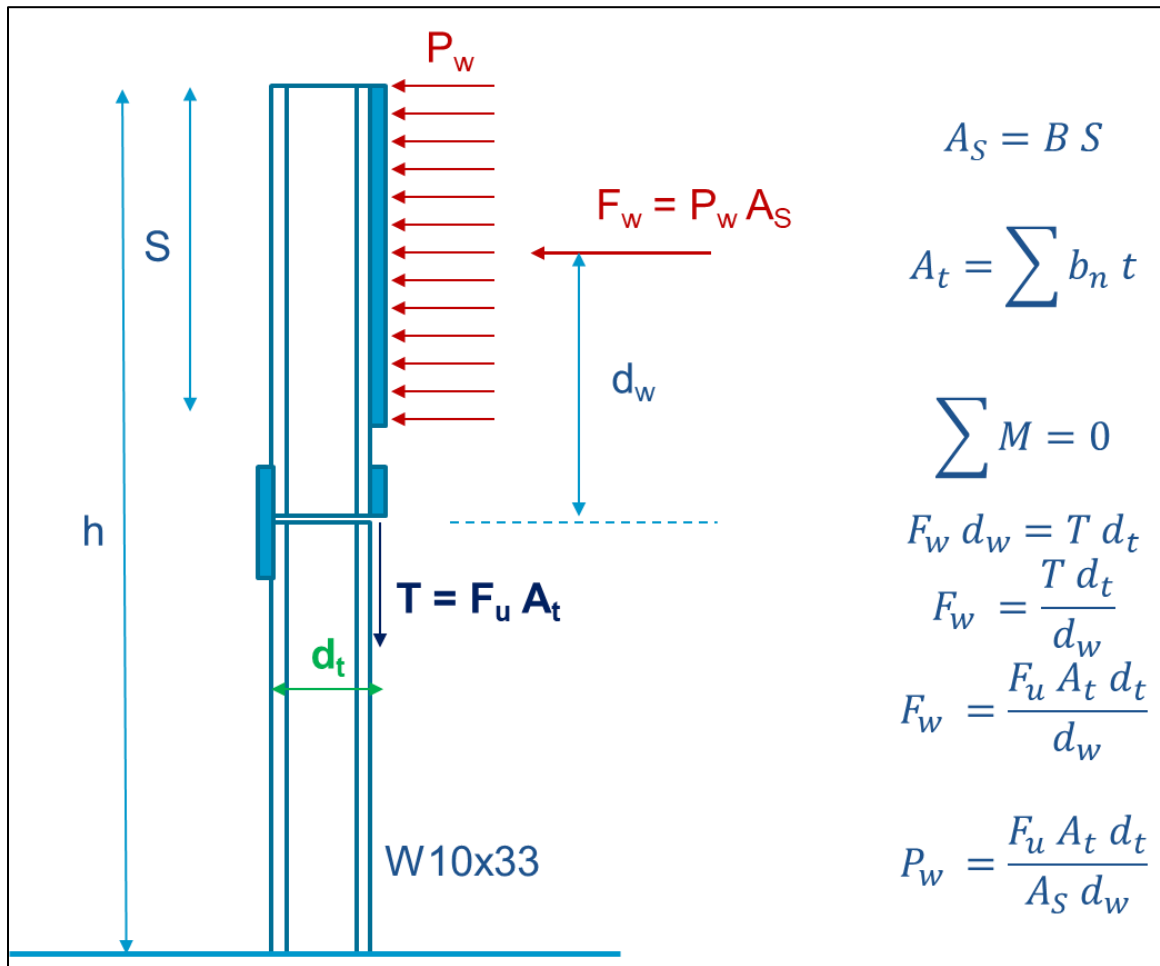


Figure 5.1: Failure model for determination of wind speed

For the model, the flexural capacity of the hinge plate was disregarded, even though it remained connected. The gravitational load of the different elements was also disregarded.

A uniform wind pressure on the sign was assumed, which is consistent with Case A of the ASCE 7 Standard, as discussed in Section 2.3.

Following the ASCE 7 Standard, from Equation (2-2), the wind pressure on the sign can be computed as:

$$P_w = \frac{F}{A_s} = 0.00256K_zK_{zt}K_dK_eGV^2C_f \quad (5-1)$$

The case studies of this project are located in flat terrain, therefore $K_{zt} = 1$, as verified by comparing ASCE-7 wind speed maps with ATC Hazard by Location website, for which the later includes the effects of topographic wind speed-up for Puerto Rico. Also, considering the effect of the ground elevation above sea level of the sign location would yield higher wind speed estimates, therefore $K_e = 1$ was conservatively assumed. Finally, since K_d is a factor that considers the reduced probability of maximum winds coming from any given direction and of the maximum pressure coefficient occurring for any given wind direction, it was also conservatively assume to be equal to one. Therefore, for this project, Equation (5-1) reduces to:

$$P_w = 0.00256K_zGV^2C_f \quad (5-2)$$

Making Equation (5-2) equal to the P_w equation derived in Figure 5.1, and solving for the wind speed, the following formula is obtained:

$$V = \sqrt{\frac{F_u A_t d_t}{0.00256K_zGC_f A_s d_w}} \quad (5-3)$$

Equation (5-3) can then be used to estimate the 3-second gust speed (in mph) at the standardized height of 33 ft that caused the failure of the sign.

5.2 Case 1

Case 1, as shown in Figure 5.2, was a guide sign supported by dual W10x33 posts of galvanized steel. The main sign had attached a smaller exit number sign. The sign was located on highway PR-30 at km 28.3, at coordinates 18°8'10.53"N, 65°49'40.19"W (see Figure 5.3). Figure 5.4 shows relevant field measurements taken of the sign structure.



Figure 5.2: Case 1

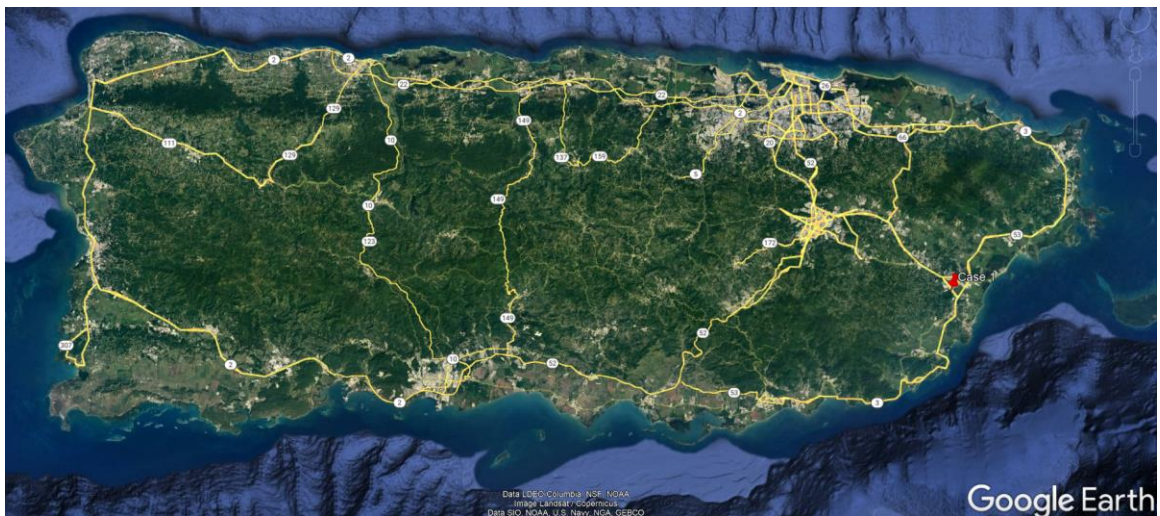


Figure 5.3 Case 1 location (adapted from Google Earth)

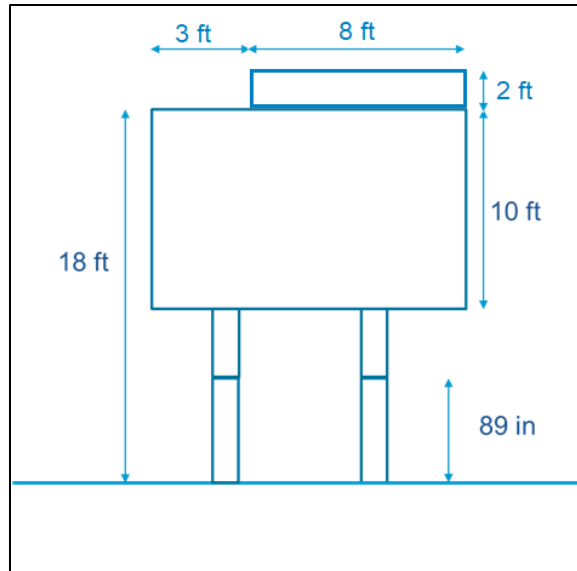


Figure 5.4: Case 1 dimensions

For this case, the two rupture fuse plates were retrieved from the posts, one of which is shown in Figure 5.5. Afterwards, the rupture fuse plates were carefully measured to determine the total tension area in the rupture plane (A_t); including both plates, it was estimated that $A_t = 1.6763 \text{ in}^2$.



Figure 5.5 Fuse plate retrieved from Case 1

Out of these plates, tension test specimens were cut using a Flow Mach2 waterjet machine, as seen in Figure 5.6(a). Afterwards, tension tests were conducted on the specimens using an Instron 300DX machine, as seen in Figure 5.6(b). Figure 5.6(c) shows some of the specimens after being tested. Calculating the average of the tension tests results presented in Table 5.1, it was assumed that the fuse plates were made of steel with an ultimate strength of $F_u = 63,963$ psi.

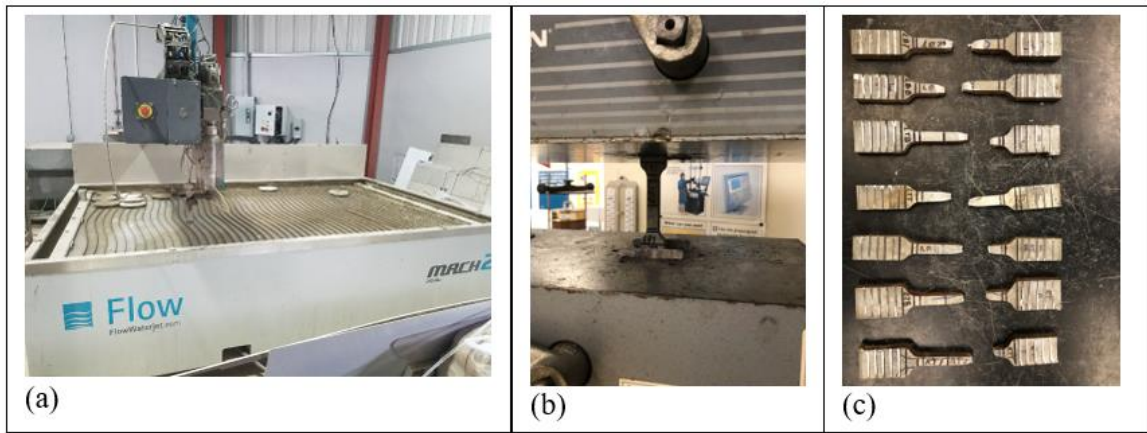


Figure 5.6: (a) Waterjet cutting machine, (b) specimens tension tested, and (c) rupture specimens.

Table 5.1: Case 1 fuse plate tensile test results

Specimen ID	Ultimate Stress F_u (psi)
LTT	68604
LTB	62051
LBB	67488
LBT	66530
RTB	59012
RBB	62322
RBT	61734

Case 1 was evaluated considering two scenarios:

- Scenario A: The smaller exit number sign attached to the main sign was disregarded, as shown in Figure 5.7.

- Scenario B: The smaller exit number sign was included in the analysis. The area of the exit number sign was computed, then divided by the width (B) of the main sign. The resulting value was added to the height of the main sign to use this as H , as shown in Figure 5.8. The result is an equivalent sign with the same total area of the main sign plus the exit number sign but disregarding small eccentricities. This was done because the ASCE 7 Standard does not offer guidance for the combination of signs.

Again, given the flexibility of the connections of the smaller signs to the main sign, the wind speed that caused the failure is probably between the estimates of the two scenarios.

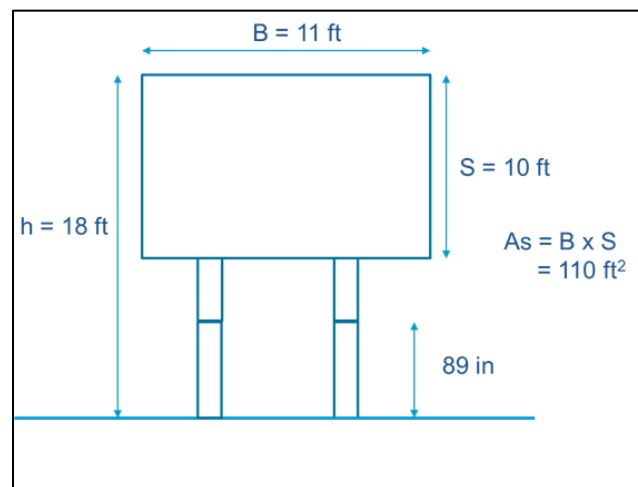


Figure 5.7 Case 1, Scenario A

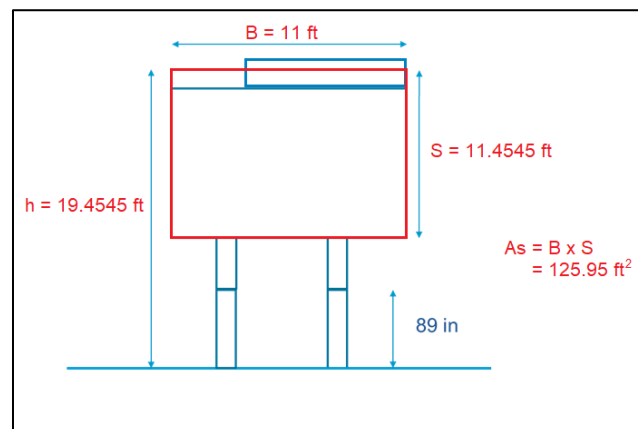


Figure 5.8: Case 1, Scenario B

5.3 Case 2

Case 2, as shown in Figure 5.9 (and previously shown in Figure 4.8), was also a guide sign supported by dual W10x33 posts of galvanized steel and a smaller exit number sign attached to the main sign. The sign was located on highway PR-30 at km 7.8, at coordinates $18^{\circ}14'58.21''\text{N}$, $65^{\circ}58'5.16''\text{W}$ (see Figure 5.10). Figure 5.11 shows relevant field measurements taken of the sign structure.



Figure 5.9: Case 2

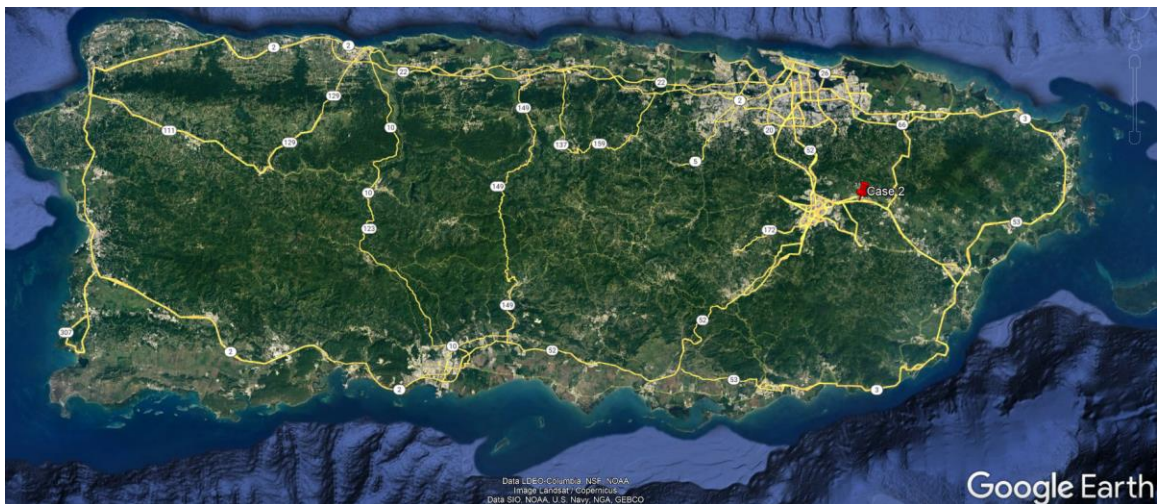


Figure 5.10: Case 2 location (adapted from Google Earth)

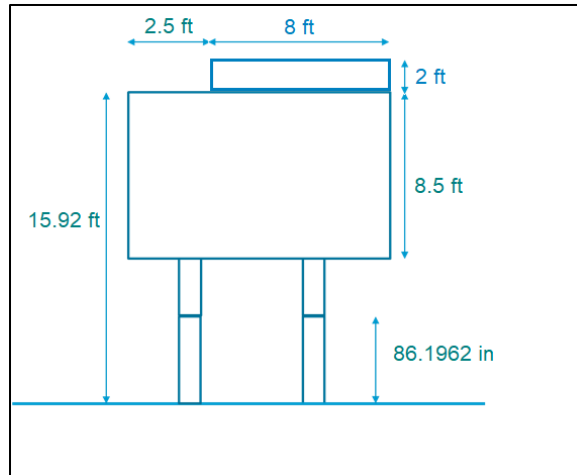


Figure 5.11: Case 2 dimensions

For this case, the two rupture fuse plates were not retrieved. The fuse plates were carefully field measured to determine the total tension area in the rupture plane (A_t); including both plates, it was estimated that $A_t = 1.414 \text{ in}^2$. It was assumed that the plates were made of the same steel of Case 1 with an ultimate strength of $F_u = 63,963 \text{ psi}$.

Case 2 was also evaluated considering two scenarios:

- Scenario A: The smaller exit number sign attached to the main sign was disregarded, as shown in Figure 5.12.
- Scenario B: The smaller exit number sign was included in the analysis, as shown in Figure 5.13.

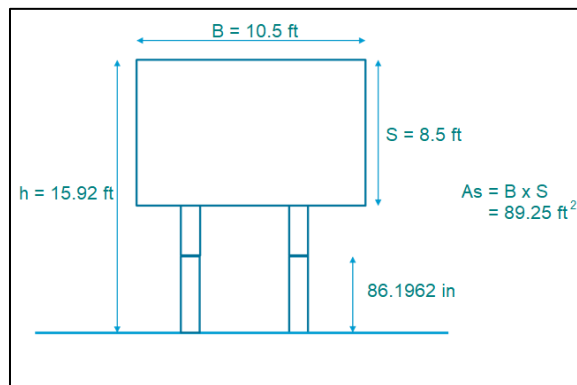


Figure 5.12 Case 2, Scenario A

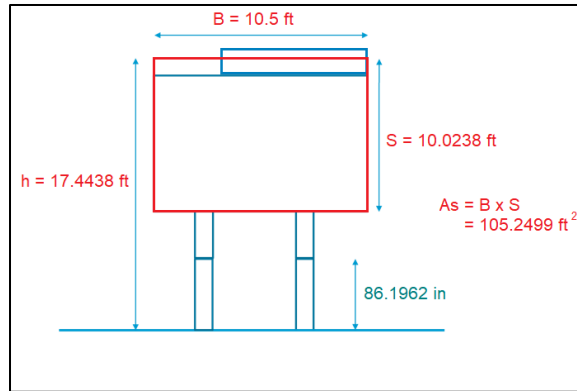


Figure 5.13: Case 2, Scenario B

5.4 Case 3

Case 3, as shown in Figure 5.14, consisted of a single W10x33 posts of galvanized steel supporting eleven small signs of assorted sizes. The structure was located on highway PR-1 at km 31.4, at coordinates $18^\circ 15' 56.68''\text{N}$, $66^\circ 2' 21.25''\text{W}$ (see Figure 5.15). Figure 5.16 shows relevant field measurements taken of the structure.

For this case, the rupture fuse plate was retrieved from the post. Afterwards, the rupture fuse plates were carefully measured to determine the tension area in the rupture plane (A_t); it was estimated that $A_t = 0.75 \text{ in}^2$.



Figure 5.14: Case 3

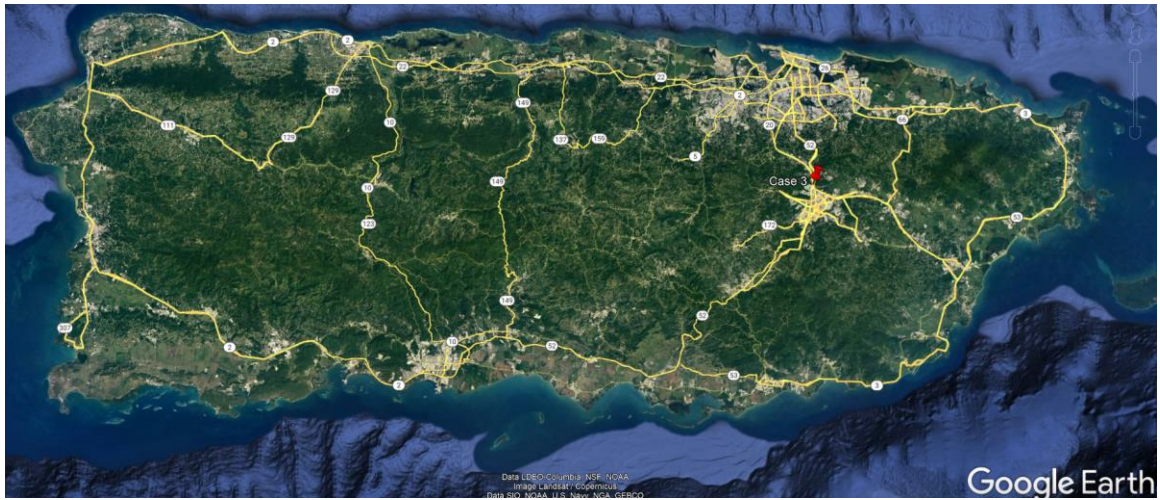


Figure 5.15: Case 3 location (adapted from Google Earth)

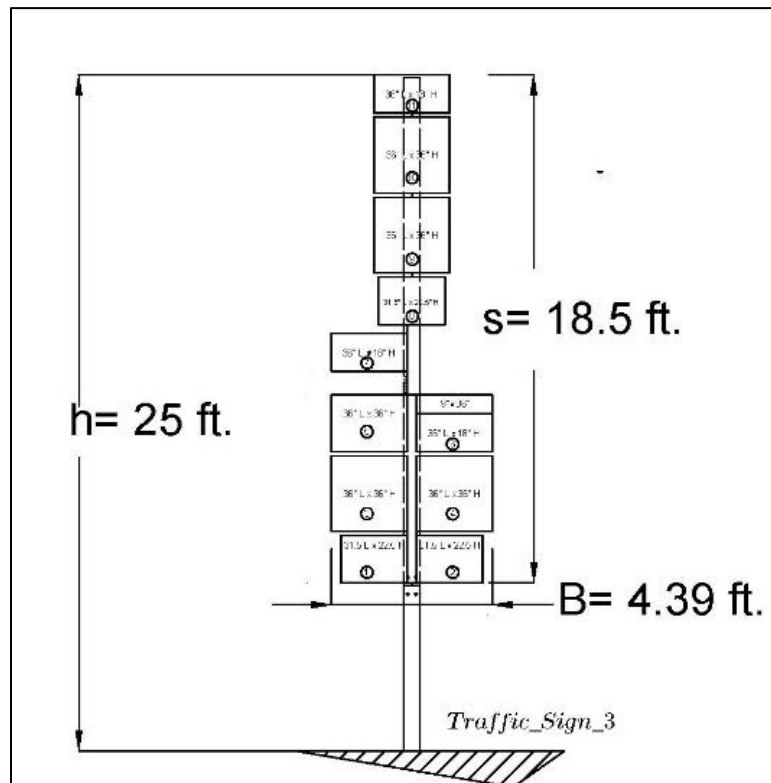


Figure 5.16: Case 3 dimensions

Similar to Case 1, out of the rupture fuse plate, tension test specimens were cut, which were then tested in tension. Calculating the average of the tension tests results presented in

Table 5.2, it was assumed that the fuse plate was made of steel with an ultimate strength of $F_u = 71,212$ psi.

Table 5.2: Case 3 fuse plate tensile test results

Specimen ID	Ultimate Stress F_u (psi)
TB	71,667
BB	71,640
BT	71,148
TT	70,392

As mentioned before, the ASCE 7 Standard does not offer guidance on how to consider a structure with several signs of assorted sizes. Therefore, it was assumed that all the smaller signs formed a larger sign with a width of 4.39 ft and height of 18.5 ft, as shown in Figure 5.17. The eccentricity of geometry formed by the different signs was disregarded.

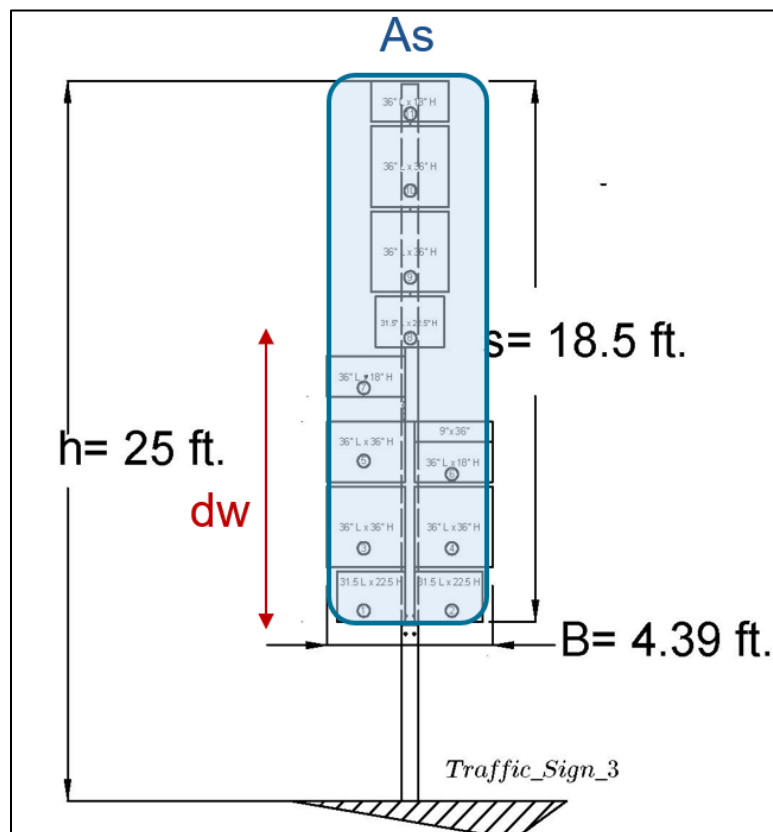


Figure 5.17: Assumed scenario for Case 3

5.5 Results

Table 5.3 summarizes the computations and results obtained from the analysis of the failure model of the three cases. The locations of the signs were consistent with Exposure C, so the height and exposure factor (K_z) and the gust effect factor (G) were calculated accordingly. The net force coefficient (C_f) was calculated according to ASCE 7's Case A, as discussed in section 2.3.

For Cases 1 and 2, gust speeds of over 178 mph were estimated to have caused the failure. This are significantly higher than the gust speeds estimated by other researchers and agree with the expected gust speeds over land for a hurricane of the magnitude of Maria. For Case 3, assuming an equivalent sign with dimensions that enclose the smaller signs may have been too conservative, therefore resulting in a wind speed significantly lower. A deeper investigation into this case may yield a higher gust speed estimate.

Table 5.3: Data and results from the three cases

		Case 1 Scenario A	Case 1 Scenario B	Case 2 Scenario A	Case 2 Scenario B	Case 3
Data (field and laboratory)	A_t [in ²] =	1.6763	1.6763	1.414	1.414	0.75
	d [in] =	9.75	9.75	9.75	9.75	9.75
	d_t [in] =	9.9785	9.9785	9.9935	9.9935	9.9785
	d_w [in] =	67	75.727	53.844	62.987	113.844
	B [ft] =	11	11	10.5	10.5	4.39
	S [ft] =	10	11.4545	8.5	10.0238	18.5
	h [ft] =	18	19.4545	15.92	17.4438	25
	F_u [psi] =	63,963	63,963	63,963	63,963	71,212
Computations	F_w [lb] =	15,968.75	14,128.41	16,786.44	14,349.86	4,681.33
	P_w [psf] =	145.17	112.13	188.08	136.34	57.64
	C_f =	1.7172	1.7074	1.7330	1.7103	1.7325
	G =	0.8970	0.8962	0.8985	0.8976	0.8968
	K_z =	0.8821	0.8966	0.8596	0.8763	0.9453
	V [mph] =	204.29	178.68	234.29	198.97	123.82

6 Conclusions and Recommendations

The results of the analysis of Cases 1 and 2 suggest that the peak gust speeds that occurred during Hurricane Maria in Puerto Rico may have been underestimated by FEMA (2018) and others. This could lead to a misinterpretation of the impact of Maria, which may eventually affect the revision of design wind speeds for Puerto Rico.

In this study, assumptions were made for the cases of a smaller exit number sign attached to a larger sign and for multiple signs of assorted sizes attached to a single post. A future area of research could be to further study these cases to determine procedures for the analysis of these structures, including appropriate values of drag and force coefficients.

Another potential area of research is comparing the performance of regular fuse plates vs slotted fuse plates. It would be of interest to determine which type of fuse had a better performance under hurricane loads.

Foundation failures suggest that the foundations were not adequately designed or constructed. Therefore, it may be appropriate to review the specification and typical drawings for foundations, such as embedment length, soil compaction, foundation size and details; or to improve quality control during construction to assure compliance with the specifications.

To increase the resiliency of the structures that were the subject of this research, the following recommendations are given:

- Only use breakaway systems if signs are not protected by guardrails. Out of the twelve failed structures documented for this study, nine were protected by guardrails. If sign structures are protected by guardrails, is not necessary to provide them with breakaway systems (AASHTO, 2015).

- Raising the location of the fuse plate as much as possible. This would cause a reduction of moment arm of the wind pressure (d_w). For Case 1, Scenario B, raising the fuse plate 10 inches would have increased the failure speed by about 13 mph, as shown in Figure 6.1.
- In regards with the exit number sign, consider implementing one of the following two alternatives:
 - Revising how the exit number sign is attached so that, during high wind speed events, the smaller sign falls back or flies off, therefore reducing the wind loads transmitted to the supporting posts. This is justified by the significant differences of gust speed estimates between Scenarios A (where the exit sign was disregarded) and B (where the exit sign was considered) for both Cases 1 and 2. Disregarding the exit sign increased the failure gust speed in 26 mph and 40 mph for Cases 1 and 2, respectively.
 - Instead of attaching an additional sign to indicate the exit number, insert this information into the main sign, without increasing its size, as shown in Figure 6.2. This is also justified by the comparison of Scenarios A and B for Cases 1 and 2.
- Develop a rotating spring hinge mechanism that connects the lower and upper segments of the W10x33 posts, as shown in Figure 6.3. After hurricanes, this type of hinge mechanism could allow the signs to be rotated back to the vertical position, aligned with the lower posts' segments.

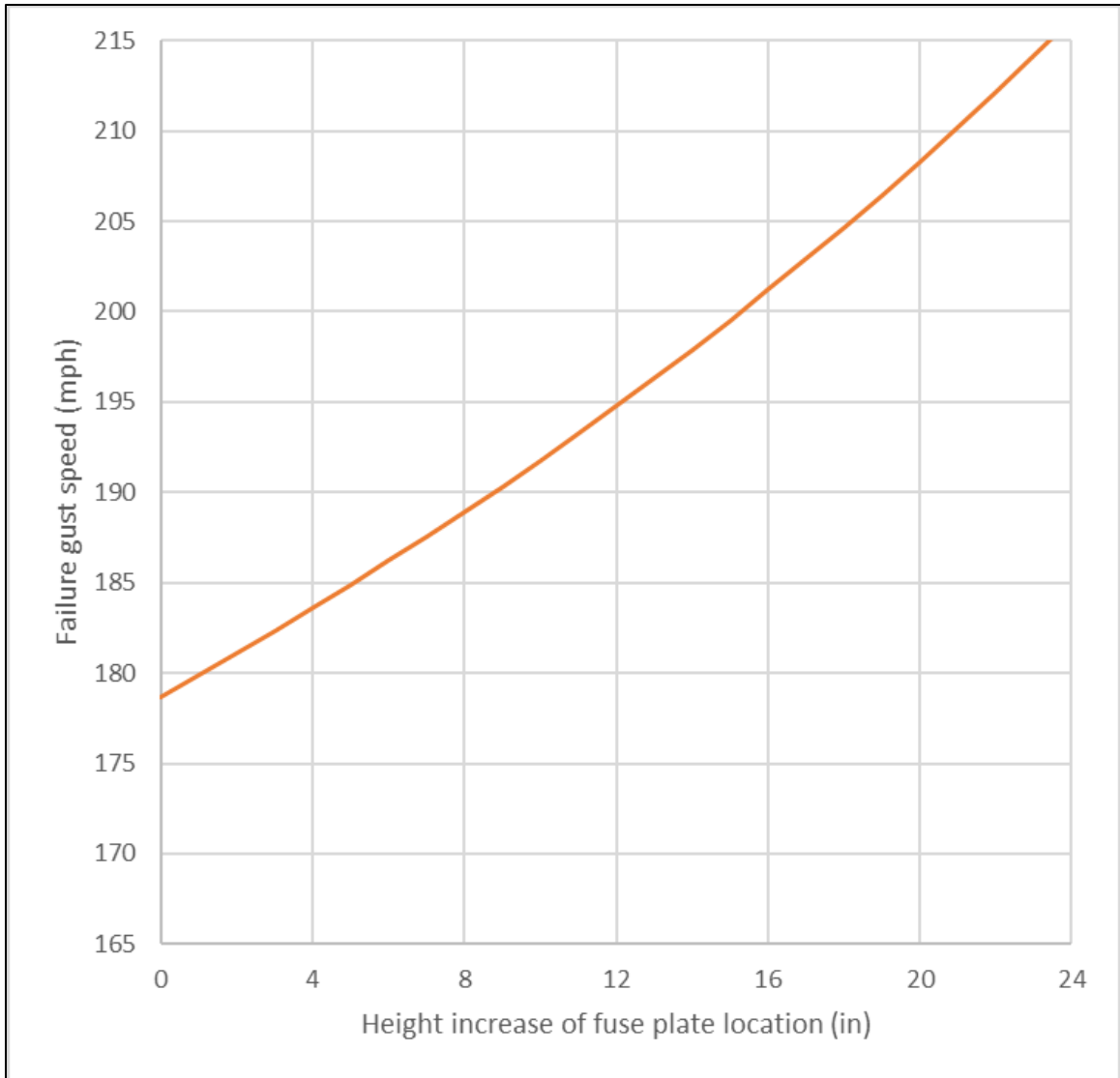


Figure 6.1: Effect of raising the location of fuse plate of Case 1, Scenario B

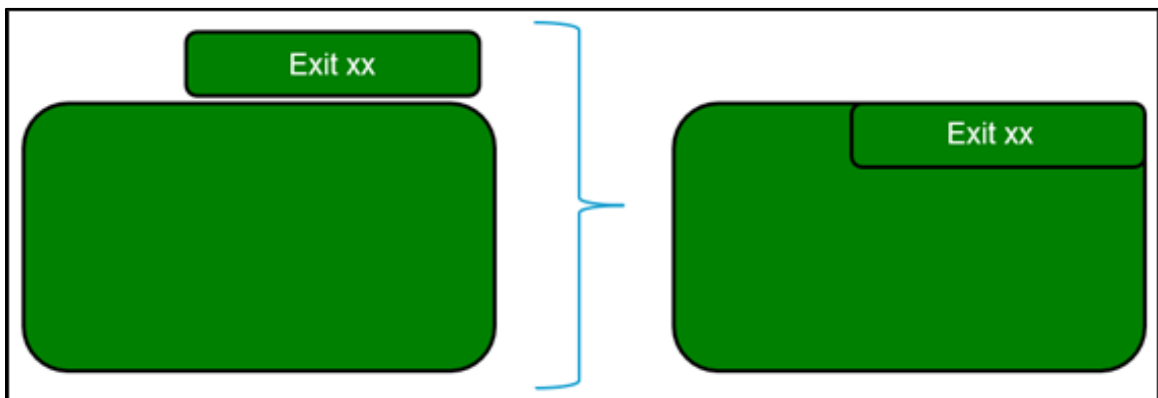


Figure 6.2: Recommendation of inserting exit number into main sign

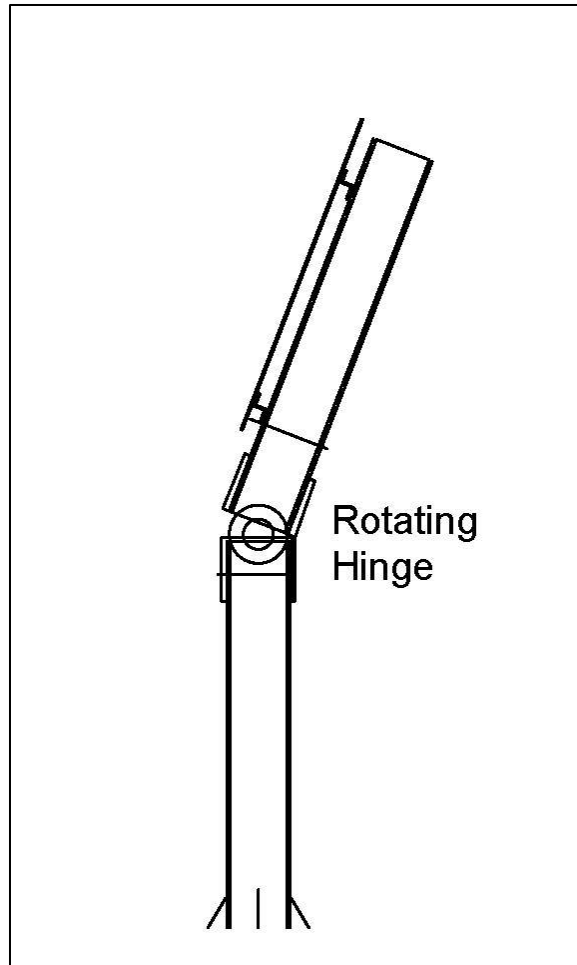


Figure 6.3: Rotating spring-loaded hinge

References

- AASHTO. (2011). *Roadside Design Guide* (4th ed.). Washington, DC: American Association of State Highway and Transportation Officials.
- AASHTO. (2015). *LRFD Specifications for Structural Supports for Highway Signs, Luminaires, and Traffic Signals* (6th ed.). Washington, DC: American Association of State Highway and Transportation Officials.
- ASCE. (2017). *Minimum design loads and associated criteria for buildings and other structures (ASCE Standard ASCE/SEI 7-16)*. Reston, VA: American Society of Civil Engineers.
- Climate.gov. (2018, August 1). Typical NEXRAD Doppler radar tower / NEXRAD Doppler radar after Hurricane Maria [Online Photo]. Retrieved from <https://www.climate.gov/news-features/understanding-climate/hurricane-marias-devastation-puerto-rico>
- FEMA. (2018). *Mitigation Assessment Team Report. Hurricanes Irma and Maria in Puerto Rico, Building Performance, Observations, Recommendations, and Technical Guidance. FEMA P-2020*. Washington, D.C: FEMA. Retrieved from https://www.fema.gov/sites/default/files/2020-07/mat-report_hurricane-irma-maria-puerto-rico_2.pdf
- FEMA. (2018). *Mitigation Assessment Team Report. Hurricanes Irma and Maria in Puerto Rico, Building Performance, Observations, Recommendations, and Technical Guidance. FEMA P-2020*. Washington, D.C: FEMA.
- Hubbard, S. (2018). *Maria Peak Windgusts [Map]*. Retrieved from https://www.ssec.wisc.edu/news/wp-content/uploads/sites/19/2018/05/maria_peak_windgusts.jpg
- NEXRAD . (1996). *NEXRAD System/Segment Specification*. Norman, OK: NEXRAD Operational Support Support Facility. Retrieved from <https://www.roc.noaa.gov/WSR88D/PublicDocs/NTR96.pdf>
- NIST. (2021, January). NIST SP 1262 A Progress Report: Learning from Hurricane Maria's Impact on Puerto Rico. Gaithersburg, MD: National Institute of Standards and Technology, U.S. Department of Commerce. Retrieved from <https://nvlpubs.nist.gov/nistpubs/SpecialPublications/NIST.SP.1262.pdf>
- NOAA. (2017). *2017 North Atlantic Hurricane Season Track Map*. Retrieved from <https://www.nhc.noaa.gov/data/tracks/tracks-at-2017.png>
- NOAA. (n.d.). *NOAA Historical Hurricane Tracks*. Retrieved from <https://www.climate.gov/maps-data/dataset/historical-hurricane-tracks-gis-map-viewer>
- NWS. (2017, November 29). *Major Hurricane Maria - September 20, 2017*. Retrieved from National Weather Service, National Oceanic and Atmospheric Administration: <https://www.weather.gov/sju/maria2017>
- Pacific Disaster Center. (2017). *Hurricane Maria - Exposure Based on Observed Wind Impacts, Puerto Rico, 21SEP17 [Map]*. Retrieved from https://reliefweb.int/sites/reliefweb.int/files/resources/PDC_TC_Maria_Wind_Exposure_Observed_Wind_PuertoRico.pdf
- Pasch, R. J., Penny, A. B., & Berg, R. (2019). *Hurricane Maria (AL 152017) 16-30 September 2017*. National Hurricane Center. Washington, DC: NOAA. Retrieved from https://www.nhc.noaa.gov/data/tcr/AL152017_Maria.pdf
- Paulsen, G., Pfeifer, B., Holloway, J., & Reid, J. (1995). *Design and Testing of a Dual Support Breakaway Sign*. Lincoln: Missouri Highway Transportation Department (MHTD).

- Pfeifer, B. G. (1993). *Safety performance evaluation of a modified perforated tension fuse plate for dual support breakaway signs*. Jefferson City: Missouri Highway Transportation Department.
- PRDOT. (2000). Ground Mounted Break-Away Signs. In *Planos Modelos* (Vol. 2). San Juan, PR: Puerto Rico Department of Transportation and Public Works. Retrieved from <https://act.dtop.pr.gov/planos-modelo/>
- PRDOT. (2011, September). Puerto Rico State Highway Map. Puerto Rico Department of Transportation and Public Works. Retrieved from <https://dtop.pr.gov/mapa-de-regionales/>

Improving Transportation Infrastructure Resilience against Hurricanes, other Natural Disasters, and Weathering: Part I - Analysis of failure of transportation signs due to Hurricane Maria

Volume 2

FINAL REPORT
July 2022

Submitted by:

Gustavo Pacheco-Crosetti, PhD, PE
Professor

Héctor J. Cruzado, PhD, PE
Professor

Guillermo López-Colón, PE
Graduate Student

Transportation Infrastructure Research Center – TIRC
Polytechnic University of Puerto Rico
377 Ponce de Leon Ave, San Juan, PR 00918

External Project Manager
Juan Carlos Rivera, Engineer
Puerto Rico Highway and Transportation Authority

<p>In cooperation with</p> <p>Rutgers, The State University of New Jersey And Puerto Rico Department of Transportation and Public Works And U.S. Department of Transportation Federal Highway Administration</p>
--

TABLE OF CONTENT

1. INTRODUCTION	1
1.1. PROBLEM DESCRIPTION	1
1.2. OBJECTIVES	2
1.3. REPORT ORGANIZATION	3
2. LITERATURE REVIEW	4
2.1. HURRICANE MARIA.....	4
2.2. SMALL TRAFFIC SIGN SUPPORTS	8
2.3. PUERTO RICO HIGHWAY AND TRANSPORTATION AUTHORITY STANDARD DRAWINGS	14
2.4. WIND LOADS ON SIGNS	24
3. RESEARCH PROGRAM.....	29
3.1. SCOPE AND OBJECTIVES	29
3.2. METHODOLOGY	30
4. DAMAGE DOCUMENTATION	32
4.1. SQUARE TUBES.....	32
4.2. U-CHANNELS	36
4.3. SUMMARY OF FINDINGS.....	49
5. CASE STUDY 1: SQUARE TUBE WITH PLASTIC BENDING	51
5.1. DESCRIPTION	51
5.2. PLASTIC MOMENT	56
5.3. WIND SPEED ESTIMATE – FIRST SCENARIO	62
5.4. WIND SPEED ESTIMATE – SECOND SCENARIO.....	65
5.5. ANALYSIS OF POST WITH LARGER CROSS SECTION	68
6. CASE STUDY 2: U-CHANNEL WITH PERMANENT TWISTING DEFORMATION	69
6.1. DESCRIPTION	69
6.2. LABORATORY TESTS	75
6.3. FIRST HYPOTHESIS – WIND PARALLEL TO SIGN PANEL	78
6.4. SECOND HYPOTHESIS – WIND PERPENDICULAR TO SIGN PANEL.....	82
7. CONCLUSIONS AND RECOMMENDATIONS	86
REFERENCES.....	88

List of Figures

Figure 1.1: Hurricane Maria approaching Puerto Rico (NWS, 2017).....	2
Figure 2.1: Hurricane Maria’s trajectory (FEMA, 2018)	5
Figure 2.2: Hurricane Maria sustained and gust speed measurements (FEMA, 2018)	5
Figure 2.3: Gust speeds estimates for Hurricane Maria (FEMA, 2018)	7
Figure 2.4: Single post roadside sign.....	8
Figure 2.5: Small wood support (McGee, 2010)	9
Figure 2.6: Holes to provide breakaway capability (McGee, 2010).....	10
Figure 2.7: U channel post (Rhino, 2019).....	11
Figure 2.8: Breakaway system for U-channel post (McGee, 2010)	11
Figure 2.9: Square tube post (Traffic Safety Products, 2019)	12
Figure 2.10: Breakaway designs for square tube posts (McGee, 2010)	13
Figure 2.11: Round tube post (Traffic Safety Products, 2019)	14
Figure 2.12: Square tube steel post dimensions (PRHTA, 2010).....	15
Figure 2.13: Square tube foundation detail for natural soil condition (PRHTA, 2010)	16
Figure 2.14: Square tube foundation detail for rock condition (PRHTA, 2010).....	17
Figure 2.15: Square tube foundation detail for location with concrete slab (PRHTA, 2010).....	18
Figure 2.16: U-channel dimensions (PRHTA, 2010).....	19
Figure 2.17: U-channel foundation detail for natural soil condition (PRHTA, 2010)	20
Figure 2.18: U-channel foundation detail for rock condition (PRHTA, 2010).....	21
Figure 2.19: U-channel foundation detail for location with concrete slab (PRHTA, 2010).....	22
Figure 2.20: EZE Erect System (PRHTA, 2010).....	23
Figure 2.21: Lap splice breakaway system (PRHTA, 2010)	23
Figure 2.22: Precast foundation (PRHTA, 2010).....	24
Figure 2.23: Wind loads on sign cases required by ASCE 7 (ASCE, 2017).....	27
Figure 4.1: Front and side views of SQ1.....	33
Figure 4.2: Aerial view of SQ1’s surroundings.....	33
Figure 4.3: Square exhibiting plasticization at the base.....	34
Figure 4.4: Out of plumb square tube due to construction defect	35
Figure 4.5: Top post without a visible base post.....	35
Figure 4.6: Example of tear-out failure	38
Figure 4.7: Examples of foundation on soil failure.....	39
Figure 4.8: Example of Backfill concrete failure	39
Figure 4.9: Example of retainer strap deformation.....	40
Figure 4.10: Examples of permanent twisting deformation.....	40
Figure 4.11: Sign facing wrong direction due to permanent twisting deformation	41
Figure 4.12: Permanent twisting deformation post that lost sign panel.....	42
Figure 4.13: Permanent twisting deformation that led to collapse by post fracture	43
Figure 4.14: Summary of U-channel failures.....	45
Figure 4.15: Sign with multiple U-channel posts where one post experienced permanent twisting deformation	46
Figure 4.16: Example of sign with permanent twisting deformation before Hurricane Maria	47
Figure 4.17: U-channel top post without a visible base post	48
Figure 4.18: U-channel with plastic reflector	49
Figure 4.19: Permanent twisting deformation in U-channels in Cambridge, MA	50
Figure 5.1: Case Study 1 location	51

Figure 5.2: Case Study 1 front view.....	52
Figure 5.3: Case Study 1 side view	53
Figure 5.4: Case Study 1 geometry	54
Figure 5.5: Case Study 1 square post dimensions (in inches)	55
Figure 5.6: Case Study 1 square post section properties	56
Figure 5.7: Material properties defined in the FE analysis.....	58
Figure 5.8: Load defined in the FE analysis	59
Figure 5.9: Load application in FE model	60
Figure 5.10: Constraints applied in the FE analysis	60
Figure 5.11: Maximum stress and deformation calculated in the FE analysis.....	61
Figure 5.12: Maximum displacement vs. load scale factor of FE analysis	62
Figure 5.13: Failure model for wind speed estimate, first scenario	63
Figure 5.14: Failure model for wind speed estimate, second scenario.....	66
Figure 6.1: Case Study 2 location	69
Figure 6.2: Case Study 2 before Hurricane Maria	70
Figure 6.3: Back view of Case Study 2 before Hurricane Maria	71
Figure 6.4: Case Study 2 after Hurricane Maria	72
Figure 6.5: U-channel post assembly at laboratory	73
Figure 6.6: U-channel post assembly longitudinal dimensions	74
Figure 6.7: U-channel cross-sectional dimensions	75
Figure 6.8: Specimens extracted from U-channel post.....	76
Figure 6.9: Universal Testing Machine.....	77
Figure 6.10: Wind loads applied in the parallel to the sign panel	78
Figure 6.11: Mesh generated for U-Channel	79
Figure 6.12: U-channel deformation under applied wind loads	80
Figure 6.13: U-channel dimensions and sectional properties (Franklin Industries, n.d.)	83
Figure 6.14: Case Study 2 geometry	85

List of Tables

Table 2.1: Approximate relationship between wind speeds in ASCE 7 and Saffir/Simpson Hurricane Scale (ASCE, 2017)	7
Table 4.1: Location of documented cases of damaged square posts	32
Table 4.2: Location and failure mode of documented cases of damaged U-channels.....	44
Table 5.1: Wind speed estimate comparison for different tubes	68
Table 6.1: Dimensions of specimens.....	76
Table 6.2: Specimens Yielding and Ultimate Stresses	78

1. Introduction

Hurricane Maria was a disastrous event in Puerto Rico which affected all aspects of the territory's infrastructure. The transportation infrastructure itself was affected with the collapse of bridges, traffic signals and signs, and luminaires. This project focused on investigating the failures of small traffic signs due to the passage of Hurricane Maria through Puerto Rico.

1.1. Problem Description

On September 20, 2017, Hurricane Maria made landfall over the municipality of Yabucoa, which is located in the southeastern part of Puerto Rico, as a near Category 5 hurricane, with sustained wind speeds of 155 mph and a pressure of 917 millibars. It left the island as a Category 3 hurricane with sustained winds of 109 mph (Pasch, Penny, & Berg, 2019). Figure 1.1 shows the magnitude and proximity of Hurricane Maria shortly before landing in Puerto Rico. Hurricane Maria is listed as the third most expensive hurricane in U.S. history, with the cost of recovery between Puerto Rico and the U.S. Virgin Islands valued at about \$90 billion (National Hurricane Center, 2018).

Hurricane Maria caused a significant amount of damage to the infrastructure of Puerto Rico, mostly affecting the debilitated electrical system, as well as the transportation infrastructure. Among the impacts to the transportation infrastructure were landslides affecting roadways, some bridges collapsing, and the failure of different types of traffic signals, signs, and luminaires.

This study focused on the damages of small traffic signs caused by Hurricane Maria's winds. For this project, small traffic signs are defined as a roadside sign panel supported

by a single post. Failures of this type of structures were geolocated and documented, taking note of the most frequent modes of failure. Also, two failed signs were taken as case studies to determine the wind speed that caused the failure and compared with the reported wind speeds of the hurricane. As a result, recommendations on how to improve the capacity of these structures are given.

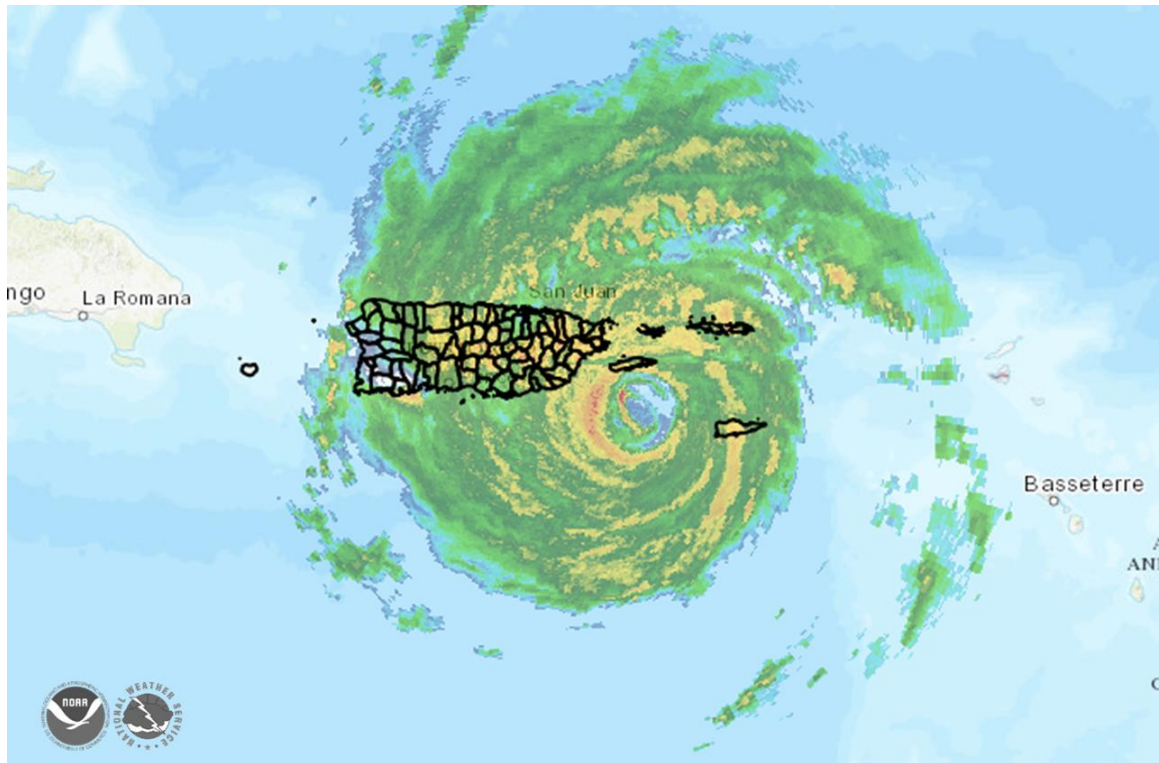


Figure 1.1: Hurricane Maria approaching Puerto Rico (NWS, 2017)

1.2. Objectives

The objectives of this project are to:

- Identify the most common modes of failures experienced by small traffic signs during Hurricane Maria.
- Estimate the gust wind speeds at which small traffic signs failed during Hurricane Maria.

- Suggest improvements to the design and construction of small traffic signs to increase their resiliency by avoiding or reducing the risk of failure in future extreme weather events.

1.3. Report Organization

Chapter 2 presents a literature review on meteorological aspects of Hurricane Maria, on general aspects of the supports of small traffic signs, on the specifications of the Puerto Rico Highway and Transportation Authority for small traffic signs, and on the calculation of wind loads on signs according to AASHTO and ASCE. Chapter 3 presents the research program followed for this project. Chapter 4 presents documented cases of small traffic signs that failed in Puerto Rico during Hurricane Maria. Chapters 5 and 6 present case studies of a sign supported by a square tube post that exhibits bending in the plastic range and another supported by a U-channel that that experienced a twisting deformation, respectively. Chapter 7 presents the conclusions and recommendations of this project.

2. Literature Review

This chapter first covers meteorological aspects of Hurricane Maria. Then, general aspects of the design and construction of small traffic signs are presented, followed by the Puerto Rico Highway and Transportation Authority specifications for this type of structure. Finally, a comparison is made between the calculation of wind loads on signs in the procedures of AASHTO and ASCE.

2.1. Hurricane Maria

Figure 2.1 shows the trajectory of Hurricane Maria since it first became a tropical storm on September 16, 2017. It turned into a hurricane on September 17 and a major hurricane on September 18 (Pasch, Penny, & Berg, 2019). Maria made landfall on the island of Dominica on September 19. Afterwards, it reached its maximum intensity of 172.6 mph with a minimum pressure of 908 mb, but then went through an eyewall replacement that weakened it as it neared Puerto Rico. It made landfall in the southeast coast of Puerto Rico on September 20 at approximately 1015 UTC with an estimated sustained wind speed of 155 mph (Pasch, Penny, & Berg, 2019), close to the lower limit of 157 mph for a category 5 hurricane.

Maria's estimated landfall wind speed at Puerto Rico was an extrapolation of the weakening trend of Maria noted by an aircraft report after the eye replacement several hours earlier (Pasch, Penny, & Berg, 2019). Figure 2.2 shows the maximum sustained and gust wind speeds measured in Puerto Rico for Hurricane Maria. Two important factors to consider are that (1) several instruments failed during the hurricane and (2) the measurements may have been made at terrains or heights that differ from the standards of 33-ft height and flat open terrain (FEMA, 2018).

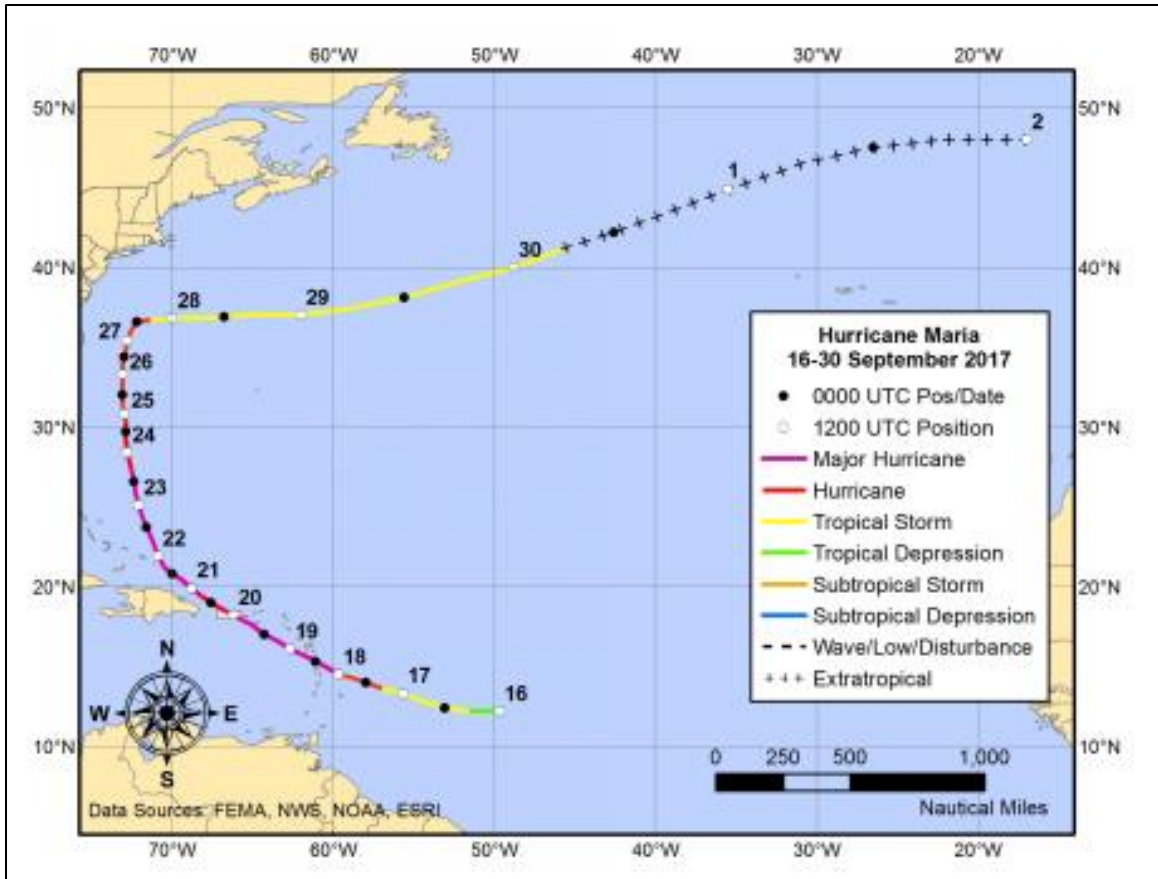


Figure 2.1: Hurricane Maria's trajectory (FEMA, 2018)

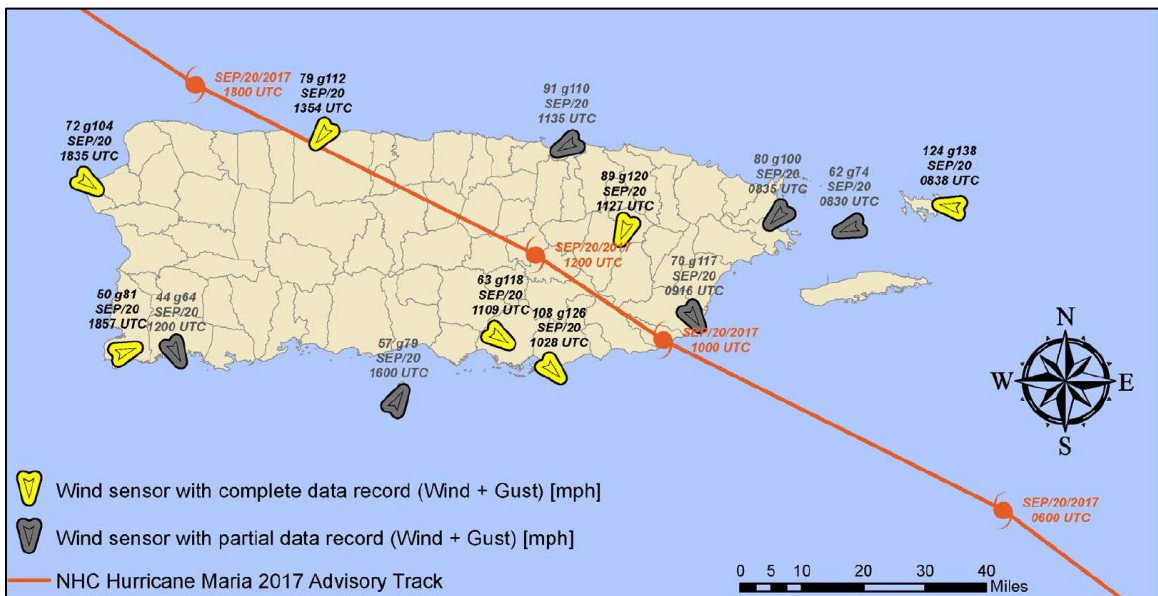


Figure 2.2: Hurricane Maria sustained and gust speed measurements (FEMA, 2018)

As the hurricane approached Puerto Rico, the main meteorological tool available to track and gather information was the San Juan WSR-88D doppler radar. The weather radar, operated by the Federal Aviation Administration and the National Weather Service, was designed for a 134 mph (60 m/s) wind speed (NEXRAD , 1996). The radar was functional until 0950 UTC on September 20, thereafter the radar was damaged and destroyed before Maria made landfall in Puerto Rico.

Hurricane Maria and its effects were extensively studied. Among the developed studies, researchers estimated the peak gust wind speeds that the hurricane produced. This type of research is extremely relevant, as they can be used to verify if the design wind speeds are adequate to lead to the construction of resilient structures against similar future weather event. Figure 2.3 presents one of these estimates; it should be considered that the estimates are for 3-second gusts 33 feet above ground for flat open terrain. In the figure, it can be seen that the maximum gust wind speed estimated was 140 mph. In other consulted studies, the maximum gust wind speed estimates range from 130 mph (Pacific Disaster Center, 2017) to 151 mph (Hubbard, 2018). No study estimating gust wind speeds higher than 155 mph, the sustained wind speed of Maria at the time of landfall, was found during the development of this study, and up to the end of year 2020. A recent report by the National Institute of Standards and Technology (2021) on Hurricane Maria included topographic effects on their wind gust estimates and presented speed higher than 155 mph in some locations.

The ASCE Standard ASCE/SEI 7-16 offers an approximate relationship between the sustained wind speed over water with gust wind speed over water and over land, as shown in Table 2.1. Performing a linear interpolation, it can be estimated that, for the sustained

wind speed of 155 mph that Hurricane Maria had at the time of landfall, the expected gust wind speed over water and over land would be 189 mph and 171 mph, respectively. A point of interest is that the gust wind speed over land of 171 mph estimated using the table of the ASCE Standard is significantly higher than the gust wind speeds estimated by the different studies consulted for this research.

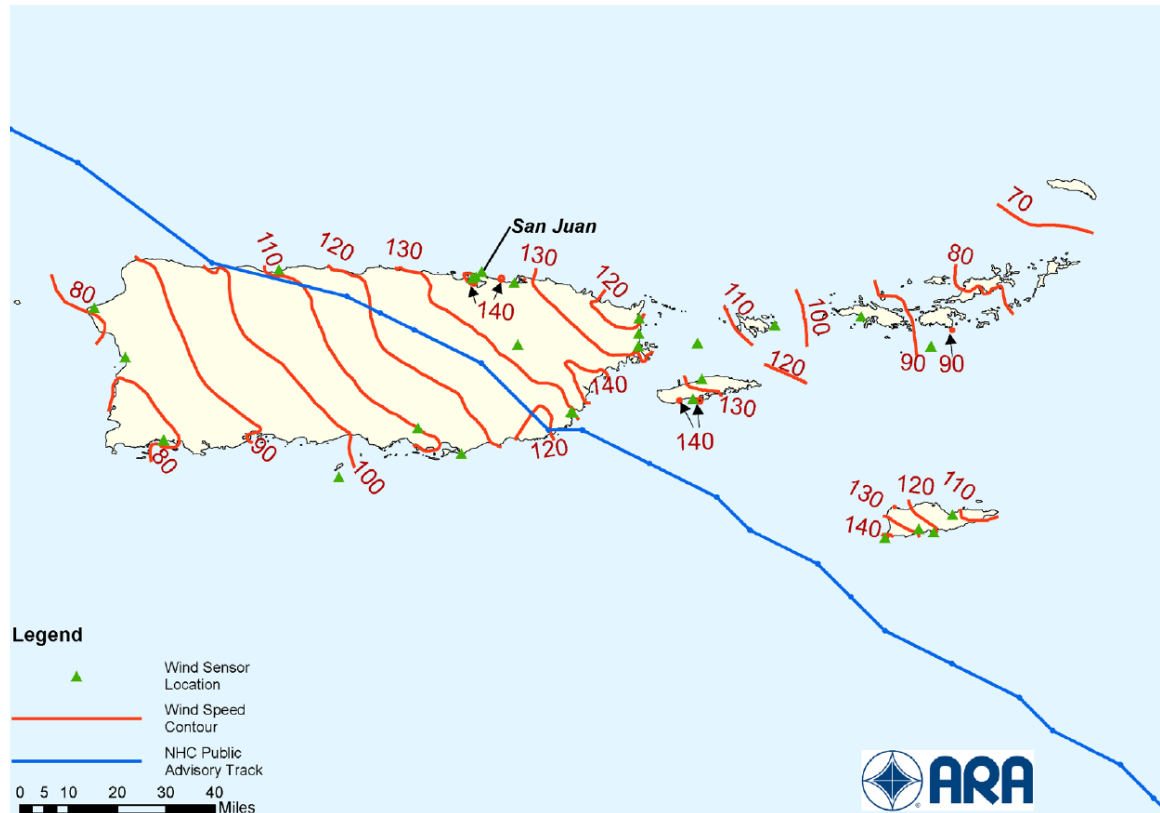


Figure 2.3: Gust speeds estimates for Hurricane Maria (FEMA, 2018)

Table 2.1: Approximate relationship between wind speeds in ASCE 7 and Saffir/Simpson Hurricane Scale (ASCE, 2017)

Saffir-Simpson Hurricane Category	Sustained Wind Speed Over Water (mph)	Gust Wind Speed Over Water (mph)	Gust Wind Speed Over Land (mph)
1	74 – 95	90 – 116	81 – 105
2	96 – 110	117 – 134	106 – 121
3	111 – 129	135 – 157	122 – 142
4	130 – 156	158 – 190	143 – 172
5	> 157	> 191	> 173

2.2. Small Traffic Sign Supports

A roadside sign is defined as one located beside the roadway and installed by a single or multiple posts (AASHTO, 2015). Figure 2.4 shows an example of a roadside sign supported by a single post. For this project, a small traffic sign is defined as a roadside sign panel supported a by single post.



Figure 2.4: Single post roadside sign

The clear zone is defined as the unobstructed, relatively flat area beyond the edge of the roadway to allow for the recovery of errant vehicles. For signs installed in the clear zone, posts must have a breakaway feature, unless they are protected by a guardrail or a barrier. This feature allows the post to yield, fracture or separate near the ground if impacted by a vehicle (AASHTO, 2015). The purpose is to protect the passengers in the case of impact.

The types of posts most commonly used for small traffic signs include wood posts and the following sections made of steel: U-channels, square tubes, and round tubes. The material used for the post depends mostly on their availability, but other factors are considered. In Puerto Rico, only hot-dip galvanized steel sections are accepted.

An example of a wood post is shown in Figure 2.5. Wood posts are used in states where wood fabrication is more economical than metal type supports (McGee, 2010). When used for permanent small traffic signs, pressure-treated redwood or coniferous ranging in size from 4x4 to 6x8 squared inches (Moeur, 2019). Poles with size greater than 4x6 squared inches are drilled perpendicular to the flow of traffic to provide the breakaway feature, but still maintaining rigidity against wind loads (Moeur, 2019), as shown in Figure 2.6.



Figure 2.5: Small wood support (McGee, 2010)



Figure 2.6: Holes to provide breakaway capability (McGee, 2010)

The U-channel steel post is a standard small traffic sign support. U-channels are characterized by its U shape, as shown in Figure 2.7. Small road constructions prefer this type of post due to its simplicity of installation (Moeur, 2019). Posts weighing 3 lb/ft or less are considered breakaway by themselves since they will bend, break, or pull out of the ground when impacted by vehicles (McGee, 2010). When the post is heavier, a stub post of the same material can be set in a concrete base with a 4-in length overlap to bolt to the post as a base connection to meet the breakaway requirements (McGee, 2010), as shown in Figure 2.8. The drawbacks of the U channel are its reduced load capacity and the inability to install the signs at right angles at the same post (Moeur, 2019).

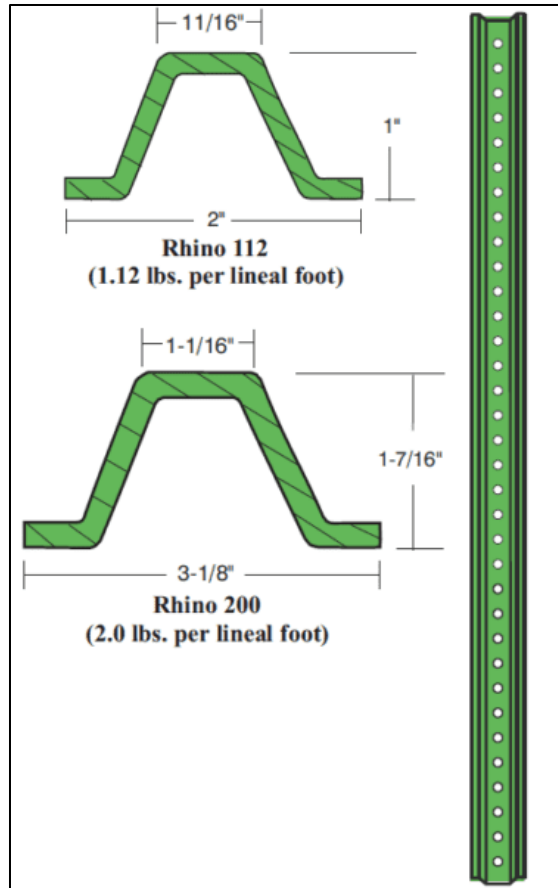


Figure 2.7: U channel post (Rhino, 2019)

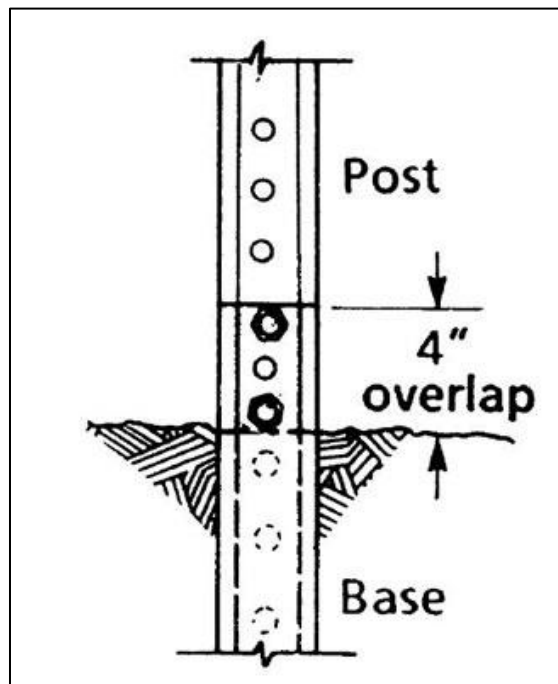


Figure 2.8: Breakaway system for U-channel post (McGee, 2010)

The square tube steel post type, as shown in Figure 2.9, is typically perforated by mounting holes at 1-in spacings (Moeur, 2019). Outside square dimensions define post sizes, with standard sizes ranging from 1-1/2 in to 2-1/2 in, with 1/4-in increments (Moeur, 2019). To increase the rigidity of these posts, higher sized posts can be selected, or a smaller sized square post can be added to join them together with a splice, forming a telescoping post (Moeur, 2019). Posts of 2-1/4 in or less are considered breakaway by themselves (McGee, 2010). Otherwise, sleeve assemblies of slip couplings may be used, as shown in Figure 2.10.



Figure 2.9: Square tube post (Traffic Safety Products, 2019)



Figure 2.10: Breakaway designs for square tube posts (McGee, 2010)

Some advantages of using square posts are that they can support higher loads than U-channels and they are more versatile in their installation, as signs can be mounted on four sides of the post (Moeur, 2019). Although they have a higher installation cost than U-channels, square tubes can be easily replaced by pulling out the old post and inserting the new one (Moeur, 2019).

Figure 2.11 shows a segment of a round tube steel post. Their nominal diameters determine the sizes, with the sign panels either screwed directly to the pole or clamped to the outside of the pole (Moeur, 2019). Some of the advantages of using these signs are that they are relatively inexpensive, easy to obtain because they are common steel parts, and can support the signs at any desired angle (Moeur, 2019). Their disadvantages include the need to drill them on-site or the use of special brackets to attach the signs, and the requirement to use specialized proprietary hardware for larger pole sizes when breakaway systems are required (Moeur, 2019).



Figure 2.11: Round tube post (Traffic Safety Products, 2019)

2.3. Puerto Rico Highway and Transportation Authority Standard Drawings

The Puerto Rico Highway and Transportation Authority (PRHTA) has a series of standard drawings that function as specifications for the design and construction of various aspects of highway and transportation projects. Any deviation from these drawings requires approval from the agency (PRHTA, 2010). The drawings include details for square tubes and U-channels supporting small traffic signs.

Figure 2.12 presents the required dimensions for square steel tubes, including the base post that would be working as part of the foundation. The post to which the signs are directly attached is denoted as the top post. Figure 2.13, Figure 2.14, and Figure 2.15 present foundation details for natural soil condition, rock condition, and location with a concrete slab, respectively. It should be noticed that, for the natural soil condition, a soil plate is required, while for the rock condition, a concrete foundation is required. Also, all three types of foundations require the use of a 2 $\frac{1}{4}$ -in base post. The 2-in top post telescopes from the base post.

Figure 2.16 presents the required dimensions for U-channels. (The PRHTA standard drawings refer to U-channels as steel flanged channels). Figure 2.17, Figure 2.18, and Figure 2.19 present foundation details for natural soil condition, rock condition, and location with a concrete slab, respectively. Notice that, similar to the square tube, a soil plate is required for the natural soil condition and a concrete foundation is required for the rock condition. Also, all foundations have a base post, to which then a top post is connected. Figure 2.20 and Figure 2.21 each present a detail that may be used to connect the base post to the top post.

Finally, Figure 2.22 presents the details of a precast concrete foundation. This detail can be used to support either a square tube or a U-channel.

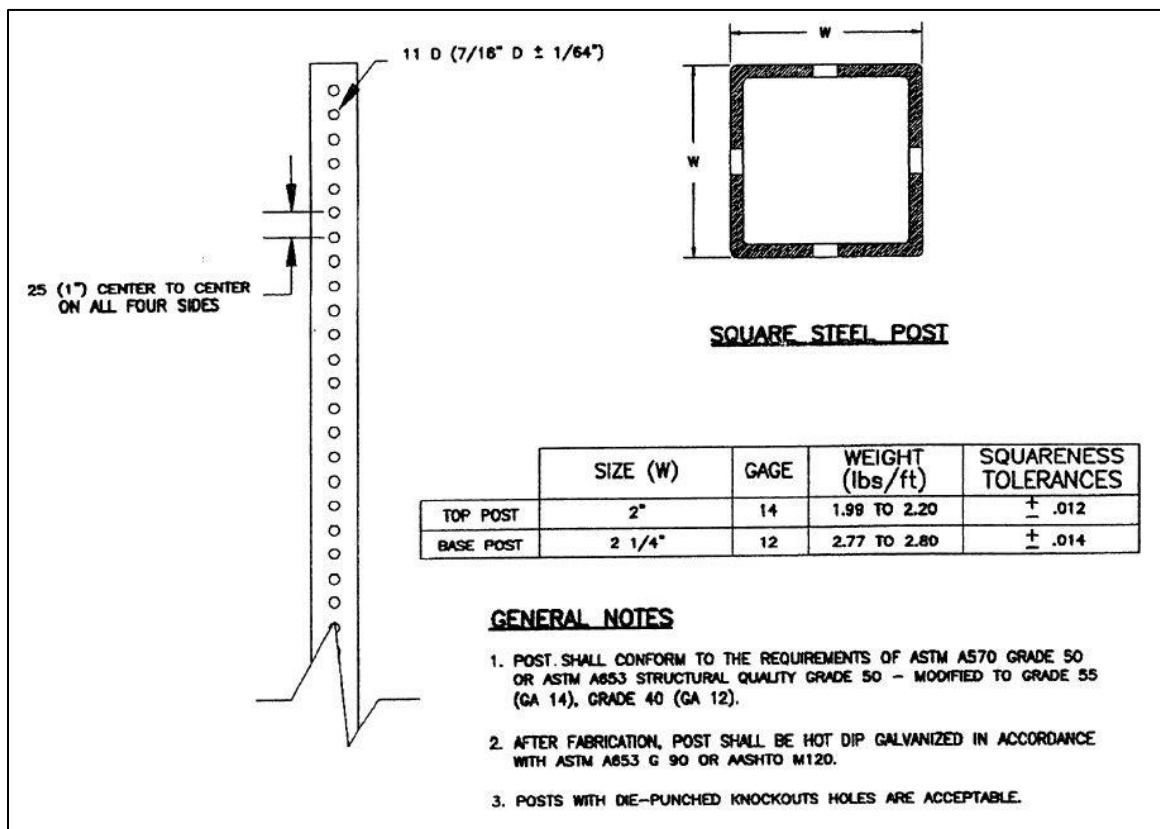


Figure 2.12: Square tube steel post dimensions (PRHTA, 2010)

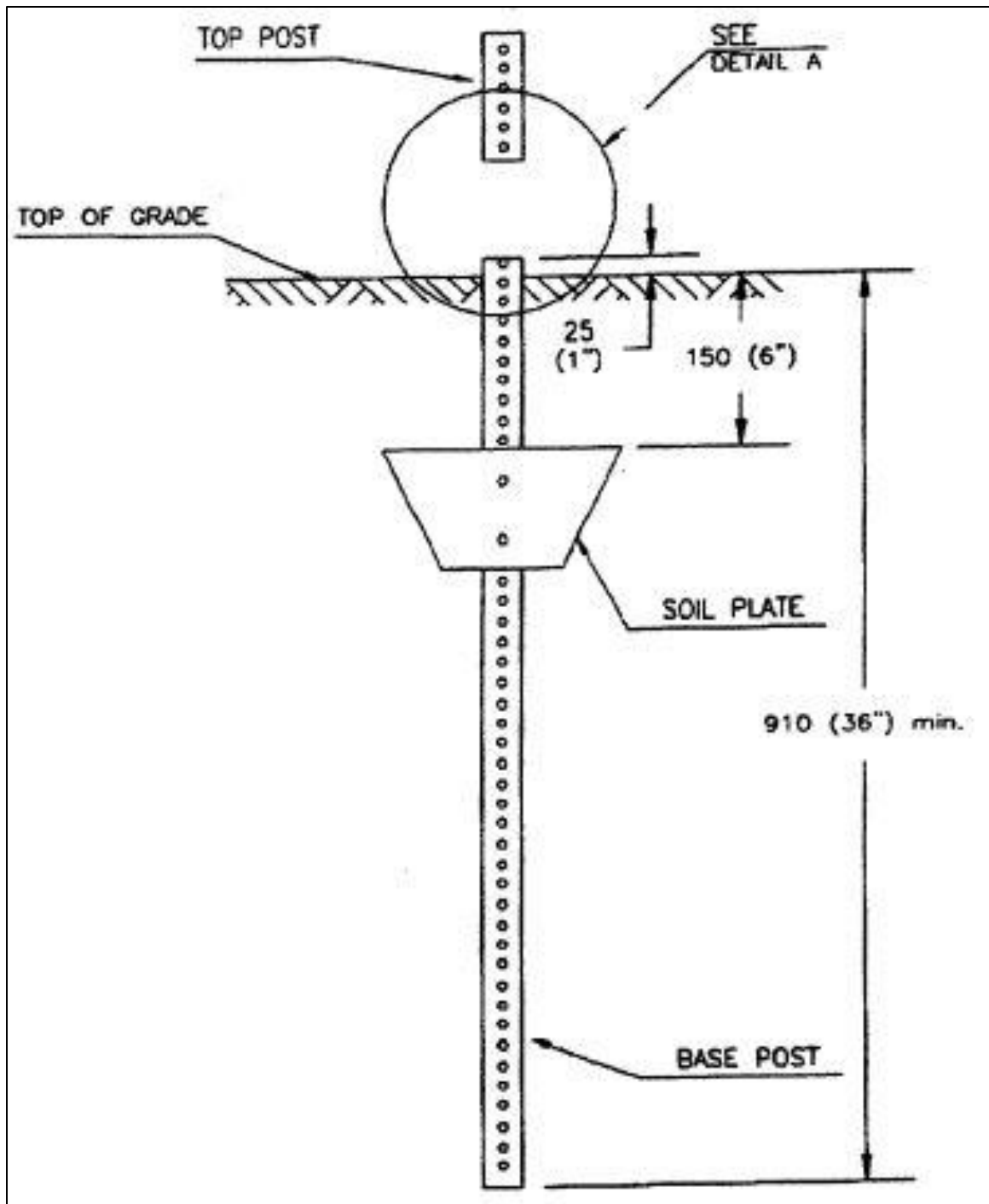


Figure 2.13: Square tube foundation detail for natural soil condition (PRHTA, 2010)

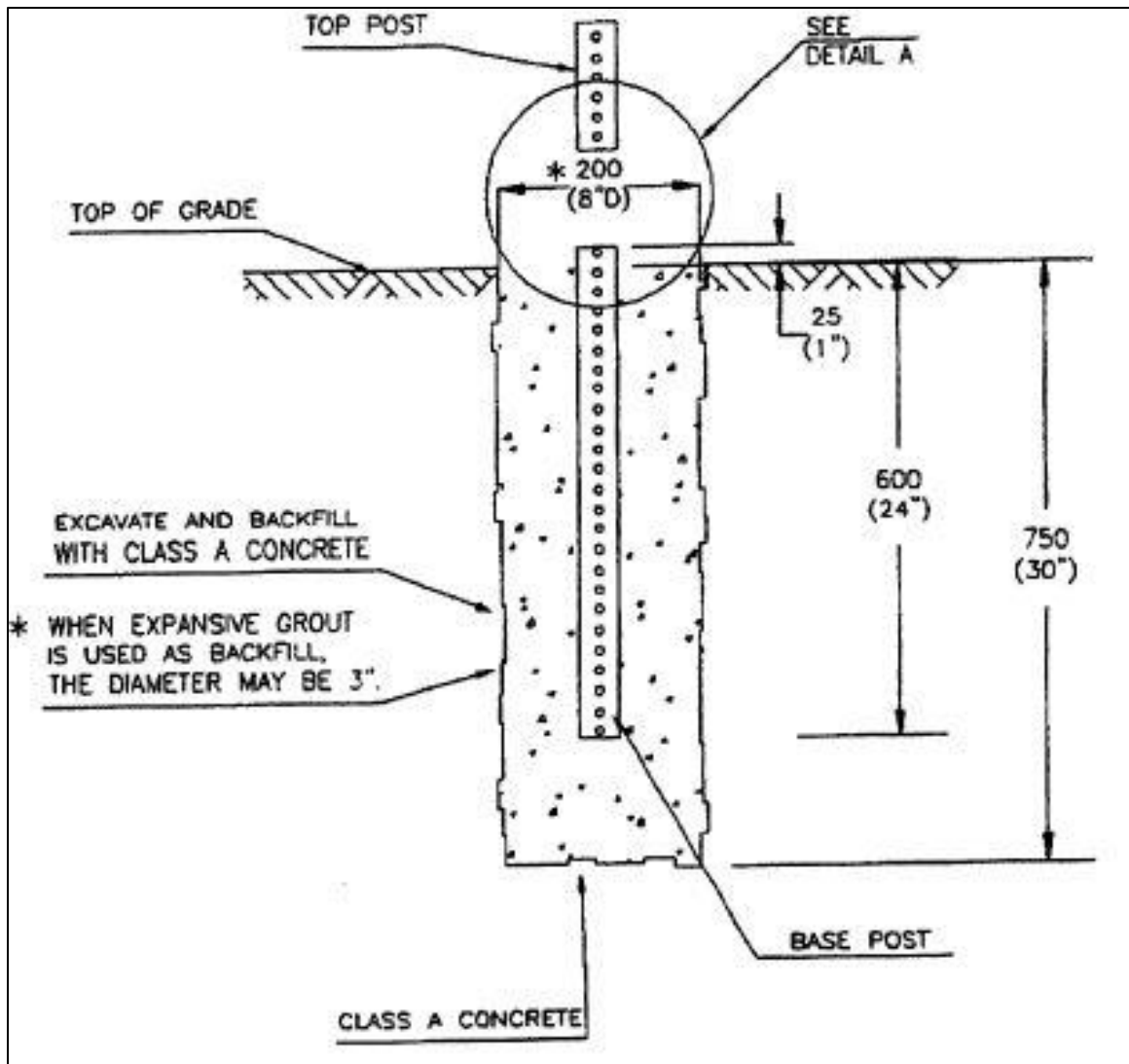


Figure 2.14: Square tube foundation detail for rock condition (PRHTA, 2010)

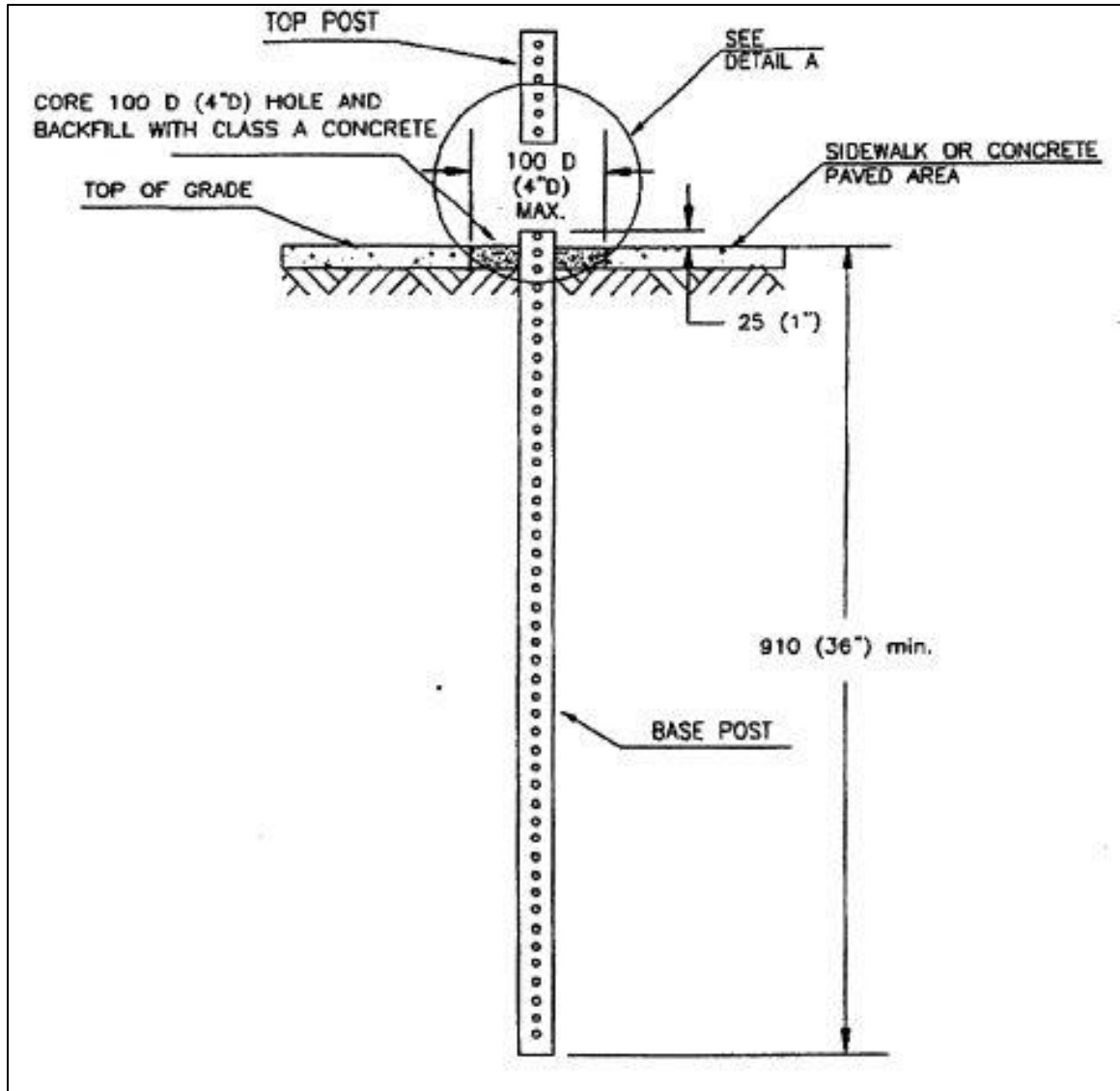


Figure 2.15: Square tube foundation detail for location with concrete slab (PRHTA, 2010)

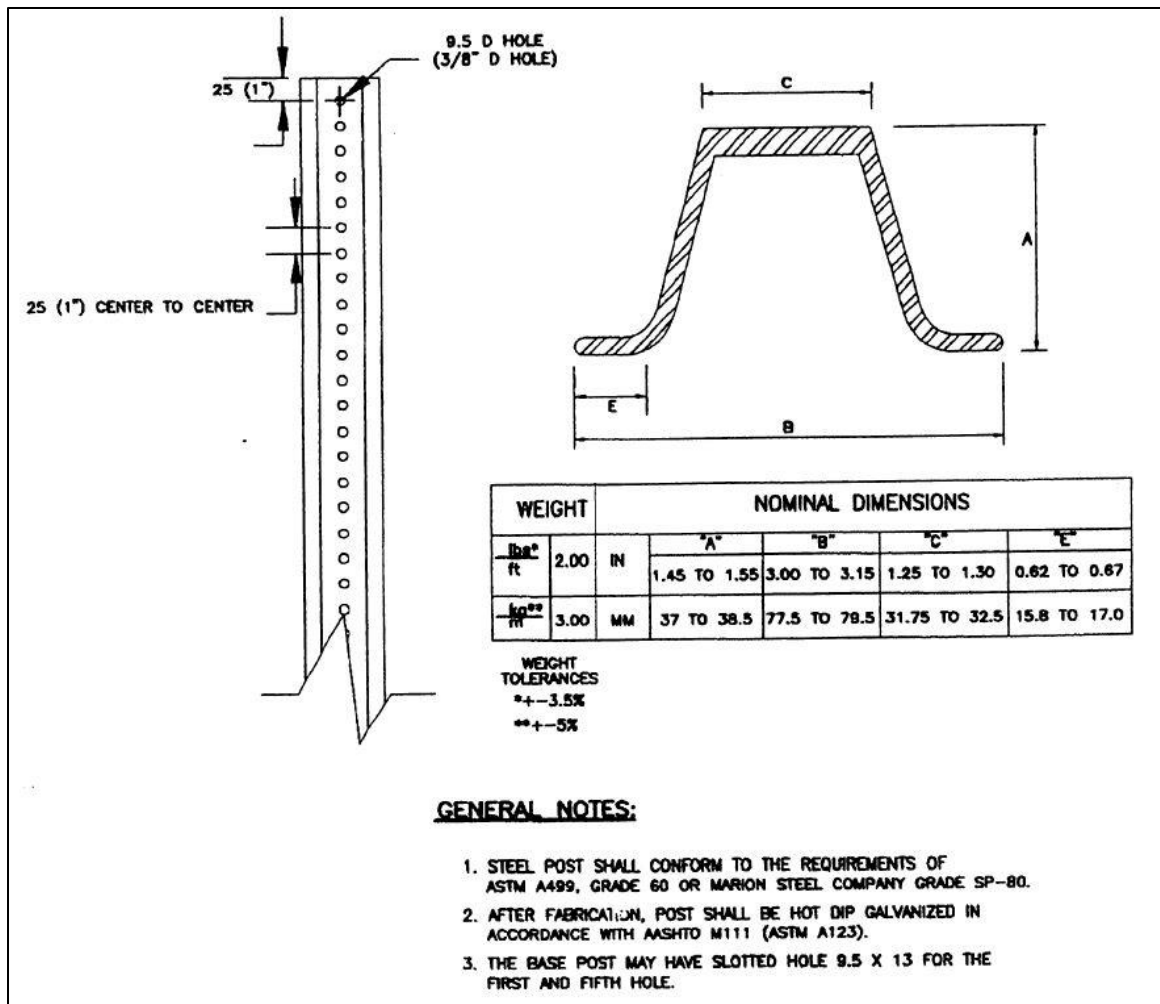


Figure 2.16: U-channel dimensions (PRHTA, 2010)

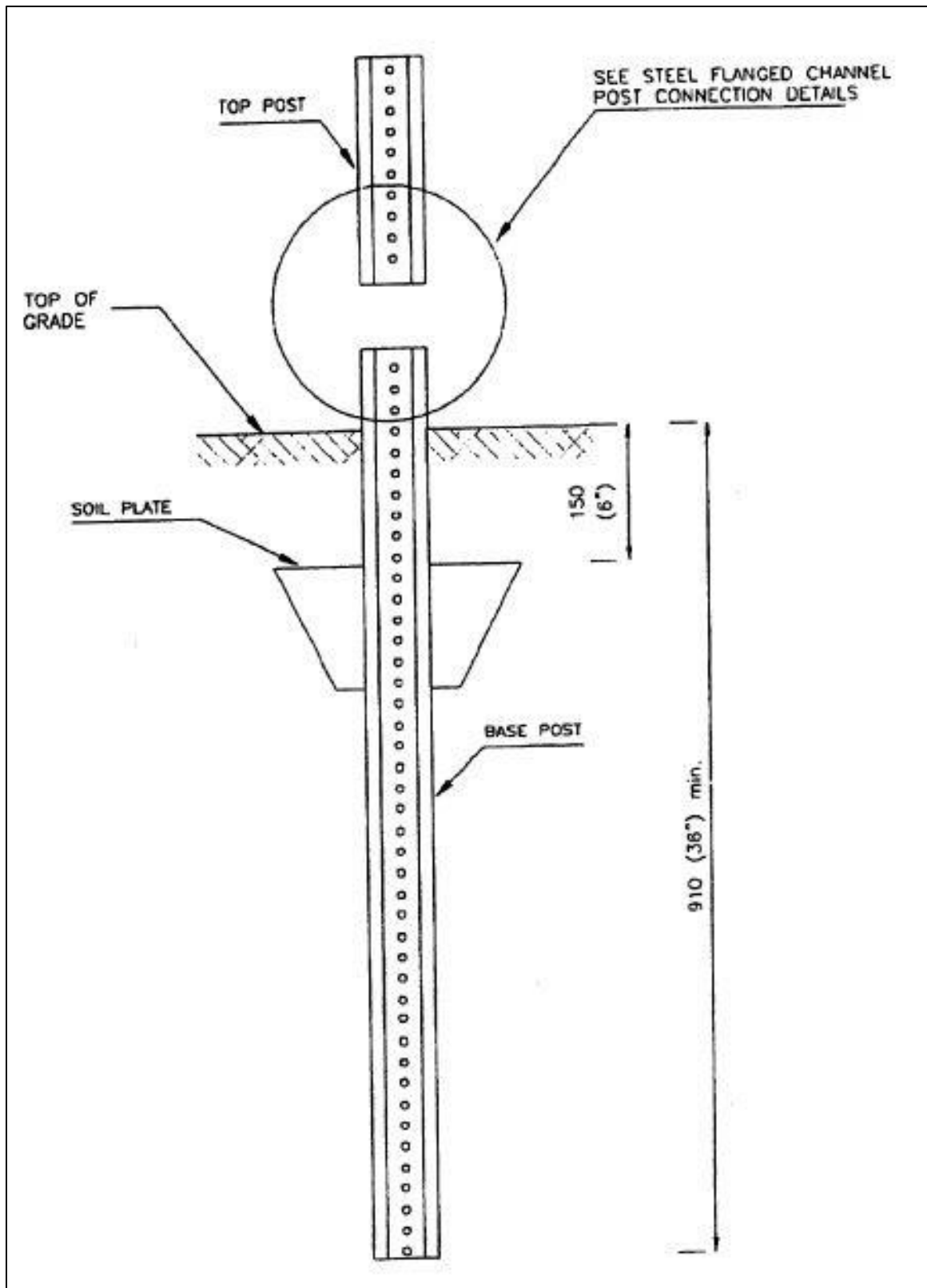


Figure 2.17: U-channel foundation detail for natural soil condition (PRHTA, 2010)

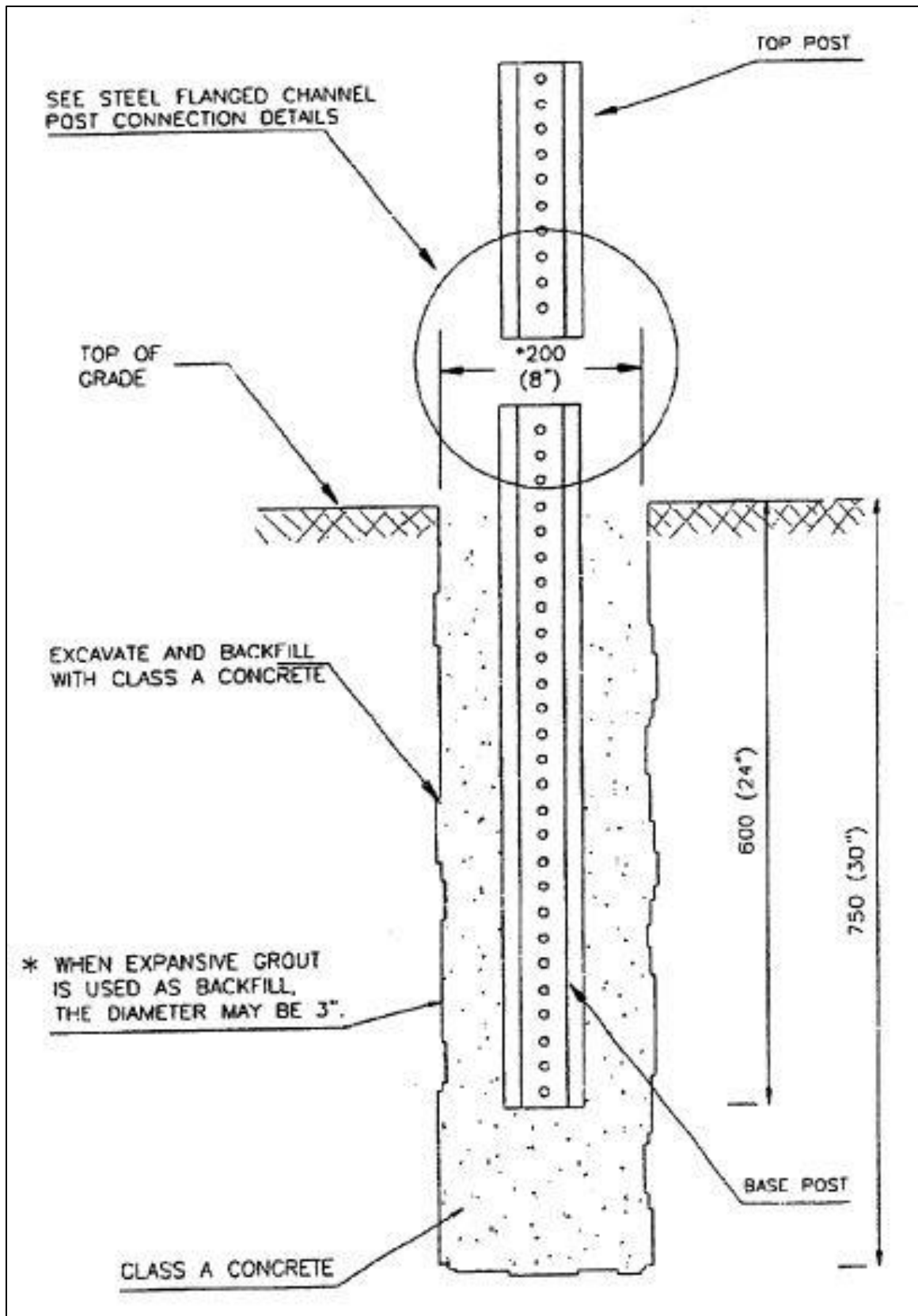


Figure 2.18: U-channel foundation detail for rock condition (PRHTA, 2010)

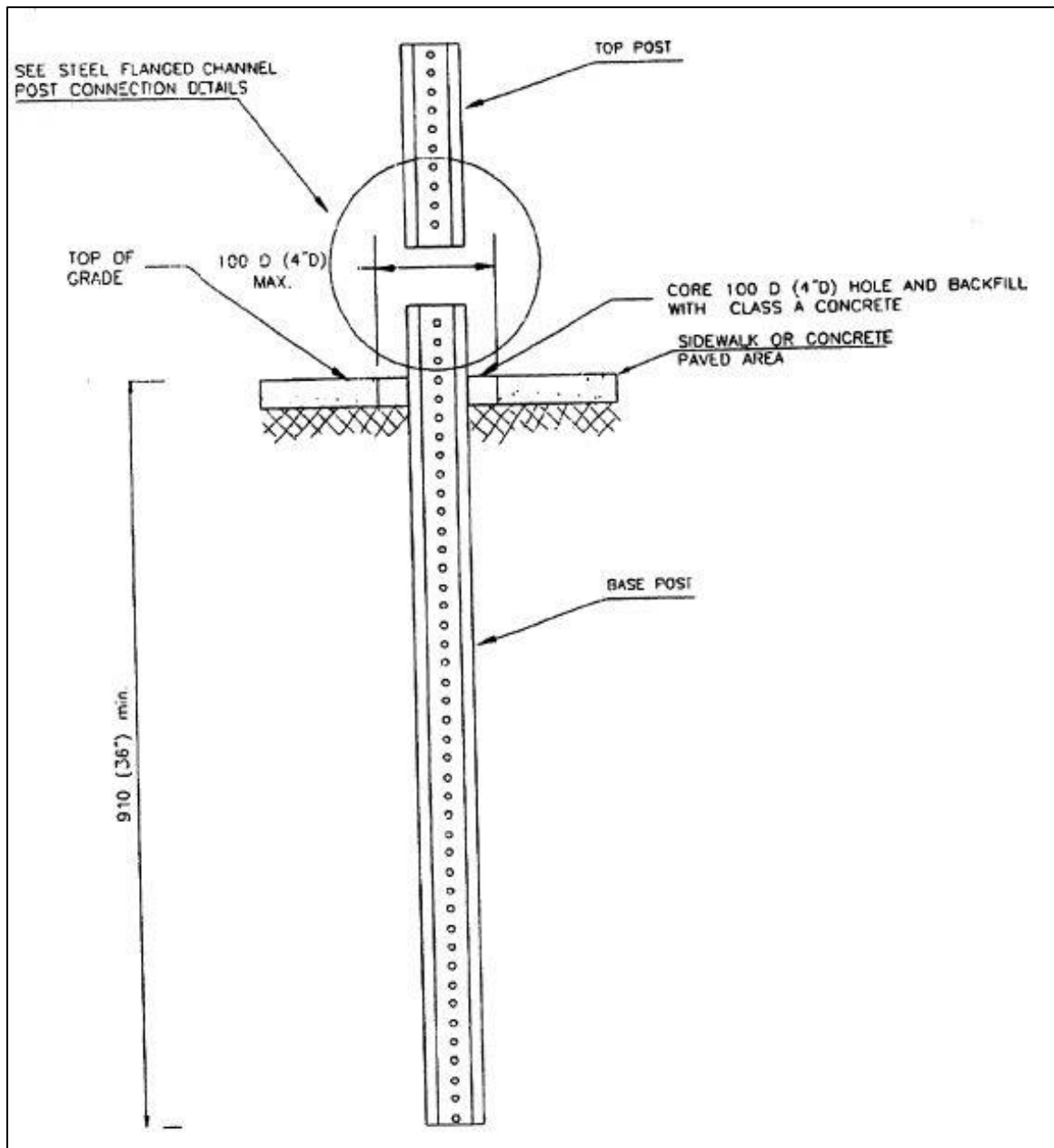


Figure 2.19: U-channel foundation detail for location with concrete slab (PRHTA, 2010)

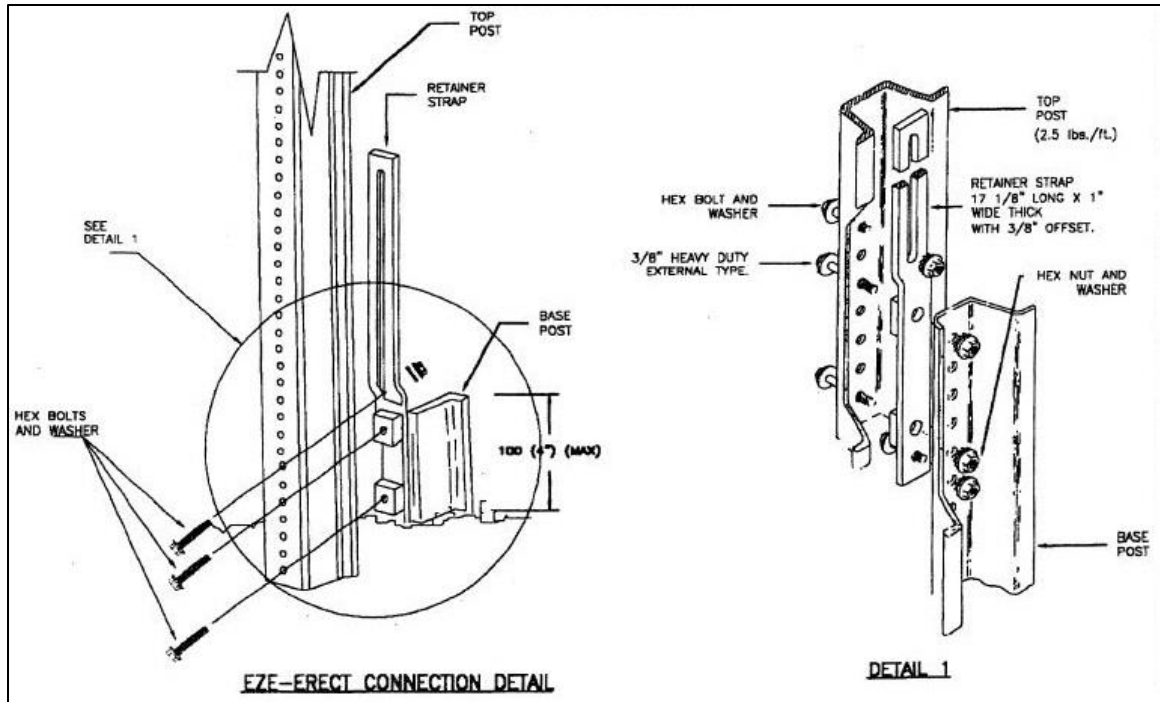


Figure 2.20: EZE Erect System (PRHTA, 2010)

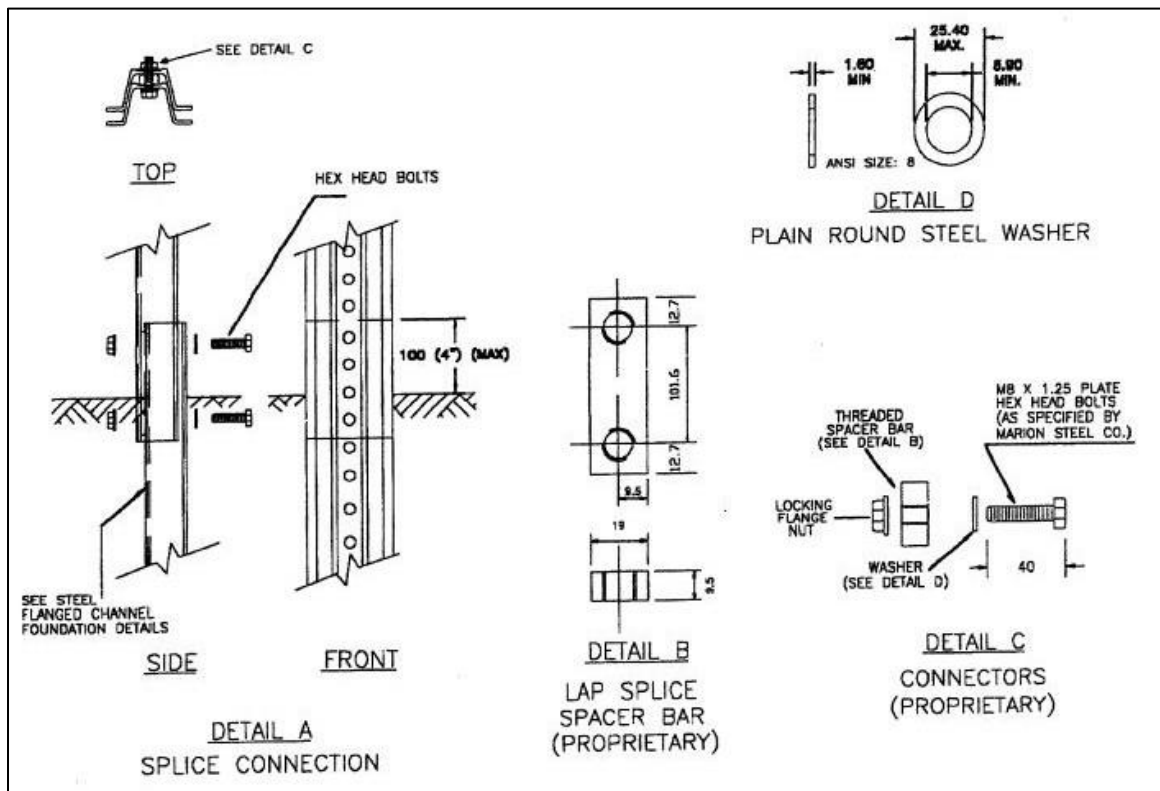


Figure 2.21: Lap splice breakaway system (PRHTA, 2010)

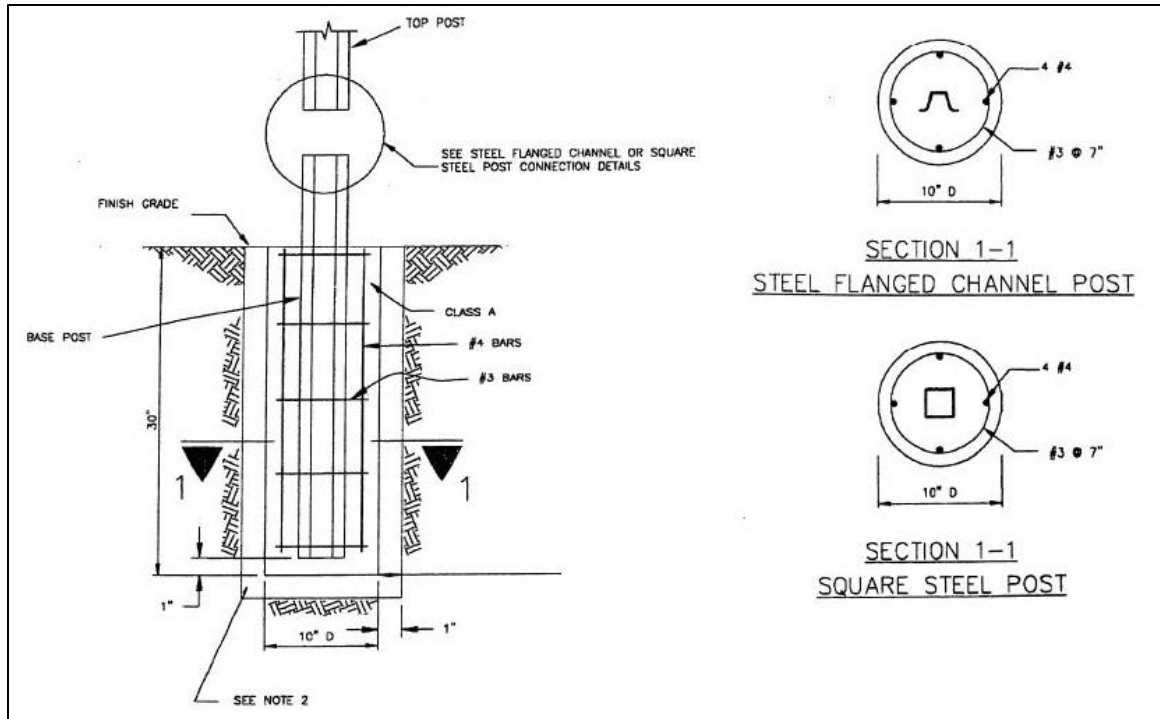


Figure 2.22: Precast foundation (PRHTA, 2010)

2.4. Wind Loads on Signs

In the U.S., there are two references that are the most widely used for the calculation of wind loads on signs and their supporting structures. These are:

- *LRFD Specifications for Structural Supports for Highway Signs, Luminaires, and Traffic Signals* by AASHTO (2015), for which the first edition was published in 2015. This edition was based on previous editions that used the ASD methodology instead of the LRFD methodology.
- *Minimum design loads and associated criteria for buildings and other structures* (ASCE Standard ASCE/SEI 7-16) by ASCE (2017).

The wind loads section of AASHTO Specifications is based on previous versions of the ASCE 7 Standard, so in fact both documents offer similar procedures for the calculation of wind loads on signs.

In the AASHTO Specifications, the design wind pressure in pounds per square foot (psf) is calculated as:

$$P_z = 0.00256K_zK_dGV^2C_d \quad (2-1)$$

where:

K_z = height and exposure factor

K_d = directionality factor

G = gust effect factor

V = basic wind speed in miles per hour

C_d = drag coefficient

Meanwhile, in the ASCE Standard, the design wind force in pounds (lb) is calculated as:

$$F = 0.00256K_zK_{zt}K_dK_eGV^2C_fA_s \quad (2-2)$$

where:

K_z = height and exposure factor

K_{zt} = topographic factor

K_d = directionality factor

K_e = ground elevation factor

G = gust effect factor

V = basic wind speed in miles per hour

C_f = net force coefficient

A_s = gross area of sign in ft²

The two main differences between the AASHTO and ASCE procedures that may lead to significant differences in the calculation of wind loads are:

- The Gust Effect Factor (G): The ASCE 7 Standard offers a procedure to calculate G in accordance with the fundamental frequency of the structure. Meanwhile, the AASHTO Specifications indicates that the ASCE 7 states that all structures with a fundamental frequency of 1 Hz or with a height to least horizontal dimension ratio greater than 4 should be considered wind-sensitive, and since most of the structures covered by the specification meet the second criteria, the minimum value of G that may be used is 1.14.
- AASHTO's Drag Coefficient (C_d) vs ASCE's Force Coefficient (C_f): For rectangular signs, the determination of C_d is based only on the dimensions of the sign. Meanwhile, the determination of C_f requires the sign dimensions plus its elevation with respect to the ground.

Other differences are:

- The inclusion of the topographic factor (K_{zt}) and the ground elevation factor (K_e) in the ASCE 7 Standard, but not on the AASHTO Specifications, which may also lead to significant differences for signs not located on flat terrain or for signs located at high elevations above sea level, respectively.
- The AASHTO Specification does indicate that three load cases must be considered:
 - Case 1: Full wind normal to the plane of the structure.
 - Case 2: Full wind transverse to the plane of the structure.

- Case 3: Three quarters of the full wind load in both directions applied simultaneously.

Meanwhile, the ASCE 7 Standard considers three different cases (as shown in Figure 2.23):

- Case A: Resultant force acting on the sign's geometric center.
- Case B: Resultant force acting at a distance e from the geometric center.
- Case C: The total area of the sign is divided into segments and a resultant force is calculated for each segment.
- The AASHTO Specification has procedures on how to calculate fatigue loads due to wind-induced vibrations, while the ASCE 7 Standard does not.

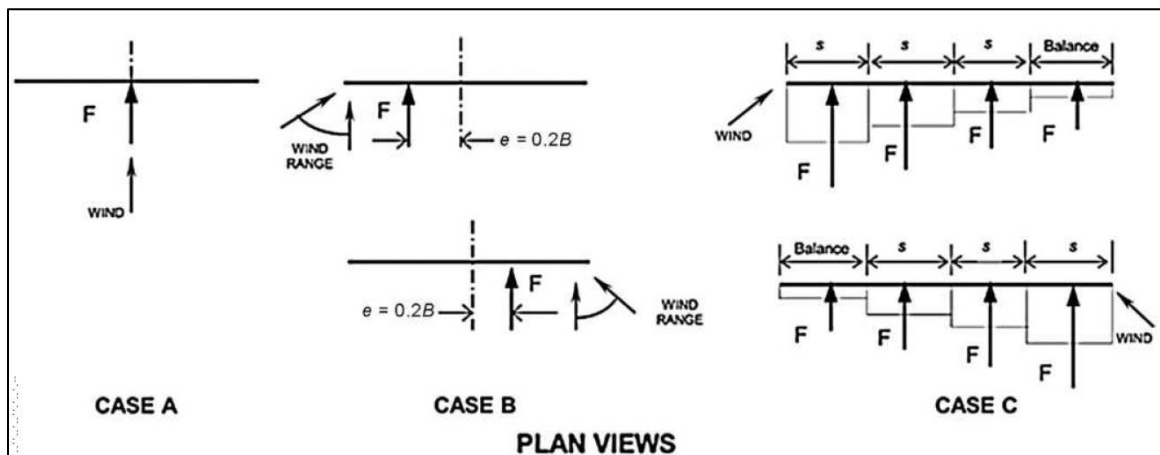


Figure 2.23: Wind loads on sign cases required by ASCE 7 (ASCE, 2017)

Both the AASHTO Specification and the ASCE 7 Standard have the following limitations:

- They do not offer any guidance on how to calculate wind loads on U-channel and square tube posts.

- They do not offer any guidance on how to calculate wind loads on non-rectangular sign panels.

Summarizing, in terms of wind loads calculations, the ASCE Standard is not only the basis for the AASHTO Specifications, but it also considers more variables and is more detailed. Therefore, the ASCE approach is considered to be more advanced and comprehensive than the AASHTO method.

3. Research Program

This chapter discusses the scope and objectives of this project. Also, the methodology followed to complete the project is presented.

3.1. Scope and Objectives

This project studies the failure of small traffic signs that failed due to the wind loads caused by Hurricane Maria in Puerto Rico. For this project, a small traffic sign is defined as a roadside sign panel supported by a single post. The project was limited to small traffic signs supported by steel U-channels and the square steel tubes, which are the only type of posts used in Puerto Rico for this type of sign. The only types of failures considered were the ones that caused the post to be damaged. If the sign itself broke away from the post without the post being damaged, the failure was not considered.

The objectives of this project are the following:

- To identify modes of failure in small traffic signs affected by Hurricane Maria.
- To determine the wind speed that caused the failure of a square tube that experienced bending in the plastic range.
- To determine the wind speed that caused the failure of a U-channel that experienced a permanent twisting deformation.
- To suggest improvements to the design and construction of small traffic signs to increase their resiliency by avoiding or reducing the risk of failure in future extreme weather events.

3.2. Methodology

In the first stage of the project, a field study was performed to evaluate the types of failures in small traffic signs in Puerto Rico after Hurricane María. Initially, the streets of the municipality of San Juan were randomly explored to find and document cases of failures of small traffic signs. These observations were made randomly in passing, meaning that there was not a systematic process of trying to document all the failures in the area. Also, cases that were incidentally found in other municipalities were included. Google Earth Pro was used to geolocate all the cases. The different modes of failure were identified, taking notice of the most frequent modes.

In the second stage, two posts supporting small traffic signs were selected as case studies:

- A square tube that experienced bending in the plastic range.
- A U-channel that experienced a permanent twisting deformation.

For the square tube case, once the geometry information was collected, the cross-sectional properties were obtained by using RISA Section software. The material properties were assumed to be those required by the PRHTA (2010). To determine the moment that caused the bending in the plastic range, calculations were made manually and compared to the results using the finite element modeling software Autodesk Inventor 2019. The percentage difference between both methods was verified to detect if there were any mistakes. Once there was confidence in the results, these were used to estimate the wind speed that produced the failure. Two scenarios were considered for this case: one that considers the wind loads acting only on the sign panel (disregarding the loads acting on the post), and another that considers the wind loads acting on both the sign panel and the post.

Also, an exercise was made of theoretically increasing the cross-sectional size of the post of this case study, to determine the required increase in wind speed to cause a similar failure.

For the U-channel case study, data was collected on the geometry and specimens were extracted from the post to conduct tensile tests to obtain the mechanical properties of the material. Initially, a hypothesis that lateral wind loads on the post caused lateral torsional buckling was evaluated. For this, a finite element model of the post was developed and subjected to a lateral pressure to determine the load that cause yielding. This load was then used to estimate the wind speed, but this was deemed too high, therefore this hypothesis was rejected. A second hypothesis was then developed, based on the published results of other researchers. The second hypothesis also considered the post twisting due to lateral torsional buckling, but not due to lateral loads, but to the wind blowing directly into the sign panel. To evaluate this hypothesis, the field measurements were used together with the finding of the other researcher to estimate the wind speed that may have caused the lateral torsional buckling.

Finally, based on the findings of previous steps of this project, recommendations were developed on how to make small traffic signs more resilient against future hurricanes.

4. Damage Documentation

This chapter presents the findings from field inspections of posts supporting small traffic signs. The main focus was to identify damages caused by Hurricane Maria to small traffic signs in Puerto Rico. The findings on square tubes are presented first, followed by the findings on U-Channels. Other findings not related to Hurricane Maria are included.

4.1. Square tubes

It was observed that most square tubes supporting small signs performed adequately during Hurricane Maria. All the inspected posts had sides measuring 2 in. No square tube was found to have collapse and only two cases were found to be damaged by hurricane winds. The location of these two posts, denoted as SQ1 and SQ2 for this project, is presented on Table 4.1. Both SQ1 and SQ2 failed due to wind loads on the sign and post, causing the post to bend in the plastic range.

Table 4.1: Location of documented cases of damaged square posts

ID	Municipality	Latitude	Longitude
SQ1	Carolina	18°26'32.22"N	66° 0'41.55"W
SQ2	San Juan	18°26'52.46"N	66° 4'2.07"W

Figure 4.1 shows SQ1's square post bended with respect to its base post. Figure 4.2 shows the areas surrounding SQ1. It can be noticed that is close to the north coast (less than 1,000 ft), while it has the Luis Muñoz Marín Airport to the south and east, and the San Jose Lagoon to the southwest.

Meanwhile, SQ2 was selected as a case study for this project to estimate the wind speed that caused it damage. Therefore, it is presented in detail in Chapter 5.



Figure 4.1: Front and side views of SQ1



Figure 4.2: Aerial view of SQ1's surroundings

Other findings not related to Hurricane Maria are the following:

- Two posts exhibited plasticization at the base. An example of this is shown in Figure 4.3. At first it was considered that Hurricane Maria caused these, but through Google Map's Street View, it was determined that the posts already presented this damage in 2016, prior to Maria's arrival.
- A few posts were out of plum due to construction defects. The base post appeared to have been improperly installed, as shown in an example presented in Figure 4.4.
- A few cases did not appear to have the base post required by the PRHTA (refer to Figure 2.13, Figure 2.14, and Figure 2.15). Figure 4.5 presents an example where the base post is not visible.



Figure 4.3: Square exhibiting plasticization at the base



Figure 4.4: Out of plumb square tube due to construction defect



Figure 4.5: Top post without a visible base post

4.2. U-channels

This project documented the failure of 60 small traffic signs supported by U-channels. Five modes of failure due to the wind loads produced by Hurricane Maria were identified for U-channels posts:

- **Tear-out:** In this mode of failure, the wind loads acting on the sign and the top post cause the bolts connecting the top and base posts to rip through the base post. An example of this is shown in Figure 4.6.
- **Foundation on soil failure:** This type of failure applies to posts installed in natural soil or rock conditions. In these cases, the ground that supports the foundation did not resist the load transferred to it from the wind loads acting on the sign and its supporting post, causing the post to tilt (see example in Figure 4.7 left) or collapse by overturning (see example in Figure 4.7 right). In these failures it was noticed that there is an apparent lack of compliance with the PRHTA standard drawings. The base posts did not have the required depth of 36-in, nor the soil plate required for natural soil conditions (refer to Figure 2.17), nor did they have the 30-in deep concrete foundation required for the rock conditions (refer to Figure 2.18).
- **Backfill concrete failure:** This type of failure occurred in posts installed in locations with a concrete sidewalk, where the sidewalk was drilled to accommodate the base post, and then the hole is backfilled with concrete. In these cases, the backfill concrete around the base post fails, allowing the sign to tilt. An example of this is shown in Figure 4.8. According to the standard drawings of the PRHTA, a 4-in diameter hole has to be drilled into the

concrete, as shown in Figure 2.19. It was noticed that, in the cases of backfill concrete failure, holes larger than 4-in were made to install the base posts.

- Retainer strap deformation: Only one case of this type of failure was found. It occurred in a sign that uses the connection depicted in Figure 2.20. In this case, the retainer strap had deformed, allowing the top post to tilt, as shown in Figure 4.9.
- Permanent twisting deformation: In this mode of failure, the top post twisted near its base, as it can be seen in the examples shown in Figure 4.10. This was the most predominant mode of failure observed. Several posts were found facing the wrong direction due to the deformation (see example in Figure 4.11). In other instances, the sign panel was lost (see example in Figure 4.12). In some cases, the deformation was so severe, that it led to the collapse by post fracture (see example in Figure 4.13). This mode of failure is furthered discussed in Chapter 6, as one of the failed signs was taken as a case study. In that chapter, theories on the mechanism that causes the twisting are offered.

All the documented failures were geolocated. Table 4.2 indicates the location of all the documented cases, along with their mode of failure. Again, it should be pointed out that the documentation of cases was made randomly in passing, meaning that there was not a systematic process of trying to document all the failures in an area.



Figure 4.6: Example of tear-out failure



Figure 4.7: Examples of foundation on soil failure



Figure 4.8: Example of Backfill concrete failure



Figure 4.9: Example of retainer strap deformation



Figure 4.10: Examples of permanent twisting deformation



Figure 4.11: Sign facing wrong direction due to permanent twisting deformation



Figure 4.12: Permanent twisting deformation post that lost sign panel



Figure 4.13: Permanent twisting deformation that led to collapse by post fracture

Table 4.2: Location and failure mode of documented cases of damaged U-channels

ID	Municipality	Latitude	Longitude	Failure Mode
U1	Loiza	18°25'28.55"N	65°50'34.97"W	Permanent twisting deformation
U2	Loiza	18°25'34.63"N	65°50'48.29"W	Permanent twisting deformation
U3	Loiza	18°25'28.58"N	65°50'35.06"W	Foundation on soil failure
U4	Rio Grande	18°25'14.44"N	65°49'42.35"W	Permanent twisting deformation
U5	Rio Grande	18°24'41.45"N	65°49'34.22"W	Permanent twisting deformation
U6	Rio Grande	18°23'21.00"N	65°49'35.13"W	Permanent twisting deformation
U7	San Juan	18°27'9.07"N	66° 3'26.82"W	Permanent twisting deformation
U8	San Juan	18°25'24.48"N	66° 3'27.59"W	Tear-out
U9	San Juan	18°25'32.79"N	66° 3'36.20"W	Foundation on soil failure
U10	San Juan	18°25'38.26"N	66° 4'6.78"W	Backfill concrete failure
U11	San Juan	18°25'32.02"N	66° 3'39.89"W	Foundation on soil failure
U12	San Juan	18°25'25.23"N	66° 3'30.00"W	Tear-out
U13	San Juan	18°25'32.05"N	66° 3'39.82"W	Permanent twisting deformation
U14	Humacao	18° 7'0.97"N	65°49'16.59"W	Tear-out
U15	Humacao	18° 6'58.85"N	65°49'16.12"W	Tear-out
U16	San Juan	18°26'49.39"N	66° 4'2.24"W	Backfill concrete failure
U17	San Juan	18°25'34.64"N	66° 4'12.06"W	Retainer strap deformation
U18	San Juan	18°25'43.30"N	66° 3'46.35"W	Permanent twisting deformation
U19	San Juan	18°25'44.98"N	66° 3'40.33"W	Foundation on soil failure
U20	San Juan	18°25'44.42"N	66° 3'42.67"W	Permanent twisting deformation
U21	San Juan	18°25'44.24"N	66° 3'43.56"W	Permanent twisting deformation
U22	San Juan	18°25'44.22"N	66° 3'43.75"W	Permanent twisting deformation
U23	San Juan	18°25'40.55"N	66° 4'3.17"W	Foundation on soil failure
U24	San Juan	18°25'40.95"N	66° 3'57.14"W	Permanent twisting deformation
U25	San Juan	18°25'38.83"N	66° 4'7.31"W	Permanent twisting deformation
U26	San Juan	18°25'41.78"N	66° 4'6.33"W	Foundation on soil
U27	San Juan	18°25'34.98"N	66° 3'50.78"W	Permanent twisting deformation
U28	San Juan	18°25'34.91"N	66° 3'39.73"W	Tear-out
U29	San Juan	18°25'32.74"N	66° 3'51.20"W	Permanent twisting deformation
U30	San Juan	18°25'37.11"N	66° 3'51.82"W	Foundation on soil
U31	San Juan	18°25'37.34"N	66° 3'52.22"W	Permanent twisting deformation
U32	San Juan	18°25'37.16"N	66° 3'52.20"W	Foundation on soil failure
U33	San Juan	18°25'38.11"N	66° 3'52.00"W	Foundation on soil failure
U34	San Juan	18°25'38.99"N	66° 3'52.27"W	Foundation on soil failure
U35	San Juan	18°24'56.71"N	66° 3'53.54"W	Permanent twisting deformation
U36	San Juan	18°24'55.47"N	66° 3'57.55"W	Permanent twisting deformation
U37	San Juan	18°24'55.84"N	66° 3'56.93"W	Permanent twisting deformation
U38	San Juan	18°24'57.30"N	66° 3'46.79"W	Foundation on soil failure
U39	San Juan	18°25'31.27"N	66° 3'44.86"W	Foundation on soil failure
U40	San Juan	18°25'31.59"N	66° 3'44.26"W	Foundation on soil failure
U41	San Juan	18°25'30.84"N	66° 3'43.68"W	Foundation on soil failure
U42	San Juan	18°25'22.93"N	66° 3'24.08"W	Permanent twisting deformation
U43	San Juan	18°25'23.30"N	66° 3'22.36"W	Permanent twisting deformation
U44	San Juan	18°25'31.04"N	66° 3'30.47"W	Foundation on soil failure
U45	San Juan	18°25'23.80"N	66° 3'25.65"W	Permanent twisting deformation
U46	San Juan	18°26'9.80"N	66° 3'33.90"W	Permanent twisting deformation
U47	San Juan	18°25'52.31"N	66° 3'31.76"W	Permanent twisting deformation
U48	San Juan	18°25'39.49"N	66° 3'29.16"W	Permanent twisting deformation
U49	San Juan	18°25'39.44"N	66° 3'29.16"W	Tear-out
U50	San Juan	18°25'56.16"N	66° 3'32.70"W	Permanent twisting deformation
U51	San Juan	18°25'45.84"N	66° 3'30.88"W	Permanent twisting deformation
U52	San Juan	18°22'36.21"N	66° 5'8.76"W	Permanent twisting deformation
U53	San Juan	18°26'40.71"N	66° 4'5.69"W	Permanent twisting deformation
U54	San Juan	18°26'46.11"N	66° 3'50.06"W	Permanent twisting deformation
U55	San Juan	18°26'40.14"N	66° 4'9.46"W	Permanent twisting deformation
U56	San Juan	18°26'43.25"N	66° 3'50.27"W	Permanent twisting deformation
U57	San Juan	18°26'43.05"N	66° 4'2.69"W	Backfill concrete failure
U58	Vieques	18° 9'1.58"N	65°26'33.17"W	Permanent twisting deformation
U59	Bayamón	18°23'37.15"N	66° 7'37.83"W	Permanent twisting deformation
U60	Bayamón	18°23'39.40"N	66° 7'40.43"W	Permanent twisting deformation

Figure 4.14 indicates the number of cases documented for each mode of failures. It can be seen that permanent twisting deformation was the predominant documented mode of failure with 35 out of the 60 documented cases, which represents 58%. It can also be noticed that the modes of foundation on soil failure and backfill concrete failure total 20, which represents 30%. This is of interest because it was found that these two modes of failures occurred in situations where the requirements of the PRHTA were not met.

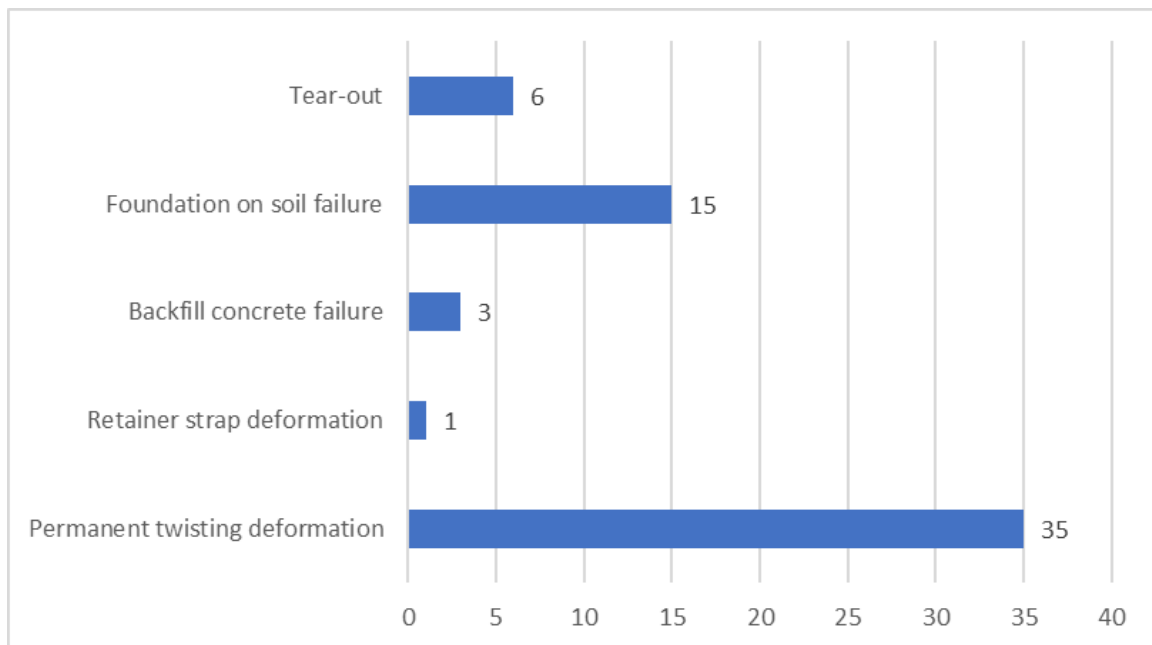


Figure 4.14: Summary of U-channel failures

In addition to the 60 documented cases, five other sign structures that failed during Hurricane Maria were also found. These were not included because they consisted in multiple U-channel posts supporting one sign, or multiple U-channel posts interconnected and supporting several small signs. Out of the five, four experienced permanent twisting deformation in one or more of the supporting U-channels (see example in Figure 4.15) and one was tilted due to foundation on soil failure.



Figure 4.15: Sign with multiple U-channel posts where one post experienced permanent twisting deformation

Twelve cases of permanent twisting deformation were at first considered to have been caused by Hurricane Maria, but through Google Map's Street View, it was noticed that the

posts already presented this damage in 2016, prior to Maria's arrival. An example of one of these cases is shown in Figure 4.16. These signs were then eliminated from the study; therefore, they are not included in the 60 documented cases.

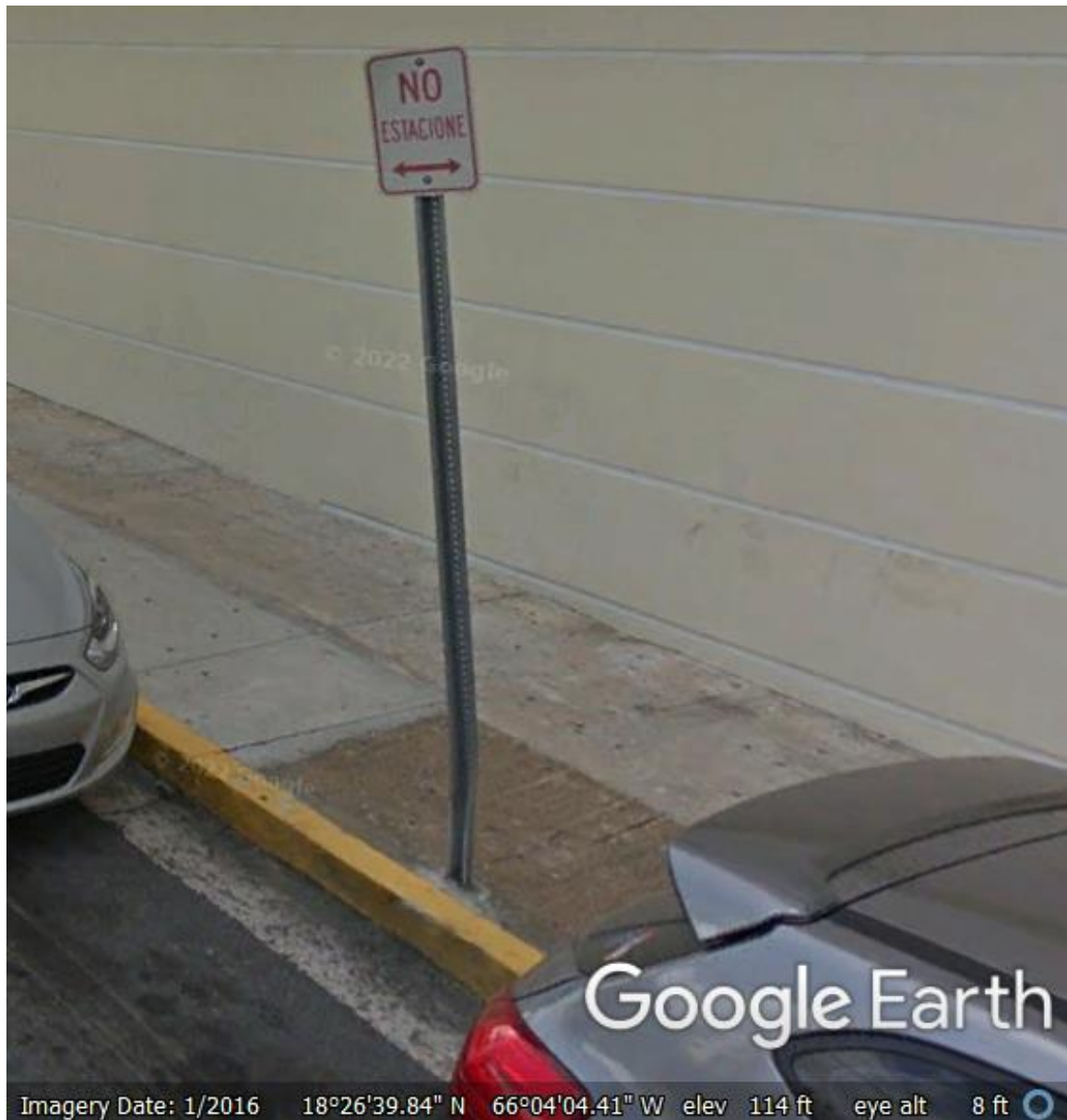


Figure 4.16: Example of sign with permanent twisting deformation before Hurricane Maria

Other findings made during the inspections were the following:

- Some cases did not appear to have the top post to base post connection as required by the PRHTA, (refer to Figure 2.20 and Figure 2.21). An example of this is shown in Figure 4.17.
- Figure 4.18 shows a U-channel post with a reflective plastic cover. This post behaved is located in a street segment of about 500 ft where five other signs failed. The reflective plastic cover may have contributed to avoid permanent twisting deformation.



Figure 4.17: U-channel top post without a visible base post



Figure 4.18: U-channel with plastic reflector

4.3. Summary of findings

Although the U-channel appears to be use much more frequently than the square tube, no square tube was found to have collapsed. Only two square tubes experienced permanent deformation due to bending in the plastic range. Still, these deformations were minor, with the posts still in use. This suggests that the square tube behaved much more adequately than the U-channel during Hurricane Maria.

In the U-channels, the most predominant mode of failure was permanent twisting deformation, which represented 58% of the documented cases. This does not include four cases of signs supported by multiple U-channels or signs that experienced this failure before Hurricane Maria.

Additionally, foundation on soil failure and backfill concrete failure combined to represent 30% of the documented cases. These failures appear to have been due to

construction not meeting the specifications of the PRHTA. Therefore, these failures could have been avoided.

The permanent twisting deformation in U-channel posts has also been observed in other parts in the United States with lower basic wind speeds. As an example, Figure 4.19 shows three posts with permanent twisting deformation in Cambridge, MA. These, together with the other cases of permanent twisting deformation that were found to have occurred before Hurricane Maria in Puerto Rico suggest that the U-channel is very susceptible to this type of failure.



Figure 4.19: Permanent twisting deformation in U-channels in Cambridge, MA

5. Case Study 1: Square Tube with Plastic Bending

This chapter presents a case study of a square tube post supporting a transit sign. The post demonstrated deformation due to plastic bending. The gust wind speed that caused this deformation is estimated.

5.1. Description

The first case study evaluated was sign with a square tube that experienced bending in the plastic range due to the winds of Hurricane Maria. For this project, this structure was identified as SQ2 in Table 4.1, which indicates the sign's location. The sign is located in an urban area, as shown in see Figure 5.1. Figure 5.2 presents a front view of the case study itself. Figure 5.3 shows a side view in which the bending failure can be appreciated.

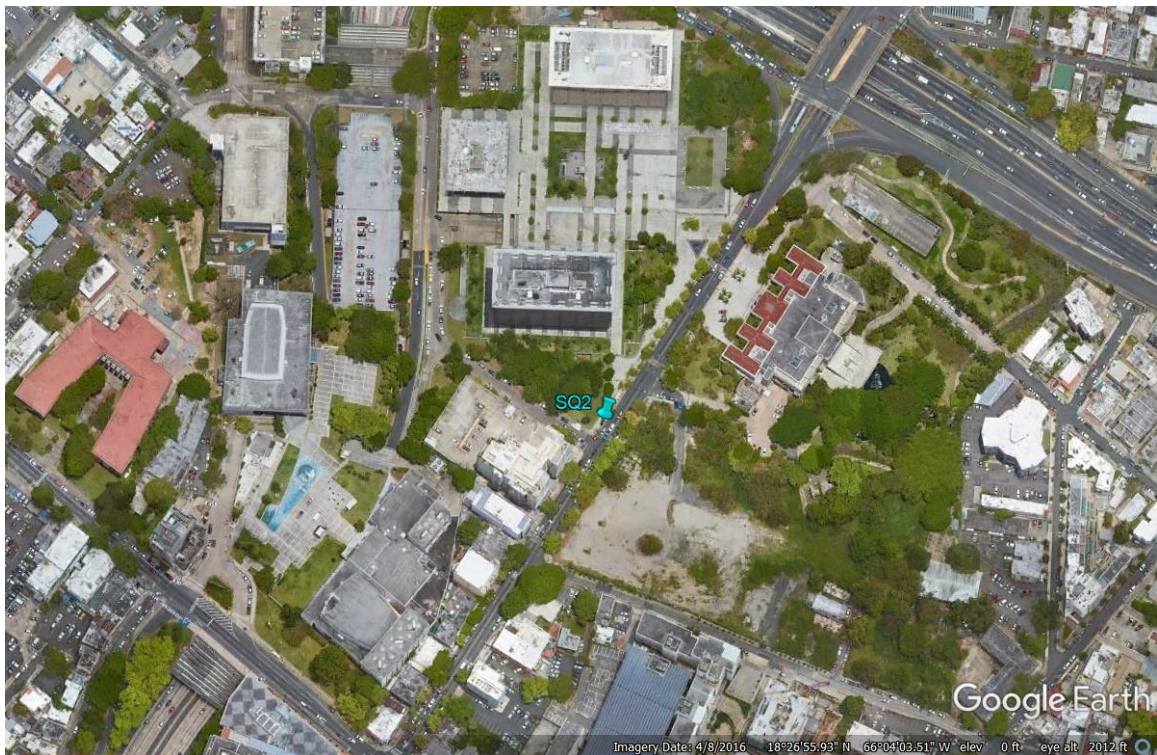


Figure 5.1: Case Study 1 location



Figure 5.2: Case Study 1 front view



Figure 5.3: Case Study 1 side view

Figure 5.4 shows the geometry of the sign structure, including the dimensions of the sign panel and its elevation above ground. Also included is the location of the plastic hinge, that is, the location where the plastic bending deformation occurred in the square tube post.

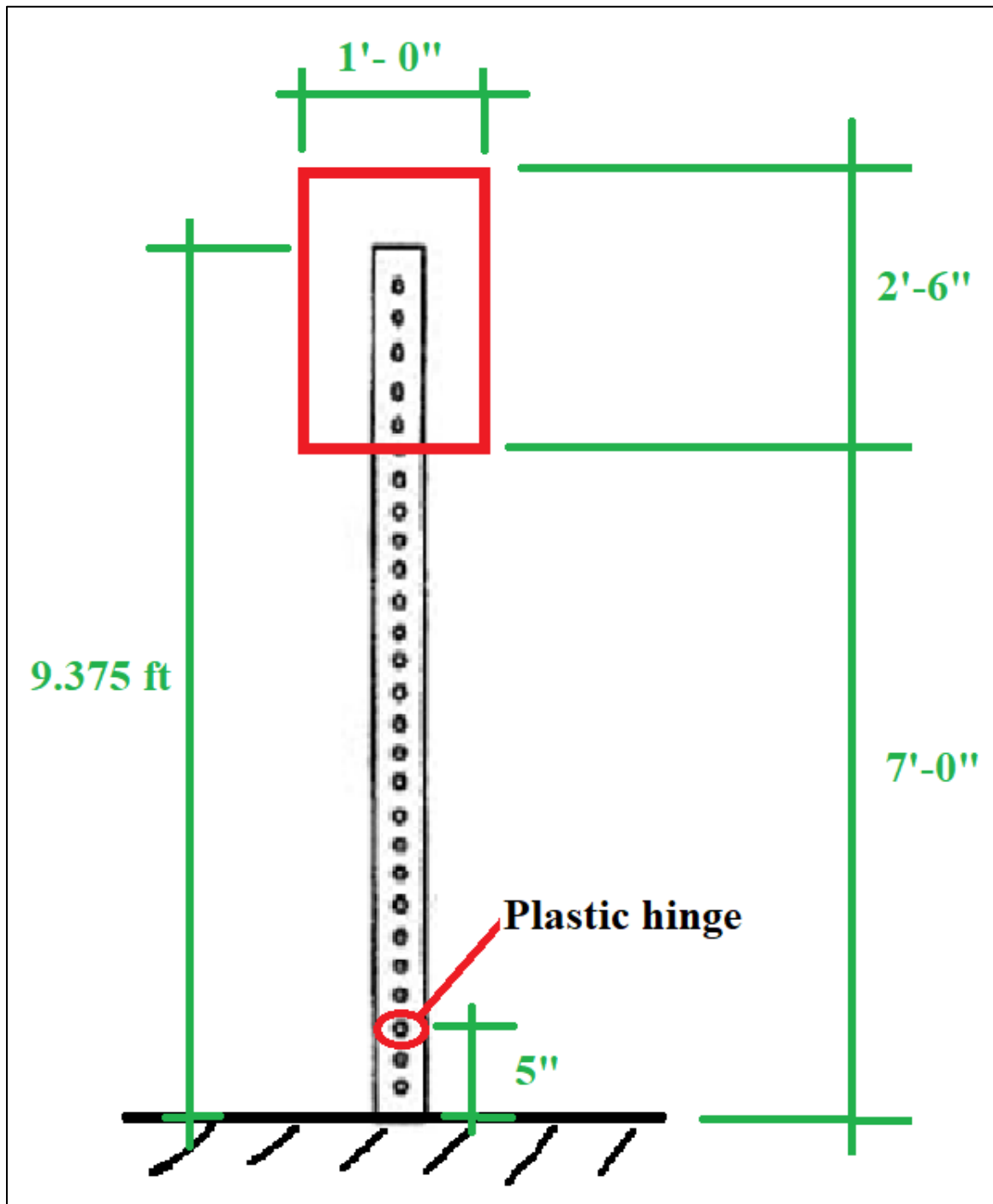


Figure 5.4: Case Study 1 geometry

Figure 5.5 shows the dimensions of the post, which has cross-sectional dimensions of 2-in by 2-in. A thickness of 0.0785 inches was assumed, based on the material indicated on the standard drawings (PRHTA, 2010), as it will be explained later.

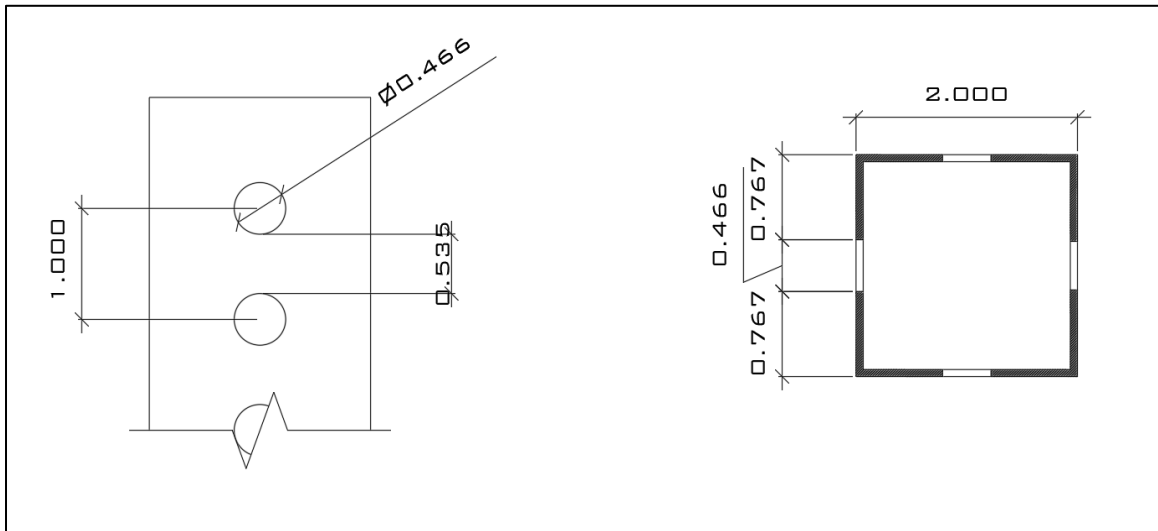


Figure 5.5: Case Study 1 square post dimensions (in inches)

At the time of this writing, the bended post was still in use, so no laboratory tests were conducted to determine the mechanical properties of the material. Therefore, it was assumed that the post was made of ASTM A570 Grade 50 steel, as indicated in Figure 2.12. Therefore, the following mechanical properties were assumed:

- Galvanized steel with gauge 14 (thickness of 0.0785 in)
- Modulus of Elasticity: 29,000,000 psi
- Ultimate Stress: 65,300 psi
- Yielding Stress: 50,000 psi
- Bulk Modulus: 23,200 ksi
- Shear Modulus: 11,600 ksi
- Poisson's ration: 0.30
- Weight: 1.99 lb/ft

5.2. Plastic Moment

RISA Section was used to compute the geometric properties of the post including area, moment of inertia, and plastic section modulus. The results are shown in Figure 5.6.

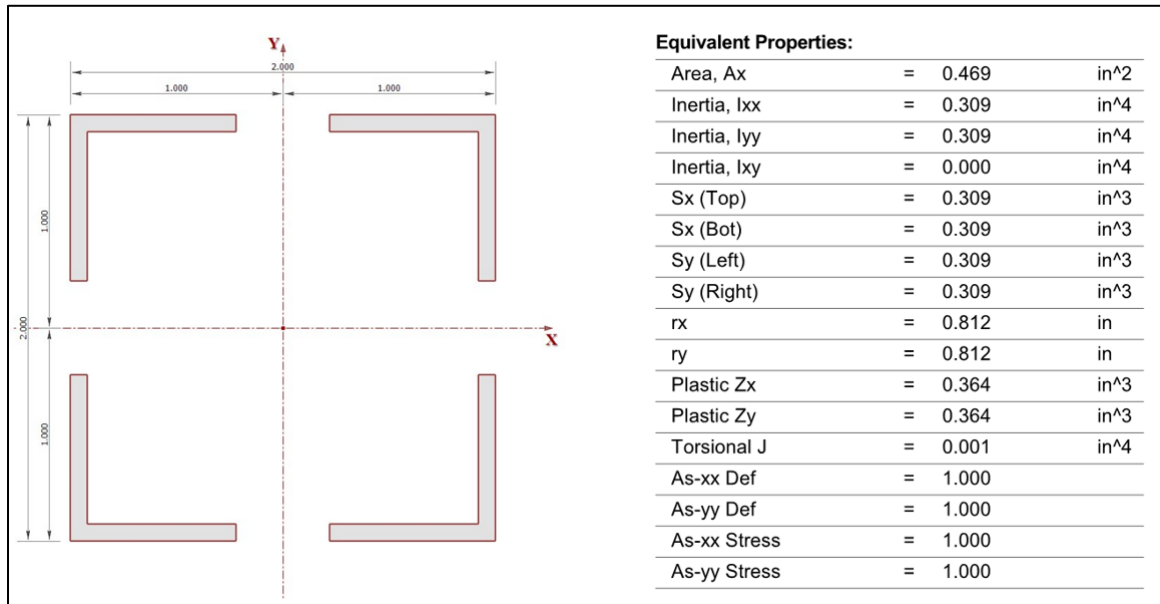


Figure 5.6: Case Study 1 square post section properties

The plastic moment is the bending moment that would produce the plastic hinge in the cross section. To determine the plastic moment, the weakest cross-sectional area of the tube was used, which is the area where the holes are. For the calculation of the plastic moment, the following equation was used (AISC, 2017):

$$M_p = F_y Z_x \quad (5-1)$$

where:

M_p = plastic moment

F_y = yield stress

Z_x = plastic section modulus

Applying Equation (5-1) to Case Study, the plastic moment is estimated as:

$$M_p = (50,000 \text{ psi})(0.364 \text{ in}^3) = 18,200 \text{ lb} \cdot \text{in} = 1,517 \text{ lb} \cdot \text{ft}$$

The Autodesk Inventor software was used for the development of the finite element analysis to verify the plastic moment previously calculated. A 3D model was created, with the data derived from the field visit and the information provided by standard drawings (PRHTA, 2010). Once the 3D model was developed, the post was assessed using the Autodesk Inventor finite element analysis tool.

In this case, a static structural model was prepared, which is commonly used to determine displacements, stress, strains, and forces in the components of a structure. Then, the material properties of the post were defined as a structural steel with a yielding stress of 50,000 psi, an ultimate stress of 65,300 psi, a Poisson's ratio of 0.3, and an elastic modulus of 29,000 ksi, as shown in Figure 5.7.

A mesh was developed to estimate deformation. In addition, fixed edge conditions were applied to the lower base of the post. A uniform pressure of 5 psi (see Figure 5.8) was applied directly to the top 27 inches of the post, as shown in Figure 5.9. The pressure load was applied directly to the post, i.e., the sign panel was not considered. Figure 5.10 shows the edge fixed condition applied in the software. Figure 5.11 presents the stresses produced by the 5-psi pressure load (the load shown in the figure is the resultant force of the pressure). It can be seen that this load produces a stress of 53.76 ksi, which is greater than the 50 ksi yield stress of the post material.

The pressure load was varied using a scale factor, as shown in Figure 5.12. In the graph it can be seen that a scale factor of 0.8 produces a change in the slope of the graph. This change represents the point where the plastic deformation starts. Therefore, the pressure that would produce the plastic moment is estimated as:

$$p = (0.8)(5 \text{ psi}) = 4 \text{ psi}$$

The area over which this pressure acts is estimated as the gross area over which the pressure acts, minus the holes over the same area:

$$A = (27 \text{ in})(2 \text{ in}) - \frac{\pi}{4}(0.466 \text{ in})^2(27 \text{ holes}) = 49.395 \text{ in}^2$$

Therefore, the resultant force is estimated as:

$$F = pA = (4 \text{ psi})(49.395 \text{ in}^2) = 197.58 \text{ lb}$$

This resultant force should act near the center of the 27" length shown in Figure 5.9.

Therefore, the moment arm of the resultant force with respect to the base of the post is estimated as:

$$d = 9.375 \text{ ft} - \frac{(27/12) \text{ ft}}{2} = 8.25 \text{ ft}$$

Material

Select Material

Name: Steel 55-415

ID: 3

Type: Isotropic

Sub Type: Neo-Hookean

Idealizations: Solid 1

Save New Material

Analysis Specific Data

Nonlinear (on)

Fatigue

PPFA

General

P: 0.00073454

GE: 0

T_{REF}

Structural

E: 2.9002e+7

G: 1.16e+7

v: 0.3

α: 6.6667e-6

Allowables

S_T: 65300

S_C

S_S

S_y: 50000

Failure Theory: von Mises Stress


Thermal

C: 46.083

K: 0.00060186

OK Cancel

Figure 5.7: Material properties defined in the FE analysis

 Load ? ×

Name:

ID:

Type: ▾

Sub Type: ▾

Selected Entities:

Subcases:

Display Options

Size:

Density:

Color:

Load Definition

Direction:

▾

Magnitude (psi):

Figure 5.8: Load defined in the FE analysis

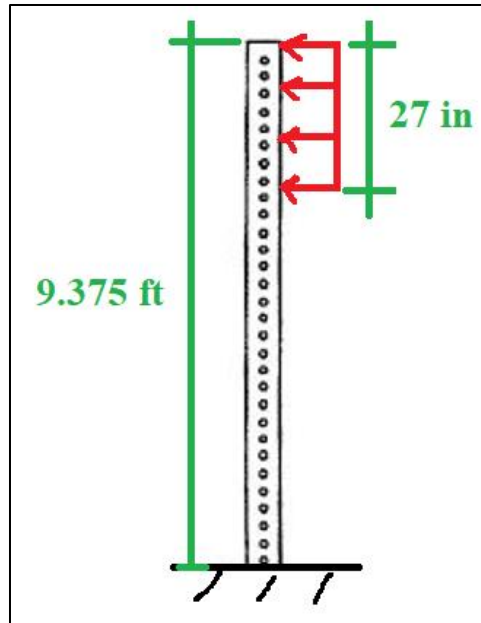


Figure 5.9: Load application in FE model

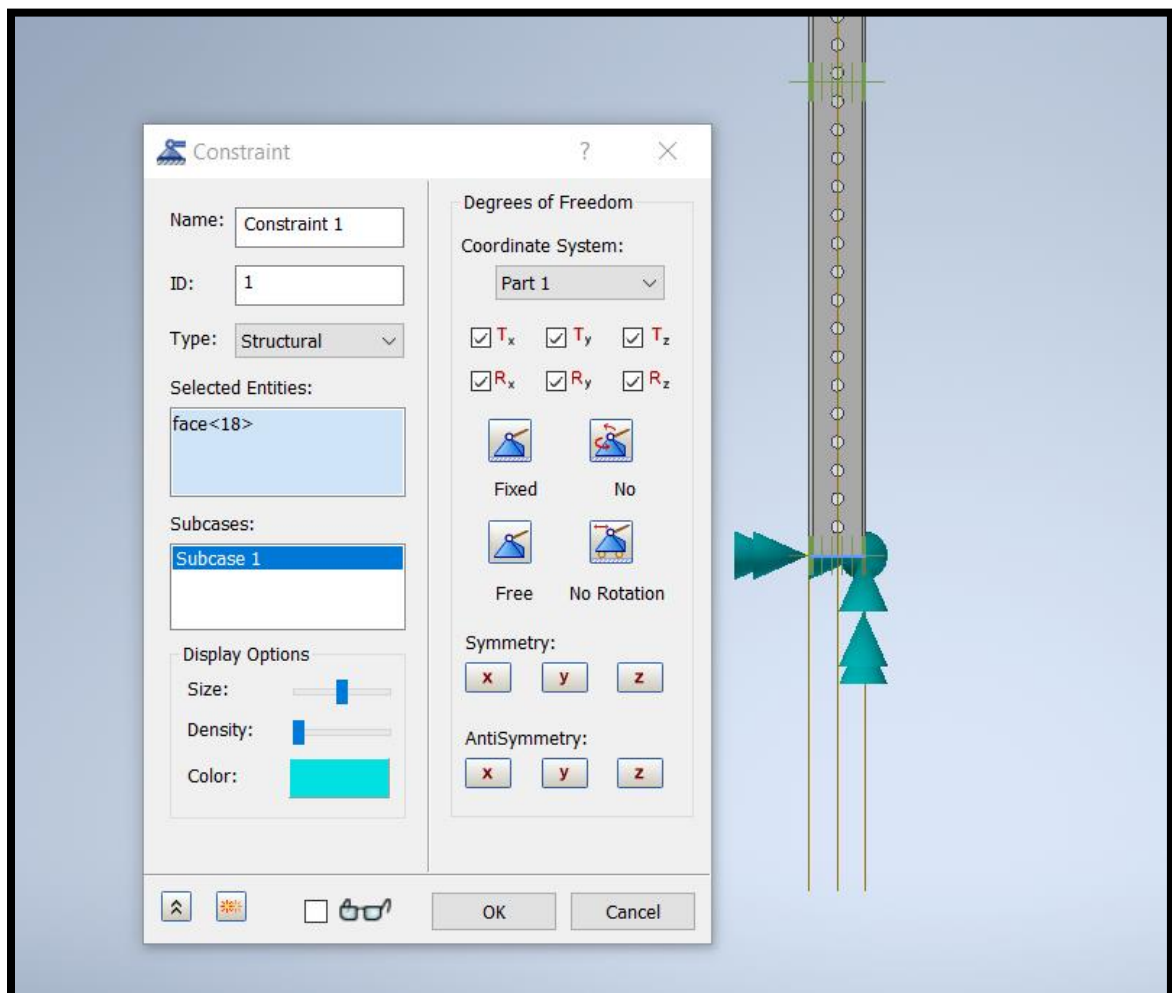


Figure 5.10: Constraints applied in the FE analysis

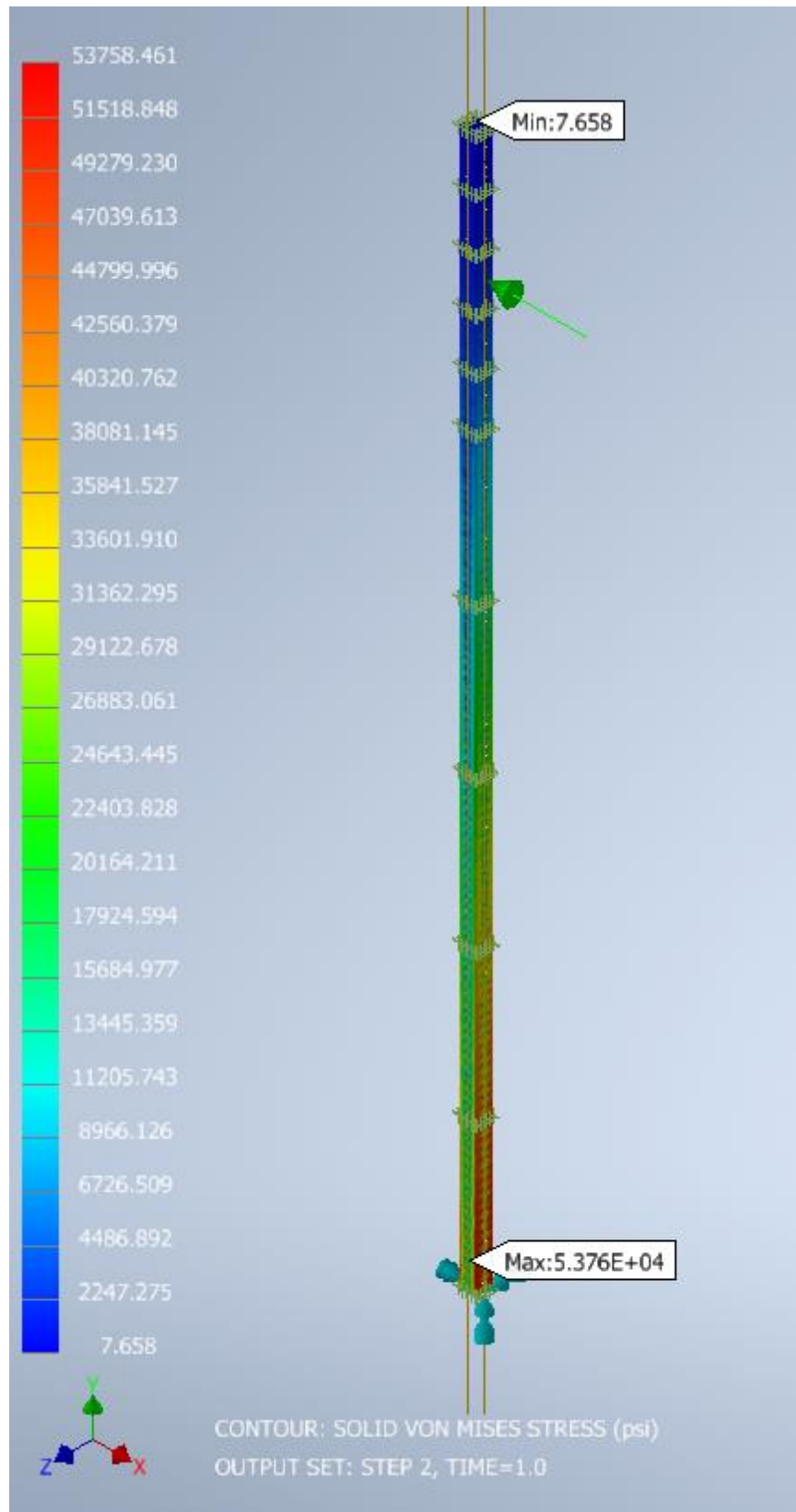


Figure 5.11: Maximum stress and deformation calculated in the FE analysis

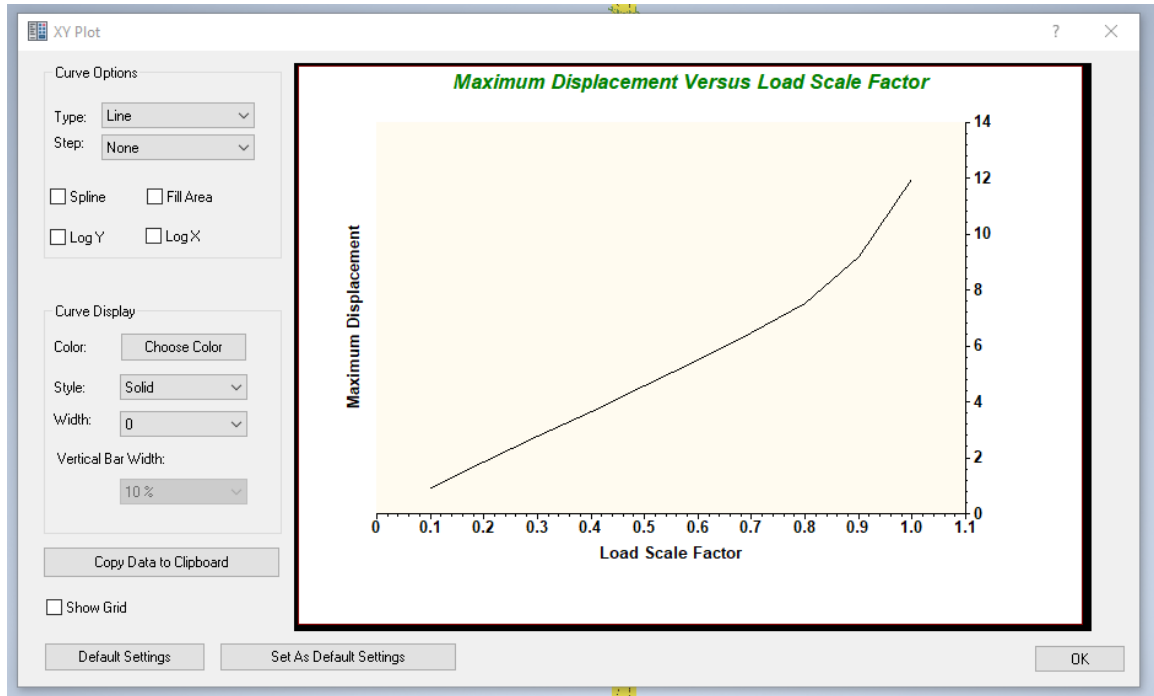


Figure 5.12: Maximum displacement vs. load scale factor of FE analysis

Finally, with the resultant force and the moment arm, the plastic moment is estimated as:

$$M_p = Fd = (197.58 \text{ lb})(8.25 \text{ ft}) = 1,630 \text{ lb} \cdot \text{ft}$$

This plastic moment estimate has a percentage difference of 7% with respect to the value calculated using Equation (5-1). This value is considered low; therefore, the estimated plastic moments are acceptable.

5.3. Wind speed estimate – first scenario

The model adopted for the failure mechanism consists of estimating the force that would produce the estimated plastic moment at the location where the plastic hinge was found, as shown in Figure 5.13. The force is estimated as:

$$F = \frac{M_p}{d} \quad (5-2)$$

This model only considers the wind loads acting on the sign panel. It disregards the effect of the wind loads on the post.

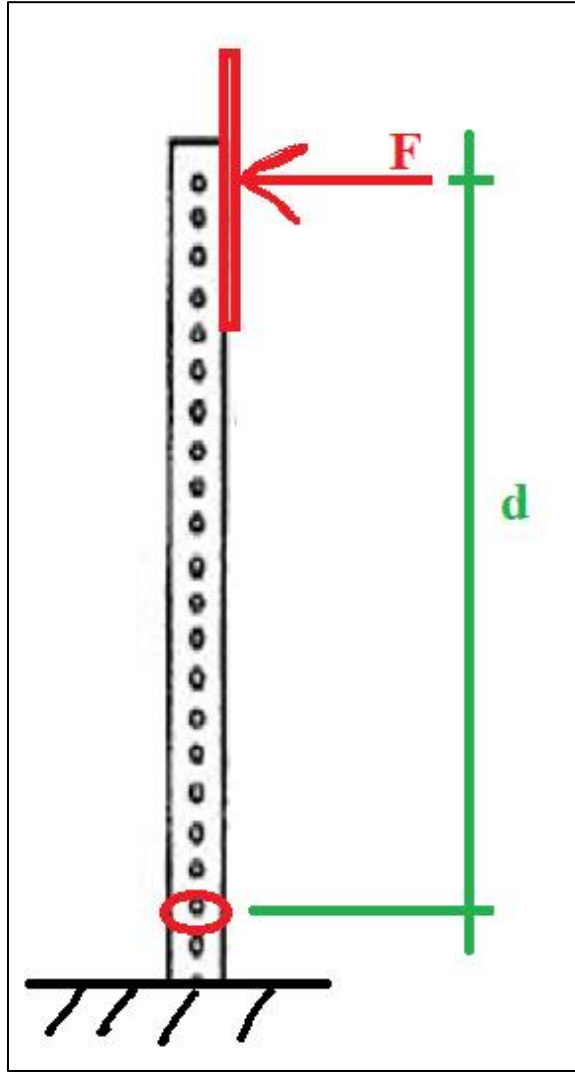


Figure 5.13: Failure model for wind speed estimate, first scenario

Equating (2-2) with (5-2), and solving for the basic wind speed, the following equation is obtained:

$$V = \sqrt{\frac{M_p}{0.00256K_zK_{zt}K_dK_eGC_fA_s d}} \quad (5-3)$$

Considering the effect of the ground elevation above sea level of the sign location would yield higher wind speed estimates, therefore $K_e = 1$ was conservatively assumed. Also,

since K_d is a factor that considers the reduced probability of maximum winds coming from any given direction and of the maximum pressure coefficient occurring for any given wind direction, it was also conservatively assume to be equal to one. Therefore, for this project, Equation (5-3) reduces to:

$$V = \sqrt{\frac{M_p}{0.00256K_zK_{zt}GC_fA_sd}} \quad (5-4)$$

To estimate the wind speed that caused the plastic bending in Case Study 1, Equation (5-4) was used with the following values:

- Of the two plastic moment values estimated in Section 5.2, the lower value ($M_p = 1,517 \text{ lb} \cdot \text{ft}$) was used to be more conservative.
- Since the sign was located in an urban area, therefore, Exposure B was assumed and a value of $K_z = 0.57$, which is the value given by the ASCE Standard for structures with a height of less than 15 ft.
- To verify if there were any topographic effects on this location, the ATC Hazard by Location website was used. For the sign location, for Risk Category I, the website indicated basic wind speeds of 161 mph and 150 mph for the Puerto Rico Building Code (PRBC) and the ASCE Standard, respectively. The PRBC includes the effects of topographic wind speed-ups. Therefore:

$$K_{zt} = \frac{161^2}{150^2} = 1.152$$

- The structure has a fundamental period of less than 1 s. Therefore, the structure is considered rigid. The gust effect factor (G) was calculated using

Equation 26.11-6 of the ASCE Standard, considering the Exposure B condition. It was estimated that $G = 0.904$.

- The net force coefficient (C_f) was calculated according to the ASCE's Case A, as discussed in Section 2.4. Using the geometry presented in Figure 5.4, a value of $C_f = 1.817$ was obtained.
- The area of the sign panel is:

$$A_s = (2.5 \text{ ft})(1 \text{ ft}) = 2.5 \text{ ft}^2$$

- Referring to Figure 5.4 and Figure 5.13, the moment arm with respect to the plastic hinge is:

$$d = 9.5 - \frac{2.5}{2} - \frac{5}{12} = 7.833 \text{ ft}$$

Therefore, the gust wind speed that is estimated to have caused the plastic bending in Case Study 1 is:

$$V = 168 \text{ mph}$$

As mentioned before, this estimate disregards the effects of wind loads on the post.

5.4. Wind speed estimate – second scenario

A second scenario was evaluated in which the wind loads acting on the post were considered, as shown in Figure 5.14. In this scenario, plastic moment is calculated as follows:

$$M_p = F_1 d_1 + F_2 d_2 \quad (5-5)$$

In Equation (5-5), each of the forces F_1 and F_2 can be calculated using Equation (2-2) as follows:

$$F_1 = 0.00256 K_z K_{zt} K_d K_e G V^2 C_f A_s \quad (5-6)$$

$$F_2 = 0.00256K_zK_{zt}K_dK_eGV^2C_{fp}A_p \quad (5-7)$$

In Equation (5-7), C_{fp} and A_p correspond to the force coefficient and the project area of the post, respectively.

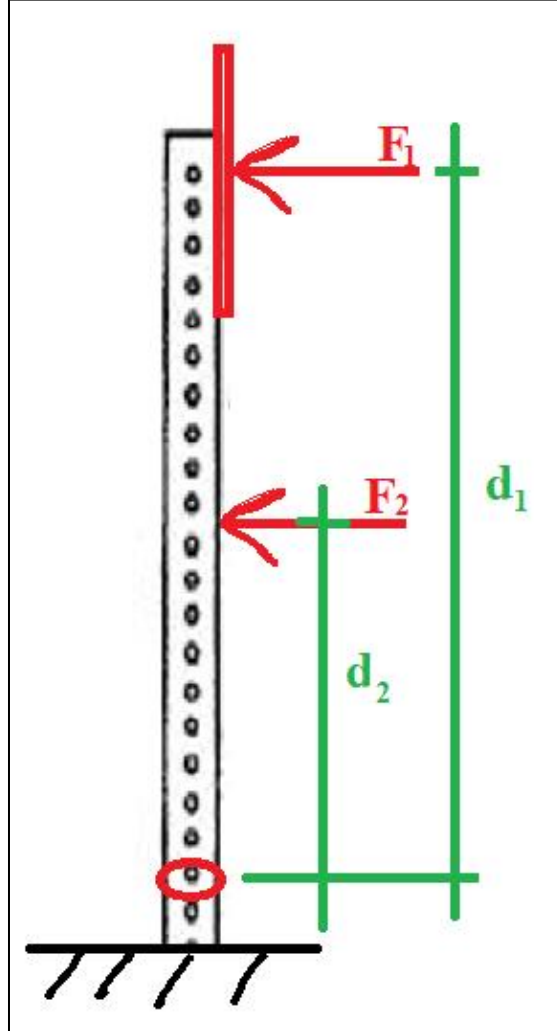


Figure 5.14: Failure model for wind speed estimate, second scenario

Substituting Equations (5-6) and (5-7) into Equation (5-5), and solving for the wind speed:

$$V = \sqrt{\frac{M_p}{0.00256K_zK_{zt}K_dK_eG(C_fA_sd_1 + C_{fp}A_pd_2)}} \quad (5-8)$$

Like before, K_d and K_e are equal to one, therefore:

$$V = \sqrt{\frac{M_p}{0.00256K_zK_{zt}G(C_fA_sd_1 + C_{fp}A_pd_2)}} \quad (5-9)$$

To estimate the wind speed that caused the plastic bending in Case Study 1, Equation (5-9) was used with the following values:

- The following were taken from the previous scenario:
 - $M_p = 1,517 \text{ lb} \cdot \text{ft}$
 - $K_z = 0.57$
 - $K_{zt} = 1.152$
 - $G = 0.904$
 - $C_f = 1.817$
 - $A_s = 2.5 \text{ ft}^2$
 - $d_1 = 7.833 \text{ ft}$
- Using Figure 29.4-1 of the ASCE Standard, the force coefficient of the post was estimated as $C_{fp} = 2.0$. This value is conservative because it does not consider that the post has holes.
- The projected area of post is:

$$A_p = \left(7 \text{ ft} - \frac{5}{12} \text{ ft}\right) \left(\frac{2}{12} \text{ ft}\right) = 1.097 \text{ ft}^2$$

- Referring to Figure 5.4 and Figure 5.14, the moment arm with respect to the plastic hinge is:

$$d = \frac{7 - 5/12}{2} = 3.292 \text{ ft}$$

Therefore, the gust wind speed that is estimated to have caused the plastic bending in Case Study 1 is:

$$V = 153 \text{ mph}$$

It is relevant to remember that this analysis disregards the presence of the holes on the post, meaning that it overestimates the drag force that the wind produced on the post. Still, this estimate is higher than most of those done by other studies, as discussed in Section 2.1.

5.5. Analysis of Post with Larger Cross Section

A square tube with 2.5-in by 2.5-in cross section was analyzed. The purpose was to determine if a 2.5-in tube had been used instead of a 2-in tube for Case Study 1, how high would the gust wind speed have to have been in order to cause the plastic bending. The 2.5" tube is available with a thickness of 0.109 in.

Like before, RISA Section was used to compute the geometric properties of the post including the plastic section modulus. Using Equation (5-1), the plastic moment was computed as:

$$M_p = (50,000 \text{ psi})(0.643 \text{ in}^3) = 32,150 \text{ lb} \cdot \text{in} = 2,679 \text{ lb} \cdot \text{ft}$$

With this value, the wind speed were estimated using Equations (5-4), which only considers wind loads on the sign; and Equation (5-9), which considers wind loads on the sign and post, although it disregards that the post has holes. The results are shown in Table 5.1. It can be seen that increasing the size of the tube would significantly increase the resistance to wind loads.

Table 5.1: Wind speed estimate comparison for different tubes

Scenario	2" tube	2.5" tube
Sign and post	153 mph	203 mph
Sign only	168 mph	223 mph

6. Case Study 2: U-Channel with Permanent Twisting Deformation

This chapter presents a case study of a U-channel post supporting a transit sign. The post demonstrated a permanent twisting deformation probably due to lateral torsional buckling. Two hypotheses were evaluated to estimate the gust wind speed that caused this deformation.

6.1. Description

The second case study concerns a sign supported by a U-channel post which was identified as U42 for this project. The post was located in the sector of Hato Rey in the municipality of San Juan, in the vicinity of the Polytechnic University of Puerto Rico (PUPR), as illustrated in Figure 6.1. It can be seen that the sign was located in an urban area.

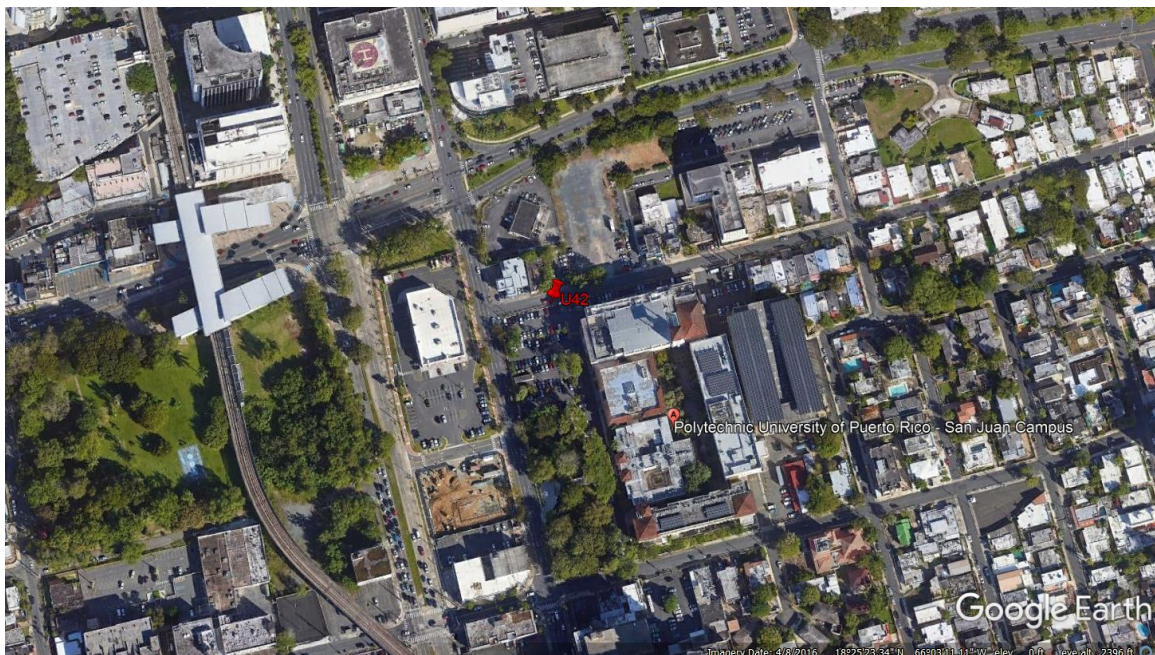


Figure 6.1: Case Study 2 location

Figure 6.2 shows the condition of the sign on February 2016, over a year before Hurricane Maria made landfall in Puerto Rico. This image was obtained using Google Street

View. It can be seen that the post supported a School Zone Speed Limit sign panel. Although the post appears to have been somewhat tilted, the post does not exhibit permanent twisting deformation.

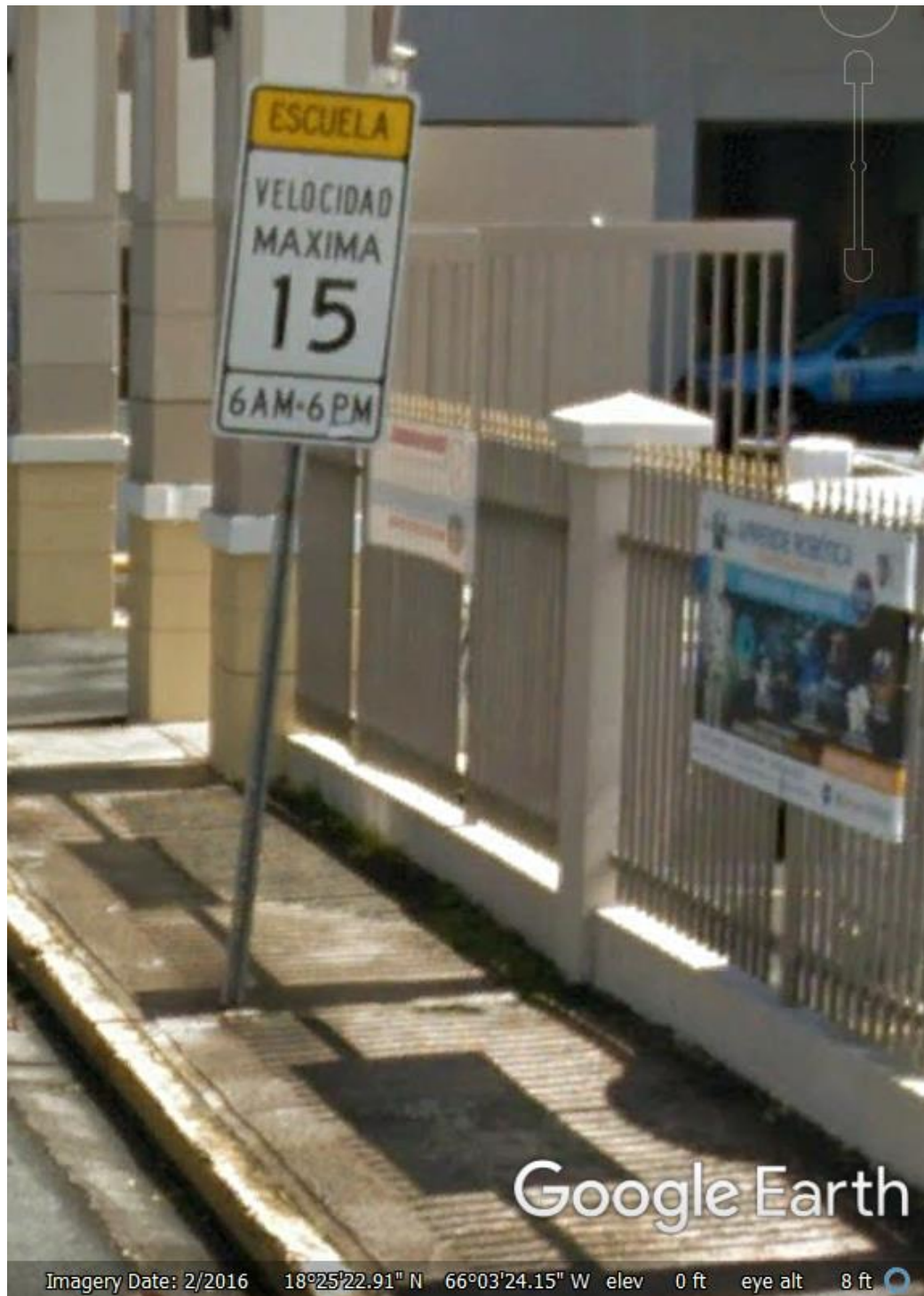


Figure 6.2: Case Study 2 before Hurricane Maria

Figure 6.3 shows a back view of the sign structure before the passing of Hurricane Maria. The change in color of the post is due to two U-channels being connected together. The darker U-channel at the top should have been the base post, while the lighter channel should have been the top post. In other words, the post assembly was incorrectly installed upside down.

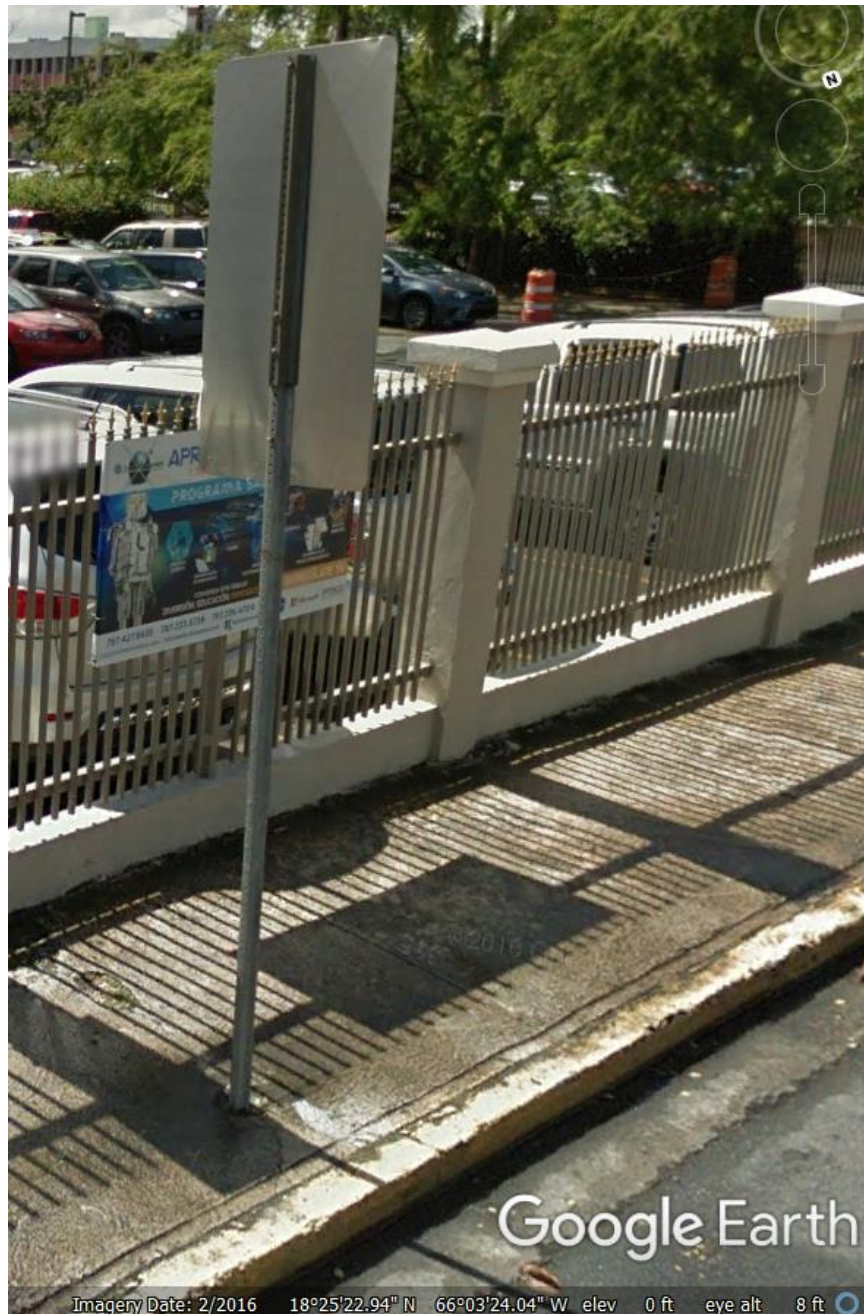


Figure 6.3: Back view of Case Study 2 before Hurricane Maria

After hurricane Maria, the post was found without the transit sign, as shown in Figure 6.4. Therefore, it was concluded that the sign panel was blown away during the hurricane. It can be noticed in the figure that the post exhibits permanent twisting deformation near its base.



Figure 6.4: Case Study 2 after Hurricane Maria

The post was eventually uninstalled and left on the sidewalk, where it was recovered by PUPR, as shown in Figure 6.5. This allowed the taking of measurements, as well as the extraction of samples to conduct laboratory tests, as it will be explained later.



Figure 6.5: U-channel post assembly at laboratory

Figure 6.6 shows how the post was installed. What should have been the base post measured 2'-3" and what should have been the top post measured 10'-9". The two posts had an overlap of 9 in, therefore, the total length of the post assembly was 12'-3". The measurement of 2'-0" at the bottom indicate the part of the post that was underground.

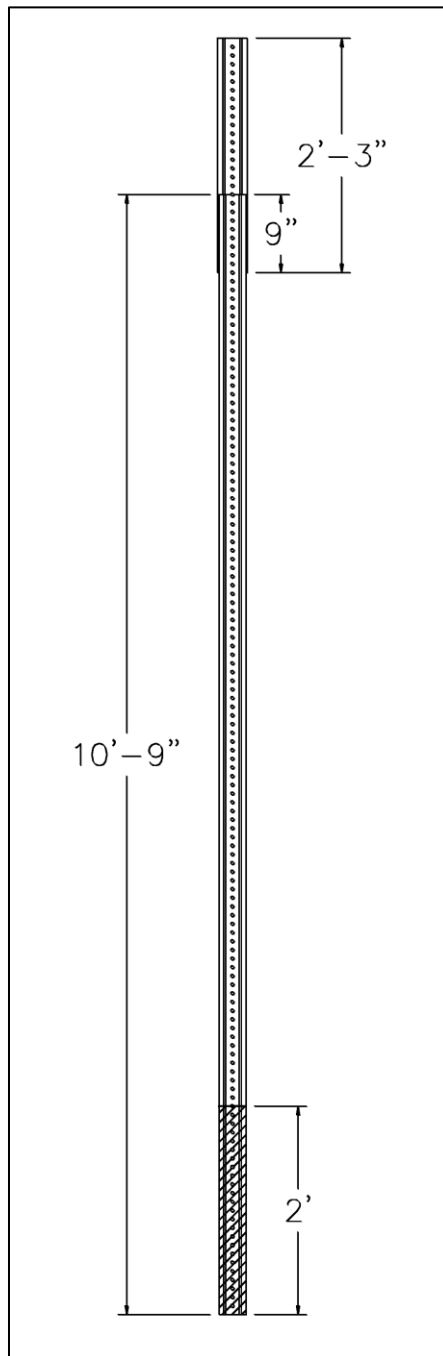


Figure 6.6: U-channel post assembly longitudinal dimensions

Figure 6.7 shows the dimensions of the cross-sectional areas of the post assembly, as measured in the laboratory. In this figure, Section 1 corresponds to what should have been the base post and Section 2 corresponds to what should have been the top post.

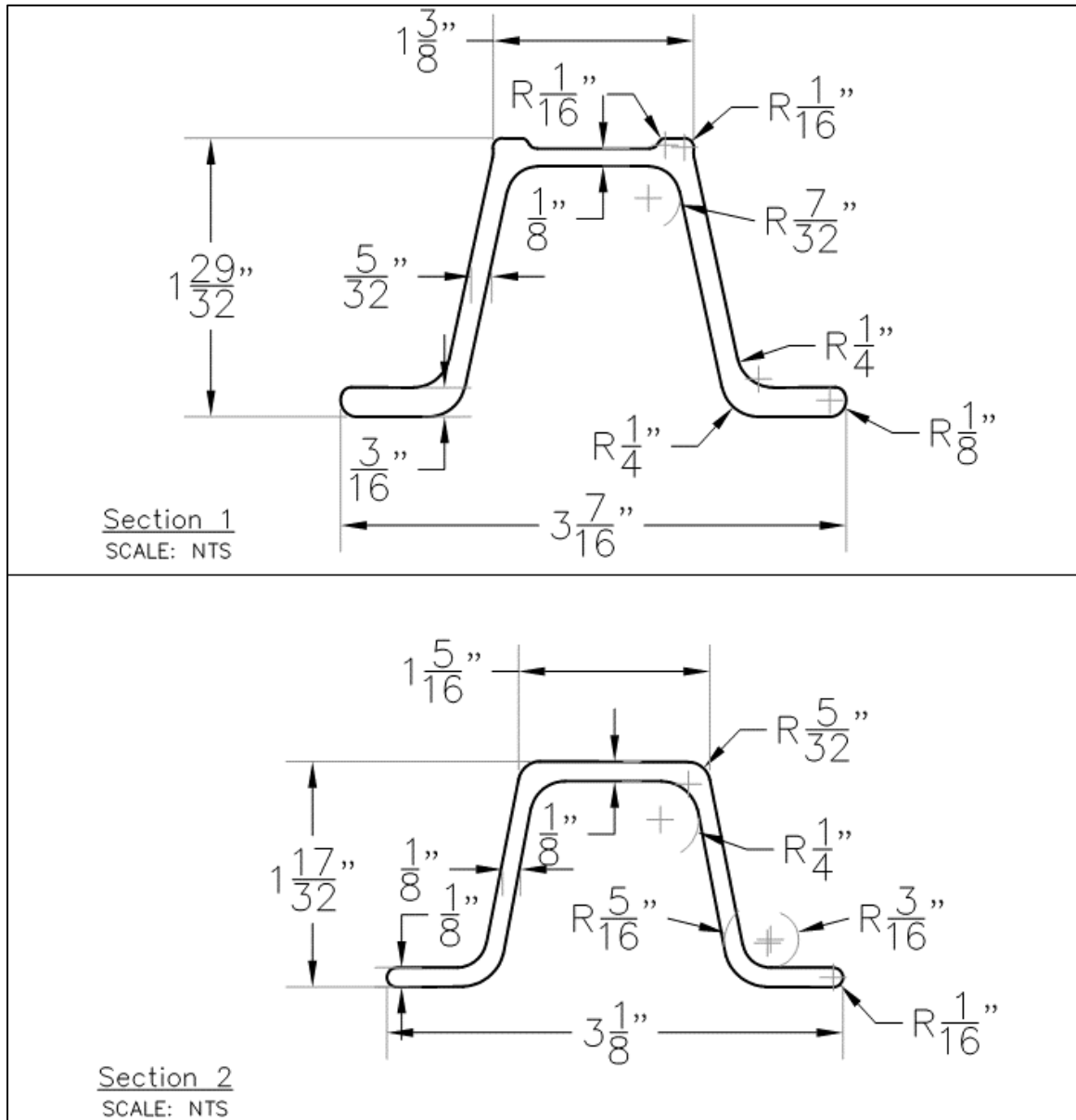


Figure 6.7: U-channel cross-sectional dimensions

6.2. Laboratory Tests

To estimate the material properties, six specimens were obtained from the U-channel using a waterjet cutting machine. This machine was used so that the properties of the

material remained unaffected. The specimens were cut in accordance with ASTM E1575 Standard Practice for Pressure Water Cleaning and Cutting, to then be subjected to tensile tests. Figure 6.8 presents the six specimens, (specimens 1 to 3 had already been tested in tension at the time of the photo). Before the tension test, each specimen was measured for thickness, length, and width; each dimension was taken in three places and then averaged. The results of these measurements are presented in Table 6.1.



Figure 6.8: Specimens extracted from U-channel post

Table 6.1: Dimensions of specimens

Specimen ID	Width (in)	Thickness (in)	Area (in ²)
1	0.4978	0.1243	0.0619
2	0.4980	0.1173	0.0584
3	0.5043	0.1205	0.0608
4	0.4992	0.1173	0.0586
5	0.5033	0.1178	0.0593
6	0.5122	0.1880	0.6090

Each specimen was subjected to a tensile test using a universal testing machine, as shown in Figure 6.9. From these tests, the yield stress and the ultimate stress of each specimen were obtained, as shown in Table 6.2. (The analysis for Specimen 3 was not completed due to technical difficulties.) The results show Specimens 1, 2 and 5 had similar yield stress values, while Specimens 4 and 6 far from the norm, therefore they were removed from this analysis. Consequently, an average yield stress of 83.30 ksi was assumed.



Figure 6.9: Universal Testing Machine

Table 6.2: Specimens Yielding and Ultimate Stresses

Specimen ID	Yield Stress (ksi)	Ultimate Stress (ksi)
1	82.55	138.69
2	84.15	142.64
3	N/A	N/A
4	90.56	136.1
5	83.21	133.40
6	74.05	125.94

6.3. First Hypothesis – Wind Parallel to Sign Panel

The hypothesis considered for Case Study 2 is based on how the post is affected when the wind has a direction parallel to the sign panel, as shown in Figure 6.10. The analysis considers the possibility that the wind applied along the post produced a failure due to lateral torsional buckling. Since the post has a permanent deformation without rupture, it is considered that the failure was due to plastic yielding. Therefore, a non-linear plastic analysis was conducted.

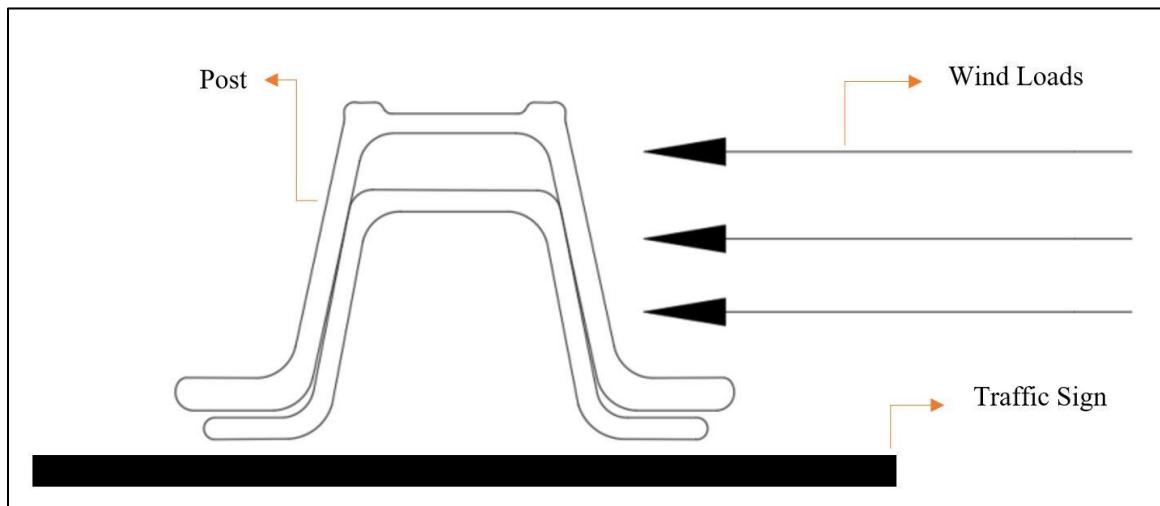


Figure 6.10: Wind loads applied in the parallel to the sign panel

Similar to the Case Study 1, a finite element model was developed using Autodesk's Inventor software, as shown in Figure 6.11. The model disregarded the presence of what should have been the base post. The model had the cross-sectional dimensions of what

should have been the top post, (Section 2 in Figure 6.7). The post was modeled with a total height of 12.25 ft, with the bottom 2ft restricted from displacing, to simulate the segment of the post that was underground.

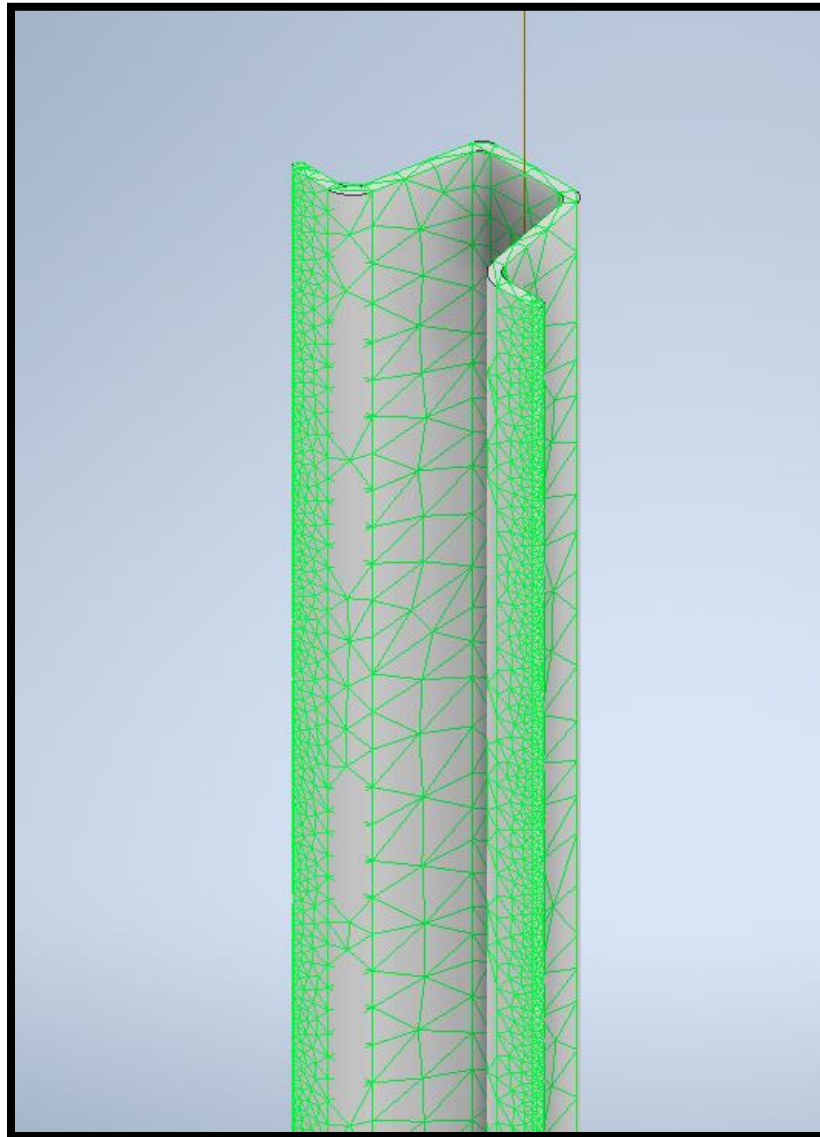


Figure 6.11: Mesh generated for U-Channel

A lateral pressure load was applied to the side of the post. It was found that with a load of 2 psi, the FE model exhibited a combination of deflection and twisting similar to the behavior of Case Study 2. This lateral pressure produced a stress of 83.07 ksi at the support, as shown in Figure 6.12. This value is close to the yield stress determined in the

tension tests. Therefore, it was assumed that a higher load would lead the post to have permanent and irreversible damage.

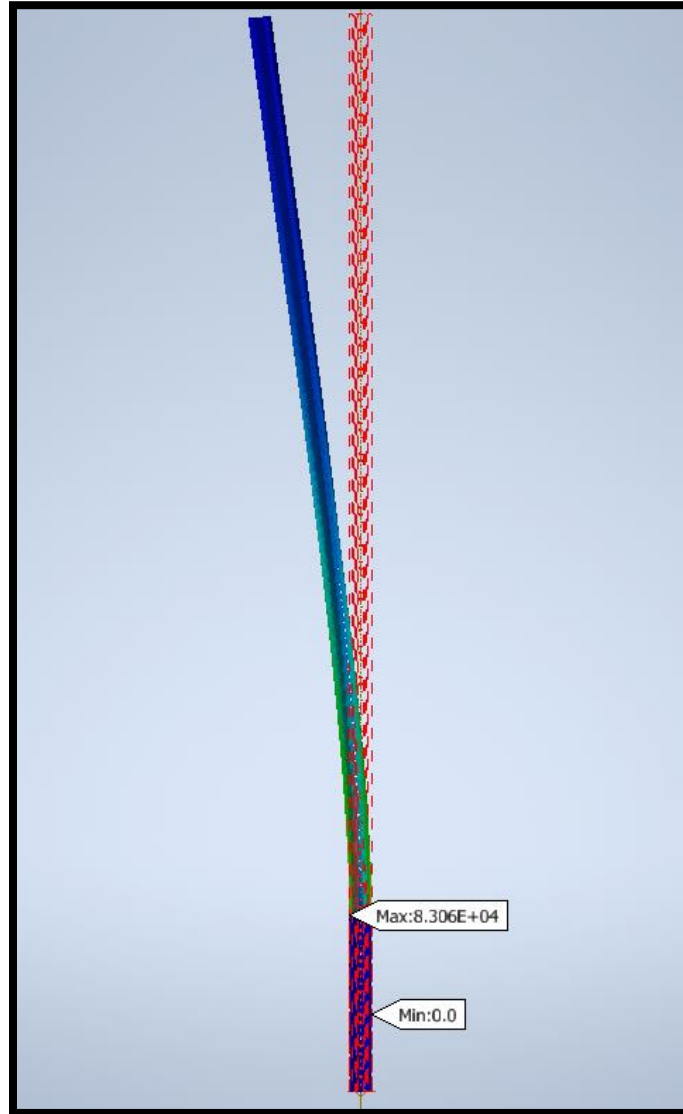


Figure 6.12: U-channel deformation under applied wind loads

To estimate the wind speed that cause the permanent twisting deformation, since only loads in the post are being considered, Equation (5-7) may be used. Solving for the basic wind speed:

$$V = \sqrt{\frac{F_2}{0.00256K_zK_{zt}K_dK_eGC_{fp}A_p}} \quad (6-1)$$

Like done for Case Study 1, it is taken that $K_e = 1$ and $K_d = 1$. Also, the lateral pressure applied to the post is made equal to F_2/A_p . Therefore, Equation (6-1) simplifies to:

$$V = \sqrt{\frac{p}{0.00256K_zK_{zt}GC_{fp}}} \quad (6-2)$$

where p represents the lateral pressure on the post in pounds per square feet.

To estimate the wind speed that caused the permanent twisting deformation in Case Study 2, Equation (6-2) was used with the following values:

- In accordance with the results of the FE analysis, $p = 2 \text{ psi} = 288 \text{ lb/ft}^2$.
- Since the sign was located in an urban area, therefore, Exposure B was assumed and a value of $K_z = 0.57$, which is the value given by the ASCE Standard for structures with a height of less than 15 ft.
- To verify if there were any topographic effects on this location, the ATC Hazard by Location website was used. For the sign location, for Risk Category I, the website indicated basic wind speeds of 148 mph and 150 mph for the Puerto Rico Building Code (PRBC) and the ASCE Standard, respectively. This implies that the value of K_{zt} for this location is less than one. It was conservatively assumed that $K_{zt} = 1$.
- The structure has a fundamental period of less than 1 s. Therefore, the structure is considered rigid. The gust effect factor (G) was calculated using Equation 26.11-6 of the ASCE Standard, considering the Exposure B condition. It was estimated that $G = 0.904$.
- Neither the ASCE Standard nor the AASHTO Specification offer guidance on how to calculate the force coefficient for a U-channel post. The net force

of the wind acting on the side of U-channel should be less than that of a 2-in square tube, as it was assumed for Case Study 1. Therefore, it was assumed that $C_{fp} = 2$.

Therefore, with the first hypothesis, the gust wind speed that is estimated to have caused the permanent twisting deformation in Case Study 2 is:

$$V = 330 \text{ mph}$$

This value is extremely high. It is very unlikely that Hurricane Maria (or any other hurricane) produced such a high gust speed. Therefore, the first hypothesis was rejected.

6.4. Second Hypothesis – Wind Perpendicular to Sign Panel

The second hypothesis evaluated was based on research by Rhee, Nevill & Lombardo (2022). They used the failure of signs supported by U-channels to estimate the wind speed of an EF-3 tornado that occurred in February 2017 in Naplate, Illinois. They noticed that the U-channel posts twisted near the base, similar to the permanent twisting deformations documented in this project due to Hurricane Maria. They conducted three-point bending moment tests on U-channel posts and noticed that the section twisted, suggesting that the posts failed due to lateral torsional buckling. The maximum moment they obtained on the experimentation was larger than the yield bending moment.

For the calculation of the yield bending moment, the following equation was used (AISC, 2017):

$$M_y = F_y S_x \quad (6-3)$$

where:

M_y = yield bending moment

F_y = yield stress

S_x = section modulus

From Figure 6.13, verifying that the measurements of post in the laboratory are very similar to the dimensions listed on the table for the section with a weight of 2 lb/ft, a section modulus of $S_x = 0.23 \text{ in}^3$ was selected. Therefore, using the yield stress value obtained through experimentation, the yield bending moment of the post of Case Study 2 is estimated as:

$$M_y = (83,300 \text{ psi})(0.23 \text{ in}^3) = 19,159 \text{ lb} \cdot \text{in} = 1,597 \text{ lb} \cdot \text{ft}$$

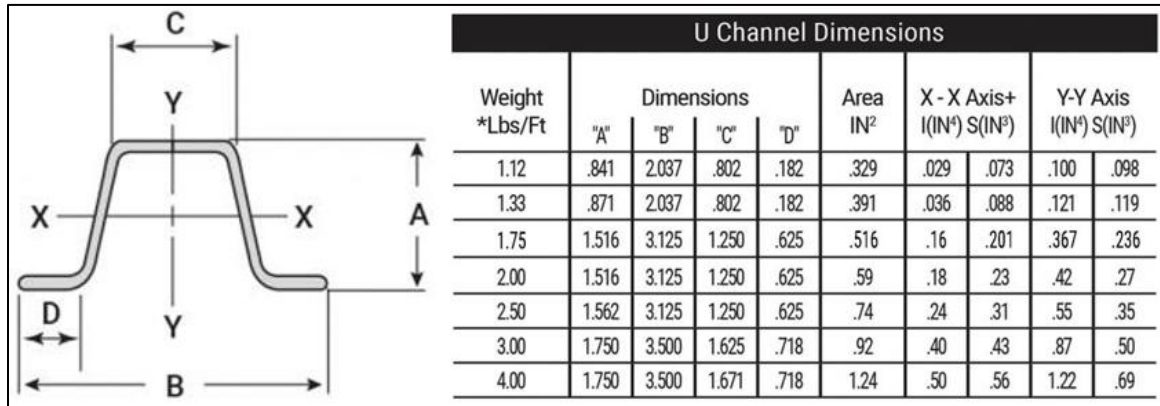


Figure 6.13: U-channel dimensions and sectional properties (Franklin Industries, n.d.)

The gust wind speed that caused the failure of Case Study 2 can then be estimated using Equation (5-4) as follows:

- The plastic moment (M_p) in the equation is replaced with yield bending moment (M_y). This is conservative, as the moment that produced the lateral torsional buckling should be higher.
- As explained before, $K_z = 0.57$.
- As explained for the previous hypothesis, $K_{zt} = 1$.
- The structure has a fundamental period of less than 1 s. Therefore, the structure is considered rigid. The gust effect factor (G) was calculated using

Equation 26.11-6 of the ASCE Standard, considering the Exposure B condition. It was estimated that $G = 0.903$.

- Given that then sign panel was not available, its dimensions were estimated using Google Street View. It was estimated that the sign panel had a height of 3ft and a width of 1.5 ft, as shown in Figure 6.14. Also, the top edge of the sign was 1” higher than the top end of the post. The net force coefficient (C_f) was calculated according to the ASCE’s Case A, as discussed in Section 2.4. A value of $C_f = 1.80$ was obtained.

- The area of the sign panel is:

$$A_s = (3 \text{ ft})(1.5 \text{ ft}) = 4.5 \text{ ft}^2$$

- The moment arm was estimated from the base of the post to the center of the sign:

$$d = 10.333 - \frac{3}{2} = 8.833 \text{ ft}$$

The estimated gust wind speed is then:

$$V = 130 \text{ mph}$$

Again, this estimate is very conservative. The failure bending moment obtained by Rhee, Nevill & Lombardo (2022) was 1.28 times larger than the yield bending moment. If that were the case for Case Study 2, the gust wind speed would increase to 147 mph.

These results demonstrate that it is possible that the permanent twisting deformations documented in U-channels for this project were caused by lateral torsional buckling. Still, further research needs to be conducted to reach a definite conclusion, as a combination of flexural and torsional forces may have caused the permanent twisting deformation due to changes in wind direction and eccentricity (Rhee, Nevill, & Lombardo, 2022).

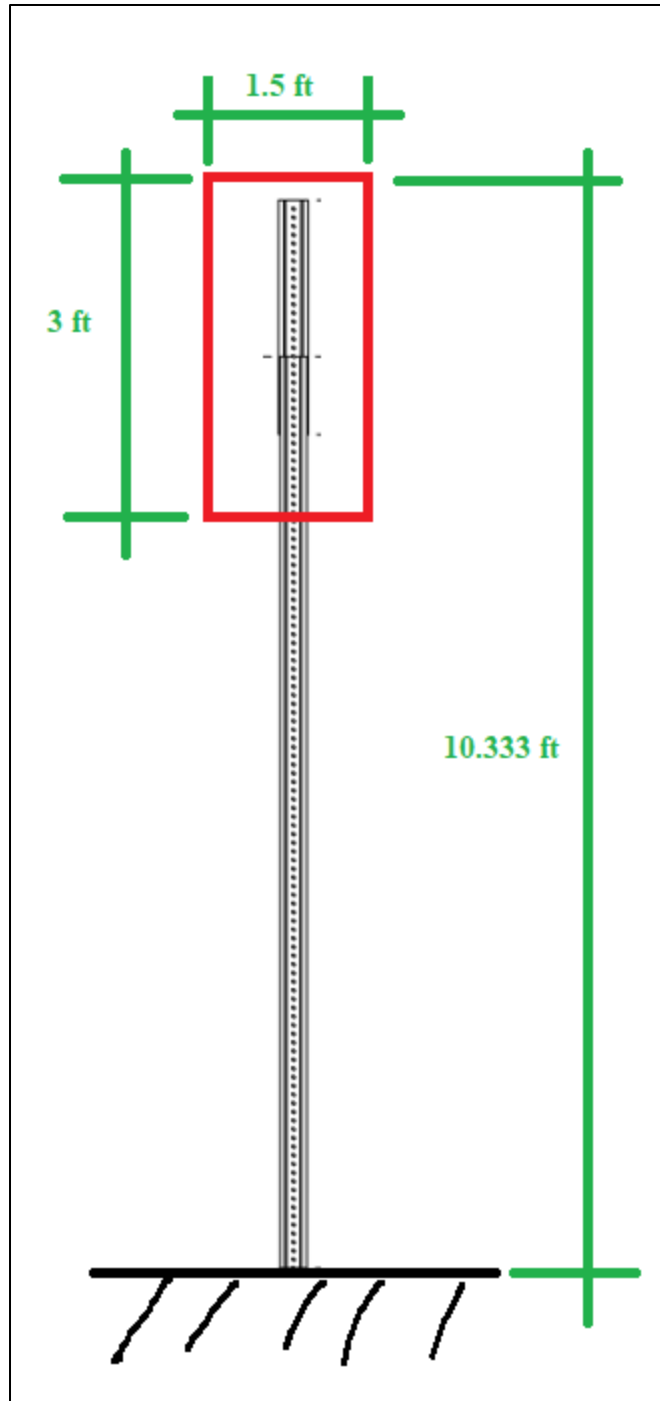


Figure 6.14: Case Study 2 geometry

7. Conclusions and Recommendations

The most important findings of this research are the following:

- It was estimated that a gust wind speed of over 153 mph caused the plastic bending deformation of Case Study 1. This wind speed is higher than the one estimated by FEMA (2018) and by other researchers. This finding reaffirms a conclusion that was presented in Volume 1; that the peak gust speeds that occurred during Hurricane Maria in Puerto Rico may have been underestimated, which may eventually affect the revision of design wind speeds for Puerto Rico.
- Square tubes appeared to have behave better than U-channels during Hurricane Maria. No collapsed square tube was found in this project.
- U-channels supporting small traffic signs appear to be very susceptible to experiencing permanent twisting deformation. Not only was it the most documented mode of failure in this project, but there were cases found to have occurred in Puerto Rico before Hurricane Maria and in places in the US mainland with lower wind speeds.
- The most probable cause of permanent twisting deformation in U-channels is lateral torsional buckling, but there are other possibilities.
- Several failed small traffic signs were found not to meet the standards of the PRHTA.

As a result of the findings of this research, and with the purpose of increasing the resiliency of small traffic signs, the following recommendations are offered:

- Phased out U-channels should be from use in small traffic signs. They should be eliminated from the standard drawings of the PRHTA, and failed and damaged posts should be replaced with square tubes. U-channels may still be used for mile markers.
- Evaluate increasing the size of square tubes from 2-in by 2-in with gauge 14 to 2.5-in to 2.5-in with gauge 12. This will represent an increase in cost of this type of structure, but it would increase their resiliency, which could be more economical eventually.
- Improve control during construction to reduce the possibility of small traffic signs not having foundations that do not meet the requirements of the PRHTA.

References

- AASHTO. (2015). *LRFD Specifications for Structural Supports for Highway Signs, Luminaires, and Traffic Signals* (6th ed.). Washington, DC: American Association of State Highway and Transportation Officials.
- AISC. (2017). *Steel Construction Manual* (15th ed ed.). Chicago: American Institute of Steel Construction.
- ASCE. (2017). *Minimum design loads and associated criteria for buildings and other structures (ASCE Standard ASCE/SEI 7-16)*. Reston, VA: American Society of Civil Engineers.
- FEMA. (2018). *Mitigation Assessment Team Report. Hurricanes Irma and Maria in Puerto Rico, Building Performance, Observations, Recommendations, and Technical Guidance. FEMA P-2020*. Washington, D.C: FEMA. Retrieved from https://www.fema.gov/sites/default/files/2020-07/mat-report_hurricane-irma-maria-puerto-rico_2.pdf
- Franklin Industries. (n.d.). *U Channel Sign Posts Available for Bulk Pricing*. Retrieved from <https://franklinindustriesco.com/u-channel-sign-post/>
- Hubbard, S. (2018). *Maria Peak Windgusts [Map]*. Retrieved from https://www.ssec.wisc.edu/news/wp-content/uploads/sites/19/2018/05/maria_peak_windgusts.jpg
- McGee, H. W. (2010). *Maintenance of Signs and Sign Supports: A Guide for Local Roads Maintenance Personnel*. Federal Highway Administration. Vienna, Virginia: Vanasse Hangen Brustlin, Inc.
- Moeur, R. C. (2019, October 30). *Manual of Traffic Signs - Sign Posts and Supports*. Retrieved from <http://www.trafficsign.us/signposts.html>.
- National Hurricane Center. (2018, January 26). *Costliest U.S. tropical cyclones tables updated*. Retrieved from <https://www.nhc.noaa.gov/news/UpdatedCostliest.pdf>
- NEXRAD . (1996). *NEXRAD System/Segment Specification*. Norman, OK: NEXRAD Operational Support Support Facility. Retrieved from <https://www.roc.noaa.gov/WSR88D/PublicDocs/NTR96.pdf>
- NIST. (2021, January). *NIST SP 1262 A Progress Report: Learning from Hurricane Maria's Impact on Puerto Rico*. Gaithersburg, MD: National Institute of Standards and Technology, U.S. Department of Commerce. Retrieved from <https://nvlpubs.nist.gov/nistpubs/SpecialPublications/NIST.SP.1262.pdf>
- NWS. (2017, November 29). *Major Hurricane Maria - September 20, 2017*. Retrieved from National Weather Service, National Oceanic and Atmospheric Administration: <https://www.weather.gov/sju/maria2017>
- Pacific Disaster Center. (2017). *Hurricane Maria - Exposure Based on Observed Wind Impacts, Puerto Rico, 21SEP17 [Map]*. Retrieved from https://reliefweb.int/sites/reliefweb.int/files/resources/PDC_TC_Maria_Wind_Exposure_Observed_Wind_PuertoRico.pdf
- Pasch, R. J., Penny, A. B., & Berg, R. (2019). *Hurricane Maria (AL 152017) 16-30 September 2017*. National Hurricane Center. Washington, DC: NOAA. Retrieved from https://www.nhc.noaa.gov/data/tcr/AL152017_Maria.pdf
- PRHTA. (2010). *Planos Modelos*. Puerto Rico Highway and Transportation Authority. Retrieved from <https://act.dtop.pr.gov/planos-modelo/>

- Rhee, D. M., Nevill, J. B., & Lombardo, F. T. (2022). Comparison of Near-Surface Wind Speed Estimation Techniques Using Different Damage Indicators from a Damage Survey of Naplate, IL EF-3 Tornado. *Natural Hazards Review*, 23(1). Retrieved from [https://doi.org/10.1061/\(ASCE\)NH.1527-6996.0000515](https://doi.org/10.1061/(ASCE)NH.1527-6996.0000515)
- Rhino. (2019). *Rhino Marking and Protection Systems*. Retrieved from Rhino: <https://www.rhinomarkers.com/product/u-channel/>
- Traffic Safety Products. (2019). *Traffic Safety Products*. Retrieved from <https://trafficsafetyproducts.net/sign-posts/telespar-square-tube/telespar-14-gauge-galvanized-sqaure-tube-sign-post.html>

Improving Transportation Infrastructure Resilience Against Hurricanes, Other Natural Disasters, and Weathering: Part I - Analysis of failure of transportation signs due to Hurricane Maria

Volume 3 Cantilever Traffic Signs

FINAL REPORT
August 2022

Submitted by:

Gustavo Pacheco-Crosetti, PhD, PE
Professor

Héctor J. Cruzado, PhD, PE
Professor

Geoffrey J. Vega-Rosado, MSCE
Graduate Student

Transportation Infrastructure Research Center – TIRC
Polytechnic University of Puerto Rico
377 Ponce de Leon Ave, San Juan, PR 00918

External Project Manager
Juan Carlos Rivera, Engineer
Puerto Rico Highway and Transportation Authority

In cooperation with

Rutgers, The State University of New Jersey
And
Puerto Rico
Department of Transportation and Public Works
And
U.S. Department of Transportation
Federal Highway Administration

LIST OF ABBREVIATIONS

ACI	American Concrete Institute
AISC	American Institute of Steel Construction
ASCE	American Society of Civil Engineers
AASHTO	American Association of State Highway Transportation Officials
DIA	diameter
DOF	degree-of-freedom
DOT	Department of Transportation
FEA	finite element analysis
NA	not available
LRFD	Load and Resistance Factor Design
PR	Puerto Rico
PRBC	Puerto Rico Building Code
PRDOT	Puerto Rico Department of Transportation and Public Works
PRHTA	Puerto Rico Highway and Transportation Authority
USGS	United States Geological Survey

GLOSSARY

The main terms related to the support structure of the cantilever traffic signs and their reinforced concrete pedestal are defined.

Base (B): Transverse plane perpendicular to the axis of the post at the lower end.

Breaking load: Load that is determined experimentally, applied in a horizontal direction and perpendicular to the axis of the post, which produces the structural collapse.

Collapse: Condition that occurs when a post, subjected to irregular loads, experiences a permanent deformation at the base, accompanied by deformations in the reinforcing steel, cracks and detachment of the concrete.

Crack: a crevice (break or fracture) that is formed in reinforced concrete and that has a width greater than 1 mm at the surface of the concrete.

Design Load: The load applied to the system for which the post is calculated and designed.

Elastic limit: The maximum stress that an elastic material can withstand without suffering permanent deformation.

Fissure: Break or fracture that forms in reinforced concrete and is up to 1 mm wide at the concrete surface.

Permanent deformation: Remaining deformed position registered after a certain load has ceased to act on the sign.

Rated breaking load: Breaking load defined by calculation and specified by the manufacturer.

Service load: Maximum load for which the post has been designed, applied in a horizontal direction and perpendicular to the axis of the post without permanent deformation of the structure.

TABLE OF CONTENT

1	INTRODUCTION.....	1
2	LITERATURE REVIEW	6
2.1	APPLICABLE CODE PROVISIONS	6
2.1.1	<i>AASHTO Specification for Supports</i>	<i>6</i>
2.1.2	<i>AASHTO Specifications, ASCE Standards, and ACI and AISC Codes</i>	<i>9</i>
2.1.3	<i>Puerto Rico Specifications and Standard Drawings.....</i>	<i>10</i>
2.2	LOADS EFFECTS ON TRAFFIC SIGNS AND LOAD DESIGN CRITERIA.....	15
2.3	WIND LOADS COMPUTATION PROCEDURES.....	18
2.3.1	<i>Wind Pressure Equation According AASHTO</i>	<i>18</i>
2.3.2	<i>Wind Pressure Equation According ASCE</i>	<i>18</i>
2.4	ANTECEDENTS	21
3	METHODOLOGY	23
3.1	SEARCH FOR BACKGROUND INFORMATION	23
3.2	CASE SELECTION AND LOCATION IDENTIFICATION	23
3.2.1	<i>Preliminary Reconnaissance.....</i>	<i>23</i>
3.2.2	<i>Identify Possible Sites by Exploratory Drives Along Puerto Rico Main Highways.....</i>	<i>24</i>
3.2.3	<i>News Analysis and PRHTA Interview</i>	<i>24</i>
3.2.4	<i>Identify Possible Sites of Signs Damages Using GIS Tools</i>	<i>24</i>
3.3	FIELD INSPECTION AND DATA COLLECTION	25
3.4	ANALYSIS, DESCRIPTION AND CLASSIFICATIONS OF FAILURES.....	26
3.5	VIRTUAL EXPLORATION TOOL DEVELOPMENT	27
3.6	MECHANICAL TESTS ON MATERIAL SAMPLES	27
3.7	SUMMARY OF FINDINGS, CONCLUSIONS AND RECOMMENDATIONS TO INCREASE RESILIENCE	28
4	IDENTIFICATION OF CANTILEVER SIGNS WITH POSSIBLE DAMAGES AND/OR COLLAPSE	29
4.1	PRELIMINARY RECONNAISSANCE	29
4.2	EXPLORATORY DRIVES ALONG PUERTO RICO MAIN HIGHWAYS.....	32
4.3	SEARCH IN NEWS OUTLETS	33
4.4	INTERVIEW PRHTA PERSONNEL TO RECEIVE THEIR INPUT	34
4.5	USE OF GIS VIRTUAL TOUR TO IDENTIFY POTENTIAL CASES	36
4.6	SUMMARY OF POTENTIAL CASE STUDIES.....	61
5	FIELD VISIT AND DATA COLLECTION.....	62
5.1	GENERAL CONSIDERATIONS REGARDING THE INSPECTION PROCEDURES	62
5.1.1	<i>Development of Field Data Collection Form</i>	<i>62</i>
5.1.2	<i>Example of the Checklist for Inspection of Cantilever Type Signs.....</i>	<i>64</i>
5.1.3	<i>Field Visits Strategy</i>	<i>64</i>
5.1.4	<i>Information Collection and Management.....</i>	<i>67</i>
5.1.5	<i>Failures Database Development</i>	<i>68</i>
5.2	INSPECTED CASES AND FAILURES FOUND	71
5.2.1	<i>Cantilever Traffic Sign Site Aguadilla P-76</i>	<i>74</i>
5.2.2	<i>Cantilever Traffic Sign Site Aguadilla P-77</i>	<i>75</i>
5.2.3	<i>Cantilever Traffic Sign Site Aguadilla P- 78</i>	<i>78</i>
5.2.4	<i>Cantilever Sign Site Arecibo P-88.....</i>	<i>80</i>
5.2.5	<i>Cantilever Sign Site Arecibo P-89.....</i>	<i>82</i>
5.2.6	<i>Cantilever Sign Site Arecibo P-90.....</i>	<i>84</i>
5.2.7	<i>Cantilever Sign Site Arecibo P-91.....</i>	<i>86</i>
5.2.8	<i>Cantilever Sign Site Barceloneta P-103</i>	<i>88</i>
5.2.9	<i>Cantilever Traffic Sign Sites Caguas P-16 and P-17</i>	<i>90</i>

5.2.10	<i>Cantilever Traffic Sign Site Caguas P-22</i>	91
5.2.11	<i>Cantilever Traffic Sign Site Caguas P-45</i>	92
5.2.12	<i>Cantilever Traffic Sign Site Caguas P-52</i>	93
5.2.13	<i>Cantilever Traffic Sign Site Caguas P-58</i>	94
5.2.14	<i>Cantilever Sign Site Camuy P-69</i>	95
5.2.15	<i>Cantilever Sign Site Canóvanas P- 106</i>	96
5.2.16	<i>Cantilever Sign Site Canóvanas P- 107</i>	98
5.2.17	<i>Cantilever Traffic Sign Site Guayama P-46</i>	99
5.2.18	<i>Cantilever Traffic Sign Site Guayama P-47</i>	101
5.2.19	<i>Cantilever Traffic Sign Site Gurabo P-57</i>	103
5.2.20	<i>Cantilever Traffic Sign Site Humacao P-61</i>	104
5.2.21	<i>Cantilever Traffic Sign Site Humacao P-100</i>	106
5.2.22	<i>Cantilever Sign Site Humacao P-105</i>	108
5.2.23	<i>Cantilever Sign Site Juana Diaz P-6</i>	110
5.2.24	<i>Cantilever Sign Site Juncos P-55</i>	111
5.2.25	<i>Cantilever Sign Site Juncos P-56</i>	112
5.2.26	<i>Cantilever Sign Site Las Piedras P-53</i>	113
5.2.27	<i>Cantilever Traffic Sign Site Las Piedras P-66</i>	114
5.2.28	<i>Cantilever Traffic Sign Site Las Piedras P-99</i>	115
5.2.29	<i>Cantilever Sign Site Ponce P-1</i>	116
5.2.30	<i>Cantilever Sign Site Ponce P-3</i>	117
5.2.31	<i>Cantilever Sign Site Ponce P-4</i>	118
5.2.32	<i>Cantilever Traffic Sign Site Ponce P- 59</i>	119
5.2.33	<i>Cantilever Traffic Sign Site Ponce P- 94</i>	120
5.2.34	<i>Cantilever Sign Site Salinas P-11</i>	122
5.2.35	<i>Cantilever Sign Site Salinas P-12</i>	123
5.2.36	<i>Cantilever Sign Site Salinas P-15</i>	125
5.2.37	<i>Cantilever Sign Site San Juan P-33</i>	126
5.2.38	<i>Cantilever Sign Site San Juan P-35</i>	127
5.2.39	<i>Cantilever Sign Site San Juan P-38</i>	128
5.2.40	<i>Cantilever Sign Site San Juan P-40</i>	129
5.2.41	<i>Cantilever Sign Site San Juan P-41</i>	130
5.2.42	<i>Cantilever Sign Site San Juan P-42</i>	131
5.2.43	<i>Cantilever Sign Site San Juan P-43</i>	133
5.2.44	<i>Cantilever Sign Site San Juan P-44</i>	134
5.2.45	<i>Cantilever Sign Site San Juan P-95</i>	135
5.2.46	<i>Cantilever Sign Site San Juan P- 98</i>	136
5.2.47	<i>Cantilever Sign Site Santa Isabel P-7</i>	137
5.2.48	<i>Cantilever Sign Site Santa Isabel P-8</i>	138
5.2.49	<i>Cantilever Sign Site Santa Isabel P-10</i>	139
5.2.50	<i>Cantilever Sign Site Santa Isabel P-36</i>	141
5.2.51	<i>Cantilever Sign Site Santa Isabel P-70</i>	142
6	ANALYSIS AND GENERAL RECOMMENDATIONS OF THE FINDINGS	143
6.1	FOUNDATION STRUCTURAL FAILURES OF THE PEDESTAL	143
6.1.1	<i>Large Lateral Deflections of Anchor Bolts</i>	143
6.1.2	<i>Anchor Bolts Located Outside the Stirrups</i>	152
6.1.3	<i>Anchor Bolts Pullout</i>	155
6.1.4	<i>Length of Longitudinal Reinforcement not Appropriate</i>	157
6.2	FOUNDATION SOIL FAILURES	159
6.2.1	<i>Foundation Torsional Failure</i>	159
6.2.2	<i>Foundation Torsional and Overturning Failure</i>	162
6.2.3	<i>Foundation Torsional and Overturning Failure on a Pronounced Slope</i>	162

7	DEVELOPMENT OF GIS VIRTUAL EXPLORATION TOOL	164
8	LABORATORY TESTING OF COLLECTED SAMPLES.....	167
8.1	TENSION TEST ON STEEL REBARS AND ANCHOR BOLTS	168
8.2	CONCRETE COMPRESSION TEST	172
8.3	SUMMARY OF LABORATORY FINDINGS.....	177
9	SUMMARY, CONCLUSIONS AND RECOMMENDATIONS	178
9.1	CONCLUSIONS AND RECOMMENDATIONS FOR THE STRUCTURAL DAMAGES	180
9.2	CONCLUSIONS AND RECOMMENDATIONS FOR SOIL-FOUNDATION DAMAGES.....	182
9.3	ADDITIONAL RECOMMENDATIONS AND FURTHER STUDY	183
	REFERENCES	184
	APPENDIX A INSPECTIONS FORMS	186
A.1	BLANK FORM	186
A.2	EXAMPLES OF ON-SITE FILLED FORMS.....	187
	APPENDIX B CURRENT WIND DESIGN SPEED (MPH) ACCORDING TO SIGN COORDINATES	193
	APPENDIX C DETAILS OF CANTILEVER TRAFFIC SIGNS ACCORDING TO PRHTA SPECIFICATIONS	198
C.1	OVERHEAD SIGNS SUPPORT SHOP DRAWINGS (CMA SEPTEMBER 4, 2020)	198
C.2	OVERHEAD SIGNS FOUNDATION FOR CANTILEVER TYPE (PRHTA)	200
	APPENDIX D STIRRUPS SPACING AND DOUBLE BENDING OF BOLTS	207
D.1	FIRST MODEL – REACH SHEAR FRACTURE BEFORE MOMENT YIELDING.....	207
D.2	SECOND MODEL – REACH SHEAR YIELDING BEFORE MOMENT YIELDING	211
D.3	THIRD MODEL – REACH SHEAR YIELDING (USING JOURAWSKY FORMULA FOR SHEAR) BEFORE MOMENT YIELDING ..	215
D.4	SUMMARY	219
	APPENDIX E CANTILEVER SIGNS GEOLOCATION PER MUNICIPALITY	221

List of Figures

Figure 1-1: Path of Historical Hurricanes that Have Impacted Puerto Rico (USGS, n.d.)	2
Figure 1-2: Path of Hurricanes Irma and Maria with Respect to Puerto Rico (Silva-Tulla & Pando, 2020)	2
Figure 1-3: Hurricane Maria's Trajectory (FEMA, 2018)	3
Figure 1-4: Example of Overhead Cantilever Sign (source: Google Earth Pro)	4
Figure 1-5: Example of Overhead Cantilever Sign Failure due to Hurricane Maria	4
Figure 2-1: Overhead Traffic Signs Specifications and Notes (PRHTA, 2010)	11
Figure 2-2: Types of Overhead Cantilever Traffic Signs Used in PR (PRHTA, 2010)	12
Figure 2-3: Foundations Specifications for Overhead Cantilever Traffic Signs (PRHTA, 2010)	13
Figure 2-4: Overhead Cantilever Traffic Sign Structures (PRHTA, 2010)	14
Figure 2-5: Overhead Cantilever Traffic Sign Structure Connection Details (PRHTA, 2010)	14
Figure 2-6: Overhead Cantilever Traffic Sign - Truss Arm Elevations (PRHTA, 2010)	15
Figure 2-7: Cantilever-type Traffic Sign Installation	17
Figure 2-8: Basic Design Wind Speeds, V, for Risk Category II Buildings and other Structures. (ASCE7-16 CH26)	20
Figure 4-1: Collapsed Cantilever Sign in PR-30 Highway	30
Figure 4-2: Collapsed Cantilever Sign in PR-30 Highway	30
Figure 4-3: Total Collapse of a Cantilever Sign Located in PR-66 Highway	31
Figure 4-4: Partial Collapse and Damages on a Cantilever Traffic Sign Located on PR-18 Highway	32
Figure 4-5: Transportation Infrastructure in Puerto Rico and Related Data (source: www.mapacarreteras.org)	33
Figure 4-6: Overhead Cantilever Traffic Sign Collapse on PR-17 (Lima, 2017)	34
Figure 4-7: Cantilever Sign Post 12 Located in Salinas (Picture 1 (12/2016), Picture 2 (10/2017))	38
Figure 4-8: Cantilever Sign Post 46 Located in Guayama (Picture 1: 10/2017, Picture 2: 1/2019)	39
Figure 4-9: Cantilever Sign Post 35 located in San Juan (Picture 1: 4/2016, Picture 2: 1/2020)	40
Figure 4-10: Cantilever Sign Post 38 Located in San Juan. (Picture 1: 4/2016, Picture 2: 4/2018)	41
Figure 4-11: Cantilever Sign Post 40 and 41 located in San Juan. (Picture 1: 4/2016, Picture 2: 4/2018)	42
Figure 4-12: Cantilever Sign Post 46 Located in Guayama (Picture 1: 10/2017)	43
Figure 4-13: Cantilever Sign Post 53 Located in Las Piedras (Picture 1: 11/2016, Picture 2: 4/2018) ..	44
Figure 4-14: Cantilever Sign Post 52 Located in Las Piedras (Picture 1: 1/2014, Picture 2: 4/2018)	45
Figure 4-15: Cantilever Sign Post 56 Located in Juncos (Picture 1: 10/2016, Picture 2: 4/2018)	46
Figure 4-16: Cantilever Sign Post 59 Located in Ponce (Picture 1: 4/2016, Picture 2: 4/2018)	47
Figure 4-17: Cantilever Sign Post 61 Located in Humacao (Picture 1: 12/2016, Picture 2: 10/2017) ...	48
Figure 4-18: Cantilever Sign Post 66 Located in Fajardo (Picture 1: 2/2017, Picture 2: 1/2018)	49
Figure 4-19: Cantilever Sign Post 69 Located in Canóvanas (Picture 1: 3/2013, Picture 2: 4/2018)	50
Figure 4-20: Cantilever Sign Post 76 Located in Aguadilla (Picture 1: 2/2017, Picture 2: 4/2018)	51
Figure 4-21: Cantilever Sign Post 77 Located in Aguadilla (Picture 1: 9/2016, Picture 2: 5/2018)	52
Figure 4-22: Cantilever Sign Post 88 Located in Aguadilla (Picture 1: 3/2016, Picture 2: 5/2018)	53
Figure 4-23: Cantilever Sign Post 88 Located in Arecibo (Picture 1: 3/2016, Picture 2 4/2018)	54
Figure 4-24: Cantilever Sign Post 91 Located in Arecibo (Picture 1: 3/2016, Picture 2: 4/2018)	55
Figure 4-25: Cantilever Sign Post 95 Located in San Juan (Picture 1: 4/2016, Picture 2: 4/2018)	56
Figure 4-26: Cantilever Sign Post 98 Located in Las Piedras (Picture 1: 4/2016, Picture 2: 4/2018)	57
Figure 4-27: Cantilever Sign Post 101 Located in Caguas (Picture 1: 10/2016, Picture 2: 10/2017)	58
Figure 4-28 Cantilever Sign Post 69 located at Canóvanas (Picture 1: 4/2018)	59

Figure 4-29 Cantilever Sign Post 94 Located in Ponce (Picture 1: 4/2016, Picture: 4/2018).....	60
Figure 5-1: Field Visits Inspection Sheet	63
Figure 5-2: Traffic Signs Identified per Exploration Region	66
Figure 5-3: Identifying the Post to Be Inspected in the Town of Quebradillas, Puerto Rico (Coordinates: 18°28'48.97"N; 66° 58'5.91"W)	68
Figure 5-4: Required Foundation Resistance to Provide Stability to the Sign Structure.....	71
Figure 5-5: Photos Showing the Rotation of the Traffic Sign at P-76 Location: 18°27'8.10"N; 67° 5'38.06"W	74
Figure 5-6: Photos of Cantilever Traffic Sign Pedestal Failures and Post Inclination at P-76	74
Figure 5-7: Photo of Cantilever Sign Foundation Failure at P-77 with Location: 18°27'13.01"N; 67° 5'20.87"W	75
Figure 5-8: Photo of Drilled Shaft Foundation of Traffic Sign P-77 with Location: 18°27'13.01"N; 67° 5'20.87"W	76
Figure 5-9: Photo of Drilled Shaft Foundation of Traffic Sign P-77	76
Figure 5-10: Photo of Cantilever Sign Soil Foundation Failure at P- 77 Location: 18° 27'13.01"N; 67°5'20.87"W (Photo 1 date: 6/2017, Photo 2 date: 4/2018)	77
Figure 5-11: Cantilever Traffic Sign P- 77 at the Time of Inspection (Post not in Place).....	77
Figure 5-12: Photo of Cantilever Sign Foundation Failure at P- 78 Photo Location: 18°26'11.95"N; 67° 8'52.33"W	78
Figure 5-13: Photo of Drilled Shaft Foundation of Traffic Sign at P-78 Photo Location: 18°26'11.95"N; 67° 8'52.33"W.	79
Figure 5-14: Continuous Gap Around the Circumference of the Drilled Shaft	79
Figure 5-15: Photo of Cantilever Sign Soil Foundation Failure at P-88 Location: 18°27'13.01"N; 66°5'20.87"W (Photo 1 date: 3/2016, Photo 2 date: 4/2018)	80
Figure 5-16: Cantilever Traffic Sign P-88 at the Time of Inspection	81
Figure 5-17: Photo of Cantilever Sign Soil Foundation Failure at P-89 Location: 18°27'10.09"N; 66°44'50.21"W (Photo 1 date: 3/2016, Photo 2 date: 4/2018)	82
Figure 5-18: Cantilever Traffic Sign P-89 at the Time of Inspection	83
Figure 5-19: Photo of Cantilever Sign Soil Foundation Failure at P-90 Location: 18°27'8.40"N; 66°43'8.03"W (Photo 1 date: 3/2016, Photo 2 date: 4/2018)	84
Figure 5-20: Cantilever Traffic Sign P-90 at the Time of Inspection	85
Figure 5-21: Photo of Cantilever Sign Soil Foundation Failure at P-91 Location: 18°27'5.98"N; 66°43'4.13"W (Photo 1 date: 3/2016, Photo 2 date: 4/2018)	86
Figure 5-22: Cantilever Traffic Sign P-91 at the Time of Inspection	87
Figure 5-23: Photo of Cantilever Sign Failure at P-103 Location: 18°26'8.06"N; 66°32'38.60"W (Photo 1 date: 11/2006, Photo 2 date: 4/2018)	88
Figure 5-24: Cantilever Traffic Sign P-103 at the Time of Inspection	89
Figure 5-25: Photos of Cantilever Traffic Sign Base Condition at P-16. Location: 18.22014722 N; - 66.04703611 W.	90
Figure 5-26: Photos of Cantilever Traffic Sign Base Condition at P-16. Location: 18.45293333N; - 66.04458333W	90
Figure 5-27: Photos of Cantilever Traffic Sign Geolocation and Rests of the Post Foundation at P-22. Location: 18.27201944N; -66.03914444W.....	91
Figure 5-28: Photos of Cantilever Traffic Sign Geolocation, damages to the traffic barrier, and Rests of a Post Foundation at P-45. Location: 18.27035278N; -66.03955556W	92
Figure 5-29: Photos of Cantilever Traffic Sign Overturning Foundation Failure and Anchor Bolts Shear/Tension Failure at P-52. Location: 18°11'7.35"N; 66° 3'17.55"W.....	93

Figure 5-30: Photos of Cantilever Traffic Sign Location and Anchor Bolts Lateral Movement Producing Cracks on the RC Base at P-58. Location: 18.25564167N; -66.02865278W	94
Figure 5-31: Additional Details of RC Base Damages due to Anchor Bolts Lateral Displacements at P-58	94
Figure 5-32: Photo of Cantilever Sign Soil and Structural Foundation Failure at P- 69 Location: 18° 29'18.024"N; 66°48'0.72"W (Photo 1 date: 1/2015, Photo 2 date: 4/2018)	95
Figure 5-33: Photo of Cantilever Sign Foundation Structural Failures on the Pedestal at P-106 Location: 18°22'20.65"N; 65°52'38.72"W	96
Figure 5-34: Photo of Cantilever Sign Foundation Structural Failures on the Pedestal at P-106	97
Figure 5-35: Photo of Cantilever Sign Foundation Structural Failures on the Pedestal at P-106	97
Figure 5-36: Photo of Cantilever Sign Foundation Torsional Rotation of the Pedestal at P-107 Location: 18.3603111°N, -65.8938111°W	98
Figure 5-37: Photo of Cantilever Sign Foundation Structural Failures on the Pedestal and Sign Position (Partial Collapse) at P-46. Location: 17°59'8.91"N; 66° 8'45.56"W	99
Figure 5-38: Photos of Cantilever Traffic Sign Foundation Structural Failure to the Pedestal at P-46; with Large Deflections and Bending on the Plastic Range and Shear Fracture of the Anchor Elements, and Fractures, Detachments and Crushing of the Concrete	100
Figure 5-39: Photo of Cantilever Sign Foundation Structural Failures on the Pedestal and Sign Position (Partial Collapse) at P-47. Location: 17.9868529°N, -66.1425048°W	101
Figure 5-40: Photos of Cantilever Traffic Sign Foundation Structural Failure to the Pedestal at P-47; with Large Deflections and Bending on the Plastic Range and Shear Fracture of the Anchor Elements, and Fractures, Detachments and Crushing of the Concrete. Bolts outside the confinement of Stirrups ..	102
Figure 5-41: Photo of Cantilever Sign Structural Failures on the Pedestal at P-57 Location: 18.25031944°N; 65.96180556°W	103
Figure 5-42: Photo of Cantilever Sign Foundation Structural Failures on the Pedestal and Sign Position (Total Collapse) at P-61. Location: 18.159975°N; 65.79745833° W	104
Figure 5-43: Photos of Cantilever Traffic Sign Foundation Structural Failure to the Pedestal at P-46; with Large Deflections and Bending on the Plastic Range and Shear Fracture of the Anchor Elements, and Fractures and Detachments of the Concrete.....	105
Figure 5-44: Photo of Cantilever Sign Structural Failures on the Pedestal at P-100 Location: 18°7'7.11"N; 65°49'16.812"W	106
Figure 5-45: Photo of Cantilever Sign Foundation Structural Failure at P-100; with Large Deflections and Bending on the Plastic Range and Shear Fracture of the Anchor Elements, and Fractures, Detachments and Crushing of the Concrete. Anchor elements outside the confinement provided by Stirrups	107
Figure 5-46: Photo of Cantilever Sign Structural Failures on the Pedestal at P-105 Location: 18° 7'20.00"N; 65°49'12.23"W	108
Figure 5-47: Photo on Cantilever Sign Foundation Structural Failure at P-105; Collapsed Post Presented Large Deflections and Bending on the Plastic Range and Shear Fracture of the Anchor Elements	108
Figure 5-48: Photo on Cantilever Sign Foundation Structural Failure at P-105; Collapsed Post Presented Large Deflections and Bending on the Plastic Range and Shear Fracture of the Anchor Elements, and Fractures and Detachments of the Concrete. Anchor elements outside the confinement provided by Stirrups.....	109
Figure 5-49: Photo of Cantilever Sign Missing Truss and Sign at P-6 Location: 18.03189444°N; 66.45465278°W.....	110
Figure 5-50: Photo of Cantilever Sign Structural Crack on the Pedestal at P-55 Location: 18.22131389°N; 65.91406944°W	111
Figure 5-51: Photo of Cantilever Sign Torsional Rotation and Possible Collapse on the Pedestal at P-56 Location: 18.22426944°N; 65.91595833°W	112

Figure 5-52: Photo of Cantilever Sign Concrete Foundation Rests at P-56.....	112
Figure 5-53: Photo of Cantilever Sign Structural Failures on The Pedestal at P-53 Location: 18°11'31.15"N; 65°53'46.75"W	113
Figure 5-54: Photos of Cantilever Traffic Sign Foundation Structural Pedestal Failure at P-53; with Large Deflections on the Plastic Range, Shear Fracture, and Pullout of the Anchor Elements, and Fractures and Detachments of the Concrete	113
Figure 5-55: Photo of Cantilever Sign Collapse at P-66 Location: 18°11'11.10"N; 65°53'28.92"W.....	114
Figure 5-56: Photo of Cantilever Sign Collapse at P-99 Location: 18.183386°N; 65.88572°W	115
Figure 5-57: Photo of Cantilever Sign P-1. Damages, Fractures on Concrete Pedestal. Location: 17°59'25.25"N; 66°37'16.63"W	116
Figure 5-58: Photo of Cantilever Sign Foundation Structural Damages on the Pedestal at P-3, Damages (Fractures on the Concrete Base) Location: 17°59'19.75"N; 66°37'0.41"W	117
Figure 5-59: Photo of Cantilever Sign Foundation Structural Damages on the Pedestal at P-4, Damages (Fractures on the Concrete Base) Location: 17.986208°N; 66.6033°W.....	118
Figure 5-60: Photo of Cantilever Sign Foundation Soil and Structural Failure at P-59. Location: 17°59'21.23"N; 66°38'46.49"W	119
Figure 5-61: Photo of Cantilever Traffic Sign Foundation Failure at P-94 Location: 17°59'16.80"N; 66°38'55.39"W	120
Figure 5-62: Photo Showing the Rotation of The Traffic Sign and the Foundation Pedestal at P-94..	121
Figure 5-63: Photo of Cantilever Sign Location and Rests Stored at Yard for Id P-11 Location: 18° 0'1.89"N; 66°14'17.05"W	122
Figure 5-64: Photo of Cantilever Sign Structural Failures on the Pedestal at P-12 Location: 18° 0'11.23"N; 66°14'29.63"W	123
Figure 5-65: Photo of Cantilever Sign Structural Foundation Failure at P-12; Collapsed Post Presented Torsional Pattern and Large Deflections of the Anchoring Elements, which also Exhibit Shear Fracture	124
Figure 5-66: Photo of Cantilever Sign Structural Failures on the Pedestal at P-15. Location: 18° 1'29.22"N; 66°14'28.42"W	125
Figure 5-67: Photo of Cantilever Sign Foundation Structural Failure at P-15; Partial Collapse; the Post Presented Large Deflections and Double Bending in the Plastic Range of the Anchoring Elements ..	125
Figure 5-68: Photo of Cantilever Sign Foundation Soil Failure (Torsional Rotation) at P- 33 Photo Location: 18°23'52.03"N; 67° 66° 4'14.19"W	126
Figure 5-69: Photo of Cantilever Sign Soil Foundation Failure (Torsional Rotation) at P- 35 Photo Location: 18°24'16.37"N; 66° 4'11.96"W.....	127
Figure 5-70: Photo of Cantilever Sign Soil Foundation Failure (Torsional Rotation) with Damages to the Pedestal at P- 38 Photo Location: 18°24'5.58"N; 66° 4'16.57"W.....	128
Figure 5-71: Satellite Image of Cantilever Sign Soil Foundation Failure (Torsional Rotation) at P- 40 Photo Location: 18.413125°N; 66.06986944°W	129
Figure 5-72: Photo of Cantilever Sign Soil Foundation Failure (Torsional Rotation) with Damages to the Pedestal at P- 41 Photo Location: 18°24'47.01"N; 66° 4'13.07"W.....	130
Figure 5-73: Photo of Cantilever Sign Foundation Failure (Torsional Rotation) at P- 42 Photo Location: 18°24'54.71"N; 66° 4'13.43"W.....	131
Figure 5-74: Gap Around the Circumference of the Drilled Shaft, and Soil Movement Downhill.....	132
Figure 5-75: Photo of Cantilever Sign Foundation Failure (Torsional Rotation), Damages to the Concrete Pedestal, and Gap Between Soil and Shaft at P- 43 Photo Location: 18.41788611°N; 66.07006111°W	133

Figure 5-76: Photo of Cantilever Sign Foundation Failure (Torsional Rotation), Damages to the Concrete Pedestal, and Small Gap Between Soil and Shaft at P- 43 Photo Location: 18.41561389°N; 66.06995°W	134
Figure 5-77: Photo of Cantilever Sign Soil Foundation Failure at P- 95 Photo Location: 18°25'25.61"N; 66° 4'20.75"W	135
Figure 5-78: Gap Around the Circumference of the Drilled Shaft	135
Figure 5-79: Photo of a Collapsed Cantilever Sign Foundation due to Structural Failures on the Pedestal at P-98 Location: 18°24'27.38"N; 66° 4'3.00"W	136
Figure 5-80: Photo of Cantilever Sign Location and Possible Collapse at P-7 Photo Location: 18.02574444°N; 66.40993889°W	137
Figure 5-81: Photo of Cantilever Sign Location and Pedestal Cracks at P-8 Photo Location: 18.01293333°N; 66.389025°W	138
Figure 5-82: Photo of Cantilever Sign Location and Pedestal Cracks at P-10 Photo Location: 18.01423056°N; 66.36989167°W	139
Figure 5-83: Photo of Cantilever Sign Location Pedestal Cracks at P-10.....	140
Figure 5-84: Photo of Cantilever Sign Location and Pedestal Cracks, Efflorescence, Water Marks and Leakage at P-36 Photo Location: 18.01324444°N; 66.38875°W	141
Figure 5-85: Photo of Cantilever Sign Location and Pedestal Cracks at P-70 Photo Location: 18.0284609°N; 66.4165331°W	142
Figure 6-1: Initial Stages of Concrete Cracks and Spalls due to Lateral Deflections of Anchor Bolts (Sign P-1).....	145
Figure 6-2: Initial Stages of Concrete Cracks and Spalls due to Lateral Deflections of Anchor Bolts (Sign P-3).....	145
Figure 6-3: Initial Stages of Concrete Cracks and Spalls due to Lateral Deflections of Anchor Bolts (Sign P-76).....	146
Figure 6-4: More Advance Stage of Concrete Cracks and Spalls due to Lateral Deflections of Anchor Bolts with Large Unconfined Length (Sign P-38).....	146
Figure 6-5: More Advance Stage of Concrete Cracks and Spalls due to Lateral Deflections of Anchor Bolts with Large Unconfined Length (Sign P-41).....	147
Figure 6-6: More Advance Stage of Concrete Cracks and Spalls due to Lateral Deflections of Anchor Bolts with Large Unconfined Length. Bolts Exhibit Double Bending Shape (Sign P-15).....	147
Figure 6-7: Large Deflections of Anchor Bolts due to Lack of Lateral Confinement (Sign P-46).....	148
Figure 6-8: Large Deflections of Anchor Bolts due to Lack of Lateral Confinement	149
Figure 6-9: Large Deflections of Anchor Bolts due to Lack of Lateral Confinement (Sign P-12).....	150
Figure 6-10: Large Deflections of Anchor Bolts due to Lack of Lateral Confinement (Sign P-12).....	150
Figure 6-11: Large Deflections of Anchor Bolts due to Lack of Lateral Confinement (Sign P-106).....	151
Figure 6-12: Several Anchor Bolts Outside the Transverse Confinement Steel / Concrete Core (Sign P-100).....	152
Figure 6-13: Some of the Anchor Bolts Outside the Transverse Confinement Steel / Concrete Core (Sign P-100)	153
Figure 6-14: Several of the Anchor Bolts Outside the Transverse Confinement Steel / Concrete Core (Sign P-105).....	154
Figure 6-15: Anchor Bolts Pullout	155
Figure 6-16: Anchor Bolts Pullout (Sign P-105).....	156
Figure 6-17: Anchor Bolts Pullout (Sign P-53).....	156
Figure 6-18: PRHTA Standard for Sign Foundations (PRHTA, 2010)	157
Figure 6-19: Interrupted Steel and Shear Fracture of the Concrete of the Drilled Shaft.....	158

Figure 6-20: Cylindrical Precast Concrete Base that Experienced Torsional Rotation. The post was Removed. PR 66 in Canóvanas	159
Figure 6-21: Cylindrical Precast Concrete Base that Experienced Torsional Rotation. PR 18 in San Juan	160
Figure 6-22: Gap Between the Soil and the Cylindrical Precast Concrete Base that Experienced Torsional Rotation. PR 18 in San Juan.	161
Figure 6-23: Foundation that Experienced Torsional Rotation and Overturning. PR 52 in Caguas.	162
Figure 6-24: Foundation that Experienced Torsional Rotation and Overturning on a Pronounced Slope. PR 2 in Ponce.	163
Figure 7-1: Google Earth Map of Puerto Rico with the Layer Activated	165
Figure 7-2: Example of the Information Revealed to the User when Using the Platform	166
Figure 7-3: Example of the Information Revealed to the User when Using the Platform	166
Figure 8-1: Samples collected from damaged pedestal	167
Figure 8-2: Tension Test of Longitudinal Rebar Specimen (Bar Size # 6, Diameter 0.097 Inches.)	168
Figure 8-3: Reinforcing steel specimen after test was conducted	169
Figure 8-4: Partial Display of the Stress-Strain Diagram for One Rebar #6	169
Figure 8-5: Anchor Bolt Tension Test	171
Figure 8-6: Anchor Bolt Sample with Plastic Deformations	171
Figure 8-7 Specimens Collected During the Field Visit	172
Figure 8-8 Example Mechanical Test to Core Obtained Concrete Cylinders	173
Figure 8-9 Pedestal Concrete Samples Confined with Fresh Concrete in a Wooden Formwork.	174
Figure 8-10 Drill Equipment Installed and Performing Extraction.....	175
Figure 8-11 Extracted Cores, Cut and Placed Inside Plastic Bags	175
Figure 8-12 Recapping and Leveling of Cores Prior to Testing	176
Figure 8-13 Compression Test on Extracted Core	176
Figure 9-1: Geolocation of Most Severe Findings by Exploration Region	179

List of Tables

Table 2-1: Main Assembly Configurations of Traffic Signs (AASHTO, 2013)	7
Table 2-2: Main Configurations of Trusses Used to Support Signs (AASHTO, 2013)	8
Table 2-3: Tubular Shapes (AASHTO, 2013).....	9
Table 2-4: Group Load Combinations (AASHTO, 2013)	16
Table 2-5: Mean Recurrence Interval (AASHTO, 2014)	19
Table 4-1: Interview questions and answers conducted with Eng. Rivera, Director of the Signs Division of PRHTA	35
Table 5-1: Post Quantity and ID per Municipality.....	72
Table 5-2: Post Quantity and ID per Municipality Grouped by Exploration Regions	73
Table 8-1: Results of the Tension Test on #6 Reinforcing Steel Rebars	170
Table 8-2: Results of Mechanical Compressive Tests Performed on Cores Extracted from The Specimens	177
Table 9-1: Summary of Damages Found on Cantilever Traffic Signs Due to Hurricane Maria.	180

1 Introduction

Puerto Rico is an island located in the Caribbean. The island is the easternmost and smallest of the Greater Antilles. Puerto Rico is a United States territory bordered in the north by the Atlantic Ocean and in the south by the Caribbean Sea. Puerto Rico measures approximately 100 mi in the east to west direction and 35mi in the north to south direction.

Puerto Rico lies in the designated Caribbean Hurricane Alley. Due to its location, the island is extremely exposed to hurricane impacts. Figure 1-1 presents a map with historical hurricanes that have impacted Puerto Rico. Several hurricanes made landfall in Puerto Rico in recent years. Examples of this are Hugo in 1999, which first made landfall in the municipal island of Vieques as a category 4 hurricane, and then made another landfall in Puerto Rico's northeastern corner as a category 3; Hortense in 1996, as a category 1; Georges in 1998, as a category 3; and Irene in 2011, which landed as a tropical storm, but turn into a category 1 hurricane before leaving the island.

Moreover, in September 2017, two hurricanes impacted Puerto Rico, first hurricane Irma and then hurricane Maria. Figure 1-2 shows the trajectory of the eyes of these hurricanes. Irma was a category 5 hurricane when it passed just to the north of Puerto Rico on September 5th, 2017. Although, it did not make landfall in the island, hurricane-strength winds extended about 80 miles from its center. Hurricane Irma left over about one million of people without electricity (Cangialosi, Latto, & Berg, 2021). Some days later, Puerto Rico was directly hit by Hurricane Maria. It was also a strong hurricane, classified as a category 4 hurricane on the Saffir-Simpson hurricane wind scale before making landfall in the municipality of Yabucoa on September 20t, 2017, with sustained winds of 155 mph. The path of the eye took a northwesterly direction. Figure

1-2 shows that hurricane-force winds extended 50 to 60 miles from its center. While Figure 1-3 shows the complete trajectory of Hurricane Maria.

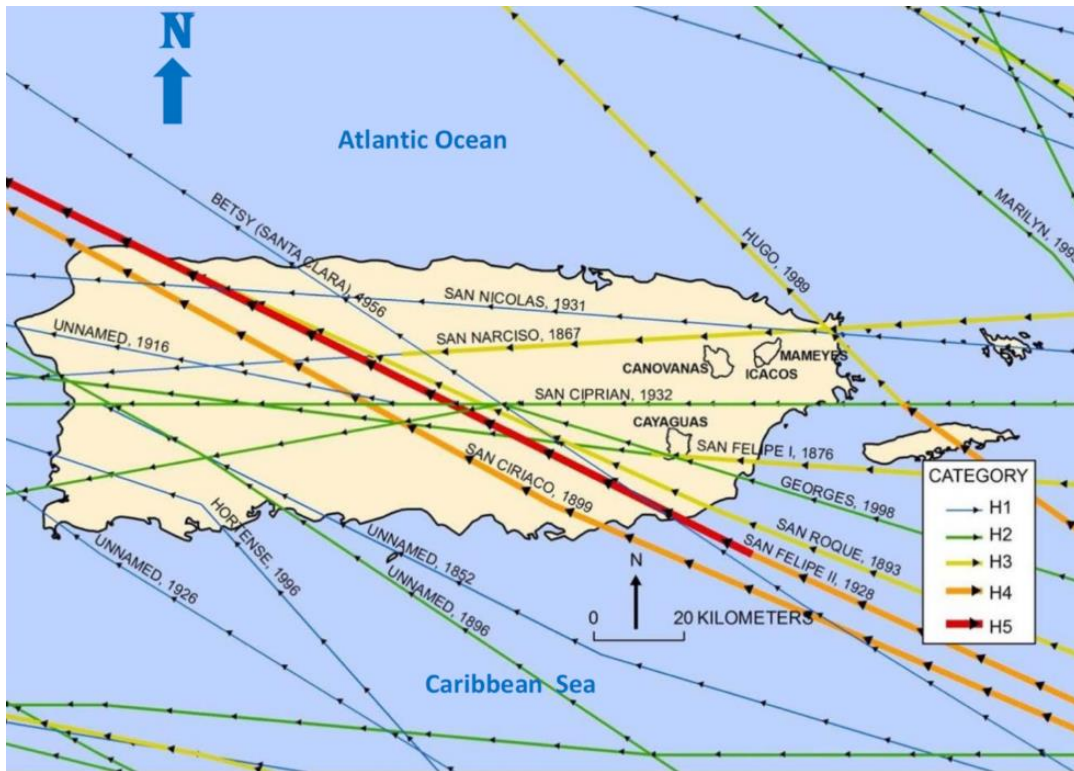


Figure 1-1: Path of Historical Hurricanes that Have Impacted Puerto Rico (USGS, n.d.)

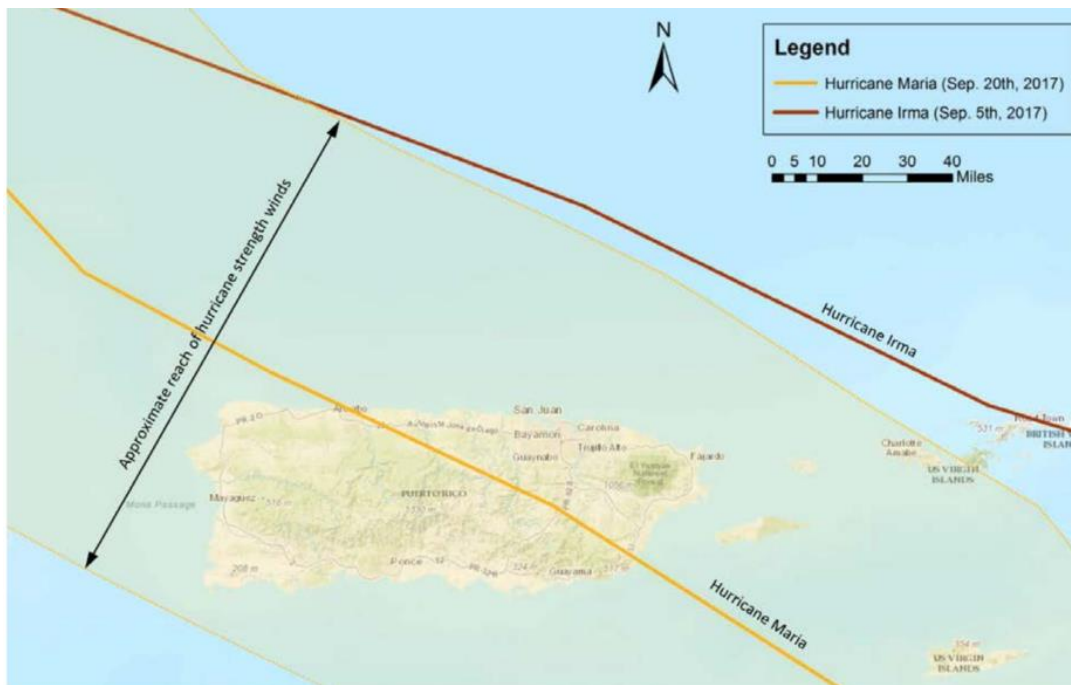


Figure 1-2: Path of Hurricanes Irma and Maria with Respect to Puerto Rico (Silva-Tulla & Pando, 2020)

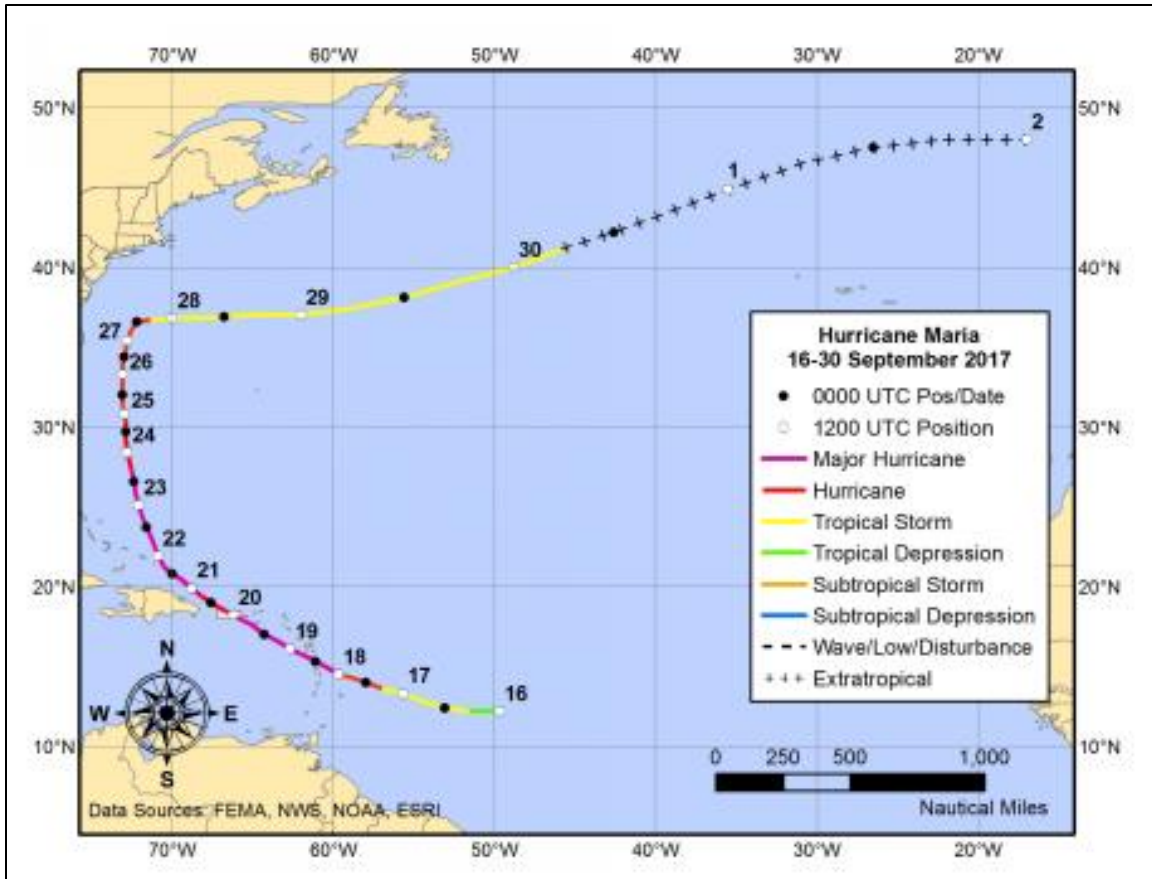


Figure 1-3: Hurricane Maria's Trajectory (FEMA, 2018)

The effects of Hurricane Maria included several failures in traffic signals, traffic signs, and traffic luminaires due to the strong winds associated with the event. For example, 881 luminaires poles under the jurisdiction of the Puerto Rico Highway and Transportation Authority (PRHTA) were affected by the impact of Hurricane Maria (Rodríguez-Caraballo, 2018).

The research project documented in this report focuses on the analysis of Overhead Signs Cantilever Types I-B and it aims to establish the types of structural failures that occurred, to help the engineering community adapt and improve design and construction practices to increase the resiliency of the infrastructure and lifelines. The cantilever-type traffic signs are used on the principal highways of the country. An example of this type of structure is presented in Figure 1-4. They are relatively common structures whose construction meets the design standards applicable

to Puerto Rico. During Hurricane Maria, some of these structures suffered different types of damages. They were exposed to lateral loads of intense winds that exceeded their capacity, resulting in the total or partial collapse of some of them. A collapse example is shown in Figure 1-5.



Figure 1-4: Example of Overhead Cantilever Sign (source: Google Earth Pro)



Figure 1-5: Example of Overhead Cantilever Sign Failure due to Hurricane Maria

This research was divided in seven main stages. The first stage was the comprehensive literature review to support the research. The second part consisted of the identification of signs that may have experienced damages by means of travelling the main highways of Puerto Rico and by using GIS programs to make a historical comparison of the traffic signs and use the comparison to identify possible case studies. The third stage was carrying out the field inspection of the signs identified as potential cases, filling inspection forms, taking photos, and collecting samples in one of the cases. The fourth stage was carrying out laboratory tests on the concrete and reinforcing steels bars collected, to assess the strength of the materials (that may help identify possible causes of the damages). The fifth step of the process was to evaluate each one of the inspected cases, and assess the type of failure that has occurred, and identify conditions that may have contributed to the damages encountered. Then, a GIS tool that allows to navigate the different cases was implemented. Finally, conclusions and recommendations to improve this type of traffic signs resilience were drawn.

2 Literature Review

This chapter summarizes important aspects found during the literature review that are relevant to the developed research project. They include applicable codes and specifications to design traffic signs, as well as the effect of winds over this type of structures.

2.1 Applicable Code Provisions

In these subsections, different codes and standards that apply to the design and construction of cantilever signs are presented and relevant information is summarized.

2.1.1 AASHTO Specification for Supports

The analysis is based upon the 2013 AASHTO Standard Specifications for Structural Supports for Highway Signs, Luminaires and Traffic Signals. The American Association of State Highway and Transportation Officials (AASHTO) has developed the Standard Specifications for Structural Supports for Highway Signs, Luminaires and Traffic Signals to regulate the design of sign structures. These specifications standardize the requirements for load application, methods of analysis, allowable stresses, and design details for sign supports. As a result, they are a primary reference for the design and standing of sign supports.

Table 2-1 show the main assembly configurations of the traffic signs installed on the highways. Element joints are identified as nodes with three degrees of freedom to promote modelling in finite element analysis programs.

Table 2-2 presents the main configurations of the trusses used to support traffic signs installed on the roads. Element joints are identified as nodes with three degrees of freedom to promote modelling in finite element analysis programs.

Table 2-3 shows the geometry of the sectional cuts of the posts used in the traffic signs installed on the roads. Reference is made to the “Stress concentration factor” that will be used during the analysis of stress distribution due to the received wind loads.

Table 2-1: Main Assembly Configurations of Traffic Signs (AASHTO, 2013)

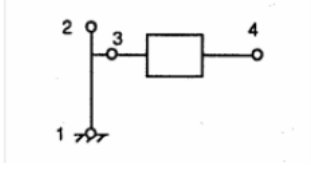
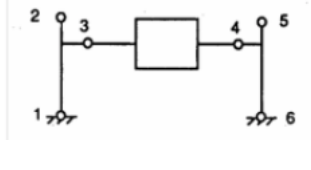
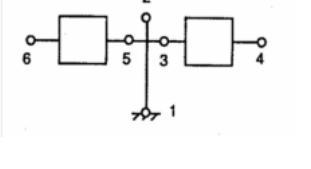
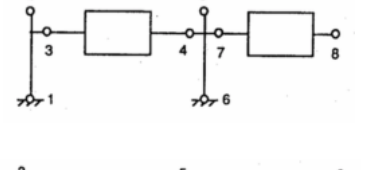
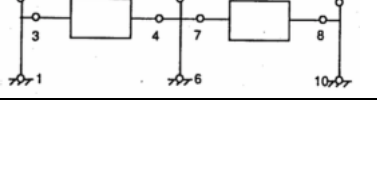
Configuration Number	Description	Basic joint and member numbering sequence
1	Cantilever	
2	Single Span	
3	Butterfly	
4	Single Span with Cantilever	
5	Double Span	

Table 2-2: Main Configurations of Trusses Used to Support Signs (AASHTO, 2013)

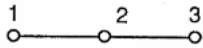
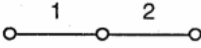
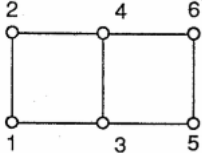
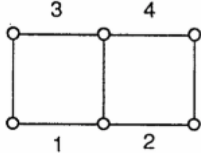
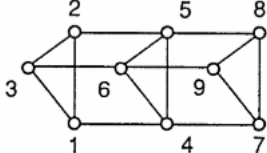
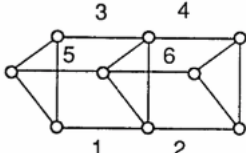
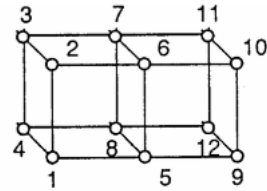
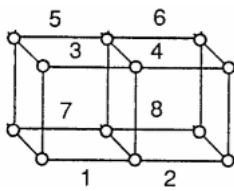
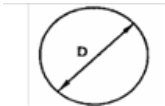
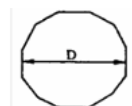
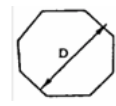
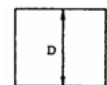
Type ID	DESCRIPTION	BASIC JOINT NUMBERING SEQUENCE	BASIC MEMBER NUMBERING SEQUENCE
1	Monotube, Cantilever		
2	Plane Truss, Cantilever		
3	Trichord Truss, Cantilever		
4	Box Truss, Cantilever		

Table 2-3: Tubular Shapes (AASHTO, 2013)

SHAPE ID	TYPE	FIGURE	STRESS CONCENTRATION FACTOR	COMMENTS
1		Not Used		
2	Round		Not Required	Note the definition of the outer diameter D.
3	Dodecagonal		Figure B-1 AASHTO Spec.	Note the definition of the outer diameter D.
4	Octagonal		Figure B-1 AASHTO Spec.	Note the definition of the outer diameter D.
5	Square		Figure B-1 AASHTO Spec.	Note the definition of the outer diameter D.

2.1.2 AASHTO Specifications, ASCE Standards, and ACI and AISC Codes

When designing a traffic sign, the interaction between these specifications, standards, and codes should be considered. This interaction can be briefly summarized as follows:

- AASHTO Specifications Current Policy: Sign structure supports shall be designed per AASHTO Standard Specifications for Structural Supports for Highway Signs, Luminaires, and Traffic Signals 2013 Edition. Sign foundations shall be designed per LRFD Bridge Design Specifications. PRHTA standard drawings for foundations were designed per LRFD Bridge Design Specifications.

- ASCE/ SEI Standard, and ACI and AISC Codes Current Policy: Shop drawings for signs in the standard drawings should be submitted to PRHTA Traffic Division for review and approval. Design calculations and shop drawings should be submitted for approval for signs that require design and are not detailed in the standard drawings in geometry. Geotechnical investigation is required for overhead sign structures.

2.1.3 Puerto Rico Specifications and Standard Drawings

As part of the literature review, the PRHTA technical specifications used as the base of the shop drawings required for the cantilever overhead traffic signs structures were obtained. Within this technical information and general notes, it was pointed out that the recommended wind speed for the design was 125 mph. These details are in place since year 2000 and were reviewed in 2012. The notes specify that the designs of this type of structures must comply with the requirements established in the AASHTO Standard Specifications for Structural Supports for Highway Signs, Luminaires and Traffic Signals, Second Draft, May 1998 or later drafts. Figure 2-1 presents page 1 of the PRHTA standard drawings for overhead signs and zooms out the design specifications.



In the drawings presented in page 4 of the PRHTA standard drawings for overhead signs, the different types of overhead cantilever signs used in Puerto Rico highways are presented, as displayed in Figure 2-7.

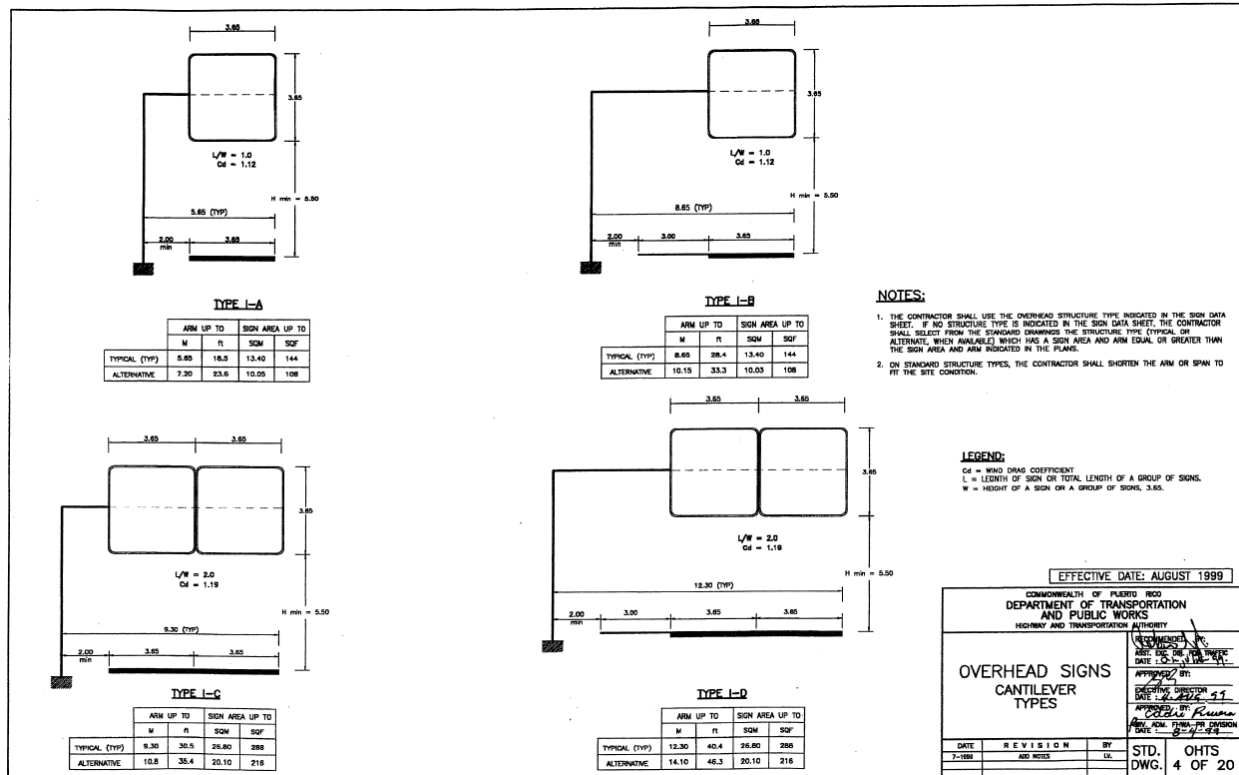


Figure 2-2: Types of Overhead Cantilever Traffic Signs Used in PR (PRHTA, 2010)

Page 10 of the PRHTA standard drawings presents the dimensions of the foundation pedestal, which vary according to the type of sign. Diagrams of the sections are also presented, to support the design process (the notes indicates that the dimensions presented are in accordance with the standard AASHTO 1998), as shown in Figure 2-3. This page also presents the following Design Criteria for the loads, foundation materials (concrete and steel), and soil:

- Wind Speed – 125 mph
- Soil Allowable Bearing Pressure – 2000 psf
- Soil Internal Friction Angle $\phi=22^\circ$
- Concrete: Class A - $f'c=3,000$ psi
- Steel: Reinforcing Steel AASHTO M31 (ASTM A615) Grade 60



For the overhead cantilever signs that are the objective of this study, the PRHTA standard drawings present structural notes, specifications, isometric views, tables presenting the list of approved manufacturers, table to presents the list of approved shop drawings, connection details, elevations of the truss used as horizontal arm, and tables with value of variables according to the type of sign, as presented in Figure 2-4, Figure 2-5 and Figure 2-6. This data was used to model the signs in the Solid Works program.

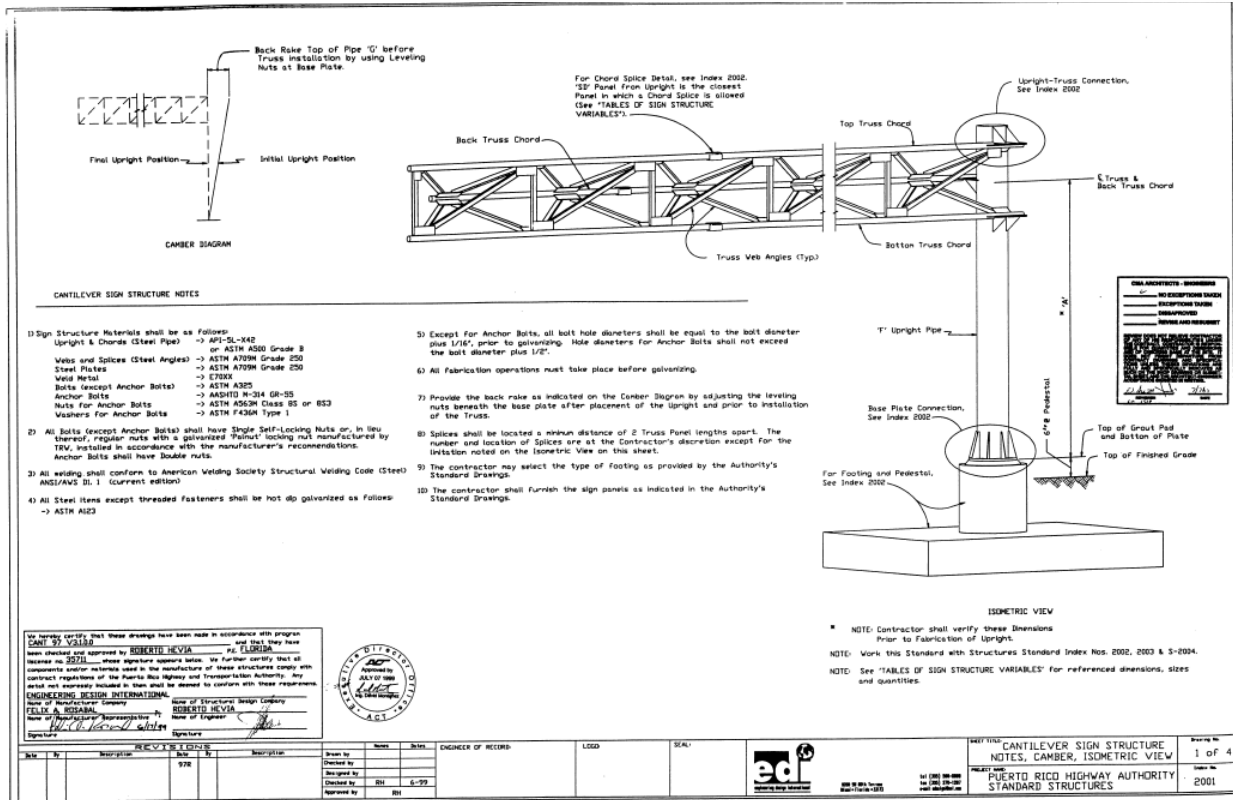


Figure 2-4: Overhead Cantilever Traffic Sign Structures (PRHTA, 2010)

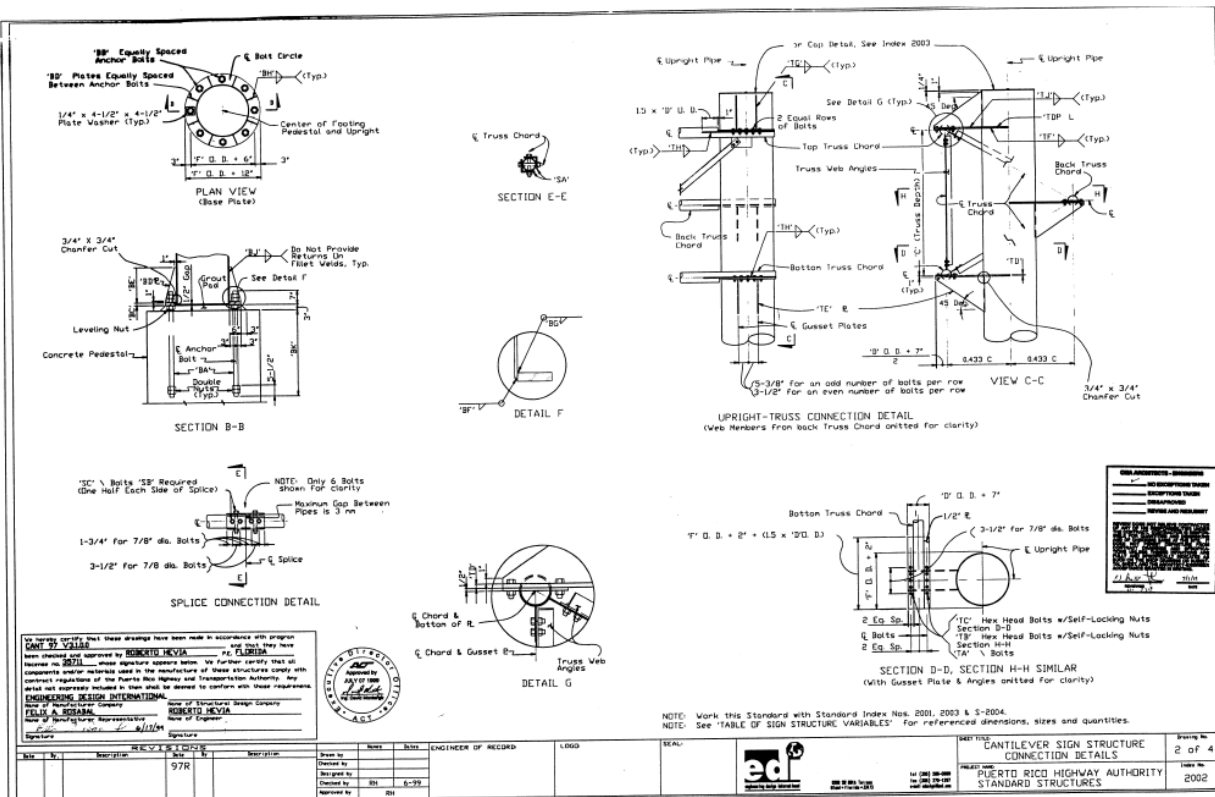


Figure 2-5: Overhead Cantilever Traffic Sign Structure Connection Details (PRHTA, 2010)

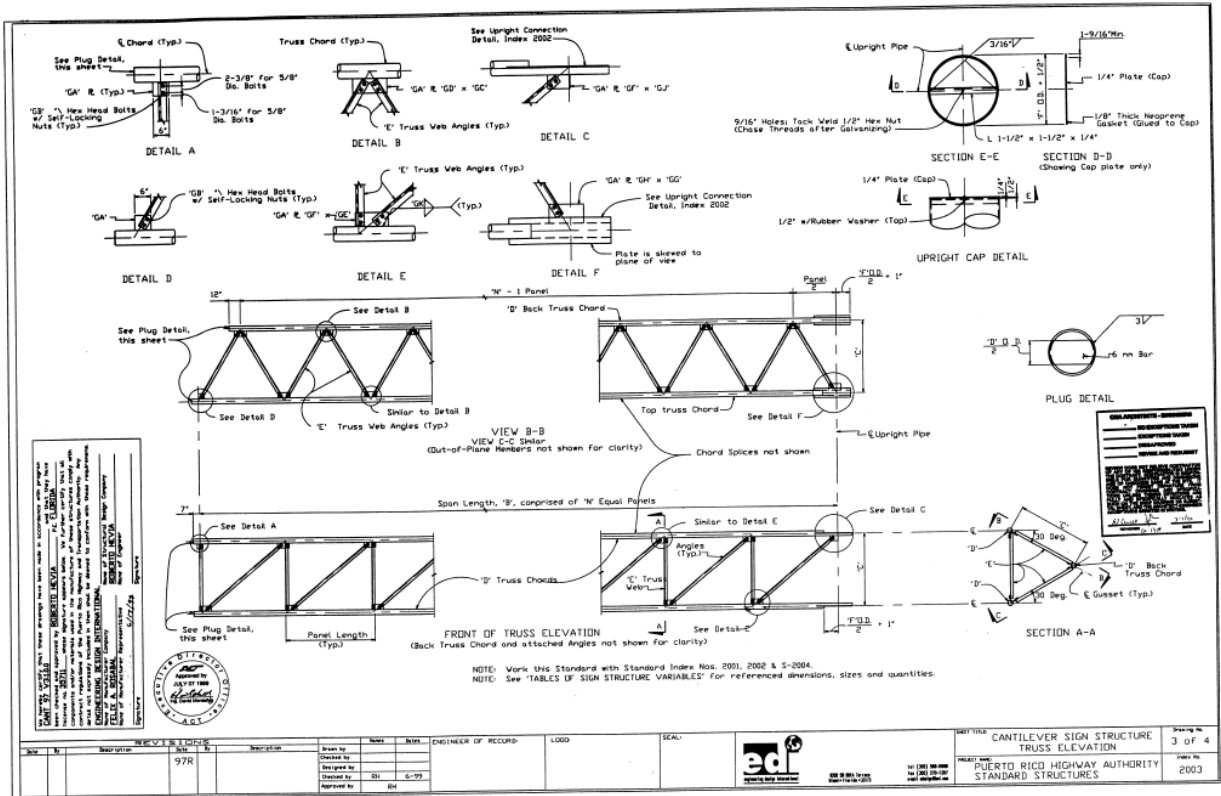


Figure 2-6: Overhead Cantilever Traffic Sign - Truss Arm Elevations (PRHTA, 2010)

2.2 Loads Effects on Traffic Signs and Load Design Criteria

Design loads for ancillary structures include dead and live loads, ice loads, and wind loads. For most structures, design will be governed by wind loads. Dead load includes the weight of the structural support itself, as well as the weights of signs, luminaires, traffic signals, lowering devices and any other appurtenances permanently attached to, and supported by, the structure. Temporary loads that may occur during maintenance should also be considered as dead load. AASHTO also requires that a live load be applied to any walkways and service platforms or ladders.

The primary loads applied to sign, signal, and luminaire structures are due to natural winds. Table 2-4 summarizes the load combinations and the percentage of allowed stress, which will be used during the analysis of the distribution of efforts due to the wind loads received, according to

the AASHTO Standard Specifications for Structural Supports for Highway Signs, Luminaires, & Traffic Signals.

Table 2-4: Group Load Combinations (AASHTO, 2013)

GROUP LOAD	LOAD COMBINATION	PERCENTAGE OF ALLOWABLE STRESS
I	<i>DL</i>	100
II	<i>DL+W</i>	133
III	<i>DL+I_{ce}+W</i>	133
IV	Fatigue	*

Note: Fatigue load is treated separately in the specification.

It is important to point out that the structure must not only have sufficient strength to withstand the maximum expected wind loads, normally a once in 50 years maximum, but also the fatigue effects of fluctuating winds of lower force. There are four wind-loading phenomena that can lead to vibration and fatigue: natural wind gusts, truck-induced gusts, vortex shedding, and galloping (AASHTO, 2013). The interaction of the support structure with the wind is dependent on the structure's stiffness and shape.

The high flexibility and low damping of cantilever support structures makes them susceptible to resonant vibration in the wind. The flexible cantilever structures have low natural frequencies of about 1 Hz (period of vibration of 1 second), which is in the range of typical wind gust frequencies. The closeness of the wind gust frequencies to the natural frequency causes resonance or dynamic amplification of the response. In addition, typical damping ratios in these structures are extremely low (less than one percent of critical damping). The low damping increases the amplification of the wind-induced vibrations.

Usually, the greater the length of the Cantilever mast arm, the more susceptible the support structure will be to wind-induced vibration. In recent years, the span length of the Cantilever mast arms has increased significantly, as displayed in Figure 2-7.



Figure 2-7: Cantilever-type Traffic Sign Installation

Personnel involved in installation, inspection, maintenance, and repair of ancillary support structures should understand the wind loading and response of various support structures. This will enable them to recognize these problems in the field and have a better understanding of the important reasons for quality control during the structure erection phase. Section 2.4 presents more detail about wind induced vibrations on traffic signs.

2.3 Wind Loads Computation Procedures

Regarding the computation of wind pressures on signs, to perform a static analysis of the effect of the wind over a traffic sign, there are two procedures available, as briefly described in the following subsections.

2.3.1 Wind Pressure Equation According AASHTO

The design wind pressure shall be computed using the following equation, according the LRFD Specifications for Structural Supports for Highway Signs, Luminaires, & Traffic Signals:

$$P_z = 0.00256 K_z G V^2 I_r C_d \text{ (psf)}$$

where:

V is the basic wind speed (mph)

K_z is the height and exposure factor

G is the gust effect factor

I_r is the importance factor as presented in table 3.8.3-1 of the AASHTO specifications

C_d is the drag coefficient, taken as 1.19 for all this type of signs

2.3.2 Wind Pressure Equation According ASCE

The design wind pressure (as described in Chapter 29, section 29.3, of ASCE 7-16 and Chapter 6, section 6.5.14 of ASCE 7-05) shall be computed using:

$$P_z = 0.00256 K_z K_d G V^2 C_f \text{ (psf)}$$

where:

V is the basic wind speed (mph).

K_z is the height and exposure factor evaluated at height z

K_d is the directionality factor

G is the gust effect factor, and

C_f is the force coefficient, which depends on the aspect ratio of the sign (horizontal to vertical dimension); its value ranges from 1.30 to 1.95

To determine the basic wind speed, one should consider the mean recurrence interval (MRI) for the wind as required by AASHTO, presented in Table 2-5, according to the average

daily traffic (ADT) of the highway. Most roads of Puerto Rico will have a typical MRI of 700 years.

Table 2-5: Mean Recurrence Interval (AASHTO, 2014)

TRAFFIC VOLUME	RISK CATEGORY		
	TYPICAL	HIGH	LOW
ADT<100	300	1700	300
100<ADT≤1000	700	1700	300
1000<ADT≤10000	700	1700	300
ADT>10000	1700	1700	300

Typical: Failure could cross travel way

High: Support failure could stop a lifeline travel way

Low: Support failure could not cross travel way

Roadside sign support: use 300 years

Figure 2-8 identifies the levels of wind speeds presented by the Puerto Rico Building Code as revised in 2018. This code is based on the International Building Code 2018, which in turns adopts the ASCE 7-16 Standard for loads on buildings and other structures. It can be noted that the design speeds on the island increased from 145 mph, which was the value required by the Puerto Rico Building Code prior to the 2018 revision (and based in ASCE 7-05), to a range from 160 to 180 mph for buildings and other structures in risk category II, that would correspond to the mean recurrence interval previously mentioned. In the notes are the design parameters that will be used for the analysis of wind pressures in the exposed structure that is the object of this investigation.

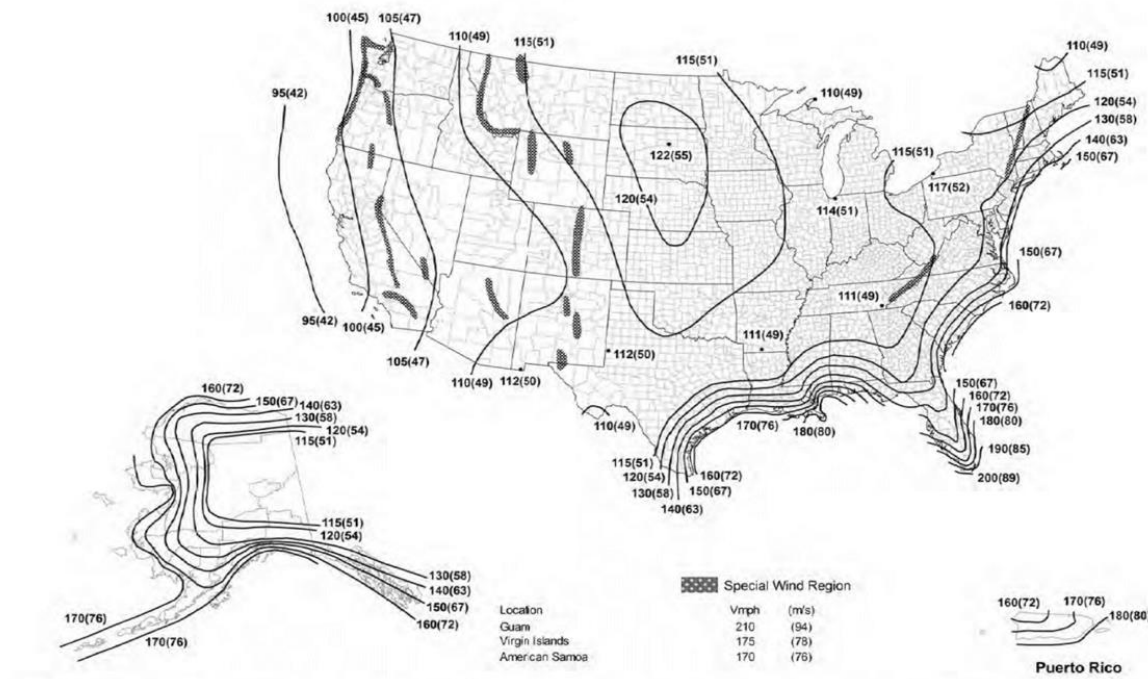


Figure 2-8: Basic Design Wind Speeds, V, for Risk Category II Buildings and other Structures. (ASCE7-16 CH26)

Notes:

1. Values are nominal design 3-second gust speeds in miles per hour (m/s) at 33 ft (10 m) above ground for Exposure C category.
2. Linear interpolation is permitted between the contours. Point values are provided to aid with interpolation.
3. Islands, coastal areas, and land boundaries outside the last contour shall use the last wind speed contour.
4. Mountain's terrain, gorges, ocean promontories, and special wind regions shall be examined for unusual wind conditions.
5. Wind speeds correspond to approximately a 7% probability of exceedance in 50 years (Annual Exceedance Probability = 0.00143, MRI = 700 Years)
6. Location-specific basic wind speeds shall be permitted to be determined using www.atcouncil.org/windspeed when applicable to ASCE 7.
7. Basic Wind Speed (Extreme Event Limit State) MRI 700 yr.

2.4 Antecedents

During the literary review process, two studies were identified that sought to understand the effect of wind loads on the overhead cantilever traffic signs that are the object of this study.

The first was the report titled Anchor Embedment Requirements for Signal/Sign Structures (Cook & Halcovage, 2007). The project focused on being able to determine the causes of rotational failures in cantilevered signs. This was the result of failures identified in the embedment of the foundation anchors during the 2004 hurricane season in the Florida area. As a result of this study, it was determined that the main failure was caused by the shear force in the anchors parallel to the edge of the pedestal. It was identified that this is a failure mode was not considered in the design procedures for this type of foundation. Upon completion of their research, they presented an alternative to increase the capacity of the structure using a carbon fiber reinforced polymer wrap around the upper part of the pedestal.

The second study consisted of three inspection reports commissioned by the Signals Division of the PRHTA to three private companies. The first of these reports was conducted by the company Kimley and Horn, which focused on conducting an inspection and recommendation of the bridge-type traffic signs located on the PR-187 highway in the Carolina area. They inspected ten signs, all showing similar damages such as corrosion of the bolts and base plate, as well as loss of parts on the sign. The second study was conducted by the company CSA Architects and Engineers, entitled "Overhead Sign Foundations Assessment Visit at PR-18". This study presents an inspection conducted on nine signs, where six of these presented problems of rotations at their base. The third study was conducted by the company R + L Structures Engineers L.L.C., entitled "Overhead Signs Assessment at PR-5" presenting an inspection report of six signs, where two of them were I-A cantilever type. No additional studies were found, thus reinforcing the importance

of conducting an inspection of the cantilever-type traffic signs that involve the main roads of the Island.

3 Methodology

The objective of this study was to perform a comprehensive field study to identify the cantilever-type traffic signs that experienced damages due to the wind loads of Hurricane María, analyze, and classify the type of damages, assess their causes, and identify vulnerable situations, and propose lines of action to improve the resilience of this type of signs. The following sections outline the methodology adopted to reach these objectives.

3.1 Search for Background Information

The principal findings of this stage were the PRHTA standard drawings; PRHTA reports on overhead signs; other standards, reports, and antecedents. The main findings were summarized in Chapter 2.

3.2 Case Selection and Location Identification

To present a representative sample of the conditions of the cantilever traffic signs, the subject of this investigation, it was required to cover all the roads of the country that use the mentioned signs. To inspect the largest number of posts affected, a strategy for data collection was established. The data was collected using different strategies, as presented in the following subsections.

3.2.1 Preliminary Reconnaissance

The preliminary visits to identify the case study were carried out during the months of October, November, and December 2017. In these preliminary visits, reconnaissance tours were carried out driving a car along some of the primary Puerto Rico highways, to identify damages, and perform preliminary inspections of the damaged structures and their pedestals. The highways visited were PR-17, PR-18, PR-30, PR-52, and PR-66, around the towns of San Juan, Caguas, Guayama, Las Piedras, Yabucoa, and Loíza.

The visits allowed to identify the cantilever traffic signs as an interesting case of study, where one can contribute significantly to improve the resilience of the system by analyzing their failure. It also allowed to establish important characteristics to be documented for the signs to assess their behavior. As results of this preliminary visits, the first seven locations were established, and preliminary data was collected.

3.2.2 Identify Possible Sites by Exploratory Drives Along Puerto Rico Main Highways

To obtain more cases, additional tours of the roads were carried out during 2018. By driving along the main highways of Puerto Rico, 32 additional cases were identified and located.

3.2.3 News Analysis and PRHTA Interview

Having selected cantilever-type signs as the focus of the study, local news outlets were analyzed during the first months of 2018 to identify reported damages. One (1) case was obtained this way.

Then, an interview was coordinated with the directive staff of the PRHTA during mid-2018, to present the project and obtain collaboration for the collection of information on the damage caused to road structures during the passage of Hurricane María. Two additional cases were obtained. PRHTA also provided three brief reports on signs damages; these reports were developed by private sub-contractors, as commissioned by the PRHTA, as mentioned in section 2.4.

3.2.4 Identify Possible Sites of Signs Damages Using GIS Tools

To broaden even more the number of cases, covering most of PR main island, a GIS based spatial technique was envisioned and implemented. Due to its availability, accessibility and adequacy, Google Earth Pro was selected as the Geographic Information Systems (GIS) to be used to perform a virtual tour along PR highways. This tour allowed to locate cantilever type traffic

signs as potential case studies; in some of the locations identified, it also allowed to assess their possible failure by comparing satellite images from dates before and after September 20, 2017. This imagery spatial analysis allows to identify sixty-six (66) potential additional cases.

3.3 Field Inspection and Data Collection

The process of collecting the data for each case implied:

1. Identifying each case by a unique number (ID using the highway code).
2. Developing an analysis of Puerto Rico Highway network, with the location of the signs, to generate the inspection schedule, where the roads and the estimated time are specified. Five main areas on the island were explored. The inspection findings were grouped in the following areas: Northwest, North, Northeast, East, Southeast, South, and part of the Central East area of the island.
3. The creation of a data collection form for the visual inspection of traffic signs that synthesizes the principal characteristics and findings that were established in the theoretical framework, selecting data that correspond to the indicators of the failures in the structure. The purpose of the document is to standardize the collection of information during the inspection. As a direct benefit, the optimization of the inspection time was observed, guaranteeing having the greatest amount of data, greater organization, avoiding the loss of information and facilitating the analysis of the data.
4. Deciding inspection tools to be carried to the field visits: primary consisting of the inspection forms, digital camera, measurement tape, and level.
5. Reviewing the process to assure that the required amount of data would be collected during the field visits.

Ninety-five (95) cantilever traffic signs were visited and fully documented with geolocated reference photos and field inspection forms. Fragments of the signs were identified in some of the areas, which were collected to obtain the mechanical characteristics of the materials, and to compare them to the technical specifications to assess if there was a deficiency in material mechanical properties. Samples were collected from the following sections of traffic signs: pedestal concrete, anchor bolts, connecting nuts between the base plates and the bolt, sign anchor element, and pedestal reinforcing steel. The identified materials were stored in the laboratory for testing.

3.4 Analysis, Description and Classifications of Failures

This was the central part of the study. During the inspection process, failures in the structure were identified, mainly the foundation. In the process of analyzing the collected data, the following failure levels of damage/failure were established:

- **Damage** – The sign was in its original position but presented some damages such as fractures in the pedestal concrete that may be related to internal stresses due to received loads. The idea of this level is to indicate that the signs were usable, but several may require repair and reinforcement to assure its resilient behavior.
- **Partial Collapse** – The sign was still standing (not on the ground), but its position and instability were compromised, presenting fractures in the concrete of the pedestal, displacements of the post base plate and anchor bolts, and/or movements of the foundation. The idea of this level is to indicate that the signs may have been providing some service, but most of them required replacement (although some of them could be reinforced and reused).

- Total Collapse – The sign was on the ground, displaying pedestal with major fractures and structure of the traffic sign on the ground. The idea of this level is to indicate that the signs were not providing any service, and that they required replacement.

When evaluating the collected data, the two main failure models identified were, associated to foundation failures: one associated to soil failure, or soil foundation interaction failure; the other associated to structural failures in the foundation pedestal. Some design/construction deficiencies were identified and documented.

3.5 Virtual Exploration Tool Development

To confirm the information obtained in the virtual investigation carried out using GIS systems, the posts were georeferenced using GPS system. With this increased precision of the location of each case study, a virtual exploration tool was developed as a layer of Google Earth Pro program. The main idea of the tool is to serve as an education and assessing tool, displaying the location all the eighty-one cases inspected, with relevant photos displaying the condition, and a summary of the principal findings. It is expected that this tool would be useful for the PRHTA, the FHWA, and the universities.

3.6 Mechanical Tests on Material Samples

The mechanical testing of the solid materials used in the design of cantilever traffic signs is determined by destructive testing. These tests are performed on standardized samples of the material, this means that the samples are subjected to a type of force until they fracture. This allows to obtain the mechanical properties of the material that are the most important during the selection of design materials, since their main function is to withstand force.

These tests were carried out in the structures laboratory of the Department of Civil & Environmental Engineering and Land Surveying at the Polytechnic University of Puerto Rico

(PUPR), and the Jaca & Sierra laboratory located in the municipality of Trujillo Alto. The methodology used to carry out the mechanical tests was governed by the applicable ASTM standards.

At the PUPR laboratories, the tests carried out were: (a) compression tests on the concrete specimens collected from the pedestals and (b) tension test on the reinforcing steel collected from the pedestal. The tension tests on the anchor bolts of the pedestal were performed in the Jaca & Sierra laboratory. This action was necessary since the laboratory had a test equipment with greater capacity to reach anchor bolt fracture capacity.

The data was analyzed, and the mechanical characteristics of the material were established for each specimen collected. These were compared with the characteristics specified in the codes and technical drawings used by PRHTA, allowing further analysis.

3.7 Summary of Findings, Conclusions and Recommendations to Increase Resilience

Finally, a summary of the findings was carried out, and conclusions and recommendations based on these findings, with the aim of increasing the resilience of these type of cantilever signs (and thus, the resilience of the transportation system), were developed.

The following chapters will describe these stages in more detail and present a summary of the findings in each phase.

.

4 Identification of Cantilever Signs with Possible Damages and/or Collapse

As mentioned in Chapter 3, to have a representative evaluation of the conditions of the cantilever traffic signs after the pass of Hurricane Maria, it was decided to cover all the highways of Puerto Rico that use the mentioned signs, to gather as much information as possible. The data was collected using different strategies and procedures, as presented in the following sections.

4.1 Preliminary Reconnaissance

As previously mentioned in Chapter 3, the preliminary visits to identify failures to the transportation infrastructure, and select the case study, were carried out during the months of October to December 2017. In these preliminary visits, reconnaissance tours were carried out by driving along some of the primary Puerto Rico highways: PR-17, PR-18, PR-30, PR-52, and PR-66, covering the towns of San Juan, Caguas, Guayama, Las Piedras, Yabucoa, and Loíza and their vicinities.

Among the damages to the transportation infrastructure, the collapse of cantilever traffic signs was identified as an important case of study, since their failure could interrupt the traffic flow (by blocking the roadway) and could affect rescue processes (since cellular data and GPS maps are seldom available after a disaster, so these traffic signs are essential to guide rescue teams, that may not be familiar with the area). The analysis of the failures could lead to suggestions that improve the resilience of these type of signs, and thus contribute to the resilience of the transportation infrastructure. Followings are some examples of the of the seven locations identified during this stage.

Figure 4-1 and Figure 4-2 show the total collapse of two cantilever traffic sign located on PR-30 highway, near Yabucoa. These cases allowed to identify failures on the foundation pedestal, with the anchor bolts experiencing large deformations, shear failure, and being place outside the

confinement provided by the stirrups. These preliminary findings suggested that a comprehensive graphical documentation of the pedestal was recommended for further field visits.



Figure 4-1: Collapsed Cantilever Sign in PR-30 Highway



Figure 4-2: Collapsed Cantilever Sign in PR-30 Highway

In Figure 4-3, the total collapse of a cantilever traffic sign located on PR-66 Highway, near Loíza, can be appreciated. The mode of failure suggested that not only rotation about a vertical axis but also about a horizontal axis was present, producing not only large deflections and shear failure on the anchor bolts, but also tension on the anchor bolts, and compression and crushing on the concrete. The necessity of documenting the pedestal condition was reinforced.



Figure 4-3: Total Collapse of a Cantilever Sign Located in PR-66 Highway

Figure 4-4 presents the condition found on a cantilever traffic sign located on PR-18 Highway, in the San Juan Area, near the Luis Muñoz Marín Park. The post was in the vertical position, but the sign experienced a rotation of more than 45 degrees. The concrete pedestal experienced damages, with concrete cracks. But the anchors bolts did not experience large lateral deflections, indicating that the hole foundation was subjected to large rotations about the vertical axis, due to lack of enough shear resistance between soil and foundation. These findings reinforced the necessity of documenting the pedestal and foundation condition.



Figure 4-4: Partial Collapse and Damages on a Cantilever Traffic Sign Located on PR-18 Highway

The seven cases identified in the preliminary reconnaissance motivated selecting these cantilever traffic signs as case study, and the development of strategies to identify more cases with damages and failures, as describes in the following sections.

4.2 Exploratory Drives Along Puerto Rico Main Highways

The second phase used to identify cases was to perform exploratory drives along some of the main highways of Puerto Rico, searching exclusively for damaged/collapsed cantilever overhead traffic signs. The Puerto Rico highway system consists of approximately 14,400 kilometers (8,948 mi) of roads (PRHTA, 2015). The road system is divided into four networks: primary network, urban primary network, secondary or inter-municipal network, and tertiary or local network (PRHTA, 2015). The cantilever overhead signs are located in the primary network. These types of

roads were identified on the road map obtained from the PRDOT, presented in Figure 4-5 as Expressways and Highways.



Figure 4-5: Transportation Infrastructure in Puerto Rico and Related Data (source: www.mapacarreteras.org)

These exploratory drives along PR-2, PR-18, PR-22, and PR-52 resulted in the identification of 32 additional cases. The signs were identified with a sequential number, in the order they were localized during the field trips.

4.3 Search in News Outlets

Local and global news outlets were reviewed, searching for articles describing damages to the transportation infrastructure in general, and to the traffic signs in particular. One case study was obtained this way, reported by journalist Jay Fonseca in the newspaper El Nuevo Día. The sign was located in PR-53 Highway, near Salinas. A BBC Mundo news report presented a case depicted in Figure 4-6 , which resulted in one of the cases identified in the preliminary tours in PR-17.



Figure 4-6: Overhead Cantilever Traffic Sign Collapse on PR-17 (Lima, 2017)

4.4 Interview PRHTA Personnel to Receive Their Input

As part of the data collection and case identification process, an interview was coordinated with the directive staff of the PRHTA on May 2, 2019. The main objective was to present the project, which could be of interest to the PRHTA. The interview also aimed to obtaining the PRHTA collaboration for the compilation of information regarding the damages caused to road infrastructure by the pass of Hurricane María, concentrating efforts on the cantilever-type traffic signs that were the main objective of this study. The interview took place at the Signs Office at the Minillas Government Center. The interviewee was Juan Carlos Rivera, Principal Director of the Division of Signs of the PRHTA. Rivera was in charge of the restoration of the existing signs and the removal and reinstallation of the signs that collapsed due to the winds produced by Hurricane María. As part of the preparation for the interview, five (5) questions were developed. Table 4-1 summarizes the interview.

Table 4-1: Interview questions and answers conducted with Eng. Rivera, Director of the Signs Division of PRHTA

QUESTIONS	ANSWERS
What reconnaissance procedure was carried out on PR main roads after Hurricane Maria?	The agency's brigades were distributed along the main roads to identify the collapsed structures and establish the removal and reconstruction plan.
Is information available on the inspections performed?	<p>The office allowed review of the Structural Evaluation reports carried out in a first phase by contracted design offices. The following reports were reviewed:</p> <ul style="list-style-type: none"> - Structures Report 1 "Overhead Signs Assessment at PR-5" Company: R+L Structures Engineers L.L.C. - Structures Report 2 "Overhead Sign Foundations Assessment Visit at PR-18" Company: CSA Architects and Engineers, LLP. - Structures Report 3 "Overhead sign report- PR-187" Bridge Type Company: Kimley Horn <p>The inspection did not focus on the traffic signs that are the subject of this investigation. They were a general inspection of the affected traffic signs in the assigned area.</p>
Where is the debris from the collapsed traffic signs stored?	Mr. Misael Cuevas Quintana, indicated that the removed sections were stored at the Service Warehouse located in the town of Bayamón.
Is it possible to access the collected material?	To gain access to the area where the collected items were stored, a permission must be granted from the agency.
Are the shop drawings of the traffic signs that are the subject of this research available?	A digital copy of the PRHTA standard drawings, as revised in August 2012, was provided.

To delve into some of the data obtained in the meeting, Mr. Rivera coordinated an interview with Mr. Misael Cuevas Quintana, Director of the Highway Division. The interview took place at the Minillas Government Center. The interview focused on the coordination of future actions for visits to the areas where the pedestals of the removed structures were stored. The objective was to obtain specimens to perform mechanical tests in the laboratory. According to the information obtained in the interview, sections of highways where traffic signs collapse were identified by department personnel. This allowed to effectively coordinate the inspection to the east area of the island.

As a result of the interviews carried out, a collaboration agreement was established by the interviewed personnel, allowing the inspection of the debris storage areas, in addition to documents about the cantilever traffic signs. Two additional cases were identified in PR-53 highway, near Salinas (as results of an additional field visit to the south division area of the PRHTA). These conversations also allowed to identify additional potential areas of study: PR-66 Km 12, Highway, in the direction of Carolina to Rio Grande Shopping Center exit on the left side, Juana Díaz Km. 84.6, PR-52 from south to north Km. 58.8.

4.5 Use of GIS Virtual Tour to Identify Potential Cases

During the literary review, codes and design standards were analyzed. This permitted to establish that the traffic signs that are the object of this investigation were located on the high-speed roads on the island. These types of roads were identified on the road map obtained from the PRHTA, as stated in section 4.2. One of the strategies established to identify cases and carry out the inspection was to use GIS programs such as Google Earth Pro. This program allowed to perform virtual tours along main highways of PR and identify and locate overhead cantilever traffic signs as potential case studies.

Keeping this in perspective, an electronically assisted inspection technique was established using satellite image systems where the primary network of the island was toured in a virtual way. For all the signs identified, a historical comparison of images was performed, using images before the landfall of Hurricane María and images after that event (September 20, 2017). Thus, at the end of this process, the posts/signs showing any change in their condition, such as rotation or collapse, were identified, having a preliminary identification of failures. In addition, the location and coordinates of the installed signs were obtained to coordinate the visit to the field.

The GIS platform used for the phase of identifying cantilever traffic sign structures, and evaluating if they had changes in their original condition or had experienced possible collapse was Google Earth Pro. This program allows to generate the required information to establish the strategy of visiting the location. Google Earth Pro is used in many branches of science as an analysis tool.

As mentioned, Google Earth Pro is a computer program that shows a virtual globe that allows you to view multiple cartography, based on satellite images. The Google Earth map is made up of an overlay of satellite imagery, aerial photography, geographic information from GIS data models from around the world, and computer-created models. This allowed to evaluate the conditions of the traffic signs prior to the passage of Hurricane María and the post-hurricane images.

A virtual investigation/tour of the following routes was carried out: PR-2, PR-52, PR-53, PR-3, PR-30, PR-66, PR-18, PR-17, PR-23, PR-22, and PR-26. The virtual tour allows to locate the cantilever traffic signs, and by comparing their condition using methods of Photogrammetry and historical satellite photography, perform a preliminary identification of possible failures due to changes in position. The dates used for the comparison ranged from March 2016 to April 2018.

After locating the sign, the location was marked with a placemark, and the date of the photo was determined to assess whether it showed visible changes. A color code was used where the apparent condition of the element was established: green for those who did not show apparent changes in their condition and red for those who showed changes in position. The position changes observed the following situations: the post presented apparent partial or total collapse, or the post showed apparent rotation at its base. The process resulted in the identification and geolocation of 66 additional cases of cantilever traffic signs as potential case studies. Examples of this

photographic evaluation for cases presenting changes, and the preliminary findings, is presented in the rest of this section.

Images in Figure 4-7 were obtained from the research carried out using the program Google Earth Pro, which works with the historical image analysis method, comparing those presented by the 10/2017 program with those of 12/2016. The inspected sign showed a foundation rotation/twisting failure. For this case (as presented in further chapters), samples of the materials were extracted to perform laboratory testing of their mechanical properties.

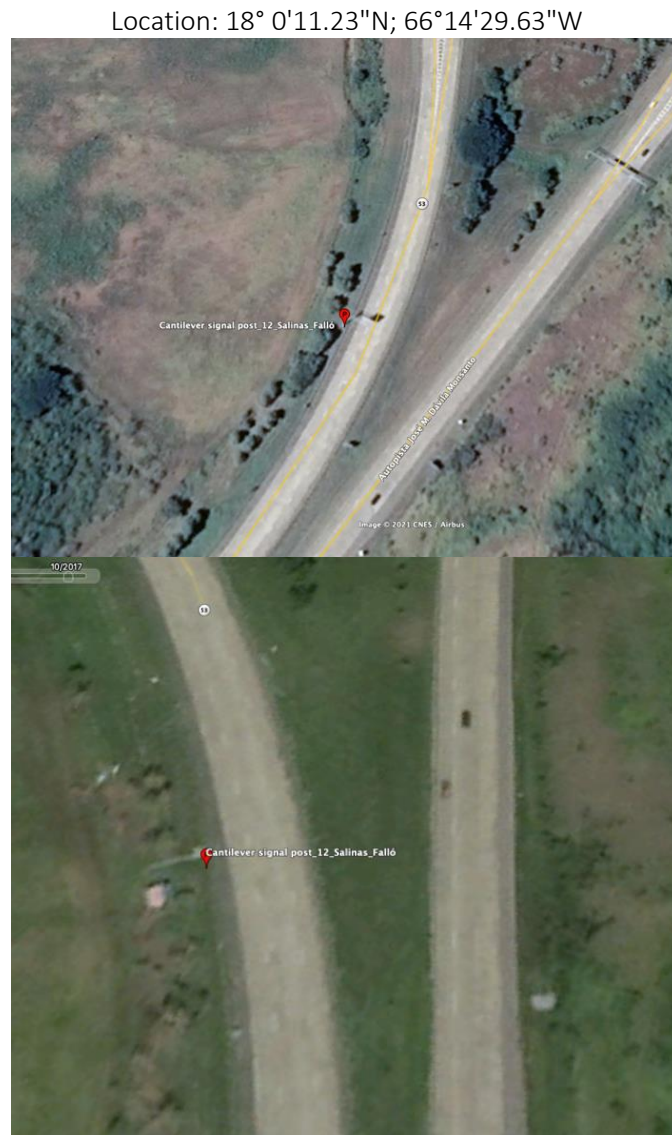


Figure 4-7: Cantilever Sign Post 12 Located in Salinas (Picture1 (12/2016), Picture 2 (10/2017))

Images in Figure 4-8 were obtained from the research carried out using the program Google Earth Pro, which works with the historical image analysis method, comparing those presented by the 1/2019 program with those of 10/2017. Apparent structural collapse, the sign appeared to be removed from the site.

Location: 17°59'8.91"N; 66° 8'45.56"W

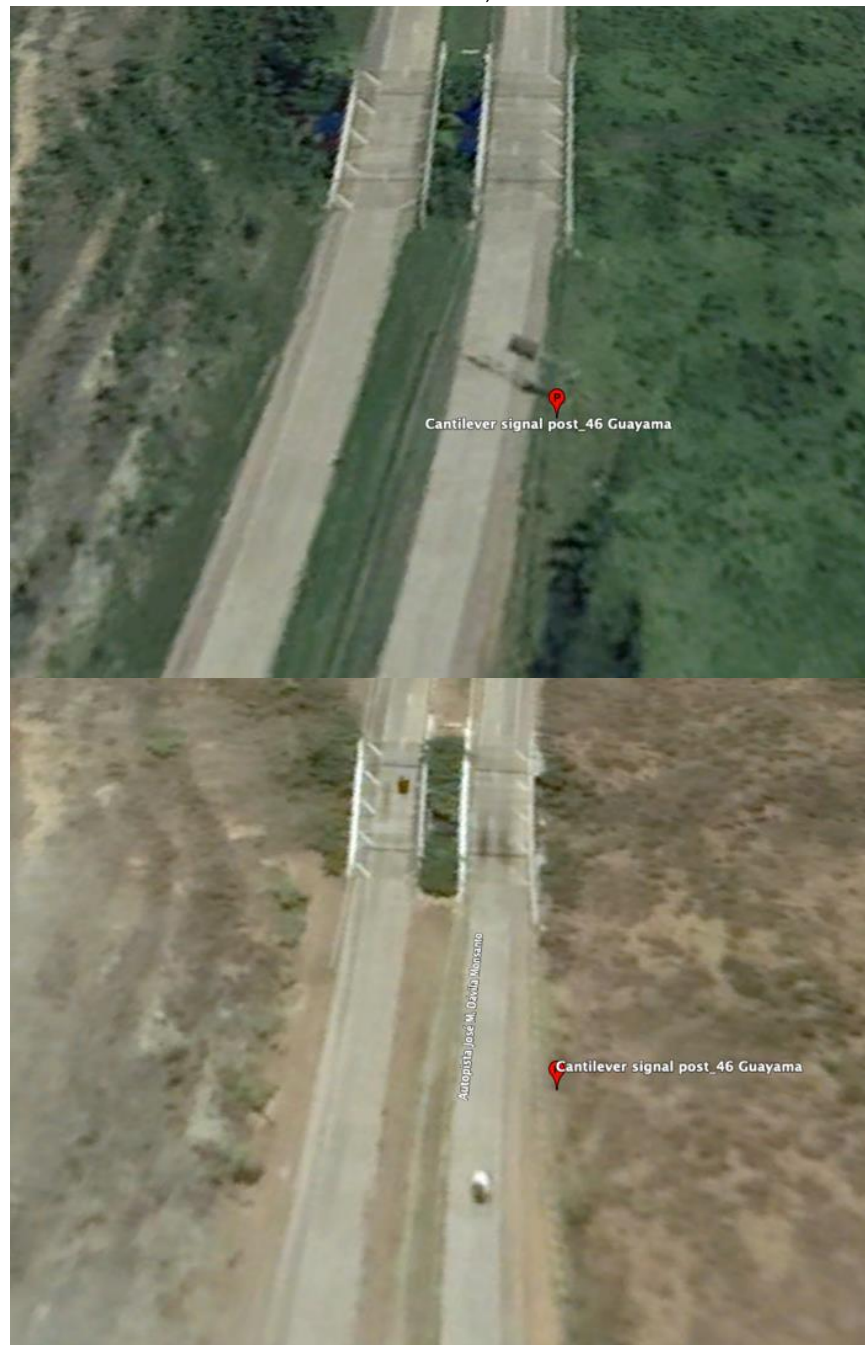


Figure 4-8: Cantilever Sign Post 46 Located in Guayama (Picture 1: 10/2017, Picture 2: 1/2019)

Photos in Figure 4-9 were obtained from the research carried out using the program Google Earth Pro, which works with the historical image analysis method, comparing those presented by the 1/2020 program with those of 4/2016. Located on PR18- N @ Km 2.80. The Cantilever sign rotated approximately 30 degrees. The concrete base could not be seen because it was covered in dirt like most of the steel bolts.

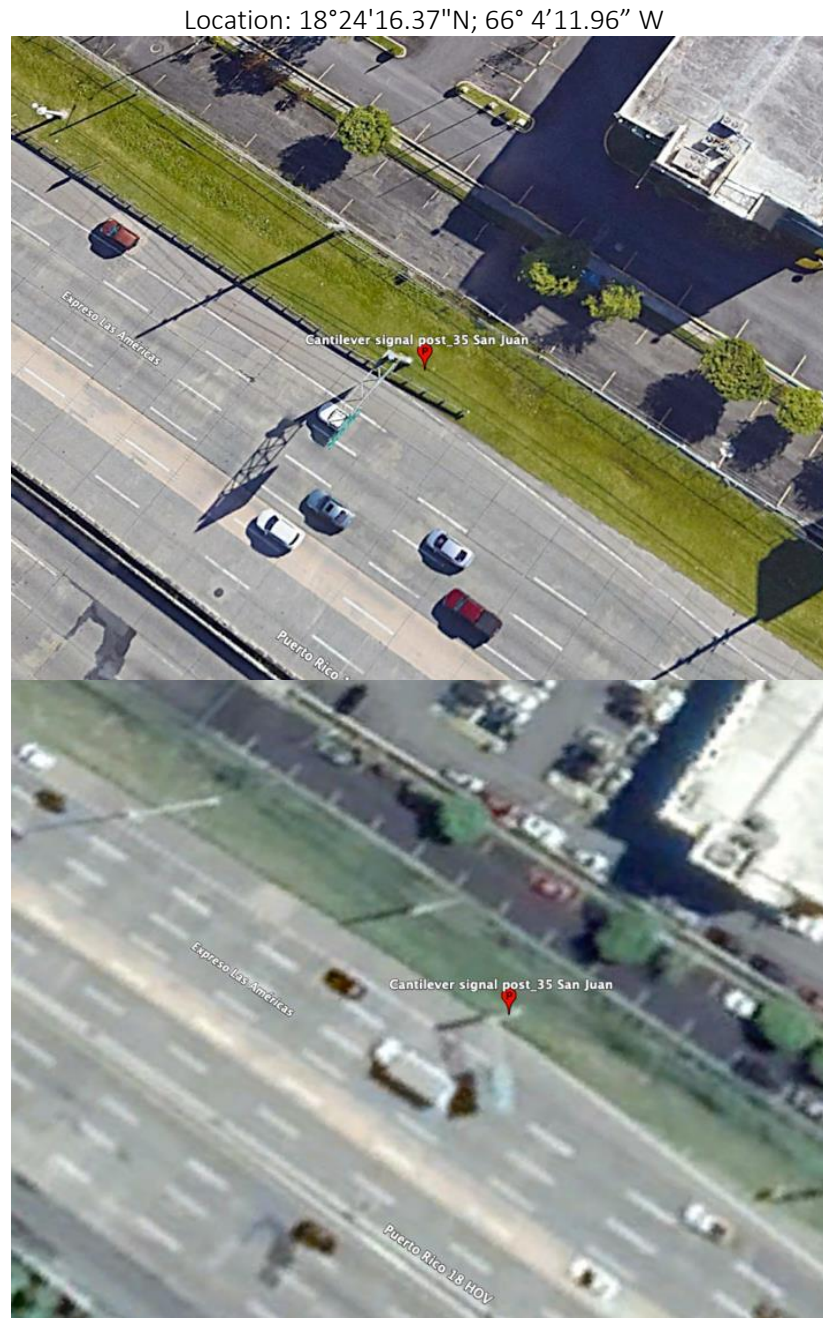


Figure 4-9: Cantilever Sign Post 35 located in San Juan (Picture 1: 4/2016, Picture 2: 1/2020)

Images in Figure 4-10 were obtained from the research carried out using the program Google Earth Pro, which works with the historical image analysis method, comparing those presented by the 4/2018 program with those of 4/2016. Located on PR18 Km 3.0 the Cantilever sign rotated 180 degrees, and the soil around the base failed allowing the base to rotate.

Location: 18°24'5.58"N; 66° 4'16.57"W



Figure 4-10: Cantilever Sign Post 38 Located in San Juan. (Picture 1: 4/2016, Picture 2: 4/2018)

Photos in Figure 4-11 were obtained from the research carried out using the program Google Earth Pro, which works with the historical image analysis method, comparing those presented by the 4/2018 program with those of 4/2016. They show two cantilever traffic signs. The base of the post identified as P-40 rotated approximately 15 degrees and the base suffered damage from loss of cover and cracking. The P-41 cantilever sign base rotated approximately 70 degrees and the concrete base suffered damage from loss of cover and cracking exposing the anchor bolts.

P-40: 18°24'47.25" N; 66° 4'11.53" W

P-41: 18°24'47.01"N; 66° 4'13.07"W

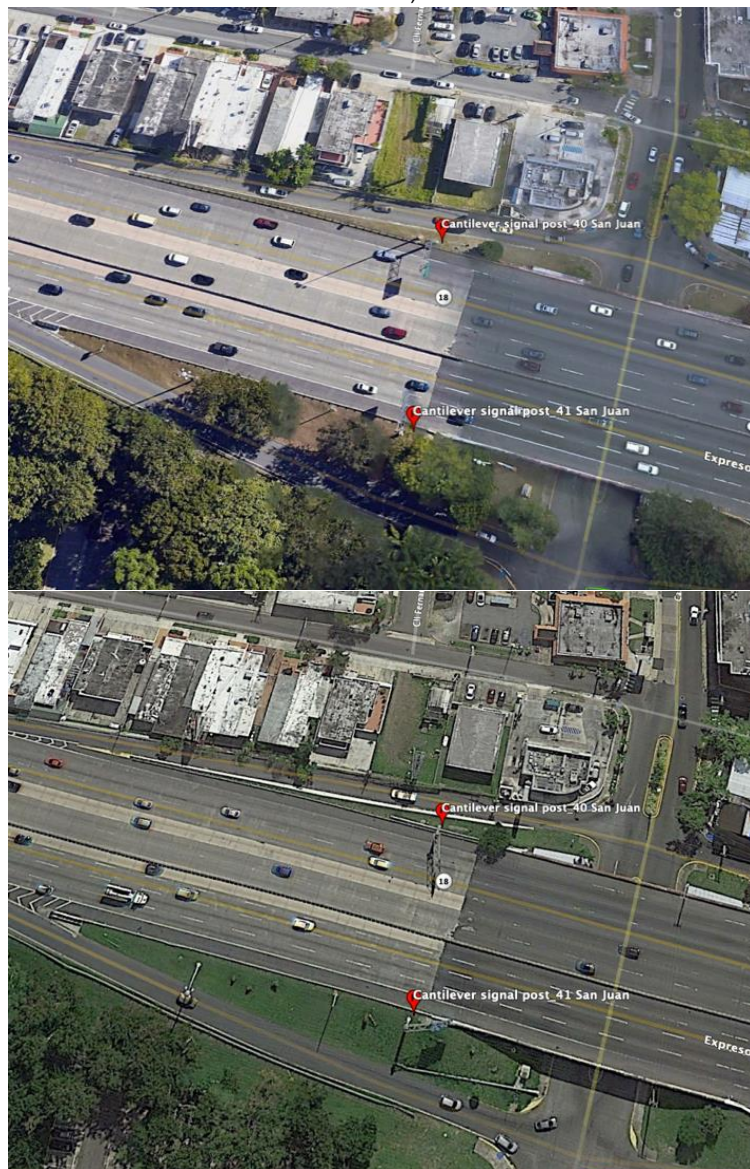


Figure 4-11: Cantilever Sign Post 40 and 41 located in San Juan. (Picture 1: 4/2016, Picture 2: 4/2018)

Figure 4-12 were obtained from the research carried out using the program Google Earth Pro, which works with the historical image analysis method, using the image from 10/2017 where the base of the pole identified as P-46 shows a rotation of approximately 20 degrees.

Location: 17°59'8.91"N; 66° 8'45.56" W



Figure 4-12: Cantilever Sign Post 46 Located in Guayama (Picture 1: 10/2017)

Images in Figure 4-13 were obtained from the research carried out using the program Google Earth Pro, which works with the historical image analysis method, comparing those presented by the 4/2018 program with those of 11/2016. This allows to identify a change in position of the post indicating a possible collapse.



Figure 4-13: Cantilever Sign Post 53 Located in Las Piedras (Picture 1: 11/2016, Picture 2: 4/2018).

Images in Figure 4-14 were obtained from the research carried out using the program Google Earth Pro, which works with the historical image analysis method, comparing those presented by the 4/2018 program with those of 1/2014. This allows to identify a change in position of the post indicating a possible collapse.

Location: 18°11'11.10"N; 65°53'28.92"W

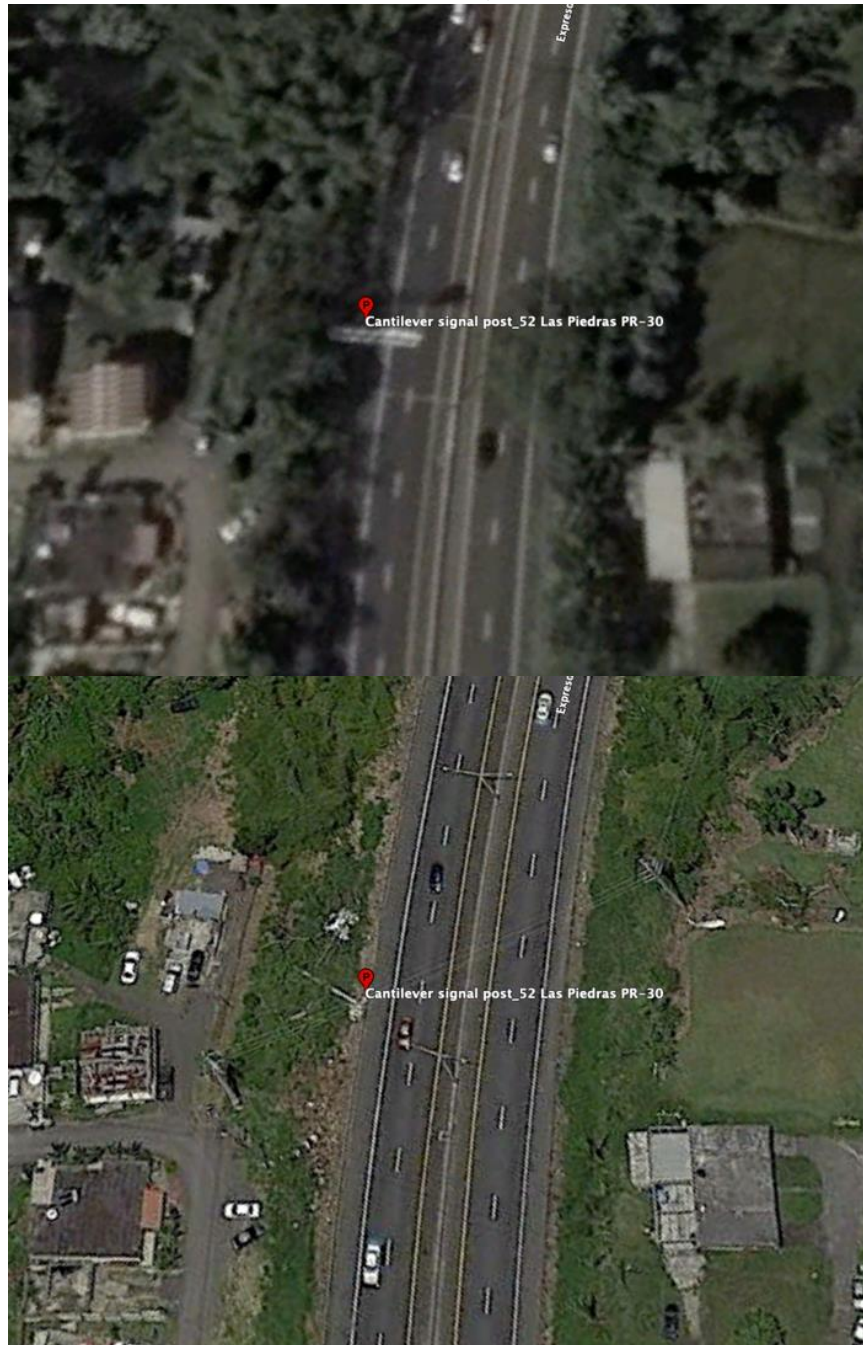


Figure 4-14: Cantilever Sign Post 52 Located in Las Piedras (Picture 1: 1/2014, Picture 2: 4/2018)

Photos in Figure 4-15 were obtained from the research carried out using the program Google Earth Pro, which works with the historical image analysis method, comparing those presented by the 4/2018 program with those of 10/2016. This allows to identify a change in position of the post indicating a possible collapse.

Location: 18°13'27.37"N; 65°54'57.45"W



Figure 4-15: Cantilever Sign Post 56 Located in Juncos (Picture 1: 10/2016, Picture 2: 4/2018)

Photos in Figure 4-16 were obtained from the research carried out using the program Google Earth Pro, which works with the historical image analysis method, comparing those presented by the 4/2018 program with those of 4/2016. This allows to identify a change in position of the post indicating a possible collapse.

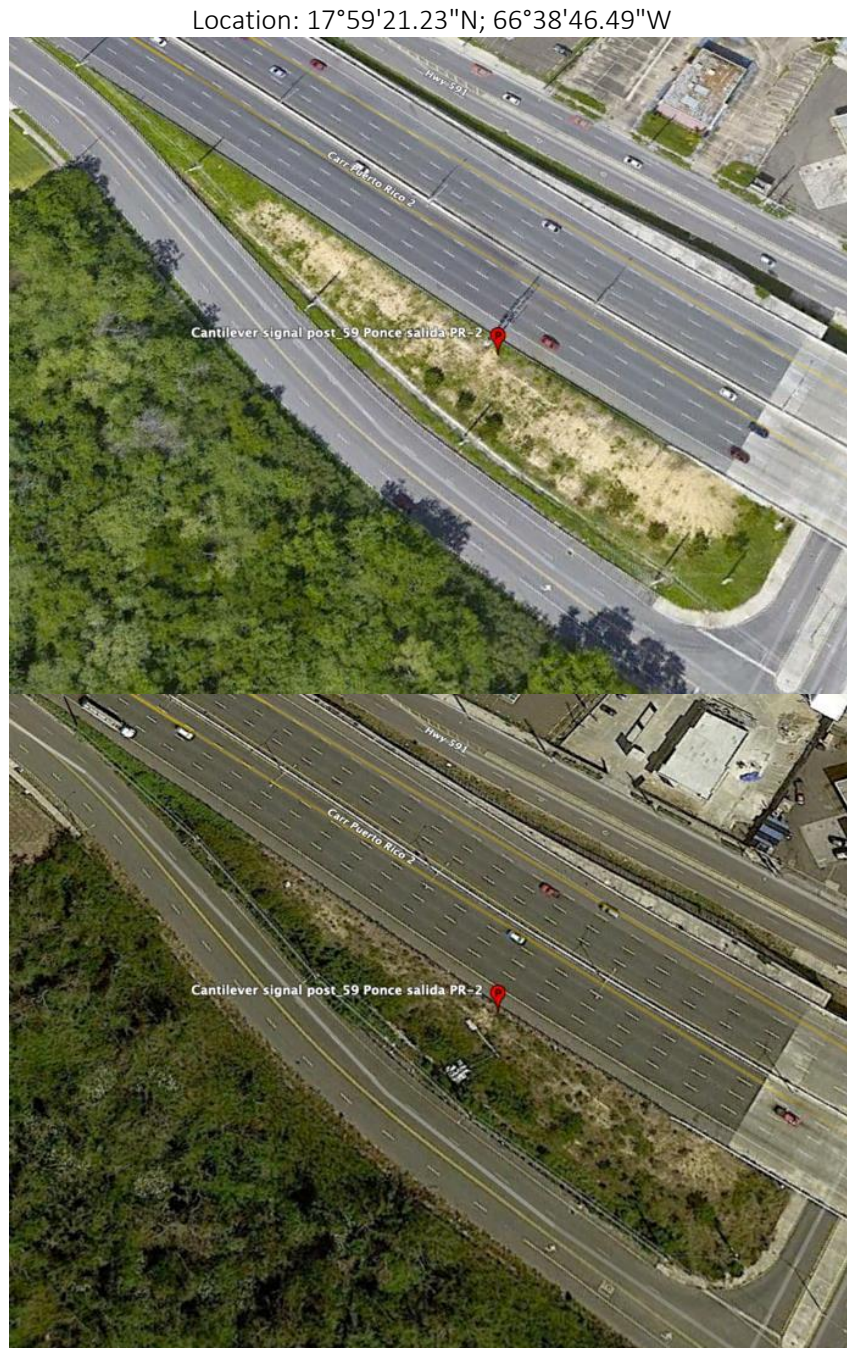


Figure 4-16: Cantilever Sign Post 59 Located in Ponce (Picture 1: 4/2016, Picture 2: 4/2018)

Images in Figure 4-17 were obtained from the research carried out using the program Google Earth Pro, which works with the historical image analysis method, comparing those presented by the 10/2017 program with those of 12/2016. This allows to identify a change in position of the post indicating a possible collapse.

Location: 18° 9'35.91"N; 65°47'50.85"W



Figure 4-17: Cantilever Sign Post 61 Located in Humacao (Picture 1: 12/2016, Picture 2: 10/2017)

Photos in Figure 4-18 were obtained from the research carried out using the program Google Earth Pro, which works with the historical image analysis method, comparing those presented by the 1/2018 program with those of 2/2017. This allows to identify a change in position of the post indicating a possible collapse.

Location: 18°17'6.38"N; 65°38'59.64"W



Figure 4-18: Cantilever Sign Post 66 Located in Fajardo (Picture 1: 2/2017, Picture 2: 1/2018)

Images in Figure 4-19 were obtained from the research carried out using the program Google Earth Pro, which works with the historical image analysis method, comparing those presented by the 4/2018 program with those of 3/2013. This allows to identify a change in position of the post indicating a possible collapse.

Location: 18°22'20.65"N; 65°52'38.72"W



Figure 4-19: Cantilever Sign Post 69 Located in Canóvanas (Picture 1: 3/2013, Picture 2: 4/2018)

Images in Figure 4-20 were obtained from the research carried out using the program Google Earth Pro, which works with the historical image analysis method, comparing those presented by the 4/2018 program with those of 2/2017. Cantilever sign foundation failure at P-76 in PR 2_Aguadilla. The Cantilever sign rotated approximately 30 degrees.



Figure 4-20: Cantilever Sign Post 76 Located in Aguadilla (Picture 1: 2/2017, Picture 2: 4/2018)

Images in Figure 4-21 were obtained from the research carried out using the program Google Earth Pro, which works with the historical image analysis method, comparing those presented by the 5/2018 program with those of 9/2016. Cantilever sign foundation failure at P-77 in PR 2_Aguadilla. The Cantilever sign rotated approximately 270 degrees.

Location: 18°27'13.01"N; 67° 5'20.87"W

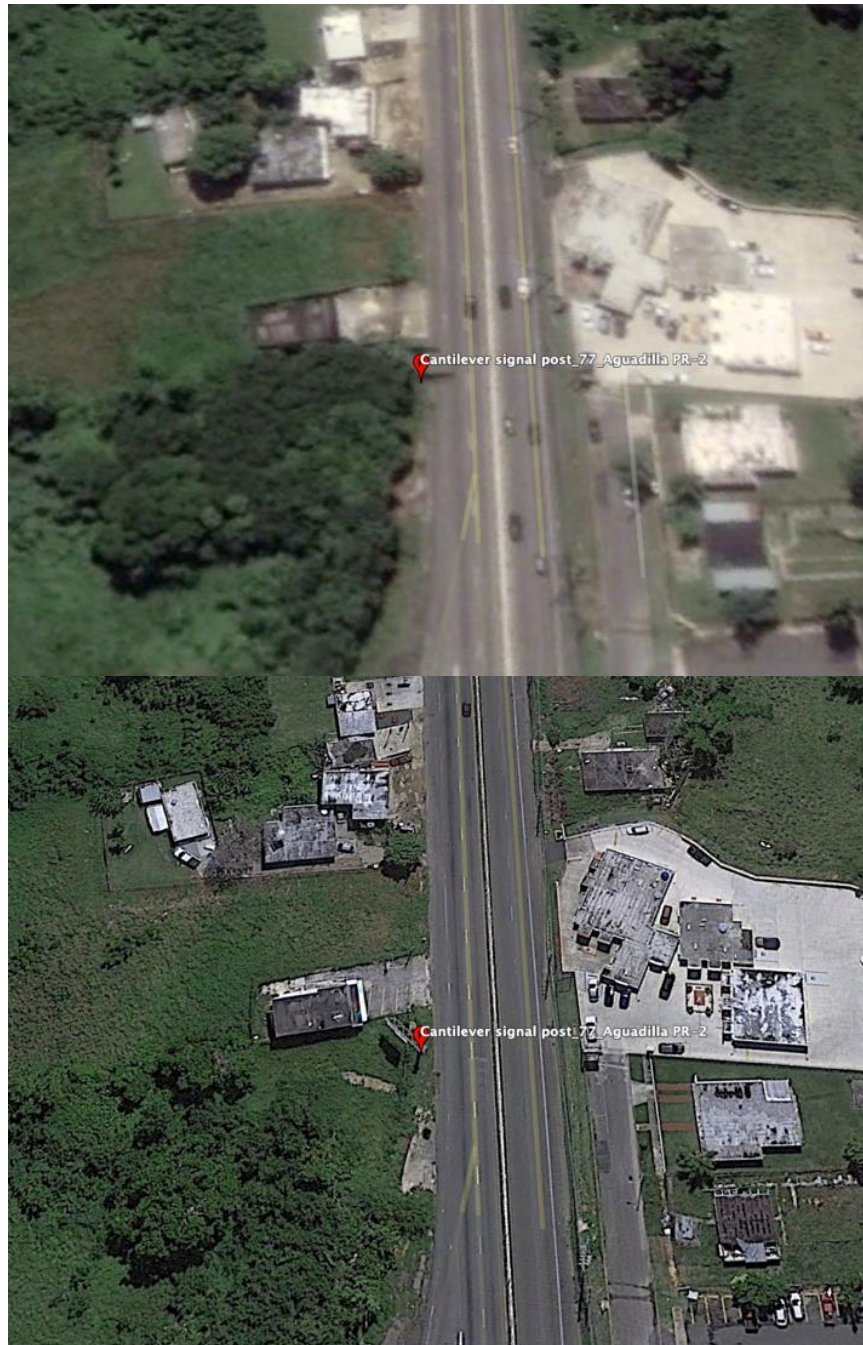


Figure 4-21: Cantilever Sign Post 77 Located in Aguadilla (Picture 1: 9/2016, Picture 2: 5/2018)

Photos in Figure 4-22 were obtained from the research carried out using the program Google Earth Pro, which works with the historical image analysis method, comparing those presented by the 5/2018 program with those of 9/2016. Cantilever sign foundation failure at P-88 in PR 2_Aguadilla. The Cantilever sign rotated approximately 100 degrees.

Location: 18°26'11.95"N; 67° 8'52.33"W



Figure 4-22: Cantilever Sign Post 88 Located in Aguadilla (Picture 1: 3/2016, Picture 2: 5/2018)

Photos in Figure 4-23 were obtained from the research carried out using the program Google Earth Pro, which works with the historical image analysis method, comparing those presented by the 4/2018 program with those of 3/2016. Cantilever sign foundation failure at P-88 in PR 22_Arecibo. The Cantilever sign rotated approximately 20 degrees.

Location: 18°27'10.09"N; 66°44'50.21"W

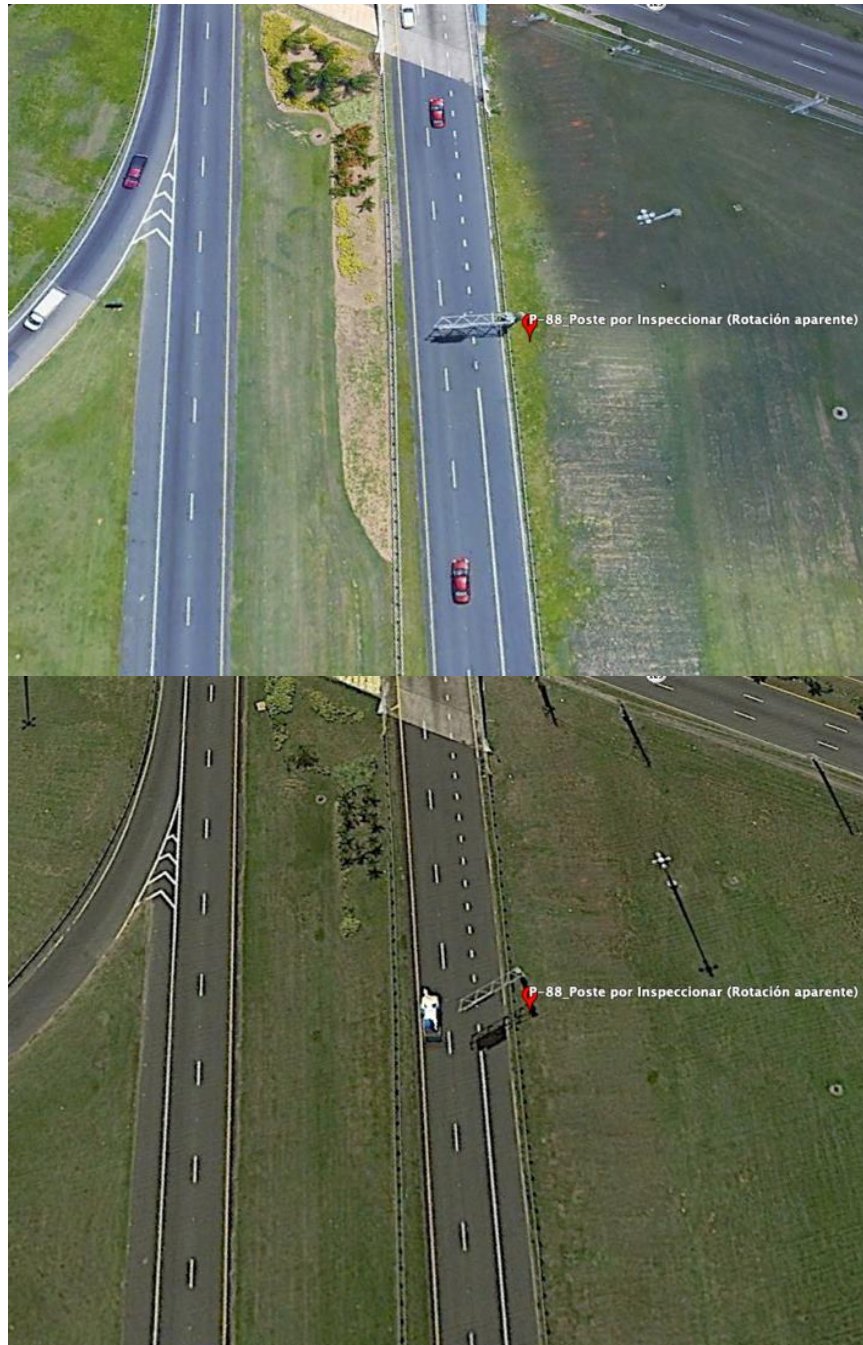


Figure 4-23: Cantilever Sign Post 88 Located in Arecibo (Picture 1: 3/2016, Picture 2 4/2018)

Photos in Figure 4-24 were obtained from the research carried out using the program Google Earth Pro, which works with the historical image analysis method, comparing those presented by the 5/2018 program with those of 9/2016. Cantilever sign foundation failure at P-91 in PR 52_Arecibo. The Cantilever sign rotated approximately 180 degrees.

Location: 18°27'5.98"N; 66°43'4.13"W



Figure 4-24: Cantilever Sign Post 91 Located in Arecibo (Picture 1: 3/2016, Picture 2: 4/2018)

Images in Figure 4-25 were obtained from the research carried out using the program Google Earth Pro, which works with the historical image analysis method, comparing those presented by the 4/2018 program with those of 4/2016. Cantilever sign foundation failure at P-95 in PR 18_San Juan. The Cantilever sign rotated approximately 180 degrees.

Location: 18°25'25.61"N; 66° 4'20.75"W



Figure 4-25: Cantilever Sign Post 95 Located in San Juan (Picture 1: 4/2016, Picture 2: 4/2018)

Images in Figure 4-26 were obtained from the research carried out using the program Google Earth Pro, which works with the historical image analysis method, comparing those presented by the 4/2018 program with those of 4/2016. This allows to identify a change in position of the post indicating a possible collapse.



Figure 4-26: Cantilever Sign Post 98 Located in Las Piedras (Picture 1: 4/2016, Picture 2: 4/2018)

Photos in Figure 4-27 were obtained from the research carried out using the program Google Earth Pro, which works with the historical image analysis method, comparing those presented by the 10/2017 program with those of 10/2016. This allows to identify a change in position of the post indicating a possible collapse.



Figure 4-27: Cantilever Sign Post 101 Located in Caguas (Picture 1: 10/2016, Picture 2: 10/2017)

Figure 4-28 was obtained from the research carried out using the program Google Earth Pro, which works with the historical image analysis method, using the image from 4/2018 where the base of the post identified as P-66. This allows to identify a change in position of the post indicating a possible collapse.

Location: 18°22'20.65"N; 65°52'38.72"W



Figure 4-28 Cantilever Sign Post 69 located at Canóvanas (Picture 1: 4/2018)

Images in Figure 4-29 were obtained from the research carried out using the program Google Earth Pro, which works with the historical image analysis method, comparing those presented by the 4/2018 program with those of 4/2016. Cantilever sign foundation failure at P-94 in PR 2_Ponce. The Cantilever sign rotated approximately 120 degrees.

Location: 17°59'16.80"N; 66°38'55.39"W



Figure 4-29 Cantilever Sign Post 94 Located in Ponce (Picture 1: 4/2016, Picture: 4/2018)

4.6 Summary of Potential Case Studies

It is important to point out that this GIS tool/process was also used with the previously identified cases. As a result, a sample of one hundred and eight (108) items was established as potential case studies for inspection. This represents a robust sample to evaluate the situation of the cantilever traffic signs after the impact of Hurricane Maria to Puerto Rico.

One complementary objective of the virtual reconnaissance exercise was the division of the island into exploration zones that would help the logistic of the visual inspection activities for the collection of field information. To this end, five main zones, for the purpose of field visits, were determined (and described in more detail in Chapter 5).

5 Field Visit and Data Collection

This chapter presents general aspects of the inspection procedure and logistics, the form developed to summarize the collected data in each location, and examples of the data collected in different sites.

5.1 General Considerations Regarding the Inspection Procedures

This section presents the process for establishing inspection logistics. The aim of this process was to determine appropriate equipment for the visual inspection, develop a data collection form for each case, and optimize inspection visits schedule to gain access to the largest number of cantilever traffic signs per trip.

To guarantee the health and safety of the inspector during the field visit process, safety parameters were established. These followed the OSHA requirements according to the code 29CFR1926 Subpart E – Personal Protective and Life Saving Equipment, where the safety equipment to be used according to the exposure and the risk analysis performed is presented. At the end of the inspection day, the documents raised are organized and filed for future actions.

Prior to the inspection, it should be checked that the necessary equipment is available. The tools required include the following: laptop, digital camera, tape measure, level, external charger for equipment, notebook, copies of inspection templates, and notepads.

5.1.1 Development of Field Data Collection Form

To standardize the data collection process and assure that all the information required is obtained, an inspection sheet to be used in the field visits was developed. This allowed the collection of data in a uniform and organized way. Figure 5-1 presents the inspection document, while Appendix A presents the images of the sheets completed during each case study visited.

Inspection sheet for cantilever sign support post

University	Polytechnic University of Puerto Rico
University Program	Civil Engineering
Proposal Center	Transportation Infrastructure Research Center
Title and Subtitle	Analysis of wind loads in cantilevered overhead sign support-truss with post
Name:	Geoffrey Vega Rosado
Inspection Date	
Town:	
Coordinates	
X=	
Y=	
Cantilever type ID number	
Geometry of the pole section	
Number of signs	
Long or short overhang	
Number of nuts in the base	
Amount of Gusset plate (rigidizador)	
Total of photos	
numeric range of photos	

Observations:

Figure 5-1: Field Visits Inspection Sheet

5.1.2 Example of the Checklist for Inspection of Cantilever Type Signs

The following checklist was created to generate the inspection document. These are elements that are considered important for the purpose of the current research and that serve as a basis for the agencies that work in road signs. Many items involve the physical location of the structure, the personnel involved in the inspection, details about the structure itself, important dimensions, and accessories. The objective is to have a useful database for the process of analysis of damage and types of failures. The information from the inspection sheet was:

- Inspection date
- Type of inspection
- Municipality code
- Latitude and longitude
- Route
- Kilometer and hectometer
- Description of the location
- Name of the structure
- Structure configuration
- Number of truss sections
- Type of material
- Town
- Identification of the sign
- Damage reports

5.1.3 Field Visits Strategy

To carry out the inspection of each case study, the high-speed routes and the strategy to be used for visiting the routes were identified. The island was divided into the following five zones: (a) West and North-West zone, (b) North and North-East zone, (c) East zone, (d) South-East zone, and (e) South zone. Most of the high-speed routes visited may be considered as coastal highways, with the exception of PR-52 from Salinas to San Juan, passing through Caguas town, which was included as part of North zone, although it is central. The zones were decided in terms of routes continuity, to facilitate inspection schedule. The zones are presented in Figure 5-2.

The following lists describes the roads and corresponding town areas and town vicinities visited, together with the total number of signs with potential damages identified in each zone.

- a) West and North-West Zone: Covers from Isabela to San German in the West, highway PR-2; and from Isabela to Manatí in the North, highways PR-2 and PR-22. The area had twenty-one (21) cantilever traffic signs identified to explore their potential failures.
- b) North and North-East Zone and Central: Covers from Vega Baja to San Juan and Carolina, highways PR-22, PR-66. It also included the only non-coastal highway visited, from Cayey to Caguas and Gurabo, highways PR-52, PR-18, PR-30. The area had thirty-two (32) cantilever traffic signs identified to explore their potential failures.
- c) East Zone: Covers the route that connects the following towns: Canóvanas, Juncos, Las Piedras, Rio Grande, Fajardo to Humacao, highway PR-66 and PR-30. The area had twenty-seven (27) cantilever traffic signs identified to explore their potential failures.
- d) South-East Zone: Covers the route that connects the following towns: Santa Isabel, Salinas and Guayama, roads PR-52, PR-53, PR-54, PR-3, and PR-30. The area had seventeen (17) cantilever traffic signs identified to explore their potential failures.
- e) South Zone: Covers from Cabo Rojo to Ponce, highways PR-2 and PR-52. The area had eleven (11) cantilever traffic signs identified to explore their potential failures

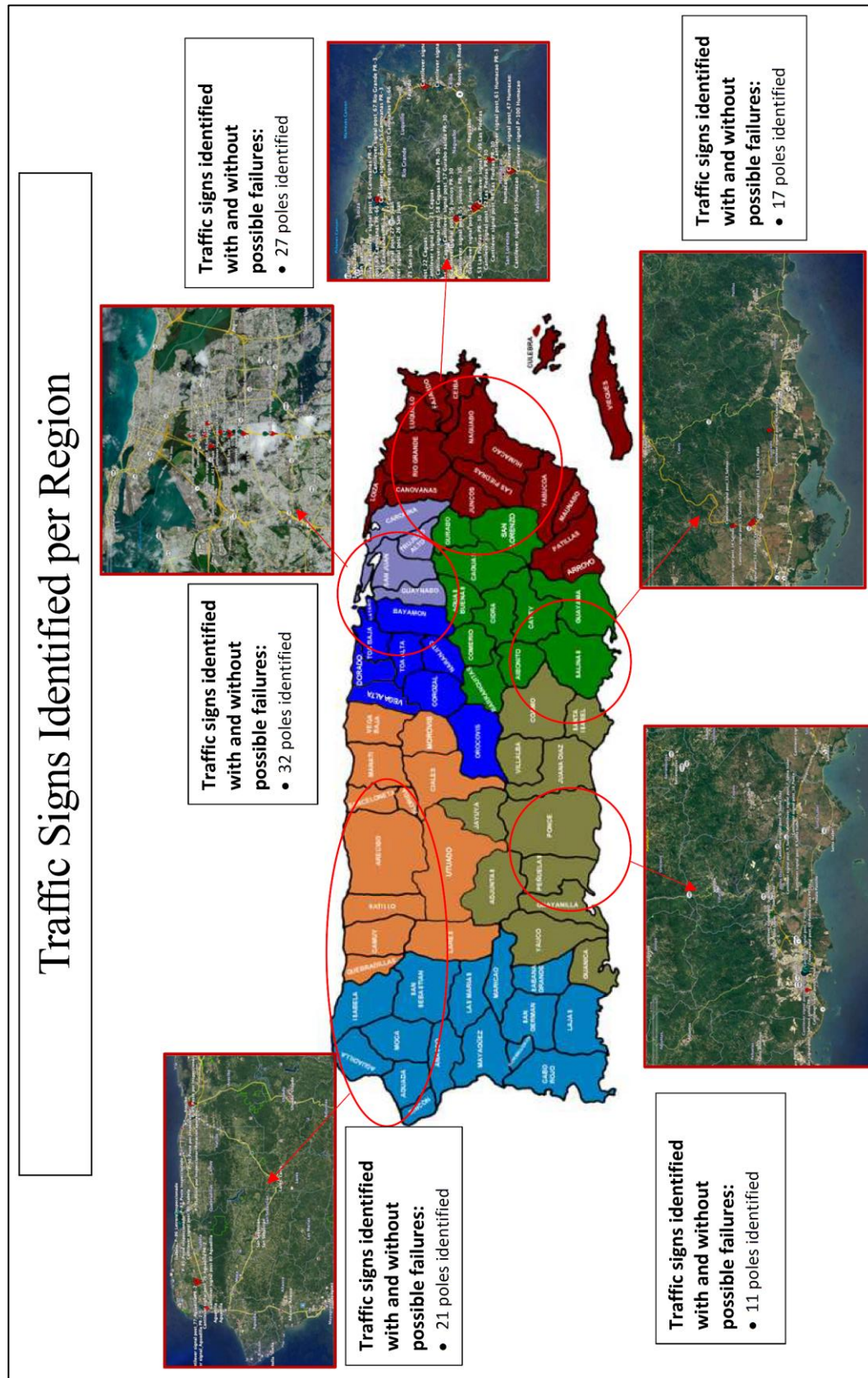


Figure 5-2: Traffic Signs Identified per Exploration Region

The field inspection began in the southern part of the island, where the signs located on the PR-2, PR-52, and PR-53 roads were examined. This inspection took about three weeks. The inspection followed a safety protocol referenced in OSHA standards 29CFR-1926, subpart D, Personal Protective Equipment (PPE). Before the inspections, the route was identified and the signs to be inspected were established. The program Google Earth Pro helped to determine the coordinates (latitude and longitude) of the targeted cantilever overhead traffic signs. On site, the coordinates were verified and refined using a GPS. By following these steps for all the field visits, one was able to optimize trips and guarantee the inspection of all identified signs.

5.1.4 Information Collection and Management

One important problem faced when carrying out the inspection of the affected structures was the lack of information and georeferenced inventory of this sign. Structures are rarely numbered for easy identification. To solve this situation, an identification nomenclature was generated for the poles inspected. Finding historical records such as construction drawings, maintenance repairs, and installation of new sign boards is difficult. Another problem is that manufacturers have replaced design drawings with their own shop drawings.

The initial collection of information from an inventory on cantilever traffic sign structures is critical. Key pieces of information include route, GPS coordinates, route association (if not on the main road), town, city, etc. Photos and measurements of sign elements are also important to help identify structures. Figure 5-3 presents examples of such photos for one of the case studies.



Figure 5-3: Identifying the Post to Be Inspected in the Town of Quebradillas, Puerto Rico (Coordinates: 18°28'48.97"N; 66° 58'5.91"W)

5.1.5 Failures Database Development

The data was collected by counting the structures that failed due to the wind loads received after Hurricane Maria. It is important to ensure a comprehensive database that helps to classify and prioritize the cantilever overhead traffic signs based on the arm length, the location, the material, the ratings (extent of the damage), and the failure types. The objective is to have a useful database for the process of analysis of damage and types of failures.

As presented in Chapter 3, in the process of analyzing the collected data, the following levels of damage/failure were established:

- a) Damages – The sign was in its original position but presented some damages such as fractures in the pedestal concrete that may be related to internal stresses due to received loads. The idea of this level is to indicate that the signs were usable, but several may require repair and reinforcement to assure its resilient behavior.
- b) Partial Collapse – The sign was still standing (not on the ground), but its position and instability were compromised, presenting fractures in the concrete of the pedestal, displacements of the post base plate and anchor bolts, and/or movements of the foundation. The idea of this level is to indicate that the signs may have been providing

some service, but most of them required replacement (although some of them could be reinforced and reused).

- c) Total Collapse – The sign was on the ground, or part of it was touching the ground, displaying pedestal with major fractures and structure of the traffic sign on the ground. The idea of this level is to indicate that the signs were not providing any service, and that they required replacement.

In terms of types or modes of failure, all the partial collapses and total collapses, and most of the damages, occurred in the cantilever traffic sign foundation system, and not on the post, cantilever truss arm, or the sign itself. Two principal modes of foundation failure were identified:

- a) Structural failures on the foundation pedestal
- b) Soil or soil-foundation interaction failures

The structural failures in the foundation pedestal presented distinctive conditions that were considered important to highlight, so it was decided to group them into the following three cases (although most of the situations more of one case was presented):

- a) Torsion – The base plate of the post experienced large rotations about the vertical axis (due to rotation of the post), leading to large lateral deflections of the anchor bolts that experienced double bending in the plastic range and shear failure. The lateral deflection of the bolts produced cracks on the concrete.
- b) Overturning - The base plate of the post rotated about a horizontal axis (due to overturning of the post) and produced compression on the concrete that experimented cracks and disintegration due to crushing.
- c) Anchor bolt misplacement

- i. Anchor bolt not confined – Anchors were outside the stirrup’s confinement core on the concrete pedestal, or the separation between the last top stirrup and the post base plate was too large (leaving an extensive length on the anchor not confined). This anchor bolts experienced extremely high lateral deflections in the case of torsion, exhibiting a double bending curvature in the plastic regimen, and producing extensive cracking on the concrete.
- ii. Anchor bolt pullout – Anchors in tension were extracted from the concrete pedestal and showed a clean face (signs of lack of adherence with the concrete of the pedestal).

The soil or soil-foundation interaction failures were grouped in the following two cases:

- a) Failures due to overturning – The foundation rotates about a horizontal axis, and the post (the hole cantilever sign) collapses. These failures may have been due to a lack of enough embedment length to activate the required soil passive thrust.
- b) Failures due to torsional rotation – The foundation rotates about a vertical axis, and the post, the cantilever arm, and the traffic signs were oriented in the wrong direction. These failures may have been due to a lack of enough shaft resistance (soil-foundation interaction shear resistance) to avoid rotation.

The large eccentric forces generated by the wind acting on the signs (and on the rest of the components of the cantilever overhead structure) requires that the foundation, to give stability to the sign structure, is able to provide adequate overturning moment resistance, torsional (twisting) moment resistance, and horizontal (shear) force resistance, as depicted in Figure 5-4.

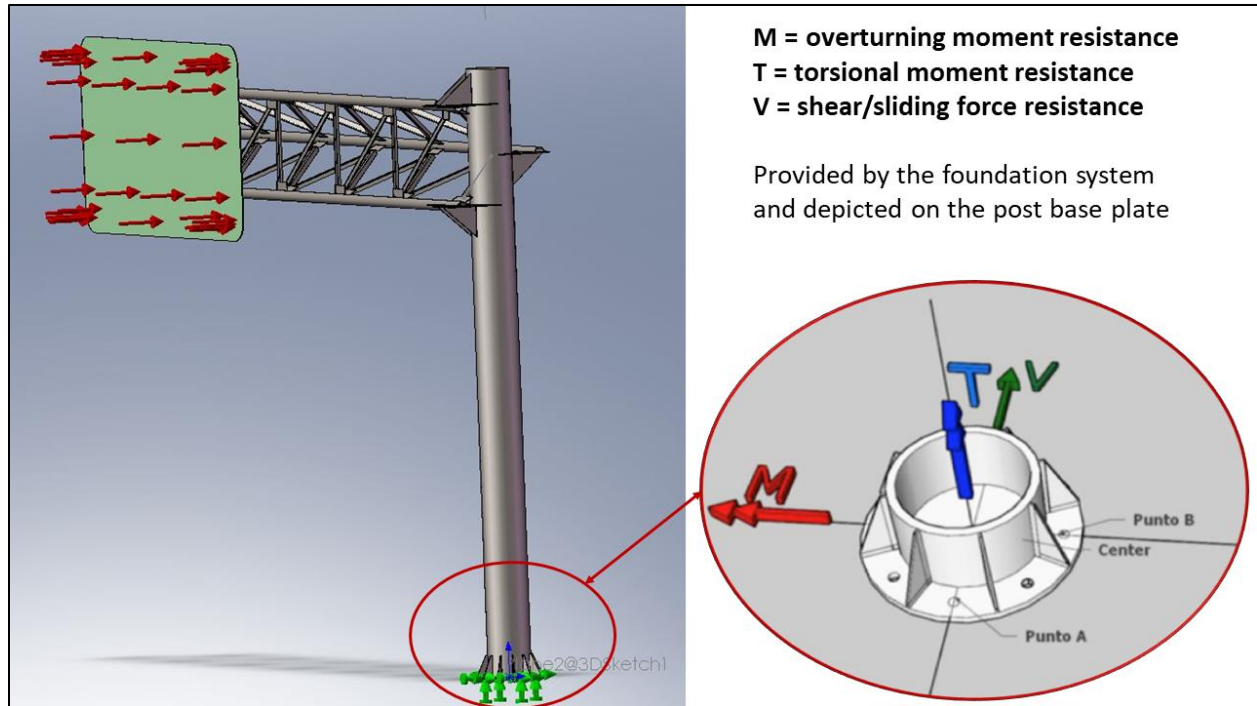


Figure 5-4: Required Foundation Resistance to Provide Stability to the Sign Structure

5.2 Inspected Cases and Failures Found

It is important to point out that of the 108 potential cases identified, 10 were discarded because they were smaller cantilever traffic signs, and the focus of the inspections was Type B cantilever overhead traffic signs, with long cantilever arms and large signs. Of the remaining 98 signs, 94 were visited and fully documented, giving priority to those cases where changes in their condition were identified in virtual tour as result of the historical comparison of satellite images. In addition, another of the 98 cases identified was obtained by interviewing PRHTA personnel working in a yard where the traffic sign was stored after removing it, for a total of 95 cases studied. 910 photos were taken to graphically document the findings. It is important to mention that several of the signs were already removed from the premises at the time of the field visit, and just the remains were documented. Table summarizes the quantity of cantilever traffic signs identified and documented in each municipality, presented in alphabetical order, and the identification given to

each post. While Table 5-2 presents the same information but grouping the municipalities by exploration zones. The 95 signs were distributed in 22 municipalities. Appendix E presents a more detailed table, specifying the locations coordinates for each cantilever traffic sign in each municipality, and a summary of the damages encountered.

Table 5-1: Post Quantity and ID per Municipality

Municipality	Quantity	Posts ID
Aguadilla	4	P-75, P-76, P-77, P-78
Arecibo	5	P-88, P-89, P-90, P-91, P-102
Barceloneta	1	P-103
Caguas	13	P-16, P-17, P-18, P-19, P-20, P-21, P-22, P-28, P-29, P-30, P-45, P-52, P-58
Camuy	1	P-69
Canóvanas	2	P-106, P-107
Dorado	1	P-62
Guayama	3	P-11, P-46, P-47
Gurabo	1	P-57
Humacao	3	P-61, P-100, P-105
Isabela	1	P-74
Juana Díaz	3	P-5, P-6, P-71
Juncos	3	P-54, P-55, P-56
Las Piedras	7	P-48, P-49, P-50, P-51, P-53, P-66, P-99
Ponce	8	P-1, P-3, P-4, P-59, P-60, P-65, P-67, P-94
Quebradillas	9	P-79, P-80, P-81, P-82, P-83, P-84, P-85, P-86, P-87
Sábana Seca	1	P-101
Salinas	6	P-11, P-12, P-13, P-14, P-15, P-26
San Juan	11	P-33, P-35, P-38, P-39, P-40. P-41, P-42, P-43, P-44, P-95, P-98
Santa Isabel	8	P-7, P-8, P-10, P-24, P-25, P-36, P-37, P-70
Toa Baja	2	P-96, P-97
Vega Alta	2	P-92, P-93
22	95	

Table 5-2: Post Quantity and ID per Municipality Grouped by Exploration Regions

Region	Municipality	Quantity	Posts ID
a) Westy and North-West	Aguadilla	4	P-75, P-76, P-77, P-78
	Arecibo	5	P-88, P-89, P-90, P-91, P-102
	Barceloneta	1	P-103
	Camuy	1	P-69
	Isabela	1	P-74
	Quebradillas	9	P-79, P-80, P-81, P-82, P-83, P-84, P-85, P-86, P-87
	Total	21	
b) North and North-East and Central	Caguas	13	P-16, P-17, P-18, P-19, P-20, P-21, P-22, P-28, P-29, P-30, P-45, P-52, P-58
	Dorado	1	P-62
	Gurabo	1	P-57
	Sábana Seca	1	P-101
	San Juan	11	P-33, P-35, P-38, P-39, P-40, P-41, P-42, P-43, P-44, P-95, P-98
	Toa Baja	2	P-96, P-97
	Vega Alta	2	P-92, P-93
	Total	31	
c) East	Canóvanas	2	P-106, P-107
	Juncos	3	P-54, P-55, P-56
	Las Piedras	7	P-48, P-49, P-50, P-51, P-53, P-66, P-99
	Humacao	3	P-61, P-100, P-105
	Total	15	
d) South-East	Guayama	3	P-11, P-46, P-47
	Salinas	6	P-11, P-12, P-13, P-14, P-15, P-26
	Santa Isabel	8	P-7, P-8, P-10, P-24, P-25, P-36, P-37, P-70
	Total	17	
e) South	Juana Díaz	3	P-5, P-6, P-71
	Ponce	8	P-1, P-3, P-4, P-59, P-60, P-65, P-67, P-94
	Total	11	

The following sub-sections section summarize the principal cases where the field visit allowed to identify that they presented damages, partial collapse, or total collapse, which resulted in 51 of the 95 studied (49 of them directly attributable to the hurricane). It is important to mention that some of the posts that were identified as having torsional rotations using the GIS tool were repaired, and in place at the time of the inspection. As previously mentioned, each sign was assigned a sequential number ##, and named P-## (P from Post, since most of the failures were located at its base); this ID is presented at the end of each post sub-section. For each case, a few photos were selected to help visualize the condition.

5.2.1 Cantilever Traffic Sign Site Aguadilla P-76

Located along the southbound lane of Highway PR-2 in Aguadilla. An image of the traffic sign structure is shown on Figure 5-5. The final position of the traffic sign was rotated about 20 degrees (negative using the right-hand sign convention with respect to a vertical Zenith axis) with respect to the original installation position. The diameter of the drilled shaft that supports this structure was measured to be 30 inches (0.76 m). The visual inspection revealed fractures and detachment of the concrete at the top of the pedestal, below the post base plate, as observed in Figure 5-6; and some stiffeners at the base plate were bent; also the post showed some degree of tilting (out of plumb by about 10 grades of the superstructure with respect to the Zenith).



Figure 5-5: Photos Showing the Rotation of the Traffic Sign at P-76 Location: 18°27'8.10"N; 67° 5'38.06"W



Figure 5-6: Photos of Cantilever Traffic Sign Pedestal Failures and Post Inclination at P-76

5.2.2 Cantilever Traffic Sign Site Aguadilla P-77

Located along the southbound lane of Highway PR-2 in Aguadilla. The image of the traffic sign structure is shown on Figure 5-7. The final position of the traffic sign was rotated about 100 degrees (measured positive or counterclockwise using the right-hand sign convention with respect to a vertical Zenith axis) with respect to the original installation position. The diameter of the precast cylindrical pedestal that supports this structure was measured to be 30 inches (0.76 m). The visual inspection revealed a deep gap around most of the perimeter circumference between the drilled shaft and the ground. Figure 5-7 shows some tilting of the superstructure with respect to the Zenith.



Figure 5-7: Photo of Cantilever Sign Foundation Failure at P-77 with Location: 18°27'13.01"N; 67° 5'20.87"W

Figure 5-8 and Figure 5-9 show photos of the top of the drilled shaft foundation where the gap formation can be observed. The gap, which likely formed due to the large bending and lateral forces transmitted to the drilled shafts, reduced the contact area between soil and foundation, and thus, the torsional resistance of the drilled shafts.



Figure 5-8: Photo of Drilled Shaft Foundation of Traffic Sign P-77 with Location: 18°27'13.01"N; 67° 5'20.87"W



Figure 5-9: Photo of Drilled Shaft Foundation of Traffic Sign P-77

The analysis of this traffic sign showed the validity of using satellite image processing to identify cases. An image of the traffic sign structure is shown in Figure 5-10, and was obtained from the research carried out using the GIS program (Google Earth Pro) that works with the historical image analysis method, comparing those presented by the 4/2018 program with those of 6/2017. In these an apparent rotation of approximately -270 degrees was identified (note that the first field visit estimate was around +100 degrees). At the time of the second field visit, the traffic sign was not found in the identified place. It appears to have been removed from the site for safety reasons, as one can appreciate in Figure 5-11.

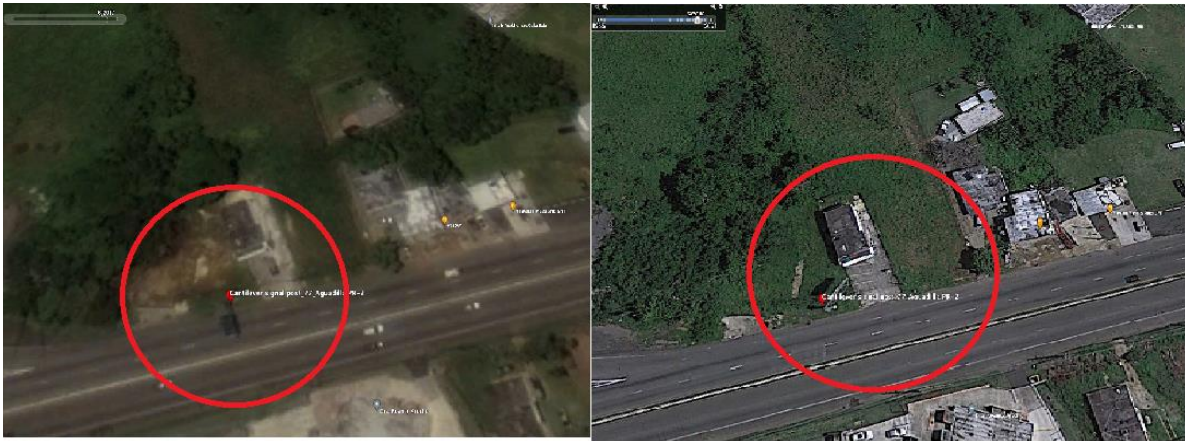


Figure 5-10: Photo of Cantilever Sign Soil Foundation Failure at P- 77 Location: 18° 27'13.01"N; 67°5'20.87"W (Photo 1 date: 6/2017, Photo 2 date: 4/2018)

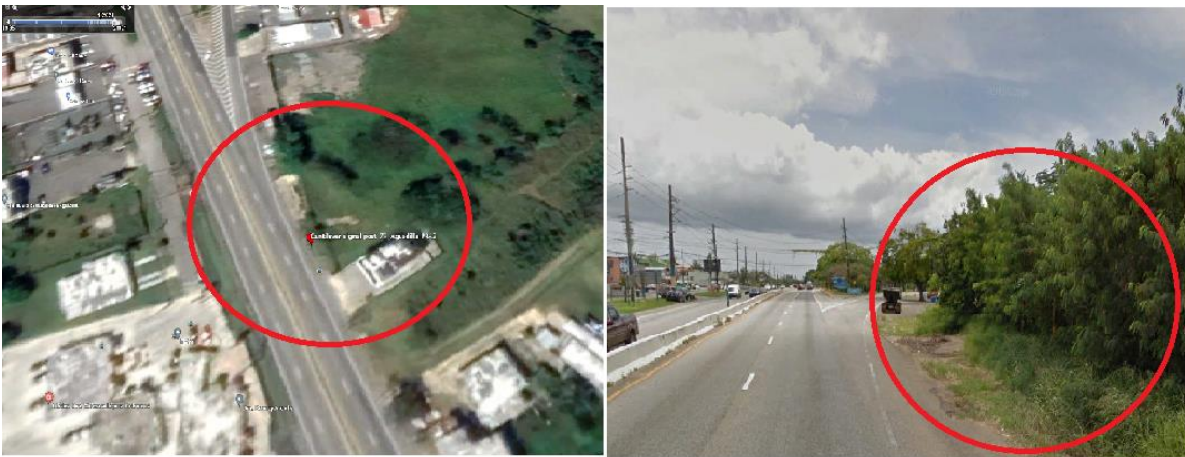


Figure 5-11: Cantilever Traffic Sign P- 77 at the Time of Inspection (Post not in Place)

5.2.3 Cantilever Traffic Sign Site Aguadilla P- 78

Located at the southwest corner of the Luis A. Canela Marquez Stadium in Aguadilla, along the northbound lane of Highway PR-2. An image of the rotated post-arm traffic sign is shown on Figure 5-12. The diameter of the drilled shaft was approximately 30 inches (0.76 m). The field inspection also revealed a near continuous gap around the circumference of the drilled shaft. In some locations, the gap was as wide as 10 inches. The observed depth of the gap was about 18 inches, as shown in Figure 5-14; however, the bottom of the gap had loose soils, which suggest that minor caving may have filled some of the gap. The post also experienced some tilt (out of plumb) as shown on Figure 5-12. The traffic sign experienced a rotation of about -100 degrees with respect to the zenith and using the right-hand rule sign convention.



Figure 5-12: Photo of Cantilever Sign Foundation Failure at P- 78 Photo Location: 18°26'11.95"N; 67° 8'52.33"W



Figure 5-13: Photo of Drilled Shaft Foundation of Traffic Sign at P-78 Photo Location: 18°26'11.95"N; 67° 8'52.33"W.



Figure 5-14: Continuous Gap Around the Circumference of the Drilled Shaft

5.2.4 Cantilever Sign Site Arecibo P-88

Located along the Highway PR-22 in Arecibo. An image of the traffic sign structure is shown in Figure 5-15, and was obtained from the research carried out using the GIS program (Google Earth Pro) that works with the historical image analysis method, comparing those presented by the 4/2018 program with those of 3/2016. In these an apparent rotation of approximately 20 degrees was identified.

At the time of the field visit no rotation was observed at the base. It appears to have been stabilized and placed in its service position. It was observed that the base of the structure is located at a distance of approximately 2 feet from the beginning of the slope, thus presenting a possible risk of stability in future situations (see Figure 5-16).

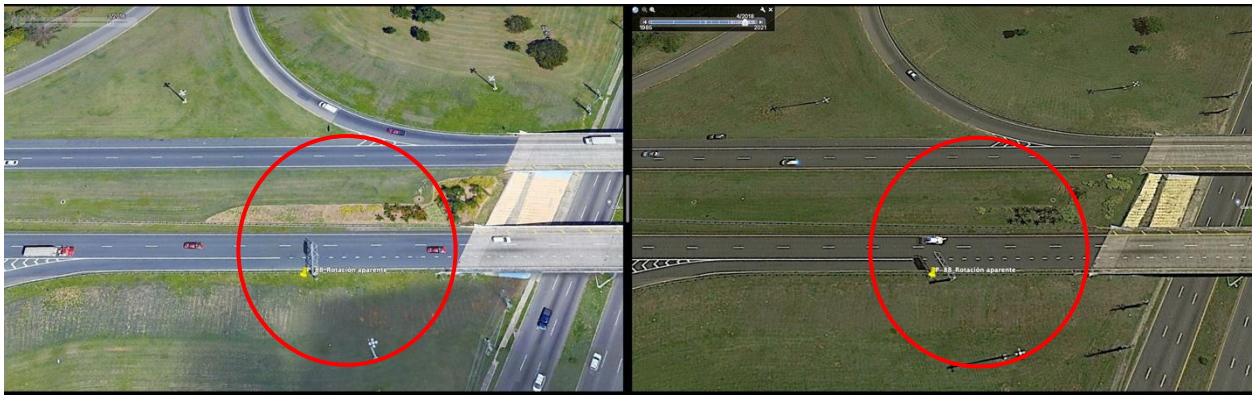


Figure 5-15: Photo of Cantilever Sign Soil Foundation Failure at P-88 Location: 18°27'13.01"N; 66°5'20.87"W (Photo 1 date: 3/2016, Photo 2 date: 4/2018)



Figure 5-16: Cantilever Traffic Sign P-88 at the Time of Inspection

5.2.5 Cantilever Sign Site Arecibo P-89

Located along the Highway PR-22 in Arecibo. An image of the traffic sign structure is shown in Figure 5-17, and was obtained from the research carried out using the GIS program (Google Earth Pro) that works with the historical image analysis method, comparing those presented by the 4/2018 program with those of 3/2016. In these an apparent rotation of approximately 15 degrees was identified.

At the time of the field visit no rotation was observed at the base. It appears to have been stabilized and placed in its service position. It was observed that the base of the structure is located just at the beginning of the slope, thus presenting a possible risk of stability in future situations (see Figure 5-18).



Figure 5-17: Photo of Cantilever Sign Soil Foundation Failure at P-89 Location: 18°27'10.09"N; 66°44'50.21"W (Photo 1 date: 3/2016, Photo 2 date: 4/2018)



Figure 5-18: Cantilever Traffic Sign P-89 at the Time of Inspection

5.2.6 Cantilever Sign Site Arecibo P-90

Located along the Highway PR-22 in Arecibo. An image of the traffic sign structure is shown in Figure 5-19, and was obtained from the research carried out using the GIS program (Google Earth Pro) that works with the historical image analysis method, comparing those presented by the 4/2018 program with those of 3/2016. In these an apparent rotation of approximately 10 degrees was identified.

At the time of the field visit no rotation was observed at the base. It appears to have been stabilized and placed in its service position. It was observed that the base of the structure is located just at the beginning of the slope, thus presenting a possible risk of stability in future situations (see Figure 5-20).



Figure 5-19: Photo of Cantilever Sign Soil Foundation Failure at P-90 Location: 18°27'8.40"N; 66°43'8.03"W (Photo 1 date: 3/2016, Photo 2 date: 4/2018)



Figure 5-20: Cantilever Traffic Sign P-90 at the Time of Inspection

5.2.7 Cantilever Sign Site Arecibo P-91

Located along the Highway PR-22 in Arecibo. An image of the traffic sign structure is shown in Figure 5-21, and was obtained from the research carried out using the GIS program (Google Earth Pro) that works with the historical image analysis method, comparing those presented by the 4/2018 program with those of 3/2016. In these an apparent rotation of approximately 180 degrees was identified.

At the time of the field visit no rotation was observed at the base. It appears to have been stabilized and placed in its service position. It was observed that the base of the structure is located at a distance of about 5 ft from the beginning of the slope, thus presenting a possible risk of stability in future situations (see Figure 5-22).



Figure 5-21: Photo of Cantilever Sign Soil Foundation Failure at P-91 Location: 18°27'5.98"N; 66°43'4.13"W (Photo 1 date: 3/2016, Photo 2 date: 4/2018)

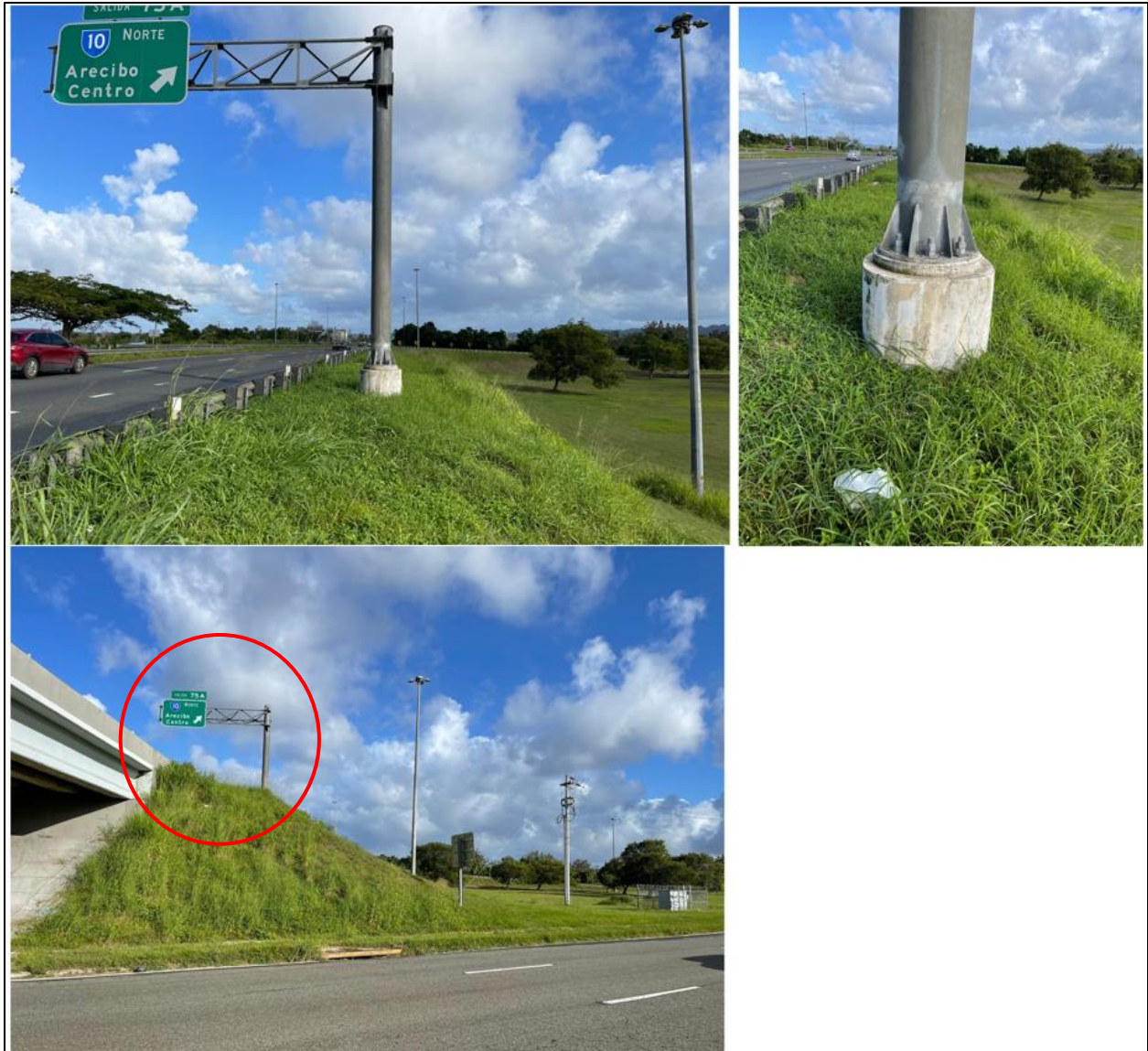


Figure 5-22: Cantilever Traffic Sign P-91 at the Time of Inspection

5.2.8 Cantilever Sign Site Barceloneta P-103

Located along the Highway PR-2 in Barceloneta. An image of the traffic sign structure is shown in Figure 5-23, and was obtained from the research carried out using the GIS program (Google Earth Pro) that works with the historical image analysis method, comparing those presented by the 4/2018 program with those of 11/2006. In these an apparent detachment of sign itself was identified.

At the time of the field visit it was identified that the sign was not of the type I-B, but since it had experienced damages (detachment of the sign itself) it was documented (see Figure 5-24). This was the only case inspected where the sign itself had apparently blown away.



Figure 5-23: Photo of Cantilever Sign Failure at P-103 Location: 18°26'8.06"N; 66°32'38.60"W (Photo 1 date: 11/2006, Photo 2 date: 4/2018)



Figure 5-24: Cantilever Traffic Sign P-103 at the Time of Inspection

5.2.9 Cantilever Traffic Sign Sites Caguas P-16 and P-17

Located along the Highway PR-52 in Caguas, an image of the traffic sign structure base is shown on Figure 5-29 for sign P-16, and Figure 5-26 for sign P-17. Although there was no evidence of post rotation or tilt, the concrete base of both posts showed vertical cracks at anchor bolt location, that appeared to be evidence of bolt lateral movement in the initial stages. Sign P-17 also showed lack of adequate bearing support (that may have been caused by construction defects, or by concrete crushing due to mall posts tilt movements).



Figure 5-25: Photos of Cantilever Traffic Sign Base Condition at P-16. Location: 18.22014722 N; -66.04703611 W.



Figure 5-26: Photos of Cantilever Traffic Sign Base Condition at P-16. Location: 18.45293333N; -66.04458333W

5.2.10 Cantilever Traffic Sign Site Caguas P-22

Located along the Highway PR-52 in Caguas, an image of the traffic sign geolocation and the rests of its base foundation structure are shown on Figure 5-27. The sign has been removed at the time of the inspection. The shape of the debris of to the concrete base suggest that large lateral displacement of the anchor bolts due to post torsional rotation took place and trigger the collapse.



Figure 5-27: Photos of Cantilever Traffic Sign Geolocation and Rests of the Post Foundation at P-22. Location: 18.27201944N; -66.03914444W

5.2.11 Cantilever Traffic Sign Site Caguas P-45

Located along the Highway PR-52 in Caguas, an image of the traffic sign geolocation displaying and apparent collapse, and the rests of a base foundation structure and damaged traffic barriers (apparently due to the collapse) are shown on Figure 5-28. The sign has appeared to have been replaced at the time of the inspection. The absence of soil movement, the shape of the damaged traffic barrier, and the satellite image suggest that a concrete base structural failure could have taken place.

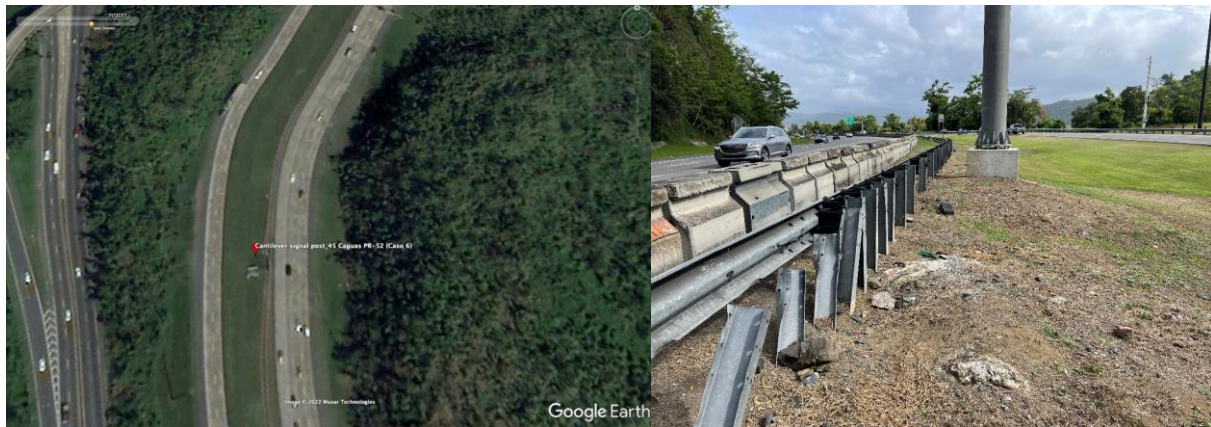


Figure 5-28: Photos of Cantilever Traffic Sign Geolocation, damages to the traffic barrier, and Rests of a Post Foundation at P-45. Location: 18.27035278N; -66.03955556W

5.2.12 Cantilever Traffic Sign Site Caguas P-52

Located along the Highway PR-52 in Caguas, an image of the traffic sign structure is shown in Figure 5-29. The final position of the traffic sign was rotated about a vertical Zenith axis. The post had a square concrete base that presented a foundation overturning failure, causing the collapse of the traffic sign, as observed in Figure 5-29. The sign showed a possible rotation around the vertical zenith axis with bolts shear and or tension failure before flipping to the ground.



Figure 5-29: Photos of Cantilever Traffic Sign Overturning Foundation Failure and Anchor Bolts Shear/Tension Failure at P-52. Location: 18°11'7.35"N; 66° 3'17.55"W

5.2.13 Cantilever Traffic Sign Site Caguas P-58

Located along the Highway PR-52 in Caguas, an image of the traffic sign structure and a detail of its base are shown in Figure 5-30. The final position of the traffic sign was not rotated about a vertical Zenith axis, but the anchor bolts lateral movement was large enough to produce wide cracks that were near to produce large spalls on the concrete base, as shown in Figure 5-31.



Figure 5-30: Photos of Cantilever Traffic Sign Location and Anchor Bolts Lateral Movement Producing Cracks on the RC Base at P-58. Location: 18.25564167N; -66.02865278W



Figure 5-31: Additional Details of RC Base Damages due to Anchor Bolts Lateral Displacements at P-58

5.2.14 Cantilever Sign Site Camuy P-69

Located along the Highway PR-2 in Camuy. An image of the traffic sign structure is shown in Figure 5-32, and was obtained from the research carried out using the GIS program (Google Earth Pro) that works with the historical image analysis method, comparing those presented by the 4/2018 program with those of 1/2015. In this case a change of situation was identified, with apparent soil and structural foundation failure. At the time of the visit, no traffic sign was found in the area. The perimeter was fenced, so no access was gained to the area to identify rests of past installation.

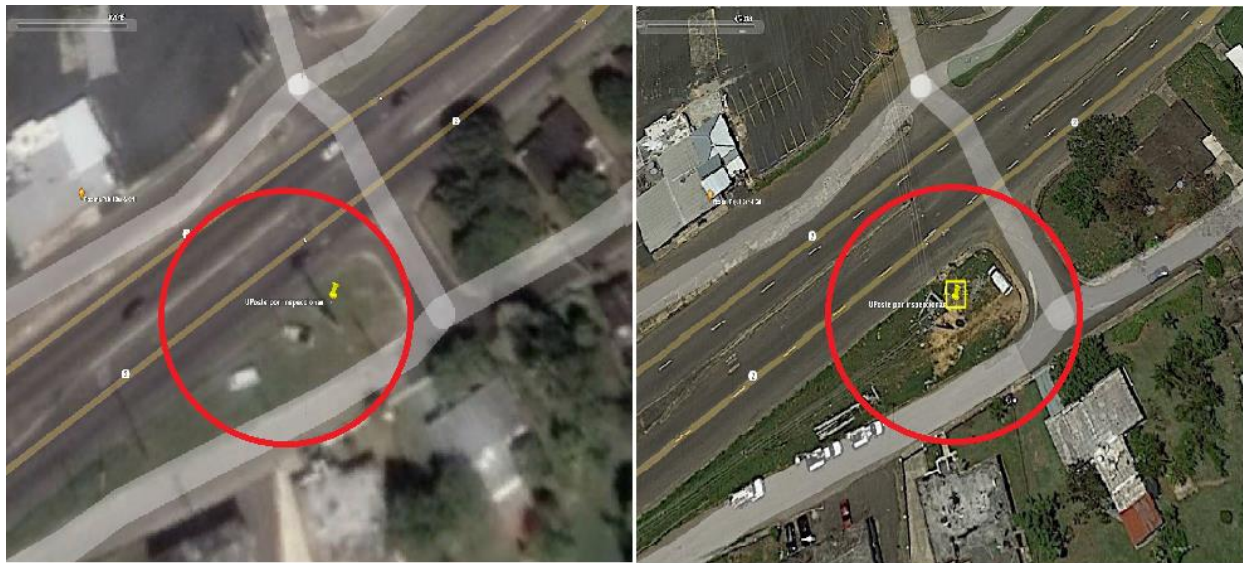


Figure 5-32: Photo of Cantilever Sign Soil and Structural Foundation Failure at P- 69 Location: 18° 29'18.024"N; 66°48'0.72"W (Photo 1 date: 1/2015, Photo 2 date: 4/2018)

5.2.15 Cantilever Sign Site Canóvanas P- 106

Located along the Highway PR-66 in Canóvanas. An image of the traffic sign structure geolocation and collapsed post is shown on Figure 5-33. The final position of the traffic sign showed a rotation around the vertical zenith axis, and also a rotation about a horizontal axis (leading to a tilt of the post). The visual inspection revealed that the collapsed traffic sign presented anchoring elements with large lateral displacements, bending on the plastic range, and shear fracture; the concrete pedestal presented large fractures and detachments as a consequence of the post torsional rotation (and bolts lateral movement) and post tilt (base plates crushed the concrete), as shown in Figure 5-34 and Figure 5-47.

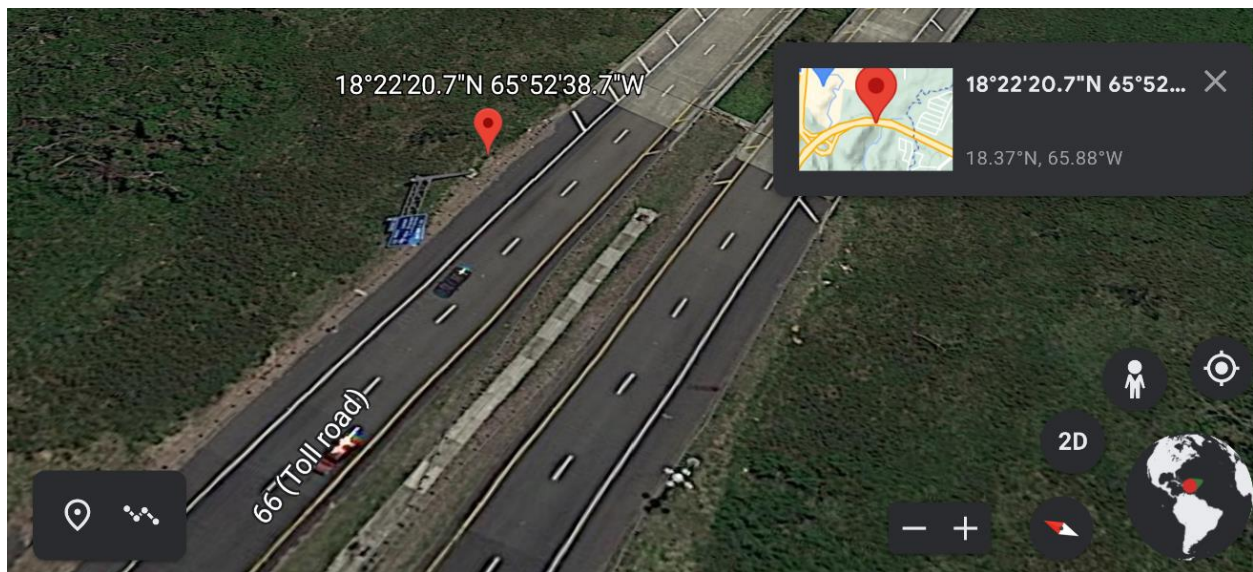


Figure 5-33: Photo of Cantilever Sign Foundation Structural Failures on the Pedestal at P-106 Location: 18°22'20.65"N; 65°52'38.72"W



Figure 5-34: Photo of Cantilever Sign Foundation Structural Failures on the Pedestal at P-106



Figure 5-35: Photo of Cantilever Sign Foundation Structural Failures on the Pedestal at P-106

5.2.16 Cantilever Sign Site Canóvanas P- 107

Located along the Highway PR-66 in Canóvanas. An image of the traffic sign structure is presented in Figure 5-36, showing a satellite image of the post indicating foundation rotation, and an image of the remaining post base with the anchor bolts in vertical position, that demonstrate that the sign had experienced torsional rotations due to soil foundation failure. The concrete base exhibit cracks due anchor bolts action. The post and the sign had been removed at the time of the field visit.

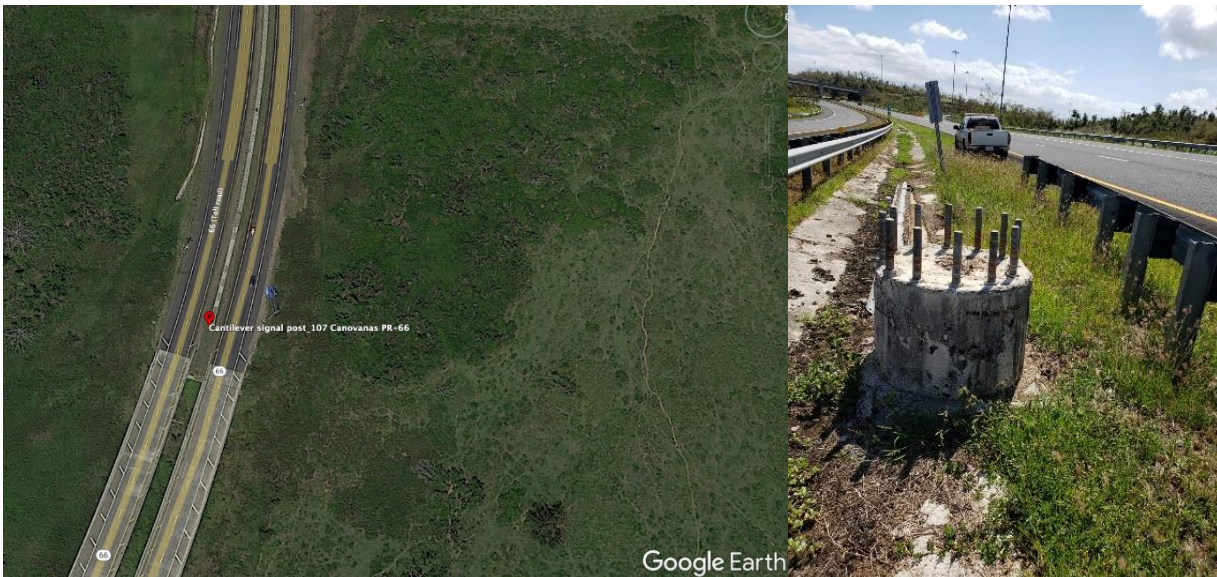


Figure 5-36: Photo of Cantilever Sign Foundation Torsional Rotation of the Pedestal at P-107 Location: 18.3603111°N, -65.8938111°W

5.2.17 Cantilever Traffic Sign Site Guayama P-46

Located along the Highway PR-53 in Guayama. An image of the traffic sign structure is shown on Figure 5-37. The final position of the traffic sign showed a rotation around the vertical zenith axis, and also a rotation about a horizontal axis (leading to a tilt of the post). The visual inspection revealed that the partially collapsed post presented large lateral displacements, bending on the plastic range, and shear fracture of the anchoring elements; the concrete pedestal presented large fractures, detachments, and crushing. One of the anchor bolts was outside the stirrups, lacking the lateral confinement, the others had a large length at the top without lateral confinement (distance between the post base plate and the first stirrup), as displayed in Figure 5-38. The concrete pedestal below the first stirrup presented few damages, in the area not affected by the plate bending. A large distance between the last stirrup and the top of the pedestal could also be appreciated.



Figure 5-37: Photo of Cantilever Sign Foundation Structural Failures on the Pedestal and Sign Position (Partial Collapse) at P-46. Location: 17°59'8.91"N; 66° 8'45.56"W



Figure 5-38: Photos of Cantilever Traffic Sign Foundation Structural Failure to the Pedestal at P-46; with Large Deflections and Bending on the Plastic Range and Shear Fracture of the Anchor Elements, and Fractures, Detachments and Crushing of the Concrete

5.2.18 Cantilever Traffic Sign Site Guayama P-47

Located along the Highway PR-53 in Guayama. An image of the traffic sign structure location and its out of plumb condition after the hurricane is shown on Figure 5-39. The final position of the traffic sign showed a rotation around the vertical zenith axis, and also a rotation about a horizontal axis (leading to a tilt of the post). During a second visit to the field the sign had been removed. The visual inspection revealed that the partially collapsed post presented large lateral displacements, bending on the plastic range, and shear fracture of the anchoring elements; the concrete pedestal presented large fractures, detachments, and crushing. Several of the anchor bolts were outside the stirrups, lacking the lateral confinement, the others had a very large length at the top without lateral confinement (distance between the post base plate and the first stirrup), as presented in Figure 5-40.



Figure 5-39: Photo of Cantilever Sign Foundation Structural Failures on the Pedestal and Sign Position (Partial Collapse) at P-47. Location: 17.9868529°N, -66.1425048°W



Figure 5-40: Photos of Cantilever Traffic Sign Foundation Structural Failure to the Pedestal at P-47; with Large Deflections and Bending on the Plastic Range and Shear Fracture of the Anchor Elements, and Fractures, Detachments and Crushing of the Concrete. Bolts outside the confinement of Stirrups

5.2.19 Cantilever Traffic Sign Site Gurabo P-57

Located along the Highway PR-30 in Gurabo. An image of the traffic sign structure location and the rests of the concrete pedestal are shown on Figure 5-41. At the time of the visit only rests of a concrete pedestal were found. A total collapse due to pedestal structural failure was assumed.



Figure 5-41: Photo of Cantilever Sign Structural Failures on the Pedestal at P-57 Location: 18.25031944°N; 65.96180556°W

5.2.20 Cantilever Traffic Sign Site Humacao P-61

Located along the Highway PR-53 in Humacao. An image of the collapsed traffic sign structure is shown on Figure 5-42. The visual inspection revealed that the collapsed post presented large lateral displacements, bending on the plastic range, and shear fracture of the anchoring elements; the concrete pedestal presented large fractures, detachments, and crushing. One of the anchor bolts was outside the stirrups, lacking the lateral confinement, the others had a large length at the top without lateral confinement (distance between the post base plate and the first stirrup), as displayed in Figure 5-43. The concrete pedestal below the first stirrup presented few damages. A large distance between the last stirrup and the top of the pedestal could also be appreciated.



Figure 5-42: Photo of Cantilever Sign Foundation Structural Failures on the Pedestal and Sign Position (Total Collapse) at P-61. Location: 18.159975°N; 65.79745833° W



Figure 5-43: Photos of Cantilever Traffic Sign Foundation Structural Failure to the Pedestal at P-46; with Large Deflections and Bending on the Plastic Range and Shear Fracture of the Anchor Elements, and Fractures and Detachments of the Concrete

5.2.21 Cantilever Traffic Sign Site Humacao P-100

Located along the Highway PR-53 in Humacao. An image of the traffic sign structure is shown on Figure 5-44. The final position of the traffic sign showed a rotation about the vertical zenith axis. The diameter of the pedestal that supports this structure was measured, resulting in a diameter of 35 inches (0.89 m). Visual inspection revealed that the collapsed post presented large lateral deflections and bending on the plastic range of the anchor elements, that also exhibited pullout and shear fracture; the concrete presented fractures and detachments (see Figure 5-45). Some of the anchor bolts were clearly located outside the confinement provided by the stirrups (see Figure 5-45). A large distance between the last stirrup and the top of the pedestal could also be appreciated.



Figure 5-44: Photo of Cantilever Sign Structural Failures on the Pedestal at P-100 Location: 18°7'7.11"N; 65°49'16.812"W



Figure 5-45: Photo of Cantilever Sign Foundation Structural Failure at P-100; with Large Deflections and Bending on the Plastic Range and Shear Fracture of the Anchor Elements, and Fractures, Detachments and Crushing of the Concrete. Anchor elements outside the confinement provided by Stirrups

5.2.22 Cantilever Sign Site Humacao P-105

Located along the Highway PR-53 in Humacao. An image of the traffic sign structure is shown on Figure 5-46. The final position of the traffic sign shows a rotation about the vertical zenith axis. The diameter of the pedestal that supports this structure was measured, presenting a diameter of 35 inches (0.89 m). Visual inspection revealed that the collapsed post showed large lateral deflections and bending on the plastic range of the anchor elements, that also exhibited pullout and shear fracture; the concrete presented fractures and detachments (see Figure 5-47). Some of the anchor bolts were clearly located outside the confinement provided by the stirrups. A large distance between the last stirrup and the top of the pedestal could also be appreciated.



Figure 5-46: Photo of Cantilever Sign Structural Failures on the Pedestal at P-105 Location: 18° 7'20.00"N; 65° 49'12.23"W



Figure 5-47: Photo on Cantilever Sign Foundation Structural Failure at P-105; Collapsed Post Presented Large Deflections and Bending on the Plastic Range and Shear Fracture of the Anchor Elements



Figure 5-48: Photo on Cantilever Sign Foundation Structural Failure at P-105; Collapsed Post Presented Large Deflections and Bending on the Plastic Range and Shear Fracture of the Anchor Elements, and Fractures and Detachments of the Concrete. Anchor elements outside the confinement provided by Stirrups

5.2.23 Cantilever Sign Site Juana Diaz P-6

Located along the Highway PR-52 in Juana Diaz. An image of the traffic sign structure is shown on Figure 5-49. The truss and the sign were missing, but the post and the concrete pedestal were in good condition, and no evidence of hurricane impact was found during the field inspection.



Figure 5-49: Photo of Cantilever Sign Missing Truss and Sign at P-6 Location: 18.03189444°N; 66.45465278°W

5.2.24 Cantilever Sign Site Juncos P-55

Located along the Highway PR-30 in Juncos. An image of the traffic sign structure is shown on Figure 5-50. The concrete base presented a wide crack that appeared to be produced by the anchor bolt lateral movement.



Figure 5-50: Photo of Cantilever Sign Structural Crack on the Pedestal at P-55 Location: 18.22131389°N; 65.91406944°W

5.2.25 Cantilever Sign Site Juncos P-56

Located along the Highway PR-30 in Juncos. An image of the traffic sign location is shown on Figure 5-51. The image clearly shows that the post experienced a large torsional rotation of more than 90 degrees, and the damaged traffic barriers may be evidence of collapse. At the time of the field visit the post was already removed, but the concrete foundation was found in place, as shown in Figure 5-52.



Figure 5-51: Photo of Cantilever Sign Torsional Rotation and Possible Collapse on the Pedestal at P-56 Location: 18.22426944°N; 65.91595833°W



Figure 5-52: Photo of Cantilever Sign Concrete Foundation Rests at P-56

5.2.26 Cantilever Sign Site Las Piedras P-53

Located along the southbound lane of Highway PR-30 in Las Piedras. An image of the traffic sign structure is shown on Figure 5-53. The final position of the traffic sign showed a rotation around the vertical zenith axis. The diameter of the pedestal that supports this structure was measured to be 35 inches (0.89 m). Visual inspection revealed that the collapsed post presents large lateral deflections and bending on the plastic range of the anchor elements, that also exhibit pullout and shear fracture; the anchor bolts seemed to have been outside of the pedestal lateral confinement; the concrete presented fractures and detachments. (See Figure 5-54).



Figure 5-53: Photo of Cantilever Sign Structural Failures on The Pedestal at P-53 Location: 18°11'31.15"N; 65°53'46.75"W



Figure 5-54: Photos of Cantilever Traffic Sign Foundation Structural Pedestal Failure at P-53; with Large Deflections on the Plastic Range, Shear Fracture, and Pullout of the Anchor Elements, and Fractures and Detachments of the Concrete

5.2.27 Cantilever Traffic Sign Site Las Piedras P-66

Located along Highway PR-30 in Las Piedras. A satellite image of the traffic sign structure is shown on Figure 5-55. The final position of the traffic sign showed a rotation around the vertical zenith axis and a total collapse. Figure 5-55 also presets that there were impact damages on the traffic barriers, possible due to the collapse of the sign. Due to narrow shoulders and traffic, the site was considered not safe to perform a more detailed inspection, but the post was already removed by the time of the field visit.



Figure 5-55: Photo of Cantilever Sign Collapse at P-66 Location: 18°11'11.10"N; 65°53'28.92"W

5.2.28 Cantilever Traffic Sign Site Las Piedras P-99

Located along Highway PR-30 in Las Piedras. A satellite image of the traffic sign structure is shown on Figure 5-56. The final position of the traffic sign showed a rotation around the vertical zenith axis and a total collapse. Figure 5-56 also presets that there were impact damages on the traffic barriers, possible due to the collapse of the sign. Due to narrow shoulders and traffic, the site was considered not safe to perform a more detailed inspection, but the post was already removed by the time of the field visit.



Figure 5-56: Photo of Cantilever Sign Collapse at P-99 Location: 18.183386°N; 65.88572°W

5.2.29 Cantilever Sign Site Ponce P-1

Located along the Highway PR-52 in Ponce. An image of the traffic sign structure is shown on Figure 5-57. Visual inspection revealed the pedestal concrete experienced fractures and detachments due to the anchor bolts lateral movement (See Figure 5-57). The position of the first stirrup was not visible.



Figure 5-57: Photo of Cantilever Sign P-1. Damages, Fractures on Concrete Pedestal. Location: 17°59'25.25"N; 66°37'16.63"W

5.2.30 Cantilever Sign Site Ponce P-3

Located along the Highway PR-52 in Ponce. An image of the traffic sign structure is shown on Figure 5-58. Visual inspection revealed the pedestal concrete experienced fractures and initial detachments due to the anchor bolts lateral movement (See Figure 5-58). The position of the first stirrup was not visible.



Figure 5-58: Photo of Cantilever Sign Foundation Structural Damages on the Pedestal at P-3, Damages (Fractures on the Concrete Base) Location: 17°59'19.75"N; 66°37'0.41"W

5.2.31 Cantilever Sign Site Ponce P-4

Located along the Highway PR-52 in Ponce. An image of the traffic sign structure is shown on Figure 5-58. Visual inspection revealed the pedestal concrete experienced fractures and initial detachments due to the anchor bolts lateral movement (See Figure 5-58). The position of the first stirrup was not visible. At the time of the visit the post was reinstalled on a new concrete square base.



Figure 5-59: Photo of Cantilever Sign Foundation Structural Damages on the Pedestal at P-4, Damages (Fractures on the Concrete Base) Location: 17.986208°N; 66.6033°W

5.2.32 Cantilever Traffic Sign Site Ponce P- 59

The Cantilever sign showing a foundation failure was located in the south area of the city of Ponce, along the Highway PR-2. It consisted of a square concrete base (pedestal) over a cast in place drilled shaft, that presented a foundation overturning failure, combined with an apparent rotation about the zenith axis before flipping, and a shear fracture of the concrete drilled shaft, as observed in the Figure 5-60. The fracture of the concrete of the drilled shaft was identified at a depth of 107 inches (measured from the top of the pedestal), just where the reinforcing steel of the shaft was discontinued.



Figure 5-60: Photo of Cantilever Sign Foundation Soil and Structural Failure at P-59. Location: 17°59'21.23"N; 66°38'46.49"W

5.2.33 Cantilever Traffic Sign Site Ponce P- 94

The Cantilever traffic was located just north of the city of Ponce along the southbound lanes of Highway PR-2. An image of the rotated state of this structure is shown on Figure 5-61. The foundation system at this site was not confirmed, as it was only possible to see a square pedestal, as shown in Figure 5-62. The sign was rotated (by about -30 degrees) and a gap between the top pedestal and the surrounding ground was observed, as shown on the images in Figure 5-62, but the concrete pedestal was not damaged, and the anchor bolts did not exhibit noticeable lateral deflections. This behavior leads to the assumptions that its foundation was the same that other exhibiting the same pattern of movement (precast cylindrical drilled shafts).



Figure 5-61: Photo of Cantilever Traffic Sign Foundation Failure at P-94 Location: 17°59'16.80"N; 66°38'55.39"W



Figure 5-62: Photo Showing the Rotation of The Traffic Sign and the Foundation Pedestal at P-94

5.2.34 Cantilever Sign Site Salinas P-11

Located along the Highway PR-53 in Salinas. The final position of the traffic sign could not be verified because at the time of the visual inspection the sign structure had been totally removed by the PR DOT. The structure was verified in the yard where it was stored. The diameter of the pole base was 35 inches (0.89 m) (See Figure 5-63). The structure was sound. Through the visual inspection of the elements on the yard, and interview with PR DOT personnel, that recover the sign from PR-53 highway, it was determined that the collapsed post experimented detachment from the pedestal, and that the anchor bolts showed large deflections, bending on the plastic range, and total shear failure due to torsional movement of the base plate, similar to P-12 (presented in next section).

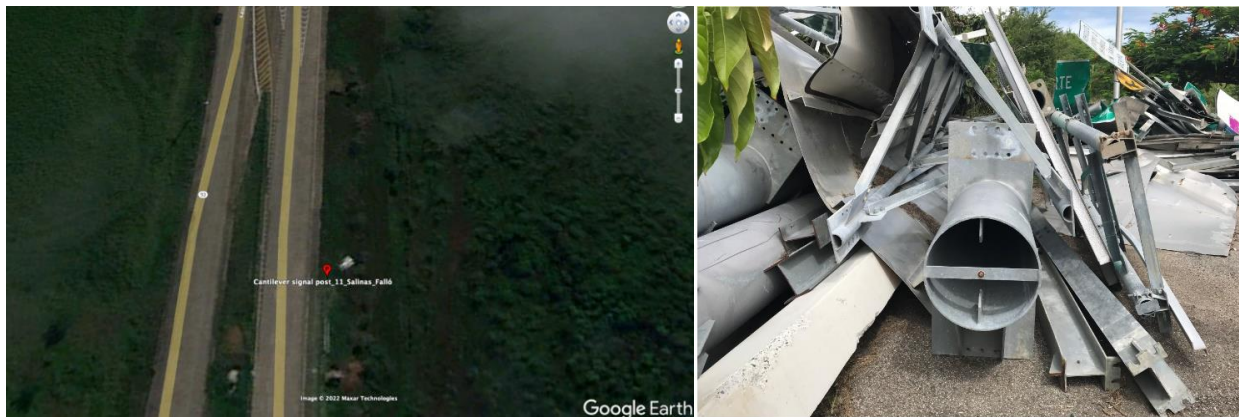


Figure 5-63: Photo of Cantilever Sign Location and Rests Stored at Yard for Id P-11 Location: 18° 0'1.89"N; 66°14'17.05"W

5.2.35 Cantilever Sign Site Salinas P-12

Located along the Highway PR-53, José M. Dávila Monsanto, in Salinas. An image of the remains of the traffic sign structure is shown on Figure 5-64. The traffic sign was removed from the scene and stored on agency property. According to the final position of the anchor bolts of the structure, a rotation of approximately 100 degrees about the vertical zenith axis was observed. Visual inspection revealed that the collapsed post presented large deflection of the anchoring elements with a torsional pattern, leading them to receive permanent deformations and shear fracture. The concrete of the pedestal reflects fractures and detachment due to the high stresses received (See Figure 5-65). A large distance between the last stirrup and the top of the pedestal could also be appreciated, and an anchor bolt outside the stirrups' confinement.



**Figure 5-64: Photo of Cantilever Sign Structural Failures on the Pedestal at P-12 Location: 18° 0'11.23"N;
66°14'29.63"W**



Figure 5-65: Photo of Cantilever Sign Structural Foundation Failure at P-12; Collapsed Post Presented Torsional Pattern and Large Deflections of the Anchoring Elements, which also Exhibit Shear Fracture

5.2.36 Cantilever Sign Site Salinas P-15

Located along the Highway PR-52 in Salinas. An image of the traffic sign structure is shown on Figure 5-66. The final position of the traffic sign showed a rotation about the zenith vertical axis (Figure 5-67). The visual inspection demonstrated that the post exhibits twisting and plastic deformations in the anchor elements. The internal stresses experienced by the concrete produced fractures and detachments in the pedestal (See Figure 5-67).



Figure 5-66: Photo of Cantilever Sign Structural Failures on the Pedestal at P-15. Location: 18° 1'29.22"N; 66° 14'28.42"W



Figure 5-67: Photo of Cantilever Sign Foundation Structural Failure at P-15; Partial Collapse; the Post Presented Large Deflections and Double Bending in the Plastic Range of the Anchoring Elements

5.2.37 Cantilever Sign Site San Juan P-33

Located along the Highway PR-18 in San Juan. An image of the traffic sign structure is shown on Figure 5-68. The visual inspection showed that the Cantilever sign rotated approximately 180 degrees about the vertical zenith axis. The ground around the base was detached from the foundation approximately 2 in, allowing the base to rotate more freely (See Figure 5-68). Not significant structural damages were found on the pedestal.



**Figure 5-68: Photo of Cantilever Sign Foundation Soil Failure (Torsional Rotation) at P- 33 Photo Location:
18°23'52.03"N; 67° 66° 4'14.19"W**

5.2.38 Cantilever Sign Site San Juan P-35

Located along the Highway PR-18 in San Juan. An image of the traffic sign structure is shown on Figure 5-69. The visual inspection revealed that the Cantilever sign rotated approximately 30 degrees about the vertical zenith axis. In addition, the connection of the base to the pedestal did not have the non-shrinkable grout material installed that must be placed between the base plate and the concrete base, to evenly distribute the loads and stresses on the concrete base.



**Figure 5-69: Photo of Cantilever Sign Soil Foundation Failure (Torsional Rotation) at P- 35 Photo Location:
18°24'16.37"N; 66° 4'11.96"W**

5.2.39 Cantilever Sign Site San Juan P-38

Located along the Highway PR-18 in San Juan. An image of the traffic sign structure is shown on Figure 5-70. During the visual inspection, it was observed that the cantilever sign rotated approximately 180 degrees about the vertical zenith axis, and the concrete base experienced fractures and detachments due to anchor bolts lateral movement. The base did not have installed the non-shrinkable grout material that must be placed between the base plate and the concrete base, to evenly distribute the loads and stresses on the concrete base (See Figure 5-70). The anchors that resulted exposed and corroded. The position of the first stirrup was not visible.



Figure 5-70: Photo of Cantilever Sign Soil Foundation Failure (Torsional Rotation) with Damages to the Pedestal at P- 38
Photo Location: 18°24'5.58"N; 66° 4'16.57"W

5.2.40 Cantilever Sign Site San Juan P-40

Located along the Highway PR-18 in San Juan. An image of the traffic sign structure is shown on Figure 5-70. During the virtual inspection, it was observed that the cantilever sign rotated approximately 10 degrees about the vertical zenith axis. This sign was not visually inspected, since it was located on a deep slope contiguous to a street without walkway; thus, the condition of the concrete pedestal could not be assessed.

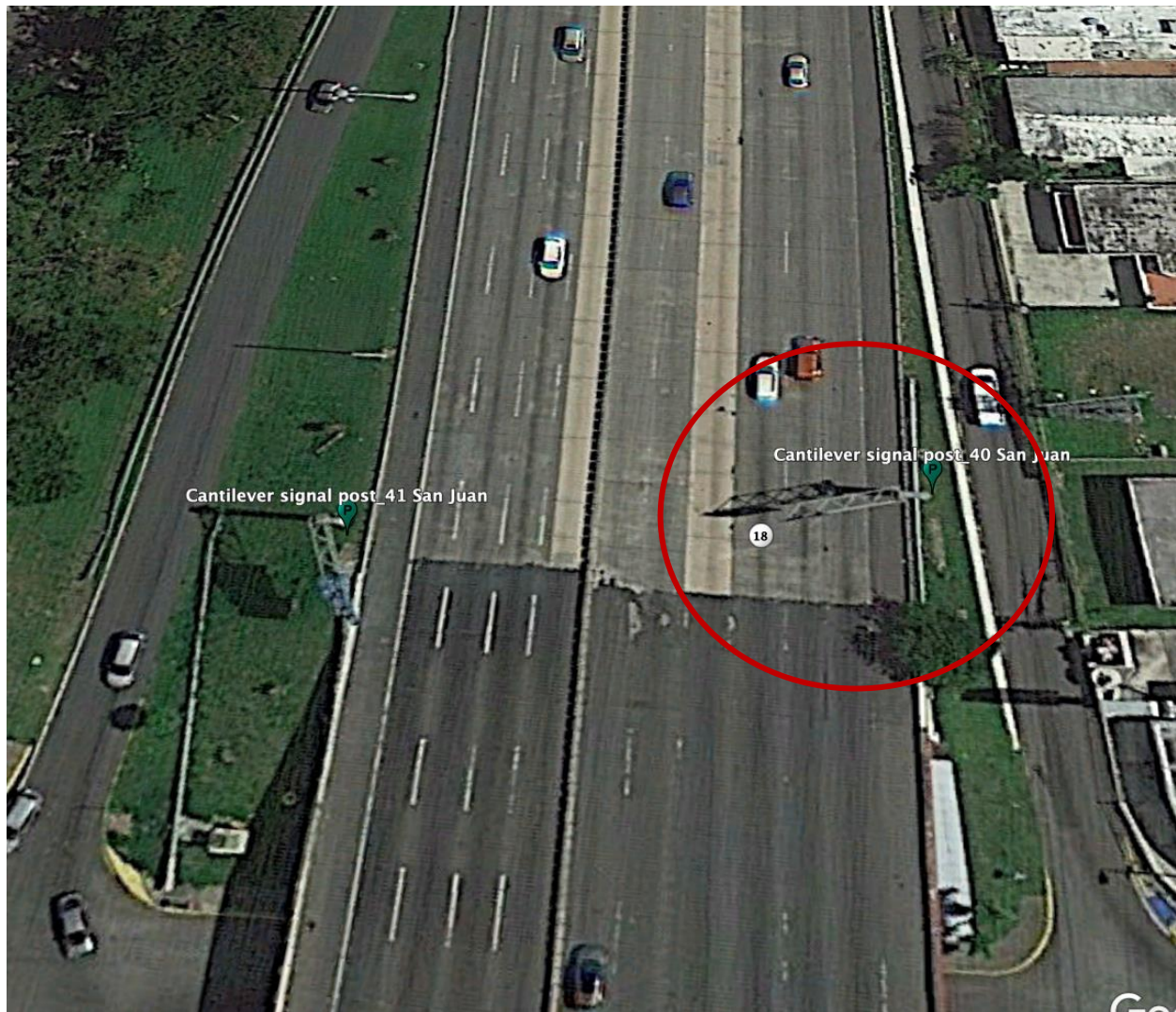


Figure 5-71: Satellite Image of Cantilever Sign Soil Foundation Failure (Torsional Rotation) at P- 40 Photo Location: 18.413125°N; 66.06986944°W

5.2.41 Cantilever Sign Site San Juan P-41

Located along the Highway PR-18 in San Juan. An image of the traffic sign structure is shown on Figure 5-72. The Cantilever sign rotated approximately 70 degrees about the vertical zenith angle, and the concrete base reflected damages (cracks and detachments) due to anchor bolts lateral movement. The bolts had some degree of permanent deformations. In the visual inspection, it was identified that the base did not have the non-shrinkable grout material installed that must be placed between the base plate and the concrete base, to evenly distribute the loads and stresses on the base of concrete (See Figure 5-72). The position of the first stirrup was not visible.



Figure 5-72: Photo of Cantilever Sign Soil Foundation Failure (Torsional Rotation) with Damages to the Pedestal at P- 41
Photo Location: 18°24'47.01"N; 66° 4'13.07"W

5.2.42 Cantilever Sign Site San Juan P-42

Located along the Highway PR-18 in San Juan. An image of the traffic sign structure is shown on Figure 5-73. The concrete base rotated 90 degrees about the vertical zenith axis, and also reflected an inclination (out of plumb) towards the bottom of the slope. In the visual inspection, it was identified that the base did not have the non-shrinkable grout material installed that must be placed between the base plate and the concrete base, to evenly distribute the loads and stresses on the base of concrete. The base was detached from the ground, creating a gap of around 3.5-4.0 in. This dimension was variable around the perimeter of the cylindrical foundation (See Figure 5-74). The granular fill material or clean sand indicated in the specifications was not identified. It was observed that part of the earth slope had experienced movement downwards (the soil located approximately 0.45 m downslope from the post) (See Figure 5-74).

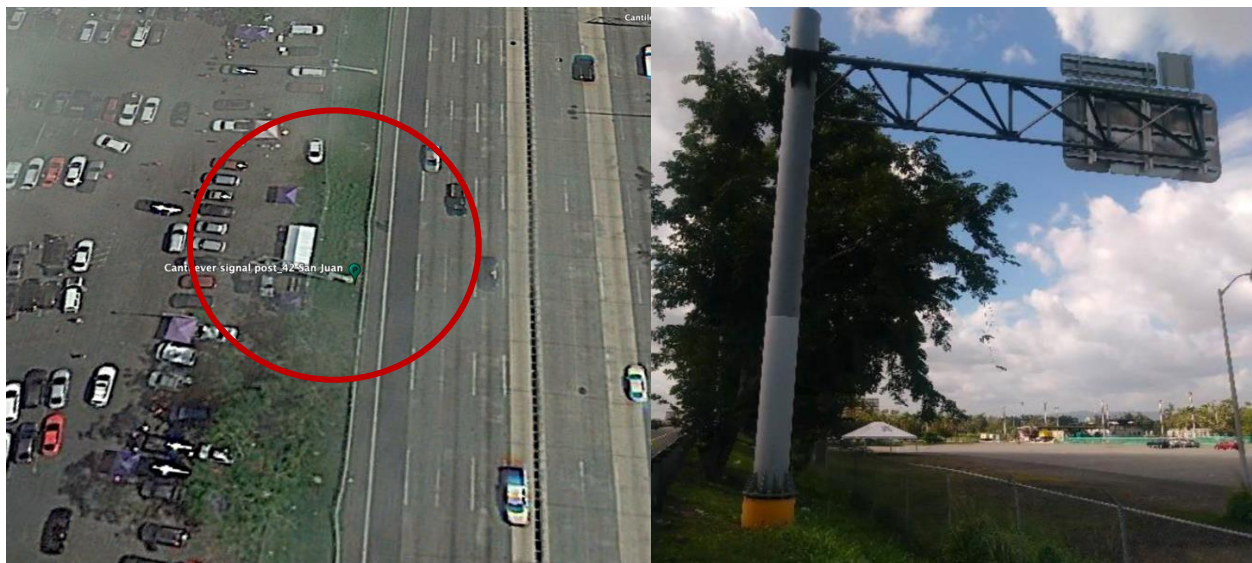


Figure 5-73: Photo of Cantilever Sign Foundation Failure (Torsional Rotation) at P- 42 Photo Location: 18°24'54.71"N; 66° 4'13.43"W



Figure 5-74: Gap Around the Circumference of the Drilled Shaft, and Soil Movement Downhill

5.2.43 Cantilever Sign Site San Juan P-43

Located along the Highway PR-18 in San Juan. An image of the traffic sign structure is shown on Figure 5-75. The concrete base appeared to have experienced small torsional rotations, there were damages to the concrete base (spall, and exposed and corroded anchor bolt), and there was a gap between the soil and de foundation shaft. Additionally, the base plate did not have the non-shrinkable grout material installed that must be placed between the base plate and the concrete base, to evenly distribute the loads and stresses on the base of concrete.



Figure 5-75: Photo of Cantilever Sign Foundation Failure (Torsional Rotation), Damages to the Concrete Pedestal, and Gap Between Soil and Shaft at P- 43 Photo Location: 18.41788611°N; 66.07006111°W

5.2.44 Cantilever Sign Site San Juan P-44

Located along the Highway PR-18 in San Juan. An image of the traffic sign structure is shown on Figure 5-76. The concrete base appeared to have experienced small torsional rotations, there were damages to the concrete base (several cracks, some at an anchor bolt embedment location), and there was a small gap between the soil and de foundation shaft.



Figure 5-76: Photo of Cantilever Sign Foundation Failure (Torsional Rotation), Damages to the Concrete Pedestal, and Small Gap Between Soil and Shaft at P- 43 Photo Location: 18.41561389°N; 66.06995°W

5.2.45 Cantilever Sign Site San Juan P-95

Located along the Highway PR-18 in San Juan. An image of the traffic sign structure is shown on Figure 5-77. The visual inspection revealed that the cantilever sign rotated approximately 180 degrees about the vertical zenith axis and exhibited a loss of contact with the ground along the entire upper circumference of the foundation. Ground detached from the base approximately 2 in around the circumference (See Figure 5-78).



Figure 5-77: Photo of Cantilever Sign Soil Foundation Failure at P- 95 Photo Location: 18°25'25.61"N; 66° 4'20.75"W



Figure 5-78: Gap Around the Circumference of the Drilled Shaft

5.2.46 Cantilever Sign Site San Juan P- 98

Located along the Highway PR-17 Avenida Jesús T Piñero in San Juan. An image of the traffic sign structure after its removal from the roadway is shown on Figure 5-79. The final position of the traffic sign shows a rotation about the vertical zenith axis, and about a horizontal axis. Visual inspection revealed that the collapsed post presented large lateral deflections and bending on the plastic range of the anchor elements, that also exhibited pullout and shear fracture; some of the anchor bolts seemed to have been out of the pedestal lateral confinement steel reinforcement; the concrete presented fractures and detachments (See Figure 5-79).



Figure 5-79: Photo of a Collapsed Cantilever Sign Foundation due to Structural Failures on the Pedestal at P-98
Location: 18°24'27.38"N; 66° 4'3.00"W

5.2.47 Cantilever Sign Site Santa Isabel P-7

Located along the Highway PR-52 in Santa Isabel. A satellite image from 2017 used to identify the location of the traffic sign structure is shown on Figure 5-80. The field visit was not conclusive, since only small fragments of what appeared to be a post foundation were found, as displayed in the other images of Figure 5-80. At the time of summarizing the findings, this one will be counted as a total collapse, considering the high probability that the remains were removed.



Figure 5-80: Photo of Cantilever Sign Location and Possible Collapse at P-7 Photo Location: 18.02574444°N; 66.40993889°W

5.2.48 Cantilever Sign Site Santa Isabel P-8

Located along the Highway PR-52 in Santa Isabel. An image of the traffic sign structure is shown on Figure 5-81. The field visit revealed some fine cracks on the pedestal, as presented in Figure 5-80; these cracks appeared to be limited to the top mortar of the concrete base, and could be a result of the construction process, and not necessarily attributed to the wind vibrations. At the time of summarizing the findings, this one will not be counted as a wind induced failure.



Figure 5-81: Photo of Cantilever Sign Location and Pedestal Cracks at P-8 Photo Location: 18.01293333°N; 66.389025°W

5.2.49 Cantilever Sign Site Santa Isabel P-10

Located along the Highway PR-52 in Santa Isabel. An image of the traffic sign structure is shown on Figure 5-82. The field visit revealed that the pedestal had cracks, as presented in Figure 5-82 and Figure 5-83. These cracks are consistent with the ones produced by anchor bolts and/or base plate movement.



Figure 5-82: Photo of Cantilever Sign Location and Pedestal Cracks at P-10 Photo Location: 18.01423056°N; 66.36989167°W



Figure 5-83: Photo of Cantilever Sign Location Pedestal Cracks at P-10

5.2.50 Cantilever Sign Site Santa Isabel P-36

Located along the Highway PR-52 in Santa Isabel. An image of the traffic sign structure is shown on Figure 5-84. The field visit revealed some fine cracks on the pedestal, as presented in Figure 5-84; these cracks appeared to be limited to the top mortar of the concrete base, and could be a result of the construction process, and not necessarily attributed to the wind vibrations. The pedestal also shows efflorescence, water marks, and leakage. At the time of summarizing the findings, this one will not be counted as a wind induced failure.



Figure 5-84: Photo of Cantilever Sign Location and Pedestal Cracks, Efflorescence, Water Marks and Leakage at P-36
Photo Location: 18.01324444°N; 66.38875°W

5.2.51 Cantilever Sign Site Santa Isabel P-70

Located along the Highway PR-52 in Santa Isabel. An image of the traffic sign structure is shown on Figure 5-85. The field visit revealed a diagonal on the pedestal, consistent with the ones produced by anchor bolts movement due to wind action (see Figure 5-85).



Figure 5-85: Photo of Cantilever Sign Location and Pedestal Cracks at P-70 Photo Location: 18.0284609°N; 66.4165331°W

6 Analysis and General Recommendations of the Findings

As mentioned in previous chapters, two principal modes of failure of cantilever overhead traffic signs were identified, both at the foundation level:

- a) Foundation structural failures on the pedestal
- b) Foundation soil/soil-structure interaction failures

Each failure was fully documented, and a collection of 910 photographs of damages was obtained to support the evaluation of these conditions. The following sections summarize the principal findings on these two predominant modes of failure.

6.1 Foundation Structural Failures of the Pedestal

The structural failures were characterized by a combination of anchor bolts large lateral deflections in the plastic range, anchor bolts shear fracture, anchor bolts pull out, concrete cracks, concrete large spalls, concrete crushing, and one case of concrete shear fracture of the drilled shaft. The following sub-section present a description of the findings supported by images that allow to appreciate the conditions.

6.1.1 Large Lateral Deflections of Anchor Bolts

It was observed that a main cause of structural damages and failures was the large lateral deflections of the anchor bolts, triggered by the torsional rotation (rotation about the vertical axis) of the post base plate due to the wind action on the signs. Most of the anchor bolts exhibit a characteristic double bending shape in the plastic regimen, with apparent plastic hinges formations at the ends (above the last stirrup, and below the post base plate).

These lateral deflections are extremely detrimental, since the bolts fail at much lower shear load than the one that would produce bolt shear fracture and are directly related to the large

separation of the top stirrup and the post base plate. Appendix D presents simplified models to estimate the required separation to assure bolt shear instead of bolt plastic bending. The models are extremely simplified and conservative, since they do not consider the concrete core resistance, and assume that the bolts are slender elements and concentrated plastic hinge model is adopted. Although the models conduct to unrealistic, too small, required distance between lateral supports, they allow to emphasize the importance of this steel detail, and strongly suggest that this is a topic for further study.

In addition, the lateral deflections of the bolts induce tension on the concrete of the pedestal that, since having a reduced tension capacity, will experience cracks and spalls. These damages to the concrete lead to uneven supports of the base plate, more cracks on the concrete, and uneven distribution of the loads on the bolts, with shear failure of overstressed bolts.

The uneven support produced by the concrete cracks, combined to the rotation of the post base plate about a horizontal axis, produced further crushing on the concrete, and pull out of the anchor bolts. Finally, $P-\Delta$ effects due to large displacements and out of plumb of the post would also contribute to the collapse.

In Figure 6-1, Figure 6-2, and Figure 6-3 one can appreciate the initial stages of pedestal damages due the torsional rotation of the post base plate, presenting cracks and spalls on the concrete triggered by the lateral deflections of the anchor bolts that exerted tension stresses on the concrete. In all these three cases the bolts did not exhibit significant deflections in the plastic regimen.



Figure 6-1: Initial Stages of Concrete Cracks and Spalls due to Lateral Deflections of Anchor Bolts (Sign P-1)



Figure 6-2: Initial Stages of Concrete Cracks and Spalls due to Lateral Deflections of Anchor Bolts (Sign P-3)



Figure 6-3: Initial Stages of Concrete Cracks and Spalls due to Lateral Deflections of Anchor Bolts (Sign P-76)

Figure 6-4, Figure 6-5, and Figure 6-6 present more advance situations of pedestal damages due the torsional rotation of the post base plate. In the first two cases the bolts did not exhibit significant defections in the plastic regimen, but in the third one the plastic deformations are present, and the double bending shape of the bolts starts to be identifiable. The large distance between the last stirrup (last lateral support of the anchor bolts) and the base plate also started to be evident.



Figure 6-4: More Advance Stage of Concrete Cracks and Spalls due to Lateral Deflections of Anchor Bolts with Large Unconfined Length (Sign P-38)



Figure 6-5: More Advance Stage of Concrete Cracks and Spalls due to Lateral Deflections of Anchor Bolts with Large Unconfined Length (Sign P-41)



Figure 6-6: More Advance Stage of Concrete Cracks and Spalls due to Lateral Deflections of Anchor Bolts with Large Unconfined Length. Bolts Exhibit Double Bending Shape (Sign P-15)

Significantly more advanced situations of damages, presenting extremely large deflections of the anchor bolts on the plastic regimen, large cracks, spalls, and deterioration of the concrete, and partial or total collapse of the traffic sign structure are displayed in Figure 6-7 to Figure 6-11. The images clearly present the double bending of the anchor bolts in the plastic range, and the large distance between the base plate of the post and the first stirrup that provides lateral support to the bolt. The images also show that in some cases the base plate did not only rotate in torsion (about the vertical axis) but also in bending (about the horizontal axis), producing crushing to the concrete, and pull out of the anchor bolts.



Figure 6-7: Large Deflections of Anchor Bolts due to Lack of Lateral Confinement (Sign P-46)



Figure 6-8: Large Deflections of Anchor Bolts due to Lack of Lateral Confinement



Figure 6-9: Large Deflections of Anchor Bolts due to Lack of Lateral Confinement (Sign P-12)



Figure 6-10: Large Deflections of Anchor Bolts due to Lack of Lateral Confinement (Sign P-12)



Figure 6-11: Large Deflections of Anchor Bolts due to Lack of Lateral Confinement (Sign P-106)

These damages and failures indicate that the confinement of the anchor bolts is essential to avoid damages. And that the specifications for stirrups separation, separation between the last stirrup and the base plate, and details of the top of the pedestal to avoid these lateral movement is of extremely importance. In several cases, the observed distance between the top stirrup and the base plate did not comply with PRHTA specifications (see Appendix C for details); a strict inspection and quality control during sign installation is also imperative.

6.1.2 Anchor Bolts Located Outside the Stirrups

The field inspection also revealed that in several situations the anchor bolts were placed outside the concrete core confined by the stirrups (transverse reinforcement). This condition made these signs more vulnerable. Figure 6-12 to Figure 6-14 are examples of this situation.

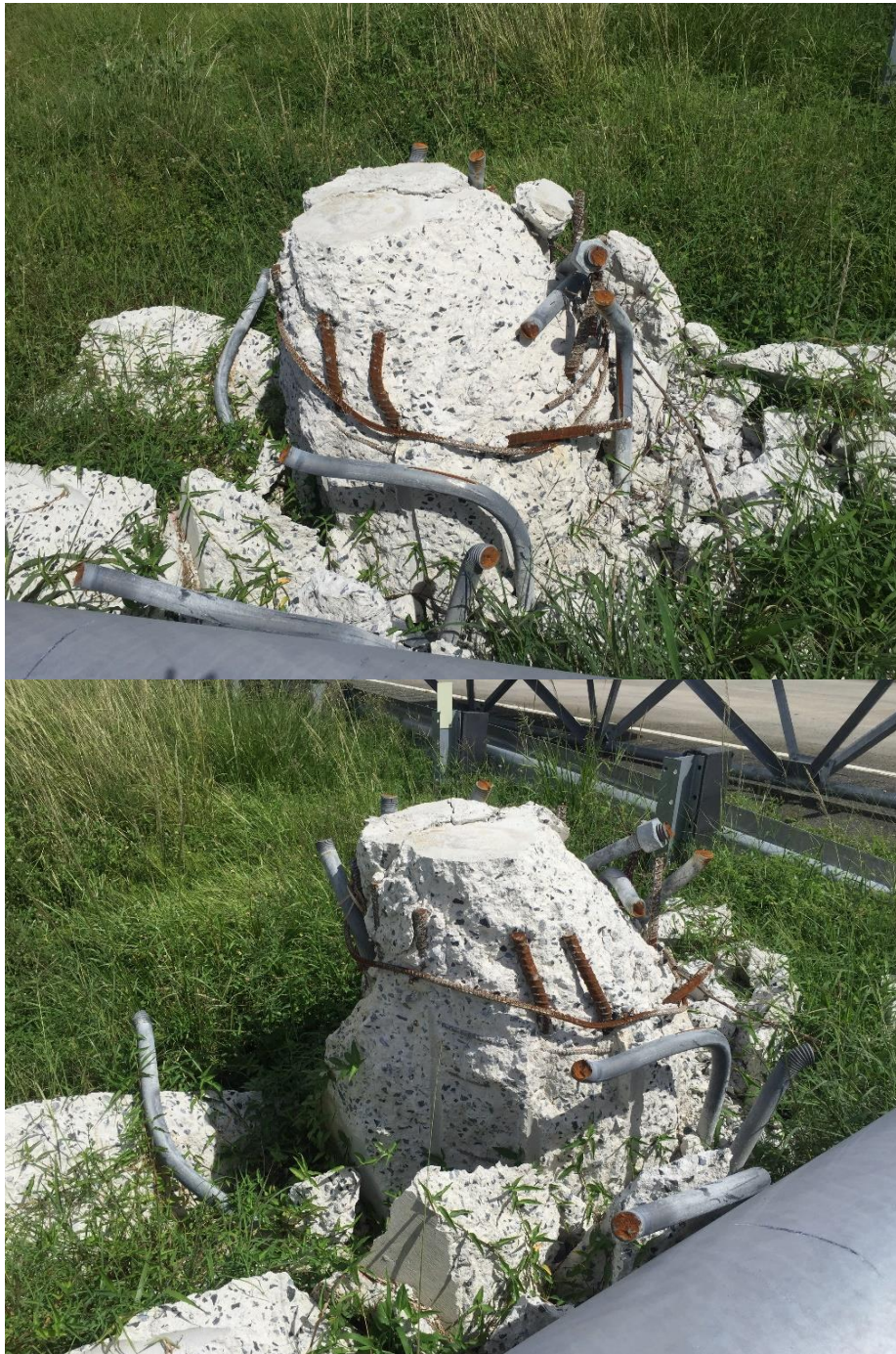


Figure 6-12: Several Anchor Bolts Outside the Transverse Confinement Steel / Concrete Core (Sign P-100)



Figure 6-13: Some of the Anchor Bolts Outside the Transverse Confinement Steel / Concrete Core (Sign P-100)



Figure 6-14: Several of the Anchor Bolts Outside the Transverse Confinement Steel / Concrete Core (Sign P-105)

The observed location of the anchor bolts strongly suggests that a review of the final proposed design for the foundation of this traffic signs, and a strict inspection and quality control during sign installation are imperative.

6.1.3 Anchor Bolts Pullout

Some of the cases presented anchor bolts clean, with no concrete adhered to its skin, giving the appearance of anchor bolts pull out due to lack of skin resistance or adequate embedment. This situation suggests that a revision of anchor bolts installation to assure proper embedment length and adherence to concrete is required. Figure 6-15 to Figure 6-17 are examples of this condition.



Figure 6-15: Anchor Bolts Pullout



Figure 6-16: Anchor Bolts Pullout (Sign P-105)



Figure 6-17: Anchor Bolts Pullout (Sign P-53)

6.1.4 Length of Longitudinal Reinforcement not Appropriate

One of the failures found on traffic sign P-59 consisted of an apparent shear failure of the concrete of the drilled shaft foundation due to torsion caused by the wind action over the sign. Figure 6-18 presents an extract of the requirement of PRHTA Standards for Sign Structures Supports (see Appendix C for more details). The inspection showed that the longitudinal steel (and the corresponding transverse steel) was interrupted at a length of 106 in, significant less than the required 157.4 in. The fact that the sign was on a slope, and the compaction conditions of the soil may have contributed to a deficient shaft resistance (load transfer), imposing significant stresses at this section. This finding also suggests that a review of the final proposed design for the foundation of this traffic sign, and a strict inspection and quality control during sign installation are imperative.

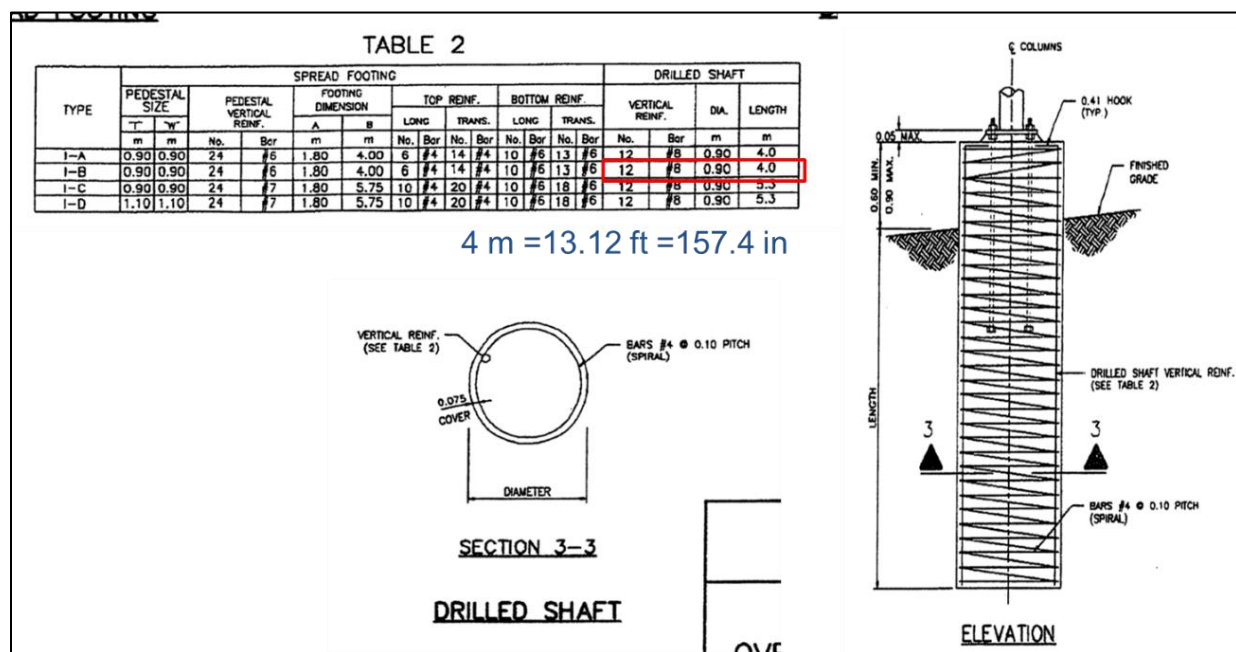


Figure 6-18: PRHTA Standard for Sign Foundations (PRHTA, 2010)

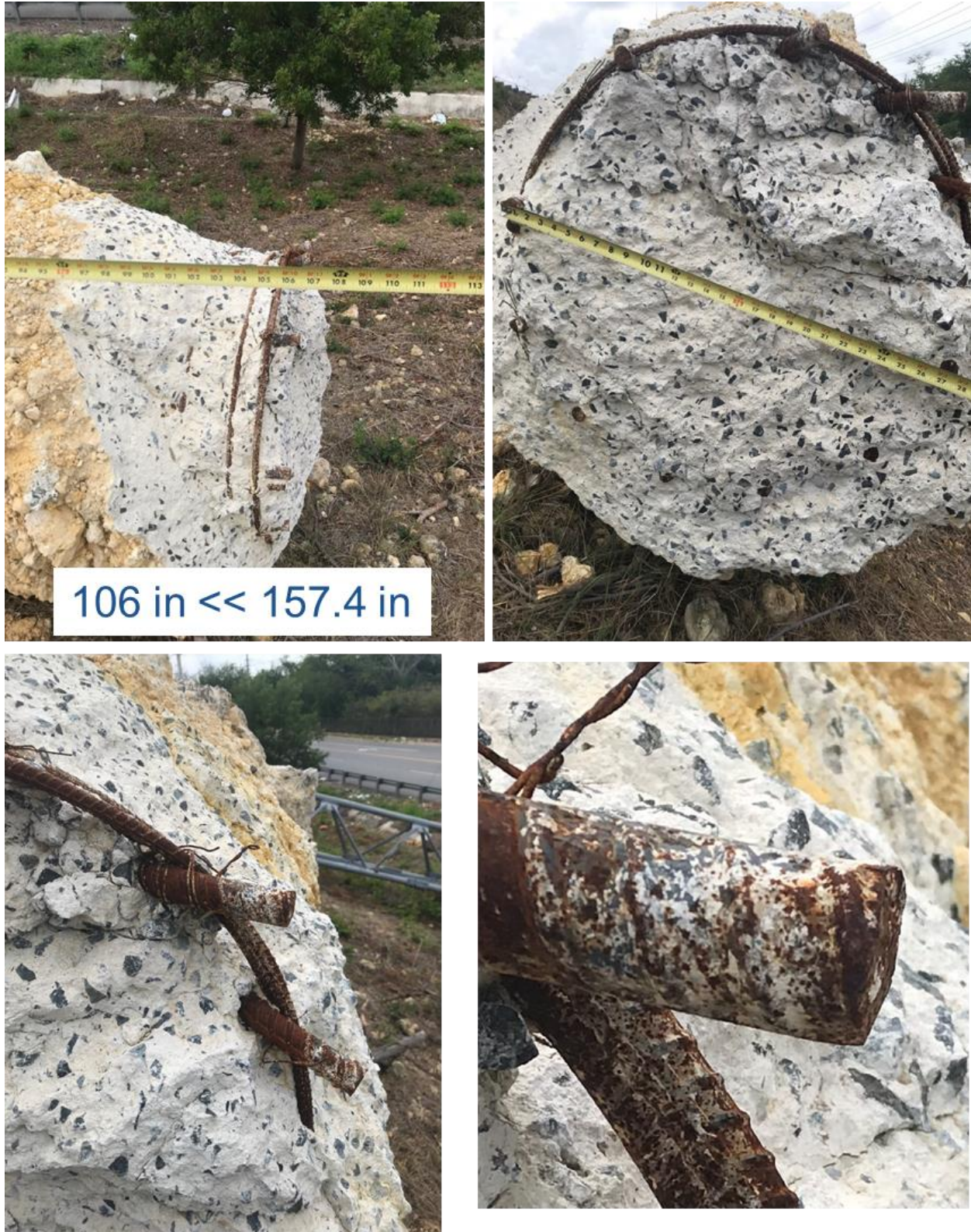


Figure 6-19: Interrupted Steel and Shear Fracture of the Concrete of the Drilled Shaft

6.2 Foundation Soil Failures

The most common soil-foundation failure observed was the rotation about the vertical axis of precast concrete cylindrical bases. There were also failures due to overturning, and failures on slopes. The following sub-sections presents examples of this modes of failure or damage.

6.2.1 Foundation Torsional Failure

Figure 6-20 and Figure 6-21 present two examples of cylindrical precast concrete bases that rotated about the vertical axis due to torsional shear stresses on the soil-shaft interface produced by the wind forces action on the traffic sign.



Figure 6-20: Cylindrical Precast Concrete Base that Experienced Torsional Rotation. The post was Removed. PR 66 in Canóvanas



Figure 6-21: Cylindrical Precast Concrete Base that Experienced Torsional Rotation. PR 18 in San Juan

This mode of failure may have been aggravated by lack of proper soil preparation. It was noticed that in some cases the concrete base was detached from the ground, creating a gap between the soil and the foundation in all the perimeter of the cylindrical shaft, as shown in Figure 6-22. Also, in these cases that presented the gap, the granular fill material or clean sand indicated in the specifications was not identified during the visual inspection. Although not related to this mode of failure, it was identified that several of the post bases did not have the non-shrinkable grout material installed that should be placed between the base plate and the concrete base, to evenly distribute the loads and stresses on the base of concrete, as can be observed in Figure 6-22.



Figure 6-22: Gap Between the Soil and the Cylindrical Precast Concrete Base that Experienced Torsional Rotation. PR 18 in San Juan.

This abundant mode of failure strongly suggests that the shaft resistance of these precast concrete cylindrical was not adequate, and a redesign of the foundations is recommended. For instance, one may consider either increasing the embedment length and the diameter of the base, changing the soil compaction requirements and the texture of the finished concrete, or changing the precast concrete base cross sectional shape from circular to square, in order to trigger soil to soil shear resistance instead of soil to concrete shear resistance. Other alternative could be to opt for cast in place concrete bases, which did not exhibit these torsional rotations.

6.2.2 Foundation Torsional and Overturning Failure

Figure 6-23 shows one of the three cases observed with this type of failure, where the base (foundation) experienced torsional rotation and collapsed by overturning. One of the other cases occurred on a more pronounced slope and is presented in the following section. The fact that there were only two cases observed in flat or not pronounced slope suggests that the overturning mode of failure was not a common problem, and not general recommendations and observations were drawn for this case.



Figure 6-23: Foundation that Experienced Torsional Rotation and Overturning. PR 52 in Caguas.

6.2.3 Foundation Torsional and Overturning Failure on a Pronounced Slope

Figure 6-24 presents the other case observed that experienced this type of failure, where the base experienced torsional rotation and collapsed by overturning, but this one occurred on a pronounced slope.

As presented in section 6.1.4, the pedestal presented lack of required length (depth) of the longitudinal and transverse steel reinforcement, that produced a shear torsional failure of the shaft.

But the shape of the soil failure suggests that there were also foundation length embedment problems. No special design details and construction plans were obtained for the case of signs on slopes from the PR DOT; This strongly suggest that this type of sign location needs special design requirements, to assure enough embedment length that allows the proper soil passive action, considering the soil discontinuity and lack of confinement downhill.

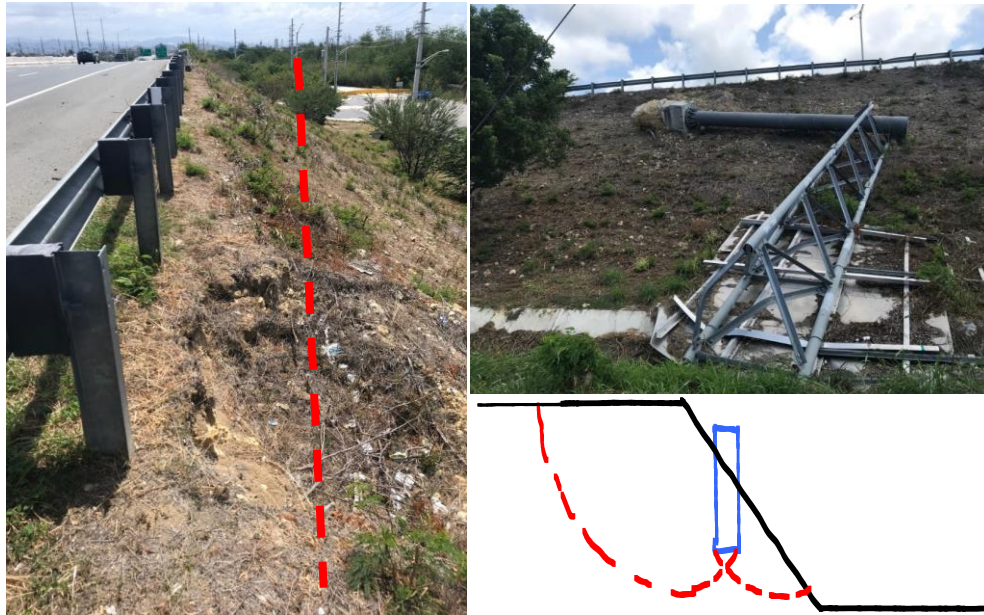


Figure 6-24: Foundation that Experienced Torsional Rotation and Overturning on a Pronounced Slope. PR 2 in Ponce.

7 Development of GIS Virtual Exploration Tool

As previously mentioned in Chapter 4, to optimize the research in the field, a spatial analysis methodology was developed performing a virtual exploration using Google Earth Pro as the GIS platform. This helped identify and locate the signs that were the objective of this research. At the end of this virtual exploration, the field visit phase continued, collecting inspection information such as: in field determined location coordinates, representative photographs, and notes of identified faults, as presented in Chapter 5. This information served as the basis for the development of a virtual exploration tool, allowing the incorporation of information obtained during the field visit and geolocation of traffic signs on the island map. This tool allows have a graphical and geospatial perception of the damages on cantilever traffic signs due to Hurricane Maria.

A nomenclature was established identifying the location of the posts that presented damage with a red dot, and those that did not present damage with a green dot. This allows to quickly locate the signs that presented damages. A higher level of information was incorporated in the established points adding value to the tool, as presented in Figure 7-1. The information presented is:

- Town
- Sign identification number
- Rectified GPS locations
- Inspection notes
- Photographs

By viewing the Google Earth map of Puerto Rico with the crated layer activated, the areas where the greatest number of faults are concentrated can be identified (see Figure 7-1).

By having access to the platform, it will be possible to easily visualize the points that locate the inspected posts, identify the damaged ones (red ones), and interact with each one of them. By interacting with the tool, users will have access to the information that summarizes the status of the sign. This gives details on the findings.

It is expected that this virtual exploration tool, complemented with this report, could be useful to PRHTA to assess the impact of Hurricane Maria on this type of traffic signs, identify most vulnerable areas, most repeated failures, contributing to develop inspection logistics and a more resilient infrastructure in future projects. This tool will allow a virtual/visual tour of all the inspected areas and the identified findings to be carried out, putting the situation found in perspective.

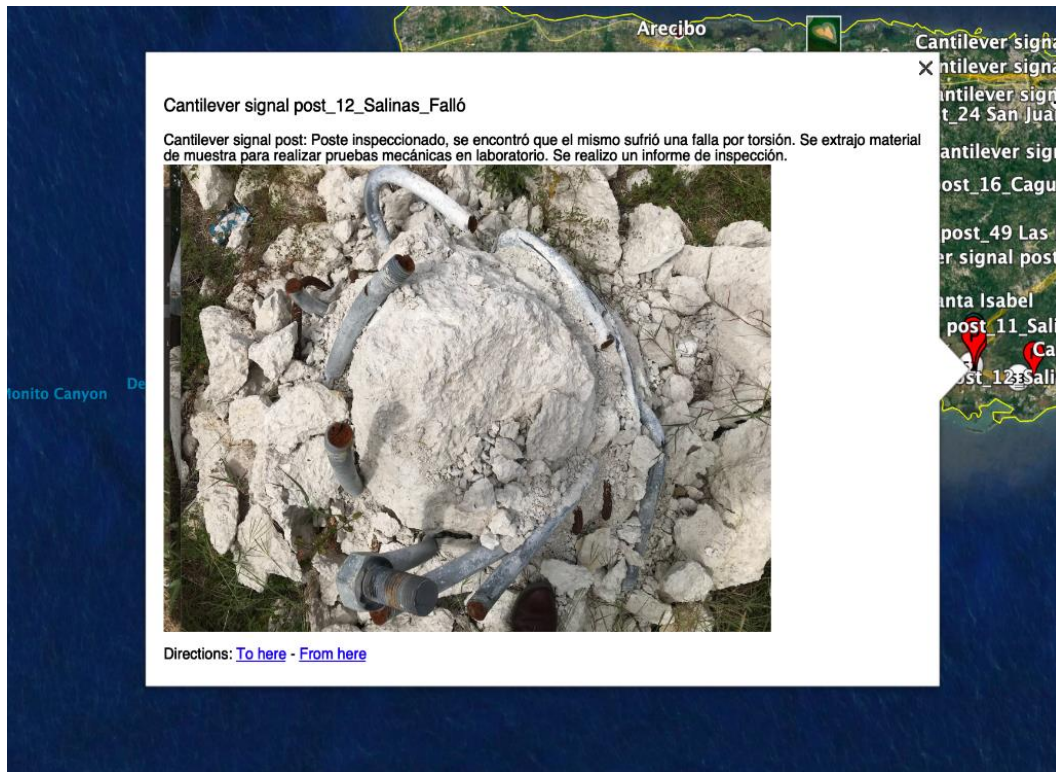


Figure 7-2: Example of the Information Revealed to the User when Using the Platform

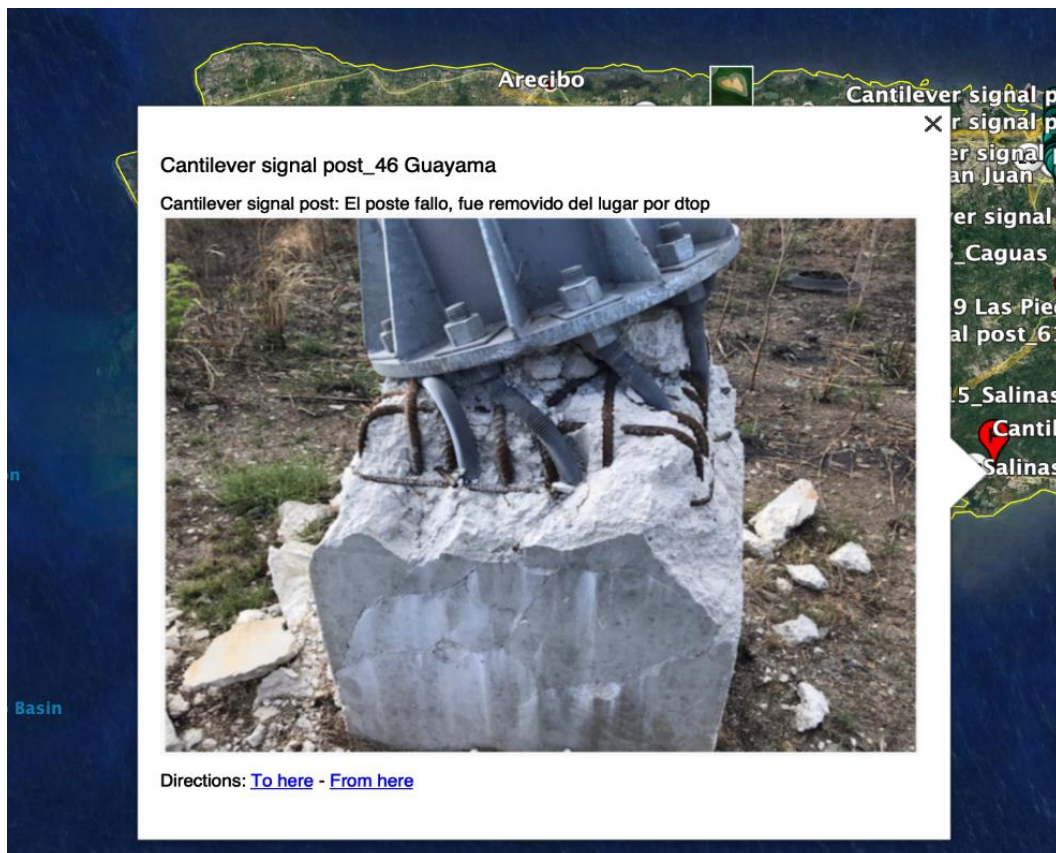


Figure 7-3: Example of the Information Revealed to the User when Using the Platform

8 Laboratory Testing of Collected Samples

For one of the sites visited, corresponding to sign P-2, samples of the pedestal structural components were collected: they consisted of pieces of detached concrete, longitudinal and transverse reinforcing steel, and anchor bolts, as presented in Figure 8-1. The main idea was to perform mechanical tests on these components, to assess if any material deficiency (lack of strength) could have contributed to the failures observed in the field visits. The following sections summarize the test performed.



Figure 8-1: Samples collected from damaged pedestal

8.1 Tension Test on Steel Rebars and Anchor Bolts

The main objective of the tension tests is to determine the yielding and ultimate resistance to normal tensile stress of the specimens. Steel specimens consisted of longitudinal and transverse reinforcing steel of the pedestals, and anchor bolts installed to anchor the bases of the posts.

To carry out the stress test of the reinforcing steel, a section of the collected #6 longitudinal reinforcing bars was extracted and manipulated with external forces to obtain three straight specimens. The specimens were subjected to a tension test, as presented in Figure 8-2.



Figure 8-2: Tension Test of Longitudinal Rebar Specimen (Bar Size # 6, Diameter 0.097 Inches.)

The specimens were subjected to tension until fracture to obtain their maximum capacity (ultimate stress). Figure 8-3 shows the three specimens after the test, where one can appreciate the

typical necking in the vicinity of the rupture surface, while Figure 8-4 presents a partial display of the stress-strain diagram provided by the tension equipment, in the region of yielding.



Figure 8-3: Reinforcing steel specimen after test was conducted

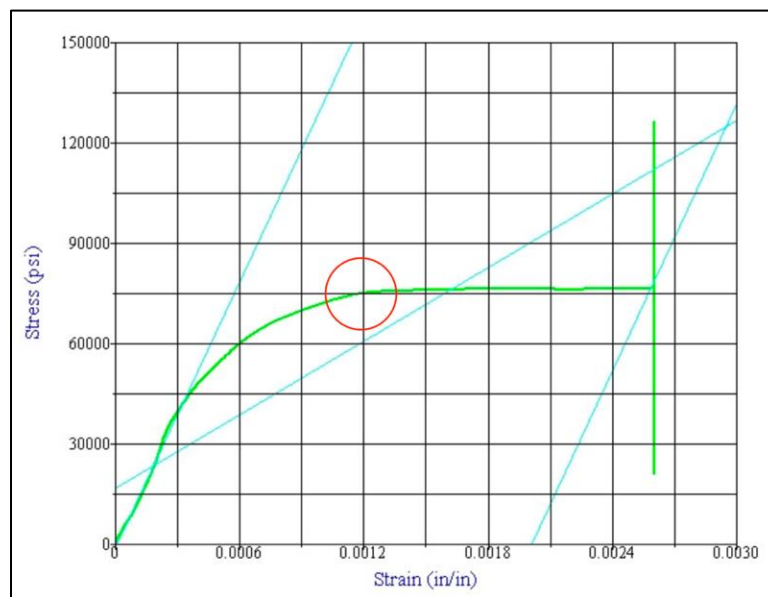


Figure 8-4: Partial Display of the Stress-Strain Diagram for One Rebar #6

The results of the tests are summarized in Table 8-1. The average ultimate stress resulted 75,762 psi, this being a representative value of a grade 60 reinforcing steel, which is the one required by the PRHTA standards for this type of signs.

Table 8-1: Results of the Tension Test on #6 Reinforcing Steel Rebars

Specimen Bar # 6	Peak Load [lb]	Ultimate Tensile Strength [psi]
1	47,947	76,556
2	47,445	74,759
3	47,724	75,970
Average	47,705	75,762

The tension test of the anchor bolts, due to their large diameter (thus requiring a tension test equipment of large capacity) was performed outside the university, in a private laboratory facility: Jaca y Sierra Testing Laboratories. They had a 300,000 lb capacity equipment, which allowed to perform a tension test of the bolt, and have its approximate strength, which resulted in:

Yielding Tensile Strength \approx 61,968 psi
 Ultimate Tensile Strength \approx 66,152 psi

Figure 8-5 presents the collected specimen, the tension test layout, and the specimen after testing. Before the test, the specimen was straightened, since it had a significant deflection in the plastic range, as displayed in Figure 8-6. The threads could not be avoided for the test. Nevertheless, the results gave a good estimate of the capacity, and the strength of the anchor bolt was considered appropriate.



Figure 8-5: Anchor Bolt Tension Test



Figure 8-6: Anchor Bolt Sample with Plastic Deformations

8.2 Concrete Compression Test

The specimens collected in the field visits are presented in Figure 8-1 and Figure 8-7. These pieces of concrete were part of the pedestal that collapsed due to the tension strains exerted on the concrete produced by the large lateral deflection of the anchor bolts, which were the consequence of the torsional rotation of post base plate due to the wind loads. Figure 8-7 shows segments of the pedestals that collapsed in the Salinas region, Sign P-2, in addition, anchoring elements such as bolts and screws with their nuts were found.



Figure 8-7 Specimens Collected During the Field Visit

To extract the cores (cylinders) from these samples it should be ensured that there is no reinforcing steel in the area so that the results of the test are not affected, and a reliable concrete strength, f'_c , is obtained.

The common way to determine the in-place strength of concrete is to drill and test cores (Arioz, Tuncan, Ramyar, & Tuncan, 2006). Although the method consists of expensive operations that require a lot of over time, the cores provide reliable and useful results because they are mechanically tested for destruction (Akçay, 2004), as shown in Figure 8-8. The general problems of core testing are well known, and the factors influencing the relationship between core strength and standard cylinder strength have been presented by many researchers (Campbell & Tobin, 1967; Petersons, 1968; Malhotra, 1977; Neville, 2001; Turkel & Ozkul, 2010).



Figure 8-8 Example Mechanical Test to Core Obtained Concrete Cylinders

The recommended procedures for cutting, testing and interpretation of results are fully established and documented in the ASTM C42 Standard (ASTM, 2018). Following the standard, the extraction, preparation, and care provided was carried out to obtain the nuclei. To extract the nuclei from the collected specimens, a wooden formwork was prepared to confine the specimen and prevent movement during the extraction of the nucleus, as presented in Figure 8-9. The surface of the pieces of concrete were clean and carefully examined, to assure steel was not present on the concrete. The specimens were confined in the concrete mix for 14 days prior to core extraction.



Figure 8-9 Pedestal Concrete Samples Confined with Fresh Concrete in a Wooden Formwork.

After the concrete set, the drilling to extract the cores took place. The drill was placed perpendicular to the surface where the core would be extracted and was anchored with two screws to the confinement concrete. Having the system installed and secured, the cutting process began.



Figure 8-10 Drill Equipment Installed and Performing Extraction

Once the nucleus was extracted, it was measured and any peculiarities that were present were recorded. Already in the laboratory, the ends of the nucleus were cut with a wet saw, so that their length complies with a 2 to 1 relationship with the diameter. The extracted core was conditioned for 5 days before the compression test was carried out, see Figure 8-11. The specimens were cut according to the diameter-height ratio required by the standard. They are covered with plastic to avoid changes in the humid conditions.



Figure 8-11 Extracted Cores, Cut and Placed Inside Plastic Bags

Before performing the mechanical compression resistance test, the specimens were recapping in accordance with the ASTM C617 standard, see Figure 8-12. This allowed to guarantee that there was a complete contact between the surfaces in the test equipment and that the applied load is distribute evenly on the concrete specimen. After recapping, it was waited at least two hours for the sulfur to acquire a resistance greater than that of the core; after this waiting time, the test was conducted, see Figure 8-13.



Figure 8-12 Recapping and Leveling of Cores Prior to Testing

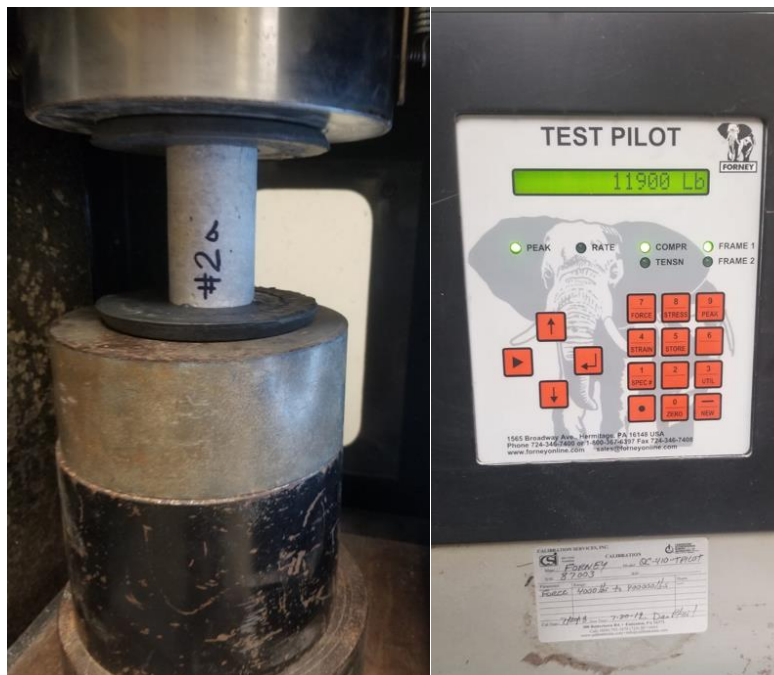


Figure 8-13 Compression Test on Extracted Core

For the interpretation of the results, the estimation of the f'_c was made through the criteria of ACI 318-S14, section 26.12 “Evaluation and acceptance of concrete”. The results of the tests carried out are summarized in Table 8-2; an average f'_c of 3,823 psi was obtained; this strength complies with the specifications in PRHTA standards for the foundations of these signs which requires 3,000 psi.

Table 8-2: Results of Mechanical Compressive Tests Performed on Cores Extracted from The Specimens

Core identification	Maximum capacity (psi)
1A	3,984
1B	3,668
2A	3,598
2B	3,040
3A	4,802
3B	3,846
Average	3,823

8.3 Summary of Laboratory Findings

The results obtained for the strength of the pedestal concrete, the pedestal reinforcing steel, and the anchor bolts was adequate and in accordance with the requirements from the PRHTA standards. Since no evidence of deficient material properties was found in this small sample, it was decided that no further investigation of material properties was advisable to support the analysis of the findings of the inspection process.

9 Summary, Conclusions and Recommendations

The purpose of this investigation was to identify the cantilever-type traffic signs that suffered damages during the passage of Hurricane María through Puerto Rico on September 20, 2017, and their primary modes of failure. After an exhaustive field investigation that covered the identification and location, the inspection, and the assessment of the modes of failure of this type of traffic signs, it was determined that the traffic signs failed primarily as the result of the torque applied to their base. This torque was a consequence of the high winds loads exerted by the hurricane on the signs and triggered structural failures on the concrete pedestal (base), and soil-foundation interaction failures.

To organize and summarize the findings, three different levels of observed damages were established:

- (a) Damages: the sign showed fractures on concrete base but was on plumb as steady, and on the right orientation.
- (b) Partial collapse: the pedestal exhibited severe damage or severe rotations, but the sign was still standing, although it may be out of plumb and not necessarily stable.
- (c) Total collapse: the pedestal presented severe damage, and the sign was on the ground or touching the ground.

In Figure 9-1 presents the geolocation of the most severe findings by region (those that produce a total or a partial collapse), with a summary of the cases observed in each mentioned level of damage observed, and the causes (mode of failure). It can be appreciated that the structural damages to the pedestal due to large lateral movements of the anchor bolts had more density to the east side of the island, where the intensity of the wind speed was higher.

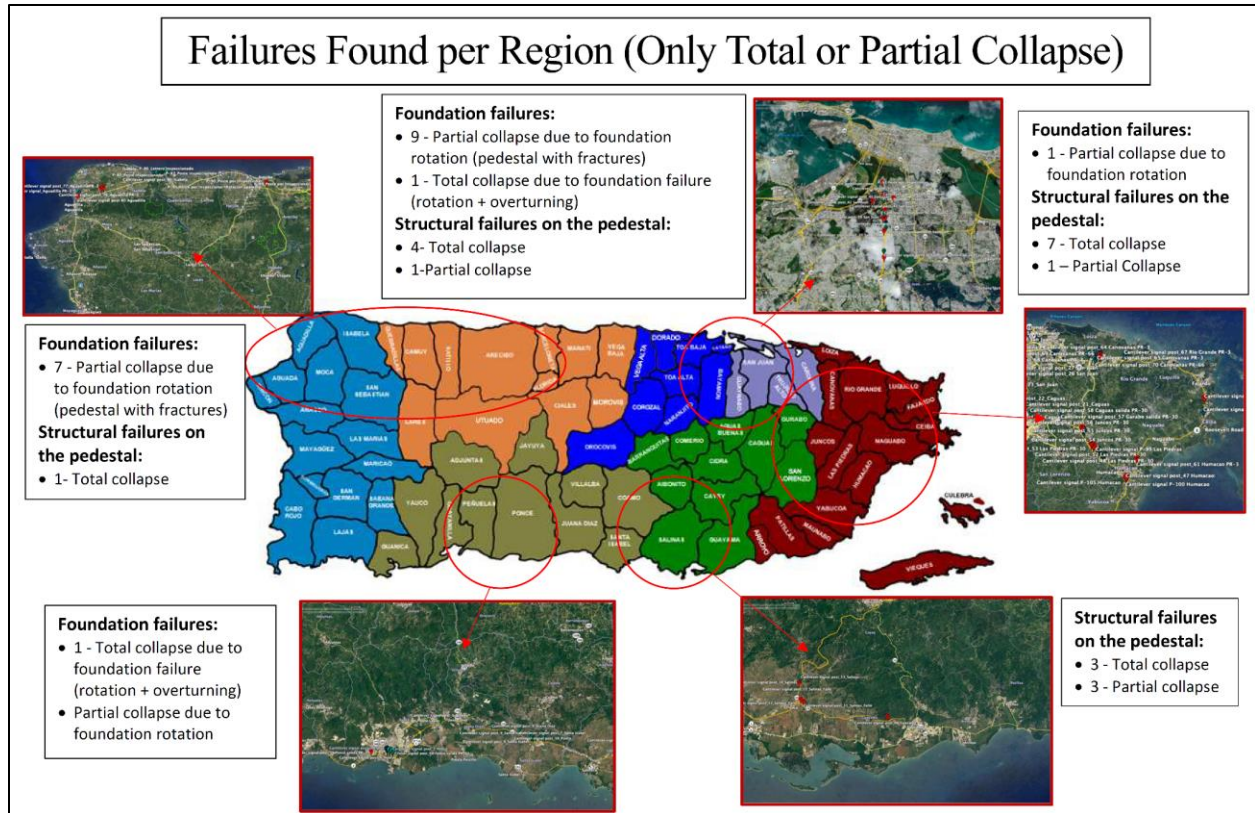


Figure 9-1: Geolocation of Most Severe Findings by Exploration Region

Table 9-1 summarized all the findings by level of damage, and by type of failure. Of the 95 traffic signs inspected, 49 presented damages associated to hurricane Maria (52%), 17 experienced total collapsed (18%), 17 failed by partial collapse (18%), and 8 exhibited damages to the pedestal (8%), while 44 were without evident damages (46%) and 2 presented damages not directly related to the pass of the hurricane (2%).

Out of the 49 (52%) that presented damages due to the hurricane (ranging from damages to collapse), 33 had structural damages to the pedestal, representing 35% of the total signs inspected and 67% of the damaged. Of the 17 that experienced total collapse, 15 (88% of the total collapsed cases) were due to structural damages to the pedestal. All these damages exhibited cracks on the concrete due to large lateral deflections of the anchor bolts.

Out of the 49 damaged signs, 19 presented torsional rotations to the precast concrete cylindrical base (20% of the inspected, and 39% of the damaged), and 2 combined the torsional rotation with overturning rotation, and damages to the RC pedestal.

Table 9-1: Summary of Damages Found on Cantilever Traffic Signs Due to Hurricane Maria.

Description Organized by Level of Damage	Number of Observed Situations	Accumulated by Level of Damage	Percentage by Level of Damage
Total collapse due to structural failures in the pedestal	15	19	20%
Partial collapse due to structural failures in the pedestal	4		
Damages to the pedestal (Fractures due to anchor bolts lateral displacement)	8	8	8%
Total collapse due to foundation failure (Rotation + overturning)	2	21	22%
Partial collapse due to foundation rotation	13		
Partial collapse due to foundation rotation (And the pedestal also presented fractures)	6		
Without evident damages	44	44	46%
Total Inspected	95	95	100%

9.1 Conclusions and Recommendations for the Structural Damages

The structural damages to the reinforced concrete pedestal, being the dominant (present in 67% of the damaged cantilever signs), require special attention to improve the resilience of this type of traffic signs. The experimental results presented in Chapter 8 for the strength of the pedestal concrete, the pedestal reinforcing steel, and the steel anchor bolts demonstrate that the resistance of the material was adequate and in accordance with the requirements from the PRHTA standards. Although the sample size was small, these results strongly suggest that the causes of damage were related to design or construction processes that need improvement.

The findings presented in Sections 6.1.2, related to anchor bolts located outside the confinement given by stirrups, and 6.1.4, related to lack of length (depth) of longitudinal and transverse steel reinforcement on the shaft foundation emphasizes the importance of having a strict

and detailed inspection process and quality control during construction and installation of these signs, and also in the process of reviewing final design drawings.

The situation addressed in Section 6.1.3, where anchors bolts appeared to be pulled out of the foundation, indicates that it is required a revision of the common practice use as the installation process of anchor bolts, to assure the anchorage has proper embedment length and adherence to concrete to avoid this failure.

The principal structural damage found was produced by the large lateral displacement of anchor bolt due to lack of lateral support at the top, and lack of concrete confinement at the top of the pedestal. Anchor bolts experienced a double bending plastic deformation, with the development of plastic hinges at the location of the base plate and the last stirrup of the concrete base, as presented in Section 6.1.1. These damages and failures indicate that the confinement of the anchor bolts and concrete confinement are essential to avoid damages. Thus, the specifications for stirrups spacings, separation between the last stirrup and the base plate, and details of the top of the pedestal to avoid these lateral movement is of extremely importance. This is an area recommended for further study, to develop best practices for steel design. Puerto Rico may evaluate if the studies by Cook at al. (2007; 2012) are applicable, and the proposed solutions address this situation.

Additionally, in several of the cases the observed distance between the top stirrup and the base plate did not comply with PRHTA specifications; this situation reinforces the fact that a strict inspection and quality control during sign installation is imperative, together with a detailed review of final design drawings.

This further study recommended to analyze pedestal design details should consider, among others: (a) the appropriate distance from the last stirrup to the post bases plate to assure shear

failure of the anchor bolt develops prior to the large lateral deflections; (b) stirrups spacings and cross ties distributions to assure proper concrete confinement; (c) anchor bolt embedment length and installation process to prevent pull out; and (d) the pedestal size to assure that over stress situations are not generated on the anchor bolts, the concrete, and the concrete base to soil interface.

9.2 Conclusions and Recommendations for Soil-Foundation Damages

All the cantilever traffic signs inspected that underwent torsional rotations (rotations about a vertical axis) had a cylindrical precast pedestal, as presented in Section 6.2.1. This situation demonstrates that rectangular and cast-in-place foundation increases the resistance of the base to these torsional rotations, since they trigger a soil-to-soil shear resistance (instead of a soil-to-concrete resistance). The findings also suggest that the usage of precast cylindrical pedestals require further study to improve the design, avoiding these rotations, and enhance the resilience of the signs. Measures to be evaluated may include, among others, consider either increasing the embedment length and the diameter of the shaft, changing the soil compaction requirements and the soil type required as filling material, modifying the texture of the finished concrete, or changing the precast concrete base cross sectional shape from circular to square in order to trigger soil to soil shear resistance instead of soil to concrete shear resistance.

Posts that are grounded on steep slopes must consider the required embedment depth based on the particular characteristics of the slope. Soil confinement and passive action on the shaft foundation depend on the soil continuity and semi-infinite extension, and the slope discontinues the soil on one side of the shaft. The present investigation did not find any special recommendation or requirement for cantilever traffic signs installed in this type of locations within the PRHTA

specifications and drawings. It is recommended to develop clear guidelines and requirements for this type of situations, being this another area of recommended further study.

9.3 Additional Recommendations and Further Study

The obtained PRHTA specifications and drawings for cantilever traffic signs indicate an unfactored design wind speed of 125 mph, which correspond to a factored wind speed of 158 mph (considering a load factor of 1.6). It is recommended to update PRHTA specifications and drawings to the PR 2018 Building code specified wind speeds (see Appendix C for examples of wind speeds in inspected sign's locations using ATC Tool that includes micro zoning due to topography). It would be also advisable to evaluate if, considering the necessity of system resilience and recovery, an increase in risk category is appropriate for this type of signs. This situation is reinforced since studies of damages of traffic signs due to hurricane Maria have addressed that the wind speeds of Maria may have reached around 200 mph at some case study locations (Pacheco-Crosetti & Cruzado, 2020), or had been well in excess to 155 mph (Morales, Sánchez, De Jesús, & Caraballo, 2021).

Polytechnic University of Puerto Rico team will continue with further study of this cantilever traffic signs, with focus on determining the wind speed required to produce specific pedestal damages, and in analyzing the implications of the different procedures of AASHTO vs ASCE wind force computation on this type of signs.

References

- AASHTO. (2013). *Standard Specifications for Structural Supports for Highway Signs, Luminaires, and Traffic Signals*. Washington, DC: American Association of State Highway and Transportation Officials.
- Akçay, B. (2004). Variation of In-Place Concrete Core Strength in Structures from Istanbul Area: Statistical Analysis of Concrete Core Data. *Journal of Materials in Civil Engineering*, 16(5).
- Arioz, O., Tuncan, M., Ramyar, K., & Tuncan, A. (2006). A comparative study on the interpretation of concrete core strength results. *Magazine of Concrete Research*, 117-122.
- ASTM. (2018). *Standard Test Method for Obtaining and Testing Drilled Cores and Sawed Beams of Concrete*. ASTM.
- Campbell, R. H., & Tobin, R. E. (1967). Core and Cylinder Strengths of Natural and Lightweight Concrete. *Journal Proceedings*, 64(4), 190-195.
- Cangialosi, J. P., Latta, A. S., & Berg, R. (2021). *National Hurricane Center Tropical Cyclone Report: Hurricane Irma (AL 112017) 30 August - 12 September 2017*. Washington, DC: National Oceanic and Atmospheric Administration (NOAA). Retrieved from https://www.nhc.noaa.gov/data/tcr/AL112017_Irma.pdf
- Cook, R. A., & Halcover, K. M. (2007). *Anchor Embedment Requirements for Signal / Sign Structures*. University of Florida, Department of Civil Engineering, Gainesville. Retrieved from <https://fdotwww.blob.core.windows.net/sitefinity/docs/default-source/research/reports/fdot-bd545-54-rpt.pdf>
- Cook, R. A., Prevatt, D. O., & Dalton, S. A. (2012). *Base Connections for Signal/Sign Structures*. University of Florida, Department of Civil and Coastal Engineering, Gainesville. Retrieved from https://fdotwww.blob.core.windows.net/sitefinity/docs/default-source/content/structures/structuresresearchcenter/final-reports/bdk75_977-32.pdf?sfvrsn=6a59e9a0_0
- FEMA. (2018). *Hurricanes Irma and Maria in Puerto Rico: Building Performance Observations, Recommendations, and Technical Guidance*. Washington, DC: FEMA. Retrieved October 15, 2020, from https://www.fema.gov/sites/default/files/2020-07/mat-report_hurricane-irma-maria-puerto-rico_2.pdf
- Lima, L. (2017, September 21). "Creí que era un sismo": por qué muchos en Puerto Rico sintieron que la tierra se "movía" durante el paso del huracán María. *BBC Mundo*. Retrieved from <https://www.bbc.com/mundo/noticias-america-latina-41351169>
- Malhotra, V. M. (1977). Contact strength requirements — Cores versus in situ evaluation. *Journal Proceedings*, 74(4), 163-172.
- Morales, J. C., Sánchez, J. N., De Jesús, S. N., & Caraballo, J. A. (2021). Morales, J., Sánchez, J., Classical Stress Analysis of a Fuse Plate that Failed During Hurricane María in Puerto Rico, RIDNAIC (2021). Vol. 19-20,. *International Journal on Natural Disasters, Accidents and Civil Infrastructure (RIDNAIC)*, 19-20`12), 188-199.
- Neville, A. (2001). Core tests: Easy to perform, not easy to interpret. *Concrete International*, 23(11), 59-68.
- Pacheco-Crosetti, G., & Cruzado, H. J. (2020). The analysis of structural failures in transportation infrastructure used to estimate wind speeds of Hurricane Maria in Puerto Rico. *International Journal on Natural Disasters, Accidents and Civil Infrastructure (RIDNAIC)*, 19-20(1), 129-144.
- Petersons, N. (1968). Should standard cube test specimens be replaced by test specimens taken from structures? *Materials & Structures*, 1(5), 435-438.
- PRHTA. (2010). *Planos Modelos*. Puerto Rico Highway and Transportation Authority. Retrieved from <https://act.dtop.pr.gov/planos-modelo/>

- PRHTA. (2015). *Guías para la selección e instalación de rótulos de orientación (suplemento al MUTCD 2009)*. Puerto Rico Highway and Transportation Authority, Área de Ingeniería de Tránsito y Operaciones. Retrieved from <https://act.dtop.pr.gov/fotos/transito/mutcd2009.pdf>
- Rodríguez-Caraballo, H. (2018, November 19). 881 postes afectados por María, asegura ACT. *Metro*. Retrieved from <https://www.metro.pr/pr/noticias/2018/11/19/881-postes-afectados-por-maria-asegura-act.html>
- Silva-Tulla, F., & Pando, M. A. (2020). Geotechnical Extreme Event Site Reconnaissance in Puerto Rico. *International Journal of Geoengineering Case Histories*, 5(4), 1-25.
- Turkel, A., & Ozkul, M. H. (2010). Size and wall effects on compressive strength of concretes. *ACI Materials Journal*, 107(4), 372-379.
- USGS. (n.d.). *Puerto Rico Hurricanes Map*. Retrieved 2018, from USGS: <https://www.usgs.gov/media/images/puerto-rico-hurricanes-map>

Appendix A Inspections Forms

A.1 Blank Form

Inspection sheet for cantilever sign support post



University	Polytechnic University of Puerto Rico
University Program	Civil Engineering
Proposal Center	Transportation Infrastructure Research Center
Title and Subtitle	Analysis of wind loads in cantilevered overhead sign support-truss with post
Name:	Geoffrey Vega Rosado
Inspection Date	
Town:	
Coordinates	
X=	
Y=	
Cantilever type ID number	
Geometry of the pole section	
Number of signs	
Long or short overhang	
Number of nuts in the base	
Amount of Gusset plate (rigidizador)	
Total of photos	
numeric range of photos	

Observations:

A.2 Examples of On-Site Filled Forms

Inspection sheet for cantilever sign support post

University	Polytechnic University of Puerto Rico
University Program	Civil Engineering
Proposal Center	Transportation Infrastructure Research Center
Title and Subtitle	Analysis of wind loads in cantilevered overhead sign support-truss with post
Name:	Geoffrey Vega Rosado
Inspection Date	25 Julio '19
Town:	Aguadilla PR-2
Coordinates	
X=	-67.0940
Y=	18.4522
Cantilever type ID number	#2 → #76
Geometry of the pole section	Circular
Number of signs	1 completo, pequeño
Long or short overhang	Long
Number of nuts in the base	10
Amount of Gusset plate (rigidizador)	10
Total of photos	23 + 1
numeric range of photos	70-81

Observations:

Number of signs

El suelo refleja problemas de sustentación. Base inclinada. $\frac{3}{4}$ "

Poste inclinado 1"

Inclinación

Rotación

Inspection sheet for cantilever sign support post

University	Polytechnic University of Puerto Rico
University Program	Civil Engineering
Proposal Center	Transportation Infrastructure Research Center
Title and Subtitle	Analysis of wind loads in cantilevered overhead sign support-truss with post
Name:	Geoffrey Vega Rosado
Inspection Date	25 Julio '19
Town:	Aguadilla PR-2
Coordinates	
X=	-67.1457255
Y=	18.4447512
Cantilever type ID number	#1 → #75
Geometry of the pole section	Circular
Number of signs	#
Long or short overhang	Long
Number of nuts in the base	10
Amount of Gusset plate (rigidizador)	10
Total of photos	6
numeric range of photos	16-1 @ 16-6

Observations:

No presenta fractura.

La base esta completamente enterrada solo se tiene acceso al plato.

Inspection sheet for cantilever sign support post

University	Polytechnic University of Puerto Rico
University Program	Civil Engineering
Proposal Center	Transportation Infrastructure Research Center
Title and Subtitle	Analysis of wind loads in cantilevered overhead sign support-truss with post
Name:	Geoffrey Vega Rosado
Inspection Date	25 Julio '19
Town:	Quebradilla PR-2
Coordinates	
X=	-66.7606
Y=	18.4825
Cantilever type ID number	#8 → #3
Geometry of the pole section	Circular
Number of signs	1 pequeño
Long or short overhang	Long
Number of nuts in the base	12 (bubles)
Amount of Gusset plate (rigidizador)	12
Total of photos	15
numeric range of photos	68 + 15 = 83

Observations:

Base $\frac{1}{4}$ "

No presenta daños estructurales.

Inspection sheet for cantilever sign support post

University	Polytechnic University of Puerto Rico
University Program	Civil Engineering
Proposal Center	Transportation Infrastructure Research Center
Title and Subtitle	Analysis of wind loads in cantilevered overhead sign support-truss with post
Name:	Geoffrey Vega Rosado
Inspection Date	25 Julio '19
Town:	Quebradilla PR-2
Coordinates	
X=	-66.9564
Y=	18.4841
Cantilever type ID number	#7 → #82
Geometry of the pole section	Circular
Number of signs	1 pequeño
Long or short overhang	Short
Number of nuts in the base	8
Amount of Gusset plate (rigidizador)	8
Total of photos	7
numeric range of photos	60 + 7 = 67

Observations:


Base $\frac{5}{8}$ "

Configuración de la base diferente a las especificaciones de AISC.

No presenta daños estructurales.


Inspection sheet for cantilever sign support post



University	Polytechnic University of Puerto Rico
University Program	Civil Engineering
Proposal Center	Transportation Infrastructure Research Center
Title and Subtitle	Analysis of wind loads in cantilevered overhead sign support-truss with post
Name:	Geoffrey Vega Rosado
Inspection Date	25 Julio '19
Town:	Quebradilla PR-2
Coordinates	
X=	-66.9543
Y=	18.4868
Cantilever type ID number	#6 \Rightarrow B1
Geometry of the pole section	Circular
Number of signs	1 Pequeño
Long or short overhang	Long
Number of nuts in the base	10 (Dobles)
Amount of Gusset plate (rigidizador)	10
Total of photos	5
numeric range of photos	54+5 = 59
Observations:	<p>• Base  5'.</p> <p>• Parece una inclinación por fatiga en el delante brazo.</p>


Inspection sheet for cantilever sign support post



University	Polytechnic University of Puerto Rico
University Program	Civil Engineering
Proposal Center	Transportation Infrastructure Research Center
Title and Subtitle	Analysis of wind loads in cantilevered overhead sign support-truss with post
Name:	Geoffrey Vega Rosado
Inspection Date	25 Julio '19
Town:	Quebradilla PR-2
Coordinates	
X=	-66.9660
Y=	18.4804
Cantilever type ID number	#5 \Rightarrow B0
Geometry of the pole section	Circular
Number of signs	1 Pequeño
Long or short overhang	Short
Number of nuts in the base	10 (Dobles)
Amount of Gusset plate (rigidizador)	10
Total of photos	4
numeric range of photos	49+4 = 53
Observations:	<p>• Base  5'.</p> <p>• Parece que es de construcción reciente (cotéjase en programa su ubicación para años anteriores)</p>


Inspection sheet for cantilever sign support post



University	Polytechnic University of Puerto Rico
University Program	Civil Engineering
Proposal Center	Transportation Infrastructure Research Center
Title and Subtitle	Analysis of wind loads in cantilevered overhead sign support-truss with post
Name:	Geoffrey Vega Rosado
Inspection Date	25 Julio '19
Town:	Entre isabela y Quebradilla PR-2
Coordinates	
X=	-66.9740 -66.98019.58" W
Y=	18.4822 18.4822 19.58" N
Cantilever type ID number	#3 \Rightarrow 78
Geometry of the pole section	Circular
Number of signs	1 completo
Long or short overhang	Long
Number of nuts in the base	10 (Dobles)
Amount of Gusset plate (rigidizador)	10
Total of photos	7
numeric range of photos	32+7 = 39
Observations:	<p>• Base cuadrada</p> <p>• Parece que es de construcción reciente (cotéjase en programa su ubicación para años anteriores)</p> <p>Base  5'.</p>

Inspection sheet for cantilever sign support post



University	Polytechnic University of Puerto Rico
University Program	Civil Engineering
Proposal Center	Transportation Infrastructure Research Center
Title and Subtitle	Analysis of wind loads in cantilevered overhead sign support-truss with post
Name:	Geoffrey Vega Rosado
Inspection Date	25 Julio '19
Town:	Quebradilla PR-2
Coordinates	
X=	-66.9723
Y=	18.4793
Cantilever type ID number	#4 \Rightarrow 79
Geometry of the pole section	Circular
Number of signs	1 Pequeño
Long or short overhang	Long
Number of nuts in the base	10 (Dobles)
Amount of Gusset plate (rigidizador)	10
Total of photos	8
numeric range of photos	40+8 = 48
Observations:	<p>• Base cuadrada  4'.</p> <p>• Parece que es de construcción reciente (cotéjase en programa su ubicación para años anteriores)</p>

Inspection sheet for cantilever sign support post



University	Polytechnic University of Puerto Rico
University Program	Civil Engineering
Proposal Center	Transportation Infrastructure Research Center
Title and Subtitle	Analysis of wind loads in cantilevered overhead sign support-truss with post
Name:	Geoffrey Vega Rosado
Inspection Date	23 de agosto de 2019
Town:	San Juan PR-18 km 1.4 to N
Coordinates	X= -66°4'15.00"W Y= 18°25'19.01"N
Cantilever type ID number	P-44
Geometry of the pole section	circular
Number of signs	1
Long or short overhang	long
Number of nuts in the base	8
Amount of Gusset plate (rigidizador)	8
Total of photos	4
numeric range of photos	F 19-22

Observations:

La base de concreto ~~de~~ no roto, sin embargo se observaron otros daños; presenta grietas verticales a lo largo del perno. Todas las grietas que se observaron coinciden con el desarrollo del anclaje dentro de la base de concreto.

Inspection sheet for cantilever sign support post



University	Polytechnic University of Puerto Rico
University Program	Civil Engineering
Proposal Center	Transportation Infrastructure Research Center
Title and Subtitle	Analysis of wind loads in cantilevered overhead sign support-truss with post
Name:	Geoffrey Vega Rosado
Inspection Date	23 de agosto de 2019
Town:	San Juan PR-18 km 1.6 to N
Coordinates	X= -66°4'15.67"W Y= 18°25'10.70"N
Cantilever type ID number	P-43
Geometry of the pole section	circular
Number of signs	1
Long or short overhang	long
Number of nuts in the base	8
Amount of Gusset plate (rigidizador)	8
Total of photos	2
numeric range of photos	F 17-18

Observations:

El letrero ~~roto~~ ~~aproximadamente~~ 30° se observaron daños a nivel de la base de hormigón y corrosión en los pernos expuestos.

Inspection sheet for cantilever sign support post



University	Polytechnic University of Puerto Rico
University Program	Civil Engineering
Proposal Center	Transportation Infrastructure Research Center
Title and Subtitle	Analysis of wind loads in cantilevered overhead sign support-truss with post
Name:	Geoffrey Vega Rosado
Inspection Date	23 de agosto de 2019
Town:	San Juan PR-18 to S km 1.9
Coordinates	X= -66°4'13.07"W Y= 18°24'47.01"N
Cantilever type ID number	P-41
Geometry of the pole section	circular
Number of signs	1
Long or short overhang	long
Number of nuts in the base	8
Amount of Gusset plate (rigidizador)	8
Total of photos	2
numeric range of photos	F 7-8

Observations:

El letrero voladizo ~~rotó~~ ~~aproximadamente~~ 70° y la base de hormigón sufrió daños de pérdida de cubierta y agrietamiento exponiendo los pernos de anclaje.

Inspection sheet for cantilever sign support post



University	Polytechnic University of Puerto Rico
University Program	Civil Engineering
Proposal Center	Transportation Infrastructure Research Center
Title and Subtitle	Analysis of wind loads in cantilevered overhead sign support-truss with post
Name:	Geoffrey Vega Rosado
Inspection Date	23 de agosto de 2019
Town:	San Juan PR-18 to N km 1.9
Coordinates	X= -66°4'11.53"W Y= 18°24'47.25"N
Cantilever type ID number	P-40
Geometry of the pole section	circular
Number of signs	1
Long or short overhang	long
Number of nuts in the base	8
Amount of Gusset plate (rigidizador)	8
Total of photos	
numeric range of photos	

Observations:

El letrero voladizo ~~rotó~~ ~~aproximadamente~~ 15° y la base de hormigón sufrió daños de pérdida de cubierta y agrietamiento.

Inspection sheet for cantilever sign support post



University	Polytechnic University of Puerto Rico
University Program	Civil Engineering
Proposal Center	Transportation Infrastructure Research Center
Title and Subtitle	Analysis of wind loads in cantilevered overhead sign support-truss with post
Name:	Geoffrey Vega Rosado
Inspection Date	23 de agosto de 2019
Town:	San Juan PR-18 km 2.2 to N
Coordinates	X= -66°4'11.42"W Y= 18°24'43.80"N
Cantilever type ID number	P-39
Geometry of the pole section	circular
Number of signs	1
Long or short overhang	short
Number of nuts in the base	5
Amount of Gusset plate (rigidizador)	5
Total of photos	2
numeric range of photos	F (15-16)
Observations:	El letrero rotó entre 20° y 30°, se encuentra inclinado hacia los carriles de la autopista. la base está parcialmente enterrada y los tornillos están expuestos a humedad continua.

Inspection sheet for cantilever sign support post



University	Polytechnic University of Puerto Rico
University Program	Civil Engineering
Proposal Center	Transportation Infrastructure Research Center
Title and Subtitle	Analysis of wind loads in cantilevered overhead sign support-truss with post
Name:	Geoffrey Vega Rosado
Inspection Date	23 de agosto de 2019
Town:	San Juan PR-18 km 2.1
Coordinates	X= -66°4'16.57"W Y= 18°24'5.88"N
Cantilever type ID number	P-38
Geometry of the pole section	circular
Number of signs	1
Long or short overhang	long
Number of nuts in the base	8
Amount of Gusset plate (rigidizador)	8
Total of photos	2
numeric range of photos	8 9-10
Observations:	Letrero voladizo roto aproximadamente 180° y la base de hormigón se rompió a nivel de los rieles. Algunos de los rieles no sufren exposición pero logran agrietar la base lo suficiente por hacerla susceptible a la entrada de agua y corrosión de los pernos.

Inspection sheet for cantilever sign support post



University	Polytechnic University of Puerto Rico
University Program	Civil Engineering
Proposal Center	Transportation Infrastructure Research Center
Title and Subtitle	Analysis of wind loads in cantilevered overhead sign support-truss with post
Name:	Geoffrey Vega Rosado
Inspection Date	23 de agosto de 2019
Town:	San Juan PR-18 km 2.8 to N
Coordinates	X= -66°4'13.91"W Y= 18°24'22.79"N
Cantilever type ID number	P-35
Geometry of the pole section	circular
Number of signs	1
Long or short overhang	long
Number of nuts in the base	8
Amount of Gusset plate (rigidizador)	8
Total of photos	2
numeric range of photos	F 13-14
Observations:	Letrero voladizo roto 30°. No se tuvo acceso a la base debido a que está cubierta de tierra, al igual que la mayoría de los pernos de acero.

Inspection sheet for cantilever sign support post



University	Polytechnic University of Puerto Rico
University Program	Civil Engineering
Proposal Center	Transportation Infrastructure Research Center
Title and Subtitle	Analysis of wind loads in cantilevered overhead sign support-truss with post
Name:	Geoffrey Vega Rosado
Inspection Date	23 de agosto de 2019
Town:	San Juan PR-18 km 3 to S
Coordinates	X= -66°4'13.86"W Y= 18°23'42.25"N
Cantilever type ID number	P-33
Geometry of the pole section	circular
Number of signs	1
Long or short overhang	long
Number of nuts in the base	8
Amount of Gusset plate (rigidizador)	8
Total of photos	2
numeric range of photos	8 11-12
Observations:	Letrero voladizo roto 180°. El suelo alrededor refleja fallo que permitieron la rotación. Se observó una separación de 2" entre suelo y base.

Inspection sheet for cantilever sign support post



University	Polytechnic University of Puerto Rico
University Program	Civil Engineering
Proposal Center	Transportation Infrastructure Research Center
Title and Subtitle	Analysis of wind loads in cantilevered overhead sign support-truss with post.
Name:	Geoffrey Vega Rosado
Inspection Date	
Town:	San Juan (Ave. Pinar)
Coordinates	
X _c	-66°4'29.5"W
Y _c	18°24'27.20"N
Cantilever type ID number	P-99
Geometry of the pole section	circular
Number of signs	1
Long or short overhang	long
Number of nuts in the base	10
Amount of Gusset plate (rigidizador)	10
Total of photos	3
numeric range of photos	
Observations:	El poste apunta estar colapsado, posible torsión de los elementos de anclaje. Se encontró el caso por la investigación literaria. Presenta colapso según la investigación literaria.

Inspection sheet for cantilever sign support post



University	Polytechnic University of Puerto Rico
University Program	Civil Engineering
Proposal Center	Transportation Infrastructure Research Center
Title and Subtitle	Analysis of wind loads in cantilevered overhead sign support-truss with post.
Name:	Geoffrey Vega Rosado
Inspection Date	23 de agosto de 2019
Town:	San Juan PR-16 to S Km.0.7
Coordinates	
X _c	-66°4'20.75"W
Y _c	18°25'25.61"N
Cantilever type ID number	P-95
Geometry of the pole section	circular
Number of signs	1
Long or short overhang	long
Number of nuts in the base	8
Amount of Gusset plate (rigidizador)	8
Total of photos	2
numeric range of photos	1-2
Observations:	Base deformó pre-fabricado rotó 180° y perdió contacto entre tierra y base en toda la circunferencia superior

Inspection sheet for cantilever sign support post



University	Polytechnic University of Puerto Rico
University Program	Civil Engineering
Proposal Center	Transportation Infrastructure Research Center
Title and Subtitle	Analysis of wind loads in cantilevered overhead sign support-truss with post
Name:	Geoffrey Vega Rosado
Inspection Date	8 abril 2019
Town:	Salinas PR 52
Coordinates	
X _c	-66°14'35.61"W
Y _c	18°1'11.92"N
Cantilever type ID number	P-15
Geometry of the pole section	circular
Number of signs	1
Long or short overhang	long
Number of nuts in the base	10
Amount of Gusset plate (rigidizador)	10
Total of photos	2
numeric range of photos	47-48
Observations:	El poste fallo y fue removido del lugar por dtop. Pudo ser inspeccionado en las oficinas de Mantenimiento Sur de la dtop donde se encontraba almacenado.

Inspection sheet for cantilever sign support post



University	Polytechnic University of Puerto Rico
University Program	Civil Engineering
Proposal Center	Transportation Infrastructure Research Center
Title and Subtitle	Analysis of wind loads in cantilevered overhead sign support-truss with post
Name:	Geoffrey Vega Rosado
Inspection Date	8 abril 2019
Town:	Salinas PR 53
Coordinates	
X _c	-66°18'33.66"W
Y _c	17°59'12.72"N
Cantilever type ID number	P-12
Geometry of the pole section	circular
Number of signs	1
Long or short overhang	long
Number of nuts in the base	10
Amount of Gusset plate (rigidizador)	10
Total of photos	2
numeric range of photos	58-59
Observations:	Poste inspeccionado, se encontró que el mismo sufrió una falla por torsión. Se extrajo material de muestra para realizar pruebas mecánicas en el laboratorio.

Inspection sheet for cantilever sign support post



University	Polytechnic University of Puerto Rico
University Program	Civil Engineering
Proposal Center	Transportation Infrastructure Research Center
Title and Subtitle	Analysis of wind loads in cantilevered overhead sign support-truss with post
Name:	Geoffrey Vega Rosado
Inspection Date	8 abril 2019
Town:	Salinas PR 53
Coordinates	X ⁿ -66°14'17.05" W Y ⁿ 18°0'1.29" N
Cantilever type ID number	P-11
Geometry of the pole section	circular
Number of signs	1
Long or short overhang	Long
Number of nuts in the base	10
Amount of Gusset plate (rigidizador)	10
Total of photos	4
numeric range of photos	71-74

Observations:

El poste falló. Fue removido del lugar por la cantidad de corrosión

Inspection sheet for cantilever sign support post



University	Polytechnic University of Puerto Rico
University Program	Civil Engineering
Proposal Center	Transportation Infrastructure Research Center
Title and Subtitle	Analysis of wind loads in cantilevered overhead sign support-truss with post
Name:	Geoffrey Vega Rosado
Inspection Date	8/abril/2019
Town:	Ponce, PR 2
Coordinates	X ⁿ -66°38'33.55" W Y ⁿ 17°59'16.19" N
Cantilever type ID number	P-98
Geometry of the pole section	circular
Number of signs	1
Long or short overhang	Long
Number of nuts in the base	8
Amount of Gusset plate (rigidizador)	8
Total of photos	2
numeric range of photos	5239-40

Observations:

Letrero voladizo roto aprox 20° y el suelo alrededor de la base falló permitiendo que este rotara. Geometría de la base 1



Inspection sheet for cantilever sign support post



University	Polytechnic University of Puerto Rico
University Program	Civil Engineering
Proposal Center	Transportation Infrastructure Research Center
Title and Subtitle	Analysis of wind loads in cantilevered overhead sign support-truss with post
Name:	Geoffrey Vega Rosado
Inspection Date	14 de febrero de 2019
Town:	Ponce PR-52
Coordinates	X ⁿ -66°37'11.092" W Y ⁿ 17°59'20.22" N
Cantilever type ID number	P-3
Geometry of the pole section	circular
Number of signs	1
Long or short overhang	Long
Number of nuts in the base	10
Amount of Gusset plate (rigidizador)	10
Total of photos	7
numeric range of photos	8890-5+1

Observations:

La base muestra una grieta vertical a lo largo del perno coinciden con el desarrollo del anclaje dentro de la base de concreto. Desprendimiento de recubrimiento en parte de sus pernos

Inspection sheet for cantilever sign support post



University	Polytechnic University of Puerto Rico
University Program	Civil Engineering
Proposal Center	Transportation Infrastructure Research Center
Title and Subtitle	Analysis of wind loads in cantilevered overhead sign support-truss with post
Name:	Geoffrey Vega Rosado
Inspection Date	1 febrero 2019
Town:	Ponce PR-52
Coordinates	X ⁿ -66°37'31.02" W Y ⁿ 17°59'27.918" N
Cantilever type ID number	P-1
Geometry of the pole section	Circular
Number of signs	1
Long or short overhang	Long
Number of nuts in the base	10
Amount of Gusset plate (rigidizador)	10
Total of photos	5
numeric range of photos	8886-9

Observations:

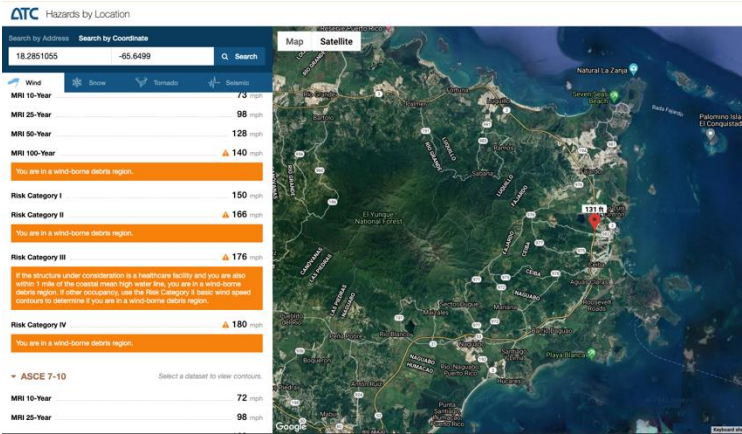
El poste fue

La base muestra una grieta vertical a lo largo del perno coincide con el desarrollo del anclaje dentro de la base de concreto. Desprendimiento de recubrimiento en parte de sus pernos.

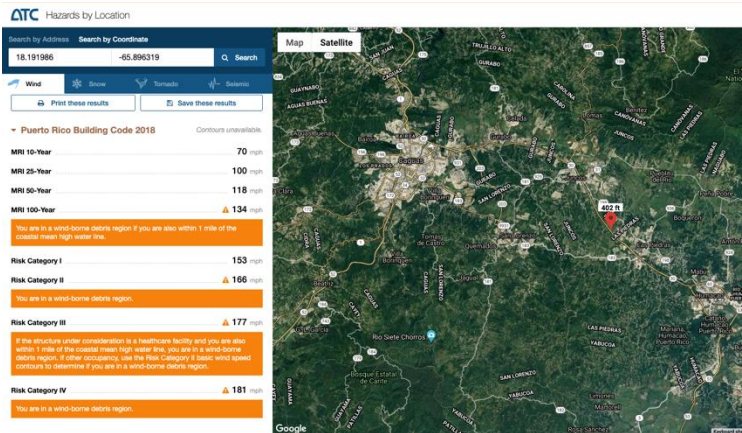
Appendix B Current Wind Design Speed (mph) According to Sign Coordinates

Applied Technology Council ATC Hazard by Location web Tool (<https://hazards.atcouncil.org/>)

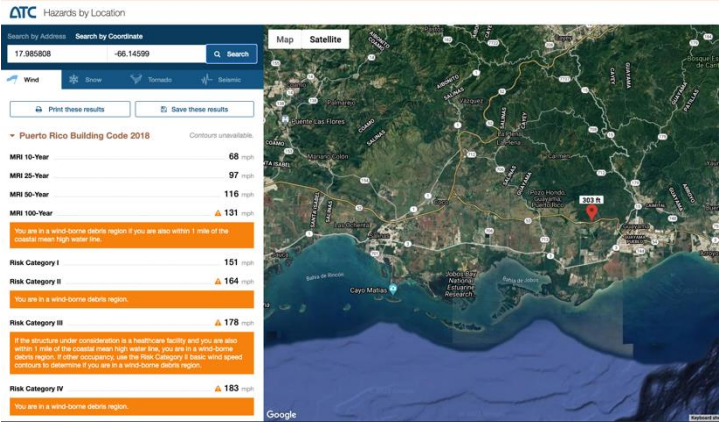
P- 66 Fajardo 18.2851055; - 65.6499



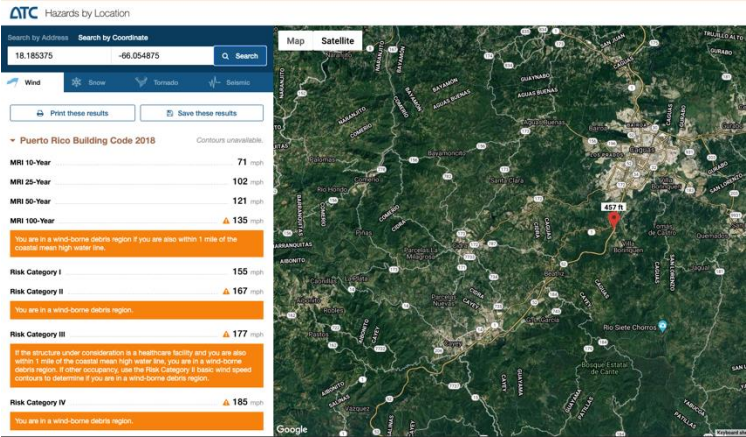
P-53 Las Piedras 18.191986; -65.896319



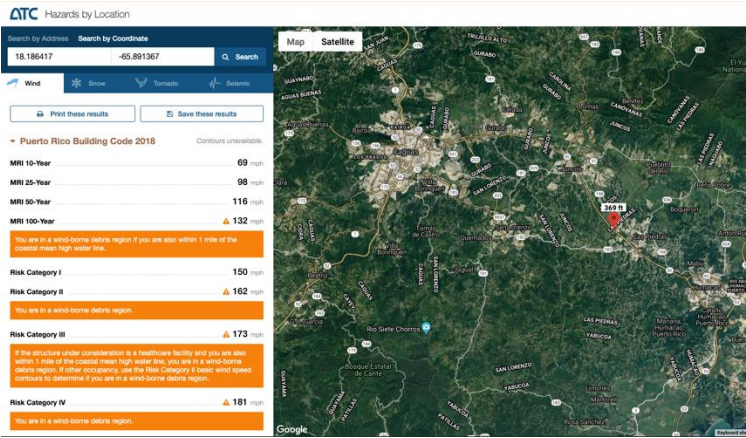
P-46 Guayama 17.985808; -66.14599



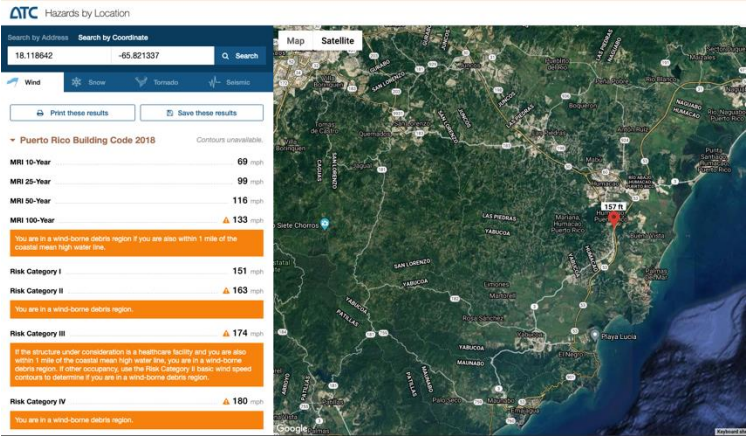
P-45 Caguas 18.185375; -66.054875



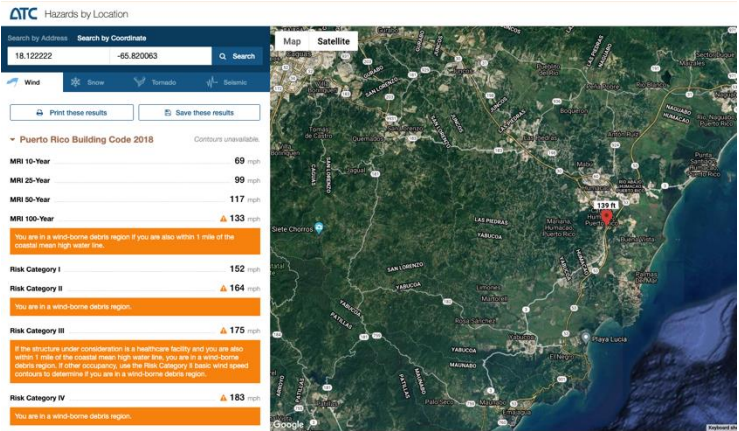
P- 52 Las Piedras 18.186417; -65.891367



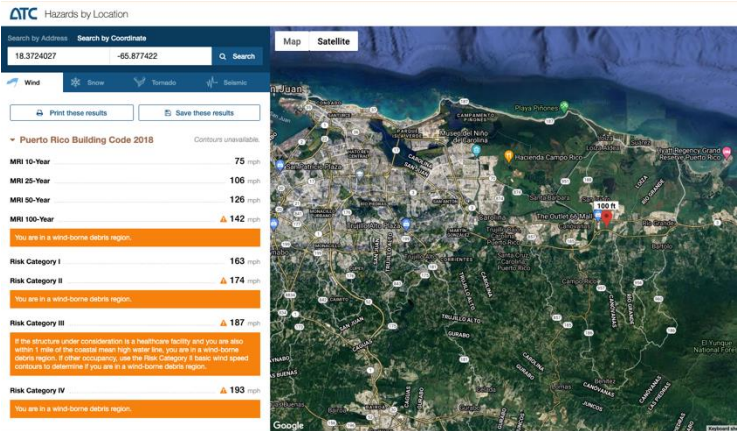
P- 100 Humacao 18.118642; - 65.821337



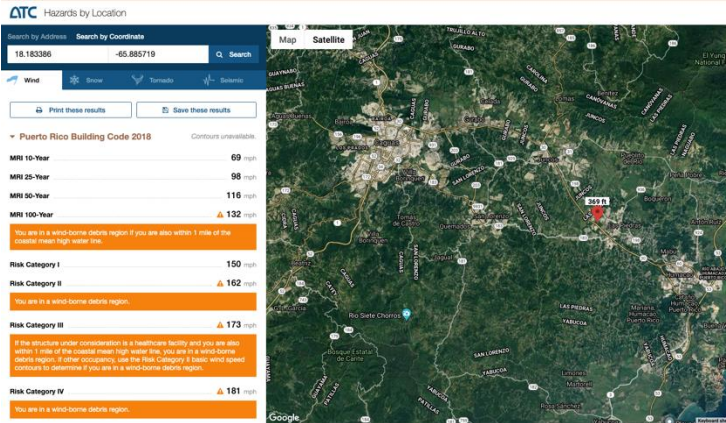
P- 105 Humacao 18.122222; - 65.820063



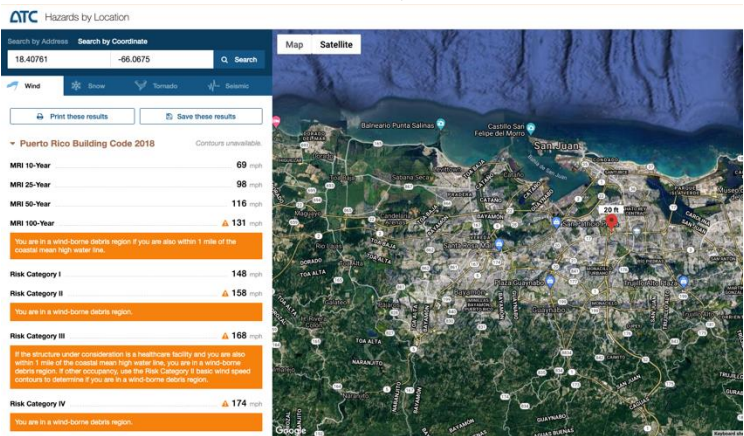
P- 106 Canóvanas 18.3724027; - 65. 877422



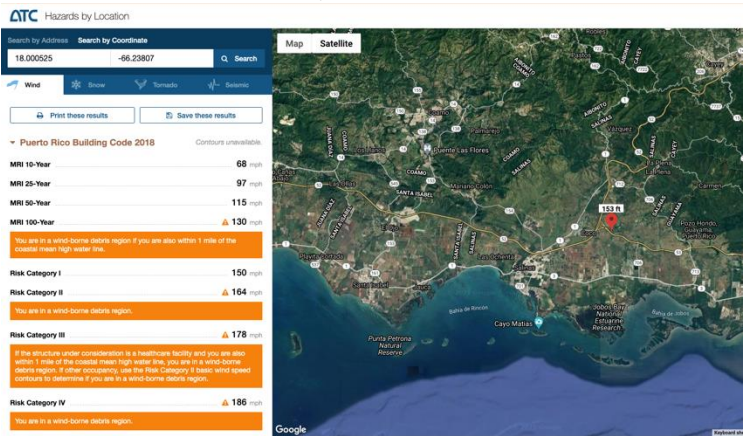
P- 99 Las Piedras 18.183386; - 65.885719



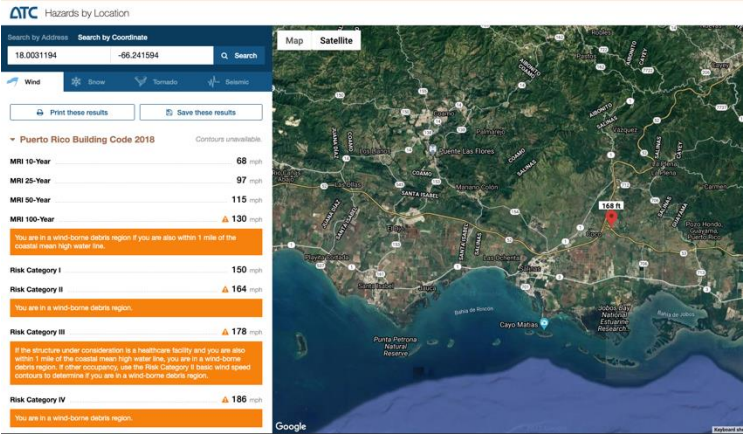
P- 98 San Juan 18.40761; - 66.0675



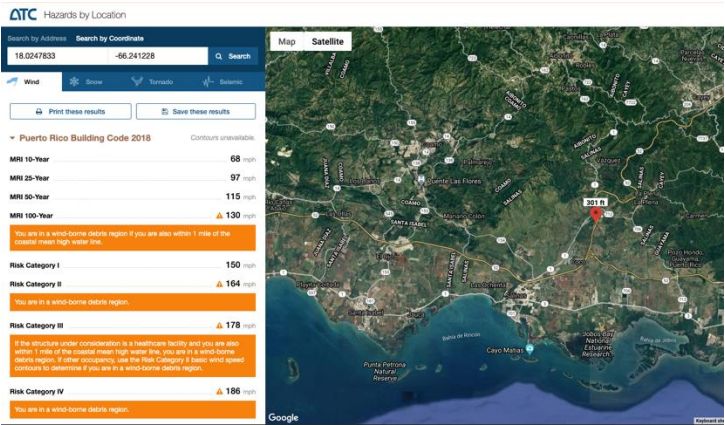
P- 11 Salinas 18.000525; -66.23807



P- 12 Salinas 18.0031194; -66.241594

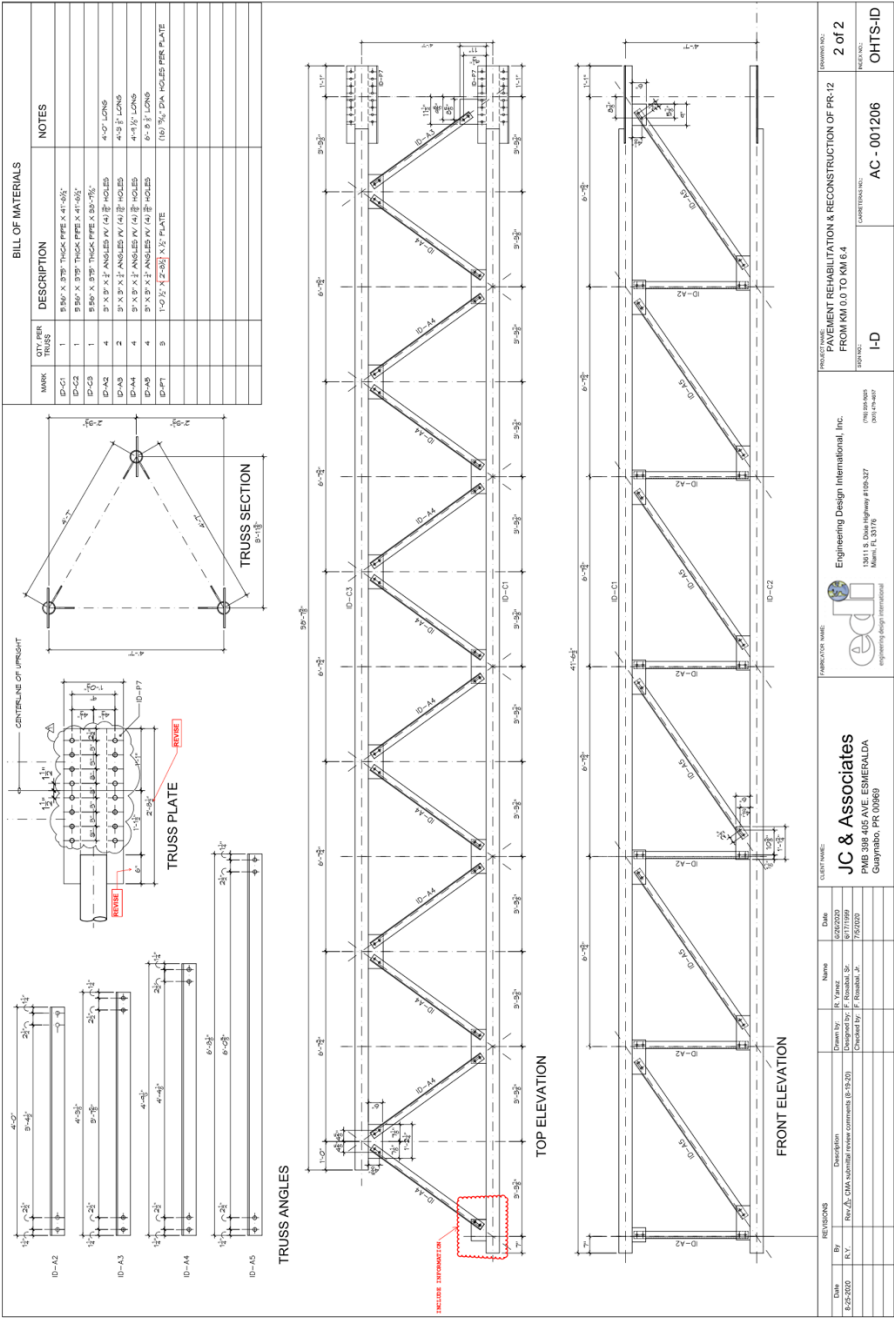


P-15 Salinas 18.0247833; -66.241228



Appendix C Details of Cantilever Traffic Signs According to PRHTA Specifications

C.1 Overhead Signs Support Shop Drawings (CMA September 4, 2020)



[illegible]

C.2 Overhead Signs Foundation for Cantilever Type (PRHTA)

SPECIFICATIONS AND NOTES APPLICABLE TO ALL OVERHEAD SIGN DRAWINGS:

FROM JUNE 30, 1999, ONLY OVERHEAD SIGN STRUCTURES INCLUDED IN THE AUTHORITY'S APPROVED LIST WILL BE ACCEPTED. AFTER THIS DATE, IF AN OVERHEAD SIGN STRUCTURE HAS NOT BEEN INCLUDED IN THE AUTHORITY'S APPROVED LIST, IT WILL BE SUBMITTED FOR EVALUATION AND INCLUSION IN THE APPROVED LIST BEFORE USING IT IN ANY OF OUR CONSTRUCTION PROJECTS. THE CONTRACTOR SHALL NOT BEGIN THE CONSTRUCTION OF ANY OVERHEAD SIGN STRUCTURE IF THE AUTHORITY HAS NOT APPROVED THE STRUCTURE.

OVERHEAD SIGN STRUCTURES THAT INCLUDE VARIABLE MESSAGE SIGNS ARE NOT INCLUDED IN THIS PROCEDURE AND PROJECT BY PROJECT SHOP DRAWINGS WILL CONTINUE TO BE SUBMITTED.

DESIGN STRUCTURES WITH CANTILEVER ARMS, SPANS AND/OR SIGN AREAS WHICH EXCEED THE MAXIMUM VALUES INCLUDED IN THE STANDARD DRAWINGS WILL BE APPROVED ON A CASE BY CASE BASIS BY SUBMISSION OF SHOP DRAWINGS BY THE CONTRACTOR AS A SUBSIDIARY OBLIGATION.

DESIGN SPECIFICATIONS AND GENERAL CRITERIA:

- OVERLAPPED SIGN STRUCTURES SHALL BE DESIGNED USING THE ASHITO STANDARD SPECIFICATIONS FOR HIGHWAY SIGNING, LUMINAIRES AND SIGN SUPPORTS, LATEST EDITION, MAY 1988, OR LATER EDITION, IF SO SPECIFICATED. HEREIN AFTER REFERRED TO AS THE ASHITO GUIDE.
- THE FOLLOWING DESIGN CONTROLLING CRITERIA WILL BE USED:
- | | |
|--|--|
| WIND SPEED (MILES PER HOUR) | 125 |
| WIND PRESSURE FACTOR (K _d) | 1.00 |
| COST EFFECT FACTOR (C ₁) | 1.00 |
| HEIGHT AND EXPOSURE FACTOR (K ₂) | 0.14 |
| WIND DIRECTION COEFFICIENT (C _d) | SHALL BE AS INDICATED IN THE DRAWINGS. |

GENERAL CRITERIA

- [illegible]

MATERIALS SPECIFICATIONS:

- [illegible]

MATERIALS SPECIFICATIONS (CONT.):

- [illegible]

DISCUSSION

- ALL DIMENSIONS SHOWN ARE IN METERS UNLESS OTHERWISE SPECIFIED. DIMENSIONS GIVEN IN MILLIMETERS SHALL BE INDICATED WITH: mm AREAS GIVEN IN SQUARE METERS SHALL BE INDICATED WITH: SQM

DISCUSSION PANELS:

- SIGN PANELS, WIND BEAMS, HANGERS AND THEIR ATTACHMENT TO THE OVERHEAD STRUCTURE SHALL BE DESIGNED AS ILLUSTRATED IN THESE STANDARD DRAWINGS.

EFFECTIVE DATE: OCTOBER 2000		COMMUNICATIONS OF PUERTO RICO DEPARTMENT OF TRANSPORTATION AND PUBLIC WORKS HIGHWAY AND INFRASTRUCTURE DIVISION	
OVERHEAD SIGNS SPECIFICATIONS AND NOTES		RECOMMENDED BY: <u> </u> REVIEWED BY: <u> </u> DESIGNED BY: <u> </u> DRAWN BY: <u> </u> CHECKED BY: <u> </u> DATE: <u>01-11-00</u> APPROVED BY: <u> </u> EXECUTIVE DIRECTOR: <u> </u> DATE: <u>1-16-00</u>	
DATE IN USE	REVISION	BY	NO.
	ISSUED WITH SPECIFICATIONS		10

SIGN STRUCTURES WITH CANTILEVER ARMS, SPANS AND/OR SIGN AREAS WHICH EXCEED THE MAXIMUM VALUES INCLUDED IN THE STANDARD DRAWINGS WILL BE APPROVED ON A CASE BY CASE BASIS BY SUBMISSION OF SHOP DRAWINGS BY THE CONTRACTOR AS A SUBSIDIARY OBLIGATION.

THE OVERHEAD SIGN STRUCTURE INCLUDES SIGN PANELS, INCLUDING DIMENSION AND HEIGHT ABOVE EXISTING GROUND, STRUCTURAL SUPPORTS INCLUDING VERTICAL AND HORIZONTAL SUPPORTS, CANTILEVER ARM, SPAN AND FOUNDATION, AND METHOD OF ATTACHMENT OF THE SIGN ASSEMBLY.

EFFECTIVE DATE: OCTOBER 2000		COMMUNICATIONS OF PUERTO RICO DEPARTMENT OF TRANSPORTATION AND PUBLIC WORKS HIGHWAY AND TRANSPORTATION AUTHORITY		RECORDED BY: _____ DEPUTY DIRECTOR FOR TRAFFIC AND SIGNALS DATE: _____	APPROVED BY: _____ EXECUTIVE DIRECTOR DATE: 12-17-00
OVERHEAD SIGNS SPECIFICATIONS AND NOTES				STD. DWG. 1A OF 20 HTS	
DATE	REVISION				

APPROVED LIST OF MANUFACTURERS AND PRODUCTS

OVERHEAD TYPE	ENGINEERING DESIGN INTERNATIONAL		REMINGTON STEEL & SIGNS CORP.		COMPANY NAME	
	SHOP DRAWING APPROVAL DATE	OVERHEAD STRUCTURE MATERIAL	SHOP DRAWING APPROVAL DATE	OVERHEAD STRUCTURE MATERIAL	SHOP DRAWING APPROVAL DATE	OVERHEAD STRUCTURE MATERIAL
I-A	JULY 07, 1999	BOLTED GALVANIZED STEEL	JULY 23, 1999	BOLTED GALVANIZED STEEL		
I-B	JULY 07, 1999	BOLTED GALVANIZED STEEL	JULY 23, 1999	BOLTED GALVANIZED STEEL		
I-C	JULY 07, 1999	BOLTED GALVANIZED STEEL	JULY 23, 1999	BOLTED GALVANIZED STEEL		
I-D	JULY 07, 1999	BOLTED GALVANIZED STEEL	JULY 23, 1999	BOLTED GALVANIZED STEEL		
II-A	DECEMBER 15, 2000	BOLTED GALVANIZED STEEL	JUNE 23, 2000	BOLTED GALVANIZED STEEL		
II-B	DECEMBER 15, 2000 (SEE NOTE 4)	BOLTED GALVANIZED STEEL	JUNE 23, 2000	BOLTED GALVANIZED STEEL		
III-A	DECEMBER 15, 2000	BOLTED GALVANIZED STEEL	JULY 23, 1999	BOLTED GALVANIZED STEEL		
III-B	DECEMBER 15, 2000	BOLTED GALVANIZED STEEL	JULY 23, 1999	BOLTED GALVANIZED STEEL		
III-C	DECEMBER 15, 2000	BOLTED GALVANIZED STEEL	JULY 23, 1999	BOLTED GALVANIZED STEEL		
III-D	DECEMBER 15, 2000	BOLTED GALVANIZED STEEL	JULY 23, 1999	BOLTED GALVANIZED STEEL		
III-E	DECEMBER 15, 2000 (SEE NOTE 4)	BOLTED GALVANIZED STEEL	JULY 23, 1999	BOLTED GALVANIZED STEEL		
IV-A						
IV-B						
IV-C						
IV-D						

GENERAL NOTES:

1. THE CONTRACTOR SHALL NOTIFY THE ENGINEER, WITHIN 90 CALENDAR DAYS OF THE AWARD OF CONTRACT, THE MANUFACTURER HE INTENDS TO USE AT EACH SIGN CODE WHICH PROVIDES THE MANUFACTURER'S NAME, ADDRESS, PHONE AND FAX NUMBERS, AND TYPE OF STRUCTURE, FROM THE APPROVED LIST OF MANUFACTURERS AND PRODUCTS AT THE DATE OF SUBMISSION.

IF THE CONTRACT SIGN DATA SHEET DOES NOT INDICATE THE TYPE OF OVERHEAD STRUCTURE TO BE USED AT EACH OR ANY LOCATION, THE CONTRACTOR SHALL NOTIFY THE ENGINEER OF THE TYPE OF STRUCTURE HE INTENDS TO USE AT EACH SIGN CODE WHICH INCLUDES AN OVERHEAD SIGN. THE MANUFACTURER SHALL BE SELECTED FOR EACH TYPE OF STRUCTURE FROM THE APPROVED LIST OF MANUFACTURERS AND PRODUCTS AT THE DATE OF SUBMISSION.

FOR OVERHEAD SIGN STRUCTURES WHICH DO NOT HAVE STANDARD MANUFACTURERS OR MANUFACTURERS WHO DO NOT HAVE THE PROPOSED STRUCTURE APPROVED INTO THE AND/OR MANUFACTURER MUST HAVE THE PROPOSED STRUCTURE APPROVED INTO THE APPROVED LIST PRIOR TO ITS PROPOSED UTILIZATION.

FOR SIGNS AND SIGN STRUCTURES WHICH EXCEED THE SPAN AND SIGN MAXIMUM LIMITS SPECIFIED IN THE STANDARD DRAWINGS, THE CONTRACTOR SHALL SUBMIT SHOP DRAWINGS IN COMPLIANCE WITH THE CONTRACT REQUIREMENTS.

2. THE CONTRACTOR SHALL USE THE OVERHEAD STRUCTURE TYPE INDICATED IN THE SIGN DATA SHEET. IF THE CONTRACTOR WISHES TO USE A STRUCTURE TYPE NOT LISTED IN THE APPROVED LIST, HE SHALL SELECT FROM THE STANDARD DRAWINGS THE STRUCTURE TYPE (TYPICAL OR ALTERNATE, WHEN AVAILABLE) WHICH HAS A SIGN AREA AND ARM EQUAL OR GREATER THAN THE SIGN AREA AND ARM INDICATED IN THE PLANS.

3. ON STANDARD STRUCTURE TYPES, THE CONTRACTOR SHALL SHORTEN THE ARM OR SPAN TO FIT THE SITE CONDITION.

4. BOLT CIRCLE DOES NOT FIT PER STA STANDARD FOUNDATIONS. CONTRACTOR MUST SUBMIT FOUNDATION DESIGN FOR APPROVAL BY PHRA AS A SUBSIDIARY OBLIGATION.

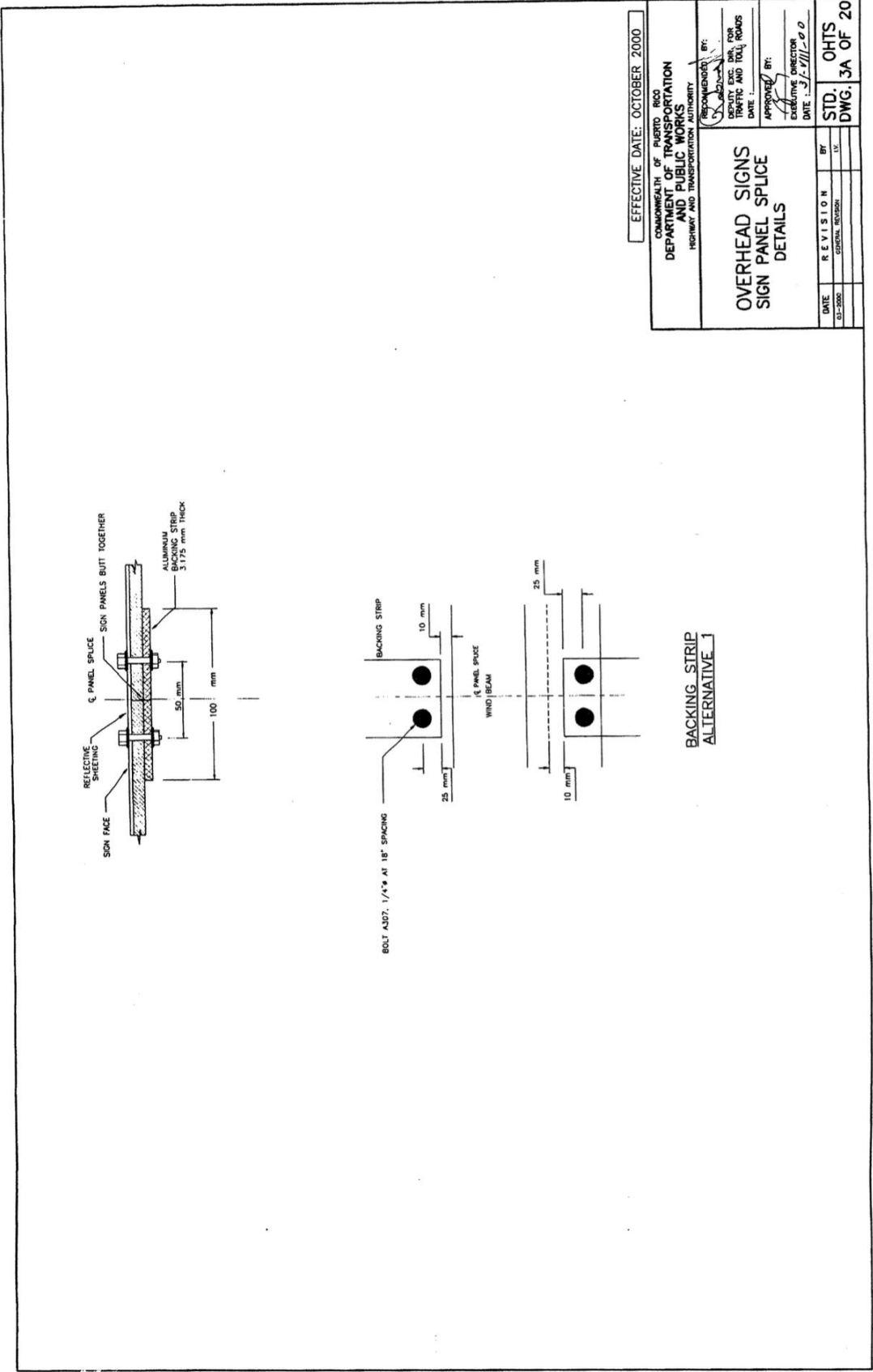
EFFECTIVE DATE: DECEMBER 2000

COMMONWEALTH OF PUERTO RICO
DEPARTMENT OF TRANSPORTATION
HIGHWAY AND PUBLIC WORKS
HIGHWAY AND TRANSPORTATION AUTHORITY

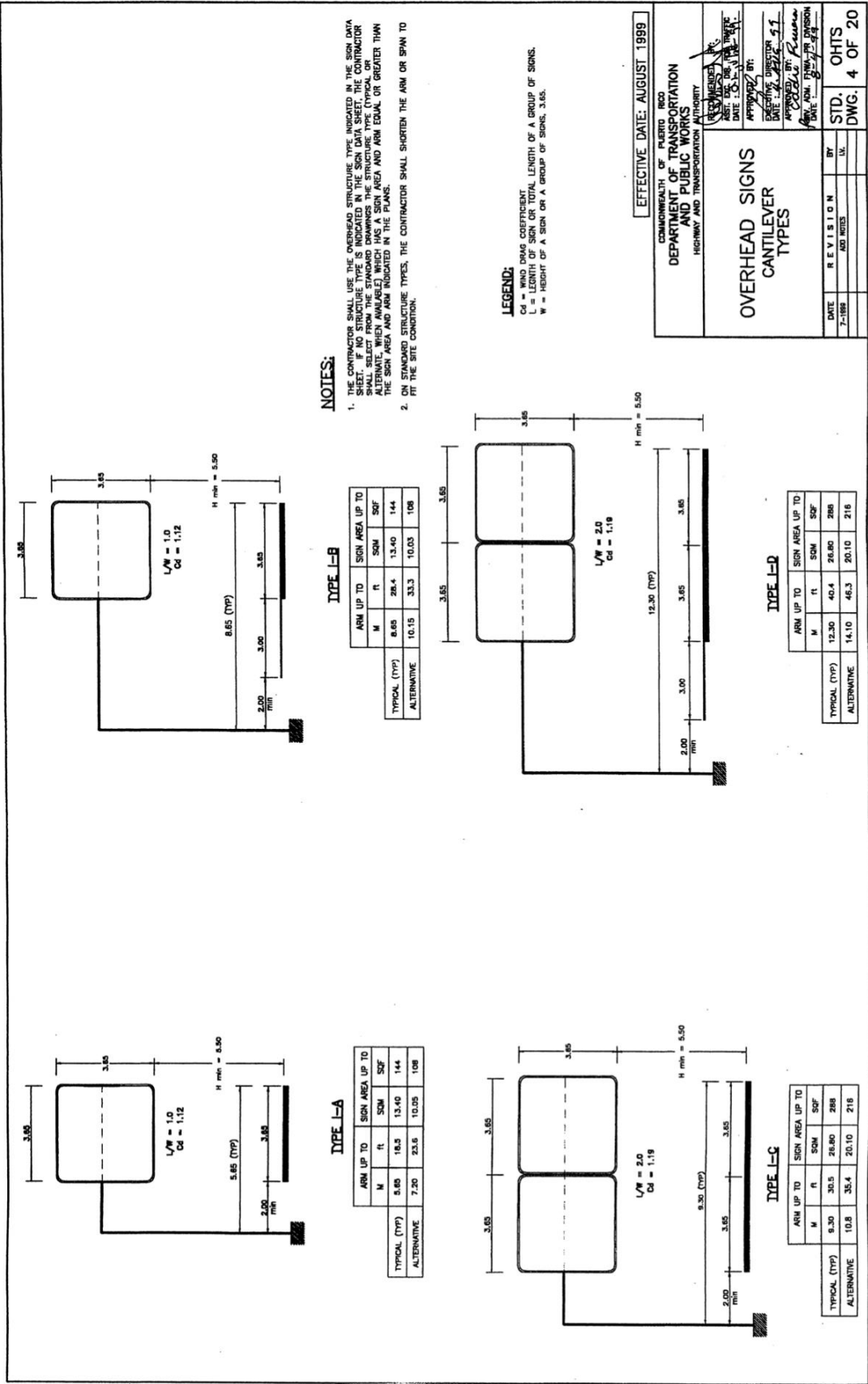
OVERHEAD SIGNS
APPROVED LIST OF
MANUFACTURERS FOR
OVERHEAD STRUCTURES
TYPES

DATE: 12-1999
12-2000
BY: [Signature]
DATE: 12-1999
12-2000
OHTS
DWG. 2 OF 20





EFFECTIVE DATE: OCTOBER 2000	
COMMONWEALTH OF PUERTO RICO DEPARTMENT OF TRANSPORTATION HIGHWAY AND TRAVEL DIVISION	
OVERHEAD SIGNS SIGN PANEL SPLICE DETAILS	
DATE: 03-2002	REVISION: GENERAL REVISION
BY: IV	DATE: 3-11-00
APPROVED BY: EXECUTIVE DIRECTOR	
DATE: 3-11-00	
STD. DWG. 3A OF 20	OHTS



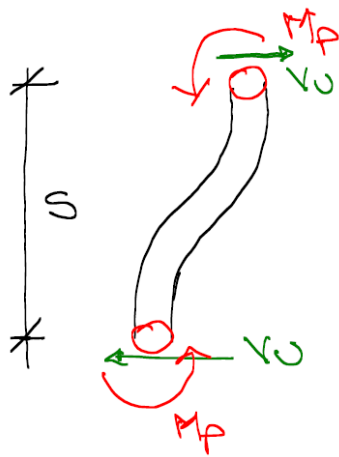


Appendix D Stirrups Spacing and Double Bending of Bolts

A simplified analysis was developed to evaluate, considering a concentrated plastic moment model, the distance S required to avoid that this double bending in the plastic regime of the anchor bolt occurs previous to the shear fracture or reaching yielding.

D.1 First Model – Reach Shear Fracture Before Moment Yielding

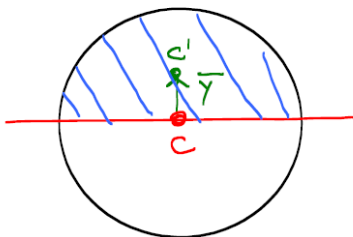
reach shear fracture before moment yielding



V_u = shear force required for shear fracture (rupture)
 M_p = plastic moment (required to produce a plastic hinge)
 FS = factor of safety
 S = spacing between last lateral confinement steel and base plate

$$V_u S FS < 2 M_p$$

$$S < \frac{2 M_p}{V_u FS}$$



$$A' = \frac{\pi r^2}{2}$$

$$y' = \frac{4}{3} \frac{r}{\pi}$$

$$Z = 2 A' y' = 2 \frac{\pi r^2}{2} \frac{4}{3} \frac{r}{\pi}$$

$$Z = \frac{4}{3} r^3$$

$$M_p = F_y Z$$

$$V_0 = F_{0y} A$$

$$V_0 = 0.6 F_0 \pi r^2$$

without considering threads

$$S < \frac{2 M_P}{V_0 F_S} = \frac{2 F_y Z}{F_{0y} A} \frac{1}{F_S}$$

$$< \frac{2 F_y \frac{4}{3} r^3}{0.6 F_0 \pi r^2} \frac{1}{F_S}$$

$$< \frac{2 F_y \frac{4}{3} r}{\frac{3}{5} F_0 \pi} \frac{1}{F_S}$$

$$S < \frac{40}{9} \frac{F_y}{F_0} \frac{r}{\pi} \frac{1}{F_S}$$

considering Threads

$$A_n = 0.75 A = \frac{3}{4} \pi r^2$$

$$S < \frac{2 M_P}{V_u F_S} = \frac{2 F_y Z}{F_u A} \frac{1}{F_S}$$

$$< \frac{2 F_y \frac{4}{3} r^3}{0.6 F_u \frac{3}{4} \pi r^2} \frac{1}{F_S}$$

$$< \frac{2 F_y \frac{4}{3} r}{\frac{3}{5} \frac{3}{4} F_u \pi} \frac{1}{F_S}$$

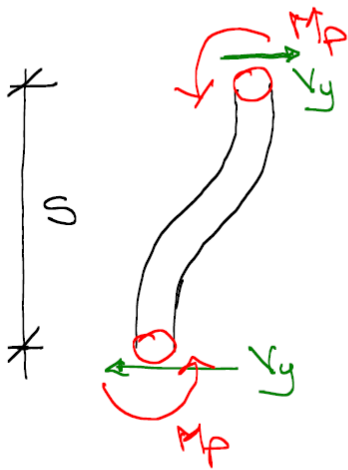
$$S < \frac{160}{27} \frac{F_y}{F_u} \frac{r}{\pi} \frac{1}{F_S}$$

Maximum Stirrup Spacing to avoid double bending failure previous the shear rupture

	Steel		FS	d [in]	S ₁ [in]	S ₂ [in]
	Fy [Ksi]	Fu [Ksi]	Factor of Safety	Anchorage element diameter	without considering threads	considering threads
A36	36	58	1	1	0.439048119	0.585397492
A572	42	60	1	1	0.495148712	0.660198282
	50	65	1	1	0.544119464	0.725492618
	55	70	1	1	0.555779166	0.741038888
	60	75	1	1	0.565884242	0.754512323
	65	80	1	1	0.574726183	0.766301578
A449	58	90	1	1	0.455851195	0.607801593
	81	105	1	1	0.545674091	0.727565454
	92	120	1	1	0.542305732	0.723074309
A354	99	115	1	1	0.608940652	0.811920869
	109	125	1	1	0.616813824	0.822418432
	115	140	1	1	0.581041856	0.774722474
	130	150	1	1	0.613041262	0.81738835
A193	75	100	1	1	0.530516477	0.707355303
	95	115	1	1	0.584336989	0.779115986
	105	125	1	1	0.594178454	0.792237939

D.2 Second Model – Reach Shear Yielding Before Moment Yielding

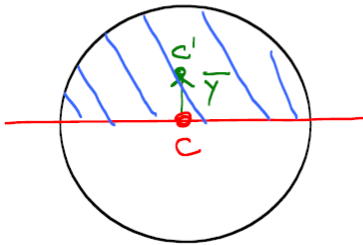
reach shear yielding before moment yielding



V_y = shear force required for shear yielding
 M_p = plastic moment (required to produce a plastic hinge)
 FS = factor of safety
 S = spacing between last lateral confinement steel and base plate

$$V_y S FS < 2 M_p$$

$$S < \frac{2 M_p}{V_y FS}$$



$$A' = \frac{\pi r^2}{2}$$

$$y' = \frac{4}{3} \frac{r}{\pi}$$

$$Z = 2 A' y' = 2 \frac{\pi r^2}{2} \frac{4}{3} \frac{r}{\pi}$$

$$Z = \frac{4}{3} r^3$$

$$M_p = F_y Z$$

$$V_y = F_{yv} A$$

$$V_y = 0.6 F_y \pi r^2$$

without considering threads

$$S < \frac{2 M_p}{V_y F_S} = \frac{2 F_y Z}{F_{yv} A} \frac{1}{F_S}$$

$$< \frac{2 F_y \frac{4}{3} r^3}{0.6 F_y \pi r^2} \frac{1}{F_S}$$

$$< \frac{2}{\frac{3}{5}} \frac{\frac{4}{3} r}{\pi} \frac{1}{F_S}$$

$$S < \frac{40}{9} \frac{r}{2\pi} \frac{1}{F_S}$$

considering Threads

$$A_n = 0.75 A = \frac{3}{4} \pi r^2$$

$$S < \frac{2 M_P}{V_y F_S} = \frac{2 F_y Z}{F_y V A} \frac{1}{F_S}$$

$$< \frac{2 F_y \frac{4}{3} r^3}{0.6 F_y \frac{3}{4} \pi r^2} \frac{1}{F_S}$$

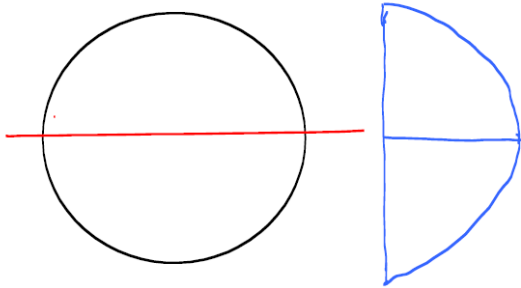
$$< \frac{2 F_y \frac{4}{3} r}{\frac{3}{5} \frac{3}{4} F_y \pi} \frac{1}{F_S}$$

$$S < \frac{160}{27} \frac{r}{\pi} \frac{1}{F_S}$$

Maximum Stirrup Spacing to avoid double bending failure previous to shear yielding						
	Steel		FS	d [in]	S ₁ [in]	S ₂ [in]
	Fy [Ksi]	Fu [Ksi]	Factor of Safety	Anchorage element diameter	without considering threads	considering threads
A36	36	58	1	1	0.707355303	0.943140404
A572	42	60	1	1	0.707355303	0.943140404
	50	65	1	1	0.707355303	0.943140404
	55	70	1	1	0.707355303	0.943140404
	60	75	1	1	0.707355303	0.943140404
	65	80	1	1	0.707355303	0.943140404
A449	58	90	1	1	0.707355303	0.943140404
	81	105	1	1	0.707355303	0.943140404
	92	120	1	1	0.707355303	0.943140404
A354	99	115	1	1	0.707355303	0.943140404
	109	125	1	1	0.707355303	0.943140404
	115	140	1	1	0.707355303	0.943140404
	130	150	1	1	0.707355303	0.943140404
A193	75	100	1	1	0.707355303	0.943140404
	95	115	1	1	0.707355303	0.943140404
	105	125	1	1	0.707355303	0.943140404

D.3 Third Model – Reach Shear Yielding (Using Jourawsky Formula for Shear) Before Moment Yielding

Considering stress formula for beams



$$\tau_{max} = \frac{VQ}{Ib}$$

$$Q = A' y' = \frac{\pi r^2}{2} \cdot \frac{4}{3} \frac{r}{\pi}$$

$$= \frac{4}{6} r^3$$

$$I = \frac{\pi r^4}{4} \quad b = 2r$$

$$\tau_{max} = \frac{V \cdot \frac{4}{6} r^3}{\frac{\pi r^4}{4} \cdot 2r}$$

$$= \frac{V}{\pi r^2 \cdot \frac{12}{16}}$$

$$= \frac{V}{\pi r^2 \cdot \frac{3}{4}}$$

$$V_y = \frac{3}{4} \pi r^2 \tau_y = \frac{3}{4} \pi r^2 \cdot 0.6 F_y$$

$$= \frac{3}{4} \pi r^2 \cdot \frac{3}{5} F_y$$

$$= \frac{9}{20} \pi r^2 F_y$$

without considering threads

$$\begin{aligned}
 S &< \frac{2 M_p}{V_y F_S} = \\
 &< \frac{2 F_y \frac{4}{3} r^3}{\frac{9}{20} F_y \pi r^2} \frac{1}{F_S} \\
 &< \frac{2}{\frac{9}{20}} \frac{\frac{4}{3} r}{\pi} \frac{1}{F_S}
 \end{aligned}$$

$$S < \frac{160}{27} \frac{r}{\pi} \frac{1}{F_S}$$

considering threads

$$V_y = \frac{9}{20} \frac{3}{4} \pi r^2 F_y = \frac{27}{80} \pi r^2 F_y$$

$$S < \frac{2 M_p}{V_y F_S} =$$

$$< \frac{2 F_y \frac{4}{3} r^3}{\frac{27}{80} \pi r^2 F_y} \frac{1}{F_S}$$

$$< \frac{2 \frac{4}{3} r}{\frac{27}{80} \pi} \frac{1}{F_S}$$

$$S < \frac{640}{81} \frac{r}{\pi} \frac{1}{F_S}$$

Maximum Stirrup Spacing to avoid double bending failure previous to shear yielding using shear distribution from beam (Jourawsky) formula						
	Steel		FS	d [in]	S ₁ [in]	S ₂ [in]
	F _y [Ksi]	F _u [Ksi]	Factor of Safety	Anchorage element diameter	without considering threads	considering threads
A36	36	58	1	1	0.943140404	1.257520538
A572	42	60	1	1	0.943140404	1.257520538
	50	65	1	1	0.943140404	1.257520538
	55	70	1	1	0.943140404	1.257520538
	60	75	1	1	0.943140404	1.257520538
	65	80	1	1	0.943140404	1.257520538
A449	58	90	1	1	0.943140404	1.257520538
	81	105	1	1	0.943140404	1.257520538
	92	120	1	1	0.943140404	1.257520538
A354	99	115	1	1	0.943140404	1.257520538
	109	125	1	1	0.943140404	1.257520538
	115	140	1	1	0.943140404	1.257520538
	130	150	1	1	0.943140404	1.257520538
A193	75	100	1	1	0.943140404	1.257520538
	95	115	1	1	0.943140404	1.257520538
	105	125	1	1	0.943140404	1.257520538

D.4 Summary

Six alternate analyses were evaluated, and a maximum spacing formula obtained as a function of the bolt diameter d , and the bolt material properties (F_y and F_u). The previous model for the anchor bolts implies slender beam behavior, and concentrated plasticity (zero length plastic hinges).

Case	S Vn at hole section	S Vn at threaded section (0.75 Ag)
$V_n = V_u = \text{fracture}$ Average shear stresses	$S < \frac{20}{9} \frac{F_y}{F_u} \frac{d}{\pi}$	$S < \frac{80}{27} \frac{F_y}{F_u} \frac{d}{\pi}$
$V_n = V_y = \text{yielding}$ Average shear stresses	$S < \frac{20}{9} \frac{d}{\pi}$	$S < \frac{80}{27} \frac{d}{\pi}$
$V_n = V_y = \text{yielding}$ Beam shear stresses	$S < \frac{80}{27} \frac{d}{\pi}$	$S < \frac{320}{81} \frac{d}{\pi}$

The model resulted not appropriate, according to results, giving values of S too small (in the range of d). The analysis of S required to avoid double bending should include a full plastic model for the bolts, also include de group action, and the effect of the enclosed concrete that produces confinement and increases resistance in the overall behavior of the bolts.

Nevertheless, the model could be used to evaluate the impact of having a large spacing S , since the slender beam behavior and the concentrated plasticity model would be more appropriate, and the concrete, due to the large space unconfined, would provide smaller additional capacity. For instance, if the bolt is $1 \frac{3}{4}$ in diameter, with a yielding stress of 60 ksi, the shear force required to reach the formation of plastic moments (hinges) in an isolated bolt is about 10% of the force required to reach the condition of yielding by shear in the cross section of the bolt, as shown below.

A more refined model would give a smaller impact, but this simplified model could be used to assess that the impact of the spacing is significant.

Impact of too large spacing in reducing shear force required to reach a failure condition, V_n

$$db := 1.75 \quad [\text{in}]$$

$$F_y := 60 \quad [\text{Ksi}]$$

$$F_u := 66 \quad [\text{Ksi}]$$

$$A_b := \pi \cdot \left(\frac{db}{2} \right)^2 \quad A_b = 2.4053 \quad [\text{in}^2]$$

$$V_y := 0.6 \cdot F_y \cdot A_b \quad V_y = 86.5901 \quad [\text{Kips}]$$

Shear force to reach shear yielding

$$S := 12 \quad [\text{in}]$$

$$z := \frac{4}{3} \cdot \left(\frac{db}{2} \right)^3 \quad z = 0.8932 \quad [\text{in}^3]$$

$$M_p := F_y \cdot z \quad M_p = 53.5938 \quad [\text{Kip-in}]$$

$$V_n := \frac{2 \cdot M_p}{S} \quad V_n = 8.9323 \quad [\text{Kips}]$$

Shear force to reach plastic moment development

Appendix E Cantilever Signs Geolocation per Municipality

The following table summarizes the geolocation of each inspected cantilever traffic sign per municipality, and the damages found. The table presents the municipality name, the quantity of cantilever traffic signs identified in that jurisdiction, and for each sign (identified with an ID consisting of a letter P followed by a sequential number assigned as the signs were identified during the research process), its geolocation coordinates, and a brief description of the damage found.

Municipality	Qty	Posts ID	Location Coordinates		Identified Damage
			N	E	
Aguadilla	4				
		P-75	18.44475278	-67.14586667	None.
		P-76	18.45225	-67.09390556	Foundation torsional rotation.
		P-77	18.45361389	-67.08913056	Foundation torsional rotation.
		P-78	18.43665278	-67.14786944	Foundation torsional rotation and RC base cracks and damages.
Arecibo	5				
		P-88	18.45280278	-66.74728056	Apparent found. torsional rotation.
		P-89	18.45293333	-66.74575833	Apparent found. torsional rotation.
		P-90	18.45233333	-66.71889722	Apparent found. torsional rotation.
		P-91	18.46075278	-66.71781389	Apparent found. torsional rotation.
		P-102	18.44319444	-66.62525278	None.
Barceloneta	1				
		P-103	18.43554722	-66.54408611	Sign blown away.
Caguas	11				
		P-16	18.22014722	-66.04703611	RC base cracks.
		P-17	18.22979722	-66.04458333	RC base cracks.
		P-18	18.22991944	-66.04418889	None.
		P-19	18.23493889	-66.04304722	None.
		P-20	18.23696944	-66.04240556	None.
		P-21	18.26821944	-66.03913889	None.
		P-22	18.27201944	-66.03914444	Apparent collapse. RC base damages.
		P-28	18.2736175	-66.0374457	None.

Municipality	Qty	Posts ID	Location Coordinates		Identified Damage
			N	E	
		P-29	18.284306	-66.0362139	None.
		P-30	18.2792184	-66.0351726	None.
		P-45	18.27035278	-66.03955556	Apparent collapse. Rests of RC base.
		P-52	18.18641667	-65.89136667	Collapse. Foundation overturning and rotation.
		P-58	18.25564167	-66.02865278	RC base wide cracks and near spalls.
Camuy	1				
		P-69	18.46343611	-66.88946389	Collapsed. Foundation torsional rotation and RC base damages.
Canóvanas	2				
		P-106	18.37240278	-65.87742222	Collapse. Anchor bolts large lateral displacement, concrete cracks, and crushing.
		P-107	18.3603111	-65.8938111	Foundation torsional rotation and RC base damages.
Dorado	1				
		P-62	18.42215278	-66.27283611	None.
Guayama	3				
		P-11	17.98893611	-66.13911389	None.
		P-46	17.98580833	-66.14682222	Partial collapse: post had torsional rotation and tilt; Anchor bolts large lateral displacement, concrete cracks, and crushing on RC pedestal.
		P-47	17.9868529	-66.1425048	Partial collapse: post had torsional rotation and tilt; Anchor bolts large lateral displacement, concrete cracks, and crushing on RC pedestal.
Gurabo	1				
		P-57	18.25031944	-65.96180556	Total collapse. Only rests of pedestal.
Humacao	3				
		P-61	18.159975	-65.79745833	Total collapse: post had torsional rotation; Anchor bolts large lateral displacement, concrete cracks, and crushing on RC pedestal.
		P-100	18.11863611	-65.82133333	Total collapse: post had torsional rotation; Anchor bolts large lateral displacement, concrete cracks, and crushing on RC pedestal.
		P-105	18.12126667	-65.82057222	Total collapse: post had torsional rotation; Anchor bolts large lateral displacement, concrete cracks, and crushing on RC pedestal.

Municipality	Qty	Posts ID	Location Coordinates		Identified Damage
			N	E	
Isabela	1				
		P-74	18.47931389	-66.97209167	None.
Juana Diaz	2				
		P-5	18.03969167	-66.53639722	None.
		P-6	18.03189444	-66.45465278	Truss and sign missing. No evidence of impact from the hurricane.
		P-71	18.0318502	-66.45461	None.
Juncos	3				
		P-54	18.21683889	-65.91140306	None.
		P-55	18.22131389	-65.91406944	Concrete base wide crack.
		P-56	18.22426944	-65.91595833	Large torsional rotation. Possible pedestal damages. Removed at the time of visit.
Las Piedras	7				
		P-48	18.173503	-65.87503	None.
		P-49	18.173647	-65.87472	None.
		P-50	18.178117	-65.88028	None.
		P-51	18.180964	-65.88374	None.
		P-53	18.191986	-65.89632	Collapse. Large deformation and pullout of the anchor bolts. Possible torsional rotation of the base.
		P-66	18.186417	-65.89137	Collapse. Removed at the time of visit. Unsafe to inspect.
		P-99	18.183386	-65.88572	Collapse. Removed at the time of visit. Unsafe to inspect.
Ponce	8				
		P-1	17.990347	-66.62129	Concrete fractures and initial detachments due to the anchor bolts lateral movement.
		P-3	17.988819	-66.61678	Concrete fractures and initial detachments due to the anchor bolts lateral movement.
		P-4	17.986208	-66.6033	Concrete fractures and initial detachments due to the anchor bolts lateral movement.
		P-59	17.989231	-66.64625	Collapse. Foundation overturning, torsional rotation, and concrete shaft shear fracture.
		P-60	17.992689	-66.60524	None.
		P-65	18.033256	-66.55973	None.

Municipality	Qty	Posts ID	Location Coordinates		Identified Damage
			N	E	
		P-67	18.035453	-66.55673	None. Construction defects on the concrete pedestal (bug holes, and large exposed aggregates).
		P-94	17.987914	-66.64869	Foundation torsional rotation.
Quebradillas	9				
		P-79	18.47931389	-66.97209167	None.
		P-80	18.48031389	-66.96836944	None.
		P-81	18.48649444	-66.954625	None.
		P-82	18.48413056	-66.9564	None.
		P-83	18.48243333	-66.96057222	None.
		P-84	18.48882778	-66.95061111	None.
		P-85	18.48464444	-66.94231667	None.
		P-86	18.48128611	-66.93954722	None.
		P-87	18.48843333	-66.94520556	None.
Salinas	6				
		P-11	18.000525	66.23806944	Collapse. Removed by PR DOT. They gave input of large lateral deflections of the anchor bolts.
		P-12	18.0031474	-66.2415833	Collapse. Pedestal structural failure with large lateral deflections of the anchor bolts.
		P-13	18.02497778	-66.24146944	None.
		P-14	18.01980556	-66.243275	None.
		P-15	18.02478333	-66.24122778	Partial collapse. The post presented large deflections and double bending in the plastic range of the anchoring elements
		P-26	17.9916384	-66.3006761	None.
San Juan	11				
		P-33	18.40454722	-66.07060833	Soil foundation failure (torsional rotation).
		P-35	18.40454722	-66.06998889	Soil foundation failure (torsional rotation).
		P-38	18.40155	66.07126944	Soil foundation failure (torsional rotation) with damages to the pedestal).
		P-39	18.41216667	-66.06983889	Not evident.
		P-40	18.413125	-66.06986944	Small torsional rotation detected in satellite image.

Municipality	Qty	Posts ID	Location Coordinates		Identified Damage
			N	E	
		P-41	18.41305833	-66.07029722	Soil foundation failure (torsional rotation) with damages to the pedestal).
		P-42	18.41519722	-66.07039722	Soil foundation failure (torsional rotation). Gap between soil and shaft.
		P-43	18.41788611	-66.07006111	Soil foundation failure (small torsional rotation) with damages to the pedestal. Gap between soil and shaft.
		P-44	18.41561389	-66.06995	Soil foundation failure (small torsional rotation) with damages to the pedestal. Gap between soil and shaft.
		P-95	18.42378056	-66.07243056	Soil foundation failure (torsional rotation). Gap between soil and shaft.
		P-98	18.40760556	-66.0675	Collapse. Pedestal structural failure with large lateral deflections of the anchor bolts.
Santa Isabel	8				
		P-7	18.02574444	-66.40993889	Possible total collapse. Post no found. Probably removed.
		P-8	18.01293333	-66.389025	Cracks of the top of the concrete base; probably construction process.
		P-10	18.01423056	-66.36989167	Deep cracks on concrete base due to bolts movement.
		P-24	18.01941841	-66.4034875	None.
		P-25	18.014831	-66.3969412	None.
		P-36	18.01324444	-66.38875	Cracks of the top of the concrete base; probably construction process.
		P-37	18.01423056	-66.39175556	None
		P-70	18.0284609	-66.4165331	Diagonal crack on the pedestal.
Toa Baja	2				
		P-96	18.41868889	66.23942222	None.
		P-97	18.4187	66.23949722	None.
Vega Alta	2				
		P-92	18.428575	-66.34839444	None.
		P-93	18.43041667	-66.336275	None.